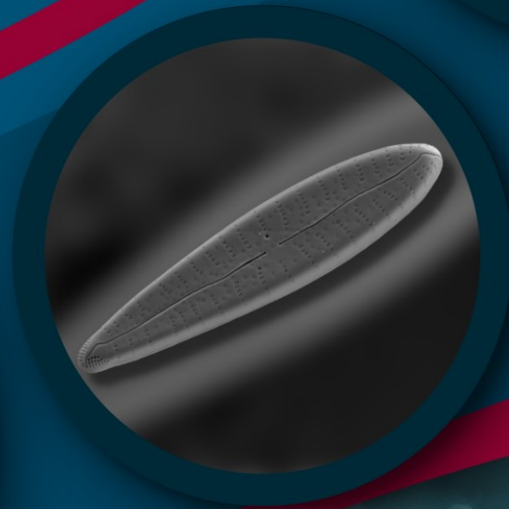


Assessment of biological activity along a metal pollution gradient applying macroinvertebrates and diatoms

by Stijn Van de Vondel

Master project submitted to obtain the degree of
Master in Biology,
specialisation Global Change Biology



Supervisors: Prof. Dr Bart Van de Vijver
Prof. Dr Lieven Bervoets
Co-supervisor: Drs Bart Slootmaekers

 University
of Antwerp

 Meise
Botanic Garden

**Assessment of biological activity along a metal
pollution gradient applying diatoms and
macroinvertebrates**

by

Stijn Van de Vondel

*Master project submitted to obtain the degree of Master in Biology,
specialisation Global Change Biology
Academic year 2019-2020*

Supervisors: Prof. Dr Lieven Bervoets & Prof. Dr Bart Van de Vijver
Co-supervisor: Drs Bart Slootmaekers

University of Antwerp – Faculty of Science: Department of Biology
Groenenborgerlaan 171, B-2020 Antwerpen, Belgium

Abstract

The European Water Framework Directive was created to monitor and establish the quality of all waterbodies within the European Union urging all member states to perform water quality assessment based on biological, physicochemical and hydro-morphological elements. Among others, diatoms and macroinvertebrates have been shown to form very reliable bio-indicators for general water quality monitoring.

The present study evaluates the impact of a metal pollution gradient caused by historical contamination in a Flemish lowland river. It follows previous research from 2006-2007 that evaluated the water quality of the Dommel using diatoms and macroinvertebrates. Biotic indices based on both diatoms and macroinvertebrates are applied to monitor the water quality of six sampling localities of the river, sampled during three campaigns. A physicochemical analysis of water, sediment and a selection of macroinvertebrates was carried out to investigate the presence of metals. Our results suggest that sites downstream of the Eindergatloop – a tributary of the Dommel – were different from upstream waters in terms of physicochemistry, showing increased levels of electrical conductivity, sulphate and chloride. Metal contents in water and sediment showed elevated levels of cadmium and lead in downstream sites, while water samples showed higher concentrations for copper, zinc and arsenic. Differences between sampling campaigns were also observed for some of these physicochemical variables. Metal concentrations in macroinvertebrates displayed increased levels of zinc, arsenic, cadmium and lead downstream of the Eindergatloop, while diatoms did not show a clear sign of metal-induced deformities. Biotic diatom indices indicated downstream sites to be of lower biological water quality, while the MMIF did not show any differences. However, the latter indicated the entire study area to be of ‘moderate’ water quality. Community analysis showed a high degree of similarity in diatom and macroinvertebrate communities, indicating increased downstream levels of pollution.

Samenvatting

De Europese Kaderrichtlijn Water werd in het leven geroepen om de waterkwaliteit van alle wateren binnen de Europese Unie te monitoren. Alle lidstaten werden hierbij verzocht om waterkwaliteitsanalyses uit te voeren die gebaseerd zijn op biologische, fysicochemische en hydromorfologische elementen. Van de biologische elementen worden diatomeeën en macro-invertebraten zeer geschikt geacht als bio-indicator voor algemene waterkwaliteitsbepalingen. Deze studie tracht de impact van een metaalverontreinigingsgradiënt, veroorzaakt door historische vervuiling, na te gaan in een Vlaamse rivier. Volgend op eerder uitgevoerd onderzoek in 2006-2007 waarin de waterkwaliteit van de Dommel werd onderzocht op basis van diatomeeën en macro-invertebraten, werden zes meetpunten bemonsterd tijdens drie verzamelcampagnes. Een fysicochemische analyse van water, sediment en een selectie van macro-invertebraten werd uitgevoerd om de aanwezigheid van metaalverontreiniging te bepalen. Onze resultaten suggereren dat meetpunten die stroomafwaarts gelegen zijn van de Eindergatloop – een zijrivier van de Dommel – verschillen in fysicochemie, gezien de daar gemeten hogere elektrische geleidbaarheid, sulfaat en chloride. Ook werden verhoogde concentraties aan cadmium en lood gevonden in water en sediment van stroomafwaarts gelegen meetpunten, terwijl waterstalen ook hogere concentraties aan koper, zink en arseen vertoonden. Daarnaast werden voor een aantal van deze fysicochemische variabelen ook verschillen gevonden tussen de verzamelcampagnes. Voor metaalconcentraties in macro-invertebraten werden verhoogde concentraties geobserveerd voor zink, arseen, cadmium en lood in locaties die stroomafwaarts gelegen zijn van de Eindergatloop, terwijl diatomeeën geen duidelijk vervormingen vertoonden door metaal-gerelateerde stress. Biotische indices op basis van diatomeeën gaven een lagere waterkwaliteit aan in stroomafwaarts gelegen samples, terwijl de MMIF hier geen verschil signaleerde. Dit laatste betekent dat het hele studiegebied kon beoordeeld worden als zijnde van ‘gematigde’ waterkwaliteit. Gemeenschapsanalyses voor zowel diatomeeën en macro-invertebraten vertoonden een hoge graad aan gelijkheid, met aanwijzingen voor een hogere verontreinigingsgraad in stroomafwaarts gelegen wateren van de Dommel.

Layman's abstract

The European Union urged all of its member states to conduct water quality evaluations for all European waters based on general water characteristics such as physicochemistry, hydromorphology and biological life. Aquatic life consists of many organisms such as diatoms and macroinvertebrates. Diatoms are microscopic, unicellular algae that are characterized by a cell wall composed of silica, which resembles the shape of a box of cheese, while macroinvertebrates consist of aquatic and often bottom-dwelling organisms that are visible to the naked eye. The species composition and the number of organisms can provide information about the ecological quality of a river, which is translated in biotic quality indices.

We investigated the impact of metal pollution caused by historical contamination in a Flemish river, the Dommel. Following research conducted in 2006-2007, water quality was investigated using both diatoms and macroinvertebrates. Six sites along the Dommel were sampled in three separate campaigns. A physicochemical analysis of water and sediment was conducted and metal contents in macroinvertebrates measured, to compare sites upstream and downstream of a possible source of contamination: the Eindergatloop, a tributary to the Dommel. Our findings showed several indications of increased levels of pollutants in sites downstream of the Eindergatloop, such as salinity. Higher concentrations of metals such as cadmium and lead were found in both water and sediment of downstream sites. Physicochemical variables also showed differences between the sampling campaigns. Higher concentrations of metals such as cadmium and lead were found in macroinvertebrates collected downstream of the Eindergatloop. Diatoms did not show any deformities caused by metals. Indices based on diatoms showed higher pollution levels in downstream sites, while macroinvertebrates valued all measuring locations to be of 'moderate' water quality. Community analysis showed similar diatom and macroinvertebrate communities between up- and downstream sites, with indications for increased levels of pollution downstream.

Acknowledgements

First of all, my sincerest gratitude goes out to my supervisors prof. Lieven Bervoets and prof. Bart Van de Vijver, both of whom played an invaluable role in giving shape to this project. Whenever any issues or discrepancies arose, Bart and Lieven would swiftly respond to help me resolve any problem at hand. They joined me during field work, guided me through the many hours in the laboratory, gave incredibly valuable feedback on all of my work, all the while keeping me sane in the process. Where Lieven was always available to solve any and every macroinvertebrate- or ecotoxicological-related complication, Bart never ceased to surprise me with his knowledge of diatom ecology and taxonomy. In other words, I simply cannot express my appreciation to a degree that would sufficiently make up for their support and expertise, other than a heartfelt thank you!

Next, I would like to profoundly thank my co-supervisor Bart Sloodmaekers for his guidance during field work, metal analysis, sorting and identification of macroinvertebrates in the lab, as well as his aid during statistical analysis, reporting of the results and general feedback. If not for his patience, the time he spent replying to my many e-mails and his down-to-Earth approach, this thesis would not have looked quite the same.

I could not have found my way through the wonderful world of macroinvertebrates, if not for the assistance of a couple of supportive individuals. For the help during the process of sorting the (many) macroinvertebrates, I want to thank Garben Logghe, Karianne Van Houtven, Margaux Pottiez, Léon Stuurman, Tess and Priscilla. Special thanks go to Garben for his assistance during macroinvertebrate identification, as well as being a sounding board for ideas in general. Same goes for Karianne Van Houtven, who helped me a great deal during sorting of macroinvertebrates, as well as being of tremendous help with measurements in the field.

With regard to the fascinating field of diatoms, I would like to thank Adrienne Mertens for helping me with the autecological calculations. Additionally, I want to extend my gratitude to the Meise Botanic Garden for granting me the opportunity to work at their institution and for allowing me to use their equipment.

Furthermore, I would like to express my gratitude to all the academic and technical personnel along the journey of this thesis. As such, I want to thank Steven Joosen and Kayawe Valentine Mubiana (SPHERE) for their time and expertise in terms of the metal analyses. Additionally, I want to thank Tom Van der Spiet and Anne Cools (ECOBÉ) for running nutrient and salt

analyses on my water samples. Additionally, I would like to thank Myriam de Haan for helping with preparation of my diatom samples. A special mention goes out to Maarten De Jonge, whose work served as the inspiration for this project.

My gratitude also goes to some individuals that I have met along the way. As such, I would like to extend my gratitude to David Williams and Paul Hamilton for inspiring me and making this journey all the more intriguing. The same sense of gratitude goes out to the NVKD and their members. Lastly, I am extremely grateful that I always had my ‘diatomaatje’ Charlotte Goeyers by my side in Meise.

Last but not least, I want to thank all of my friends (shoutout to Fergus and Justine for always rooting for me!) and family who stood by my side during this marvellous journey. Special thanks go out to both of my parents, who never stopped believing in me. I also want to express my gratitude to Ben and Emma, the most incredible couple I have ever met, for guidance with Excel-related questions, for proofreading my texts and providing feedback. And to my wonderful girlfriend, my partner in crime, thank you for joining me on this epic adventure!

My final words go out to my late grandfather Lionel, who always believed I would become a marine biologist. Even though I did not quite grow into the world of marine life as you had foreseen, I made it all the way through, nonetheless!

List of abbreviations

BBI	Belgian Biotic Index
BgK	Large Brook Kempen (Grote Beek Kempen)
BMQL	Below Method Quantification Limit
BOD	Biological Oxygen Demand – commonly expressed as BOD₅²⁰ (mgO ₂ /L of sample during 5 days incubation at 20°C)
BQE	Biological Quality Elements
CIW	Integrated Water Policy (Coördinatiecommissie Integraal Waterbeleid)
COD	Chemical Oxygen Demand
DW	Dry Weight
EC	Electrical Conductivity
EPT	Number of Ephemeroptera, Plecoptera and Trichoptera
EQS	Environmental Quality Standards
IBD	Indice Biologique Diatomées or Diatom Biological Index
IPS	Indice de Polluosensibilité Spécifique or Specific Polluosensitivity Index
MQ	Demineralized water
MMIF	Multimetric Macroinvertebrate Flanders
MTS	Mean Tolerance Score
NH₄⁺	Ammonia
NO₂⁻	Nitrite
NO₃⁻	Nitrate
NST	Number of Non-Sensitive Taxa
P	Phosphorous
PE	Polyethylene
PO₄³⁻	Phosphate
PP	Polypropylene
SO₄²⁻	Sulphate
SWD	Shannon-Wiener Diversity Index
TAX	Taxa richness
TDI	Trophic Diatom Index
TKN	Total Kjeldahl Nitrogen; a measure of the total N fraction contained within organic N, NH ₃ and NH ₄ ⁺
TU	Toxic Units
VMM	Flanders Environment Agency (Vlaamse Milieumaatschappij)
WFD	Water Framework Directive
WMS	Weighted Mean Score

Table of contents

1. INTRODUCTION	1
1.1. THE EUROPEAN WATER FRAMEWORK DIRECTIVE	1
1.2. BIOLOGICAL WATER QUALITY EVALUATION	1
1.3. BIOLOGICAL QUALITY ELEMENTS	2
1.3.1. <i>Diatoms (Bacillariophyceae)</i>	2
1.3.2. <i>Macroinvertebrates</i>	6
1.4. METALS AND METAL POLLUTION	9
1.4.1. <i>Metals and diatoms</i>	10
1.4.2. <i>Metals and macroinvertebrates</i>	10
1.5. RATIONALE & OBJECTIVES	12
2. MATERIALS & METHODS	13
2.1. STUDY AREA	13
2.2. PHYSICOCHEMICAL CHARACTERIZATION OF WATER	15
2.3. SAMPLING AND PREPARATION OF SEDIMENT	15
2.4. METAL ANALYSIS OF WATER AND SEDIMENT	16
2.5. SAMPLING AND IDENTIFICATION OF DIATOMS	16
2.6. COLLECTION AND CLASSIFICATION MACROINVERTEBRATES	18
2.7. METAL ANALYSIS OF MACROINVERTEBRATES	19
2.8. ADDITIONAL CALCULATIONS AND STATISTICAL ANALYSIS	20
2.8.1. <i>Metals in water, in sediment and biota</i>	20
2.8.2. <i>Toxic units (TU)</i>	20
2.8.3. <i>Diatom index calculations & autecology</i>	21
2.8.4. <i>Multimetric Macroinvertebrate Index Flanders (MMIF)</i>	21
2.8.5. <i>Statistical analysis</i>	21
3. RESULTS	23
3.1.1. <i>Correlation analysis of physicochemistry and metals in water</i>	24
3.1.2. <i>Principal Component Analysis of physicochemistry</i>	25
3.1.1. <i>Abundance and diversity</i>	26
3.1.2. <i>Diatom autecology</i>	28
3.1.3. <i>Diatom indices: IBD, TDI & IPS</i>	28
3.1.4. <i>Diatom community composition</i>	29
3.1.1. <i>Abundance and diversity</i>	30
3.1.2. <i>Metals in macroinvertebrates</i>	31
3.1.3. <i>Multimetric Macroinvertebrate Index Flanders</i>	32
3.1.4. <i>Community composition</i>	33
4. DISCUSSION	35
PHYSICOCHEMISTRY OF WATER AND SEDIMENT	35
DIATOMS	37
MACROINVERTEBRATES	42
PAST AND PRESENT	47
CAVEATS AND RECOMMENDATIONS	49
5. CONCLUSION	50
6. BIBLIOGRAPHY	51
7. APPENDIX	59

1. Introduction

1.1. The European Water Framework Directive

The European Water Framework Directive 2000/60/EC WFD (European Commission, 2000) is the Union's flagship legislative instrument on water protection. The Directive establishes a framework in which each of the Union's member states is urged to protect all natural and artificial water bodies, with the central objective of achieving good ecological status in the entire water system (i.e. conditions that are only slightly altered by anthropogenic activities) by 2015. If this initial WFD goal was deemed impossible to achieve within the defined time limit (of reasons such as technical feasibility or disproportionate costs), time extensions may be applicable (up until 2027). In doing so, the WFD aims to prevent further deterioration of aquatic ecosystems, promoting their protection and long-term sustainable use in reducing the discharge and emissions of priority substances. Additionally, the WFD wants to ensure the progressive reduction of groundwater pollution and facilitate the quality and quantity of ecosystem services in terms of mitigating floods and droughts. In other words, member states are tasked with the restoration and improvement of all natural, artificial and heavily modified water bodies (lakes, rivers, transitional and coastal waters). For each of these water bodies, type-specific hydromorphological and physicochemical conditions are established that represent the theoretical 'reference' situation of a given water body type with hardly any anthropogenic stressors (Birk et al., 2012; Moss, 2008). In terms of the actual evaluation, member states are to perform water quality assessment based on a list of predefined conditions (2000/60/EC Annex V), comprising of biological (e.g. composition and abundance of aquatic flora or benthic invertebrate fauna; referred to as biological quality elements or BQEs), hydromorphological (e.g. hydrological regime, morphological conditions) and physicochemical elements (e.g. thermal conditions, nutrient conditions).

1.2. Biological water quality evaluation

Much like smoke is a tell-tale sign of fire, the appearance and abundance of certain biota is mostly influenced by the ecological quality of their environment. Using these organisms to evaluate this quality is commonly referred to as biomonitoring. Historically, biomonitoring (or at least the fundamentals) of surface waters started as early as the 1850s, when scientists observed different organisms occurring in clean water opposed to polluted water (De Pauw & Vanhooren, 1983), while surface water quality assessment based on actual biological indicators

began in Germany at the end of the 19th century (Metcalf, 1989). To date, many different methods for biological water quality evaluation have been developed.

At the beginning of the 20th century, Kolkwitz & Marsson (1908) developed a saprobity system, describing how contamination of water by organic matter led to changes in the biological composition of the water body (Descy & Micha, 1988). This system formed the basis for Slàdeček's work in biotic evaluation of saprobity (Slàdeček, 1973; Slàdeček, 1986). Later, more systems were introduced, all pointing to the idea that water pollution can have important effects on aquatic communities such as changes in the composition, elimination of sensitive species and replacing them by tolerant ones, reducing the number of species and/or individuals per species and changes in the relative proportions of species within the community (Descy & Micha, 1988; Hawkes, 1979).

The basic principle for all quality monitoring systems is supported by the hypothesis that every aquatic organism exhibits specific preferences for almost any given environmental variable. A combined assessment of these preferences provides an indication of the overall quality condition of the environment these organisms are living in. For practical use, this ecological assessment was translated in the development of water quality indices (Descy & Micha, 1988). The rationale behind such biotic indices is simply the monitoring by a set of metrics representing community structure (e.g. taxa richness, relative abundance), tolerance or sensitivity to pollution, life history strategies, density, etc., to gain insight in how a given community responds to environmental changes (Klemm et al., 2003; Metcalf, 1989). A downside to the story of taxonomy-based biomonitoring is the time and knowledge required to carry out such tasks and this approach may well be overtaken by environmental DNA metabarcoding for biological monitoring in the future (Pawłowski et al., 2018; Uchida et al., 2020; Vasselon et al., 2017).

Within the Water Framework Directive, several groups of organisms were selected as bio-indicators for monitoring the water quality. Among them are benthic algae such as diatoms, as well as macroinvertebrates; both groups will be used in this thesis.

1.3. Biological quality elements

1.3.1. Diatoms (Bacillariophyceae)

Diatoms are a group of highly diverse unicellular algae encompassing more than 100 000 taxa (Mann & Droop, 1996). They are found in virtually all aquatic and moist terrestrial habitats

(Medlin, 2016; Round et al., 1990) and play a major role in all aquatic ecosystems (Dugdale & Wilkerson, 1998; Falkowski et al., 2004).

Diatoms are characterized by their unique cell wall, called frustule, made of polymerized silica (SiO₂) (Round et al., 1990). Every frustule is composed of two valves, kept together with a series of narrow bands, called the girdle (Round et al., 1990; Zurzolo & Bowler, 2001). Based on their overall shape and symmetry, diatoms can roughly be separated into radial centrics, polar centrics and pennates (Kröger & Poulsen, 2008; Round et al., 1990). The valve surface shows a distinct morphological ornamentation that allows identification of the species. Generally, diatoms are used in a wide variety of applications (Smol & Stoermer, 2010), ranging from archaeological and palaeoecological research (Li et al., 2010; Stone et al., 2011) to oil and gas exploration (Bentaalla-Kaced et al., 2017), forensic science (Piette & De Letter, 2006), the use of diatomaceous earth as building or filtration material (Smol & Stoermer, 2010), or even to produce microalgal-derived biofuels (Pienkos & Darzins, 2009).

Diatoms are distributed worldwide and found virtually anywhere water is available (Mann & Droop, 1996). As they show very specific preferences for a wide range of environmental parameters (such as pH, salinity or nutrients), they are considered excellent bio-indicators. They can rapidly shift their community composition as a response to environmental changes (Passy, 2007; Potapova et al., 2004; van Dam et al., 1994; Weckström & Juggins, 2006). Diatoms have been shown to be sensitive to eutrophication and acidification, metal and pesticide pollution, the introduction of invasive species and other anthropogenic stressors (Battarbee et al., 2001; Corcoll et al., 2012; Coste & Ector, 2000; Kelly & Whitton, 1995; Morin et al., 2012; Rott et al., 1998).

This environmental response can be evaluated in two ways, on one hand assessing the autecological conditions of a sample and on the other hand, developing indices that quantify the water quality based on the diatom composition.

The first approach derives a set of environmental conditions from the observed species composition in combination with their specific preferences for a certain parameter (Bahls, 2009; Desrosiers et al., 2013; Fore & Grafe, 2002; Kociolek, 2005; van Dam et al., 1994), a technique often applied in palaeoecological research (Bottjer, 2016; De Wolf, 1982; Denys & Lodewijckx, 1984; Stone et al., 2011; Witkowski et al., 2009). Simply put, using a diatom's 'lifestyle' in combination with that of other diatoms in an assemblage, a lot of information can be derived with regard to the site's ecology. As this is often regionally determined (due to the

often restricted biogeographical distribution of diatoms), region-bound lists were published in the last decades, an often time-consuming activity requiring an extensive amount of preparatory taxonomic and ecological work (Bahls, 2009; Kociolek, 2005, 2006).

For the Low Countries (Flanders & The Netherlands), such a list was assembled (and continuously updated) by van Dam et al. (1994), encompassing attributes such as pH, salinity oxygen requirements, saprobity and trophic state. For each of these ecological indicator values, a set of classes are distinguished for which each taxon is assigned a class value. The full classification according to van Dam et al. (1994) is available in Appendix 1.

For the second approach, a number of diatom-based indices have continuously been developed and improved since the early 1980s to quantify the ecological status of a given water body (Coste, 1982; Kelly, 1998; Kelly & Whitton, 1995; Prygiel et al., 1996; Sládeček, 1986), in terms of acidity, salinity, nitrogen uptake metabolism, oxygen requirements, saprobity, trophic state and moisture requirements (van Dam et al., 1994). Most of these indices are based on the weighted average equation of Zelinka & Marvan (1961):

$$\text{WMS} = \frac{\sum_{j=1}^n a_j v_j i_j}{\sum_{j=1}^n a_j v_j}$$

in which the weighted mean score (WMS) is calculated using a_j as the proportionate abundance of species j in a given sample, v_j as an indicator value and i_j the pollution sensitivity of species j . The indices differ in the number of species that is taken into consideration for the calculation of the index. Also the corresponding indicator and pollution sensitivity values are incorporated, which vary with respect to the pollutant or stressor under investigation. This eventually leads to differences in the obtained quality values.

Based on previous work (e.g. Besse-Lototskaya et al., 2011), several indices proved to be more accurate than others. Hence, a selection was made for this thesis: Specific Polluosensitivity Index (IPS/SPI; Coste in Cemagref (1982)), the Trophic Diatom Index (TDI; Kelly & Whitton (1995)) and the Diatom Biological Index (IBD; Lenoir & Coste (1996)).

- **Indice de Polluosensibilité Spécifique or Specific Polluosensitivity Index (IPS/SPI)**

The Specific Polluosensitivity Index was established by Cemagref (1982) and continuously updated ever since. As the index takes into account more than 2000 diatom taxa, it has an

important advantage over other indices using only a tiny fraction (less than 250 taxa) of this species database (EauFrance, 1994; Prygiel & Coste, 1995), since the obtained water quality estimate will be based on the entire community and not on a small portion of the diatoms present in the sample. On the other hand, the use of this index will require the identification up to species level of all encountered diatoms, which can be a time-consuming and not always simple achievement. Another strong point of this index is that it integrates organic pollution (expressed as biological oxygen demand (BOD), chemical oxygen demand (COD) or ammonia (NH_4^+)), salinity (expressed as conductivity and chlorides), and eutrophication (expressed as either chlorophyll levels or phosphate levels) in its species values providing a more complete assessment of the water quality (Prygiel & Coste, 1993, 1995).

IPS values can be calculated using the same procedure as shown for Zelinka & Marvan's (1961) WMS, with species abundance a_j of species j and the modified values for v_j and i_j ; the indicative ecological amplitudes and species sensitivities, respectively. These calculations result in IPS values ranging from 1 (very low) to 5 (very high water quality), after which these values can be transformed to values on 20 to facilitate comparison with other indices. Based on the 1-20 score, five quality classes are distinguished: $IPS \geq 16$ indicating no pollution or little eutrophication, $16 > IPS \geq 13.5$ a moderate level of eutrophication, $13.5 > IPS \geq 11$ as a sign of moderate pollution or strong eutrophication, $11 > IPS \geq 7$ indicating a high level pollution and $IPS < 7$ a very high level of pollution (Prygiel et al., 1996).

- **Trophic Diatom Index (TDI)**

The Trophic Diatom Index (Kelly & Whitton, 1995) was developed in response to the Urban Wastewater Treatment Directive of the European Community. It is used to monitor the trophic status of rivers based on diatom composition. Initially, the TDI used a simplified taxa list to deal with the limitations of taxonomy-heavy indices. Nowadays, the TDI is calculated using approx. 700 diatom taxa, sacrificing some taxonomic resolution compared to IPS (Kelly et al., 2008; Kelly & Yallop, 2012). If the index is used in samples free of organic pollution, TDI is highly correlated with aqueous P (phosphorous). However, when other pollutants are present and when inorganic nutrient levels are high (i.e. P is no longer the limiting nutrient), the TDI's performance may be reduced. In case of heavy organic pollution, separating eutrophication from other effects becomes increasingly difficult. To overcome this limitation, Kelly & Whitton (1995) proposed the use of pollution-tolerant taxa (i.e. the fraction of diatoms that tolerate organic pollution) as an indication of TDI reliability for estimating eutrophication.

Later, this criterion was replaced with the percentage of valves belonging to motile taxa to account for organic pollution (Kelly et al., 2001). Additionally, centric diatoms are omitted from TDI computations, along with some modifications to certain sensitivity values (Kelly, 1998; Lecoïnte et al., 2008).

As is the case for other diatom indices, computation of TDI is based on the WMS of Zelinka & Marvan (1961). Using the latter with a_j as the abundance of species j (as a proportion), v_j as an indicator value (ranging from 1 to 3) and i_j as the pollution sensitivity of species j (ranging from 1 to 5), the TDI can be calculated. After a conversion to a scale on 100, TDI scores indicate very low nutrient concentrations (TDI = 0; clean water) to very high nutrient concentrations (TDI = 100; grossly polluted water (Kelly et al., 2008; Kelly, 1998).

- **Indice Biologique Diatomées or Diatom Biological Index (IBD)**

Lastly, the Diatom Biological Index (IBD) is France's national index and is continuously updated to include the latest taxonomic and ecological diatom information. It is based on an updated list of over 800 diatom species and integrates a series of chemical (BOD, COD, NH_4^+ , nitrate (NO_3^-), nitrite (NO_2^-), total Kjeldahl nitrogen (TKN), P, phosphate (PO_4^{3-}), chlorides) and physical (pH, temperature, conductivity) parameters (AFNOR, 2000; Coste et al., 2009). The IBD is accompanied by taxonomic notes and light microscope images to facilitate identification of key species, which improves ease-of-use. Because of the increasing importance of tropical invasive species in the French hydrosystem, these are included in the IBD along with their respective 'native' ecological profiles (Coste et al., 2009). The latter is still a subject of debate, as diatom community structure is largely influenced by ecoregional parameters (Pan et al., 2000). This could present limitations to the IBD's interpretation, as a tropical species could indicate 'good water quality' in their native areas, which is not necessarily the case in non-tropical regions (Coste et al., 2009).

The basic principle of Zelinka & Marvan's WMS (1961) is also used for the calculation of IBD scores, see Coste et al. (2009). After calculation, IBD values range from 1 (very poor water quality) to 20 (very good water quality) (Lecoïnte et al., 1993; Prygiel et al., 2002).

1.3.2. *Macroinvertebrates*

Macroinvertebrates are aquatic and often bottom-dwelling organisms that are visible to the naked eye (de Paiva Magalhães et al., 2015). They are found in freshwater environments thriving in and on the sediment (benthic), in or between macrophytes or swimming around in

the water column (De Pauw & Vannevel, 1991; Sekiranda et al., 2004). Naturally, the different habitats found in a freshwater environment imply a wide variety of ecological niches and strategies.

Benthic invertebrate fauna consists of a wide variety of taxa with each their own preferred habitat and environmental conditions. They have been shown to respond to changes in stream ecosystems on a taxonomic, morphological, trophic and physiological level (Klemm et al., 2003). Macroinvertebrates have become widely used in water quality assessment because of their responsiveness to environmental changes, as well as their ubiquity, well-known taxonomy, ease of collection and their role in key ecosystem processes (Friberg et al., 2011; Wallace & Webster, 1996). Furthermore, an additional advantage of using macroinvertebrates over chemical assessments is that organisms integrate water quality over a period of time, rather than being a snapshot of a given environmental quality (De Pauw & Vanhooren, 1983). However, water quality assessment based on macroinvertebrates is also limited in a couple of aspects. For instance, many macroinvertebrates display complex life cycles that are prone to seasonality, meaning that some invertebrates may not be found at some times of the year (De Pauw et al., 2006; Šporka et al., 2006). Additionally, the distribution and community composition of these organisms (as well as diatoms) is also affected by variables that do not necessarily affect water quality. Such metrics include the current velocity of the stream, the available substrate, microhabitats and their geographic distribution (Collier, 1995; De Pauw et al., 2006).

To comply with the requirements set out by the WFD, the Multimetric Macroinvertebrate Index Flanders (MMIF; Gabriels et al. (2010)) was developed. It provides a general assessment of the ecological quality in Flemish rivers and lakes and quantifies the level of ecological deterioration based on a variety of natural and anthropogenic stressors. The MMIF is a type-specific index, i.e. its calculation depends on the type of river (or lake) a sampling site belongs to (Gabriels et al., 2010). For this purpose, Jochems et al. (2002) listed all waterbody categories in Flanders and created a typology according to the WFD requirements, of which system B is used in calculating the MMIF (see WFD Annex II 1.2.1. Rivers). This typology is based on physical and chemical factors that are expected to determine biological population structure and composition for Flemish river systems (see Jochems et al., 2002). The calculation of the MMIF is also presented here for the purpose of consistency and completeness, after which it is briefly mentioned in materials and methods. The index itself is made up of five individual metrics: taxa richness (TAX), number of Ephemeroptera, Plecoptera

and Trichoptera (EPT), number of other sensitive taxa (NST), Shannon-Wiener diversity index (SWD) and mean tolerance score (MTS). Furthermore, tolerance scores are assigned to each taxon, ranging from 1 to 10 (see Appendix 2): Low scores indicate pollution tolerant taxa, while high scores signify pollution sensitive taxa (De Pauw & Vanhooren, 1983; Gabriels et al., 2010). These scores are required to calculate two of the MMIF metrics (NST and MTS), while the other metrics (TAX, EPT, SWD) are based on the raw macroinvertebrate count data. Metrics such as taxa richness and number of Ephemeroptera, Plecoptera and Trichoptera are self-explanatory and not elaborated here. However, NST, SWD and MTS require some additional clarification.

The NST metric is based on the tolerance scores previously assigned to all identified taxa. It comprises the number of taxa with a tolerance score of 5 or higher, excluding all EPT (Gabriels et al., 2010). Next, the SWD index H' is obtained by calculating the proportion of species i relative to the total number of species in the sample p_i , after which it is multiplied by the natural logarithm of said proportion $\ln p_i$. Simply put, the Shannon index calculates the contribution of each species to the total number of individuals, which is calculated for each species in a given sample, after which the negative sum is calculated (Begon et al., 2006; Shannon, 1948):

$$\text{diversity, } H' = - \sum_{i=1}^s p_i \ln p_i$$

Lastly, the MTS is calculated by adding all tolerance scores for every taxon found and dividing this number by the total number of taxa in the sample (TAX).

In summary, the MMIF comprises of taxonomy-based metrics (i.e. species richness, diversity; TAX, SWD) and autecology-based metrics (i.e. metrics that capture sensitivity to disturbances; MTS, EPT), with NST being a combination of both categories (Birk et al., 2012; Gabriels et al., 2010). As the MMIF combines several metrics into a single evaluation, it integrates several aspects of ecosystem functioning and ecological integrity, which also tends to enhance reliability and robustness of the index. Namely, in case a specific metric was not measured accurately, or in case of accidental outliers, other metrics may still be able to smooth out the end result to some extent (Gabriels et al., 2010).

However, as mentioned by Pawlowski et al. (2018), low taxonomic resolution at the level of family or genus may limit assessing the degree of degradation or its causality, especially in environments where multiple stressors are apparent. Even though a lower taxonomic resolution

may prove to be more practical, it may also pose some challenges in relating lower index values to the actual root of the problem. For instance, F. Chironomidae encompasses a large number of genera and species. Because these can exhibit subtler differences in ecological quality of the stream, information may be lost when this group is identified at family level (Waite et al., 2004).

1.4. Metals and metal pollution

Metals and metalloids (e.g. arsenic) are among the most widespread types of pollutants as a result of the technical revolution and metallurgy, although they can also originate from natural phenomena such as rock weathering and volcanic eruptions (Palma et al., 2015; Shikhova, 2017). In terms of human activity and emissions into water, mining and industry are among the biggest point sources of metals released into the environment, though metals can also stem from diffuse sources such as atmospheric deposition, wearing of tires and municipal wastewater (Nordberg et al., 2015).

Metals are characterized by their persistency in the environment, still showing elevated concentrations in soils long after the initial release was halted or decreased (De Jonge et al., 2008; Groenendijk et al., 1999a, 1999b). Even though some metals, such as iron (Fe), zinc (Zn) and copper (Cu) are essential in certain metabolic processes, they are frequently found to be toxic to virtually all lifeforms once concentrations exceed limits within which organisms can safely metabolize the compound (Sarkar, 2002). Other metals such as cadmium (Cd) and lead (Pb), may display toxic side effects even at very low concentrations (Nordberg et al., 2015). Accumulation of metals is a dynamic process in aquatic ecosystems that is a subject of time and characterized by intensity and specificity of a toxicant (Zaikov et al., 2017). The intensity of metal accumulation is determined by its concentration in the environment, while its specificity is related to the metal's interactivity with membranes and its affinity with substrates or (intra)cellular components (Hare, 1992; Zaikov et al., 2017).

An important aspect of metal toxicity in the aquatic environment is their resistance to biodegradation, which may lead to bioaccumulation and biomagnification within the ecosystem (Palma et al., 2015). Furthermore, metal bioaccumulation is also a function of bioavailability, which in turn is determined by biotic (e.g. exchange surfaces, feeding strategies, competition for binding sites) and abiotic factors (e.g. pH, temperature, complexation) (Bervoets & Blust, 2003; Stockdale et al., 2010; Wu et al., 2016).

1.4.1. Metals and diatoms

Studies in metal-polluted rivers have shown that diatoms respond in two ways: at the community level with changes in diversity and at the individual level with changes in the morphology of their frustules (De Jonge et al., 2008; Ferreira da Silva et al., 2009; Luís et al., 2009). Metal pollution can provoke the formation of teratogenic valves with modifications in the general shape and ornamentation of the valves as a result of altered diatom metabolism (Medley & Clements, 1998; Morin et al., 2008, 2012). Such frustule deformations include abnormal valve outlines, irregular striation patterns, unusual raphe systems and overall size reductions due to faults or unfavourable modifications during reproductive processes (Falasco et al., 2009; Ferreira da Silva et al., 2009). Although these deformations are rather obvious in diatom communities of metal-polluted water bodies, they are usually not taken into account in most diatom indices.

1.4.2. Metals and macroinvertebrates

Most macroinvertebrates are net accumulators of trace metals – whether essential or not –, necessitating detoxification of metals, e.g. via excretion or storage in the organism (Rainbow, 2002). The rates at which metals are accumulated and the threshold at which toxicity occurs varies between species and functional feeding groups, with shredders-scrapers that feed on biofilm generally showing the largest concentrations of metals (Farag et al., 1998; Rainbow & Luoma, 2011).

At the community level, when comparing pristine river courses with highly polluted sites, macroinvertebrates show strong shifts in their community composition. A study in the Upper Arkansas River Basin showed reference sites (not significantly metal-polluted) dominated by mayflies (O. Ephemeroptera), while moderately polluted sites showed high numbers of caddisflies (O. Trichoptera) and high abundances for chironomids (F. Chironomidae) in highly polluted sites. However, these responses were complicated by natural seasonal changes in macroinvertebrate assemblages (Clements, 1994). Other research confirms that many (not all – a continuum of sensitivities can still exist within each order) families of Ephemeroptera, Trichoptera as well as Plecoptera display metal sensitivity (Beasley & Kneale, 2003). Such shifts are the consequence of interspecific differences in sensitivity to metals (due to differences in physiology or detoxification mechanisms), resulting in population-level effects that culminate in assemblage shifts from a sensitive to a (more) metal-tolerant community (Cid et al., 2010; Luoma & Rainbow, 2005; Schmidt et al., 2010). Often, Ephemeroptera,

Trichoptera and Plecoptera are considered to be sensitive to metals, making room for metal-tolerant taxa (e.g. F. Chironomidae) when environmental concentrations increase (Beltman et al., 1999; Clements, 1994). Furthermore, macroinvertebrates have been shown to develop some degree of adaptation to chronic metal exposure, complicating the interpretation of species and community responses to metal contamination (Groenendijk et al., 1999a; Loria et al., 2019; Postma & Groenendijk, 1999). Interestingly, recent research has shown an indication for species with lower migration rates to show an adaptive response more quickly, implying an interspecific adaptational difference (Weigand et al., 2018). Additionally, small populations tend to be more vulnerable to (local) extinctions due to demographic and environmental stochasticity, limiting their chances of overcoming and surviving the toxic conditions (Loria et al., 2019; Weigand et al., 2018).

1.5. Rationale & objectives

In 2006-2007, a first comparative study was performed on the Dommel. The response of diatoms and macroinvertebrates was evaluated with respect to the impact of historical metal contamination of the river. The present study continues this previous research, published by De Jonge et al. (2008), on the effects of historical metallurgic activity on the Dommel. This activity led to increased concentrations of metals in sediments such as Cd and Zn. It begs the question whether these increased concentrations are still distinguishable and whether these have an effect on either diatom or macroinvertebrate communities today. Given the recent changes in diatom taxonomy and the measures taken under WFD regulation, it is important to evaluate whether these changes have an effect on present-day water quality.

The central question in this dissertation is: “Does the historical pollution of the Dommel still affect diatom and macroinvertebrate communities in the river today? And, by extension, how does this translate into the river’s water quality?” In search of answers, the following hypotheses need to be tested.

- Sites downstream of the Eindergatloop – the tributary that connects the Dommel to the point source of metal contamination – are expected to show elevated metal concentrations (Cd and Zn, particularly) in sediment and dissolved in water. Likewise, metals in macroinvertebrates are expected to show elevated concentrations in downstream sites, while diatoms are hypothesized to show more teratological forms.
- Based on De Jonge’s research, diatom community composition is assumed to better reflect the decrease in water quality from the metal pollution source than macroinvertebrate communities. It is hypothesized that diatom community assemblages will shift to a more tolerant community more clearly than macroinvertebrates.
- More distinct differences in diatom indices between sites up- and downstream of the Eindergatloop are expected, compared to the macroinvertebrate-based MMIF.
- Because of the large time interval between sampling campaigns, the ‘seasonal’ effect of sampling is also taken into consideration. Riverine systems are highly dynamic, so it is expected that this variation will contribute to differences between sampling campaigns. It remains to be investigated to what degree this variation also has an effect on metal concentrations or index scores.
- As a result of improvements of the Dommel’s physicochemistry over the past decade, we expect an increase of its ecological quality compared to De Jonge (2008).

2. Materials & Methods

2.1. Study area

The Dommel is a lowland river, situated in the north-eastern part of Belgium (BE) and the southern parts of The Netherlands (NL). Only 35 km of its total 120 km length is located in the Belgian province of Limburg (Bleeker & van Gestel, 2007; Waterschap De Dommel, 2020). The river, part of the Meuse basin, originates on the Kempens Plateau in Peer (BE) and runs northward via Pelt (BE) to 's Hertogenbosch (NL), where it merges with the Aa to form the Dieze, one of the many tributaries of the Meuse (Fig. 1) (CIW, 2016; Waterschap De Dommel, 2020). The Dommel is characterized by a sandy river bed (containing a small fraction of clay), a width of 5-7 m, a depth ranging from 0.4 to 1.5 m, an irregular current velocity varying between 0.3 and 0.8 m s⁻¹ and neutral waters with a naturally high iron (Fe) content (Postma & Groenendijk, 1999; VMM, 2020), the latter originating from the Fe-rich clay minerals in the soil (Herr et al., 2014). The river is mainly fed by rainwater and seepage flowing into the Dommel through a network of tributary streams and ditches (Groenendijk et al., 1998; Waterschap De Dommel, 2020). This network runs through a mosaic of grasslands, agricultural fields, forests, suburban and industrial areas from which runoff is discharged into the river, leading to direct (e.g. increased nutrient levels) and indirect effects (e.g. sharp decreases in oxygen content) on its water quality (CIW, 2016; Herr et al., 2014). The intensive agriculture (which changed their activity from dairy to intensive livestock farming in the 1970s), the dense population (approx. 600 000 people in the entire Dommel) and the multiple wastewater treatment plants, resulted in an increased amount of dissolved elements in surface- and groundwater (CIW, 2016; Petelet-Giraud et al., 2009; VMM, 2014). More information on industrial activity and wastewater treatment plants in the study area can be found in Appendix 3A.

The Dommel river is characterized by high metal concentrations due to historical and prevailing metallurgic activity. Since 1888, a nearby zinc smelter on the banks of the Eindergatloop (a tributary of the Dommel) has been discharging their effluent into the river (Groenendijk et al., 1999a, 1999b; Waterschap De Dommel, 2019). This zinc factory is licensed to discharge high concentrations of zinc, chlorides and sulfates (among others) which – in combination with the historical contamination – resulted in significant ecological pressure on the aquatic fauna and flora (Waterschap De Dommel, 2019). Because of this historical contamination, part of the river (starting from the merge of the Eindergatloop with the Dommel

up to the Dutch-Belgian border) was dredged within the context of contaminant remediation (De Jonge et al., 2012).

Finally, in terms of WFD classification, the Dommel is categorized as ‘Grote Beek Kempen’ (or ‘Large Brook Kempen’) and abbreviated to ‘BgK’ (Maarten De Jonge et al., 2008; Jochems et al., 2002).

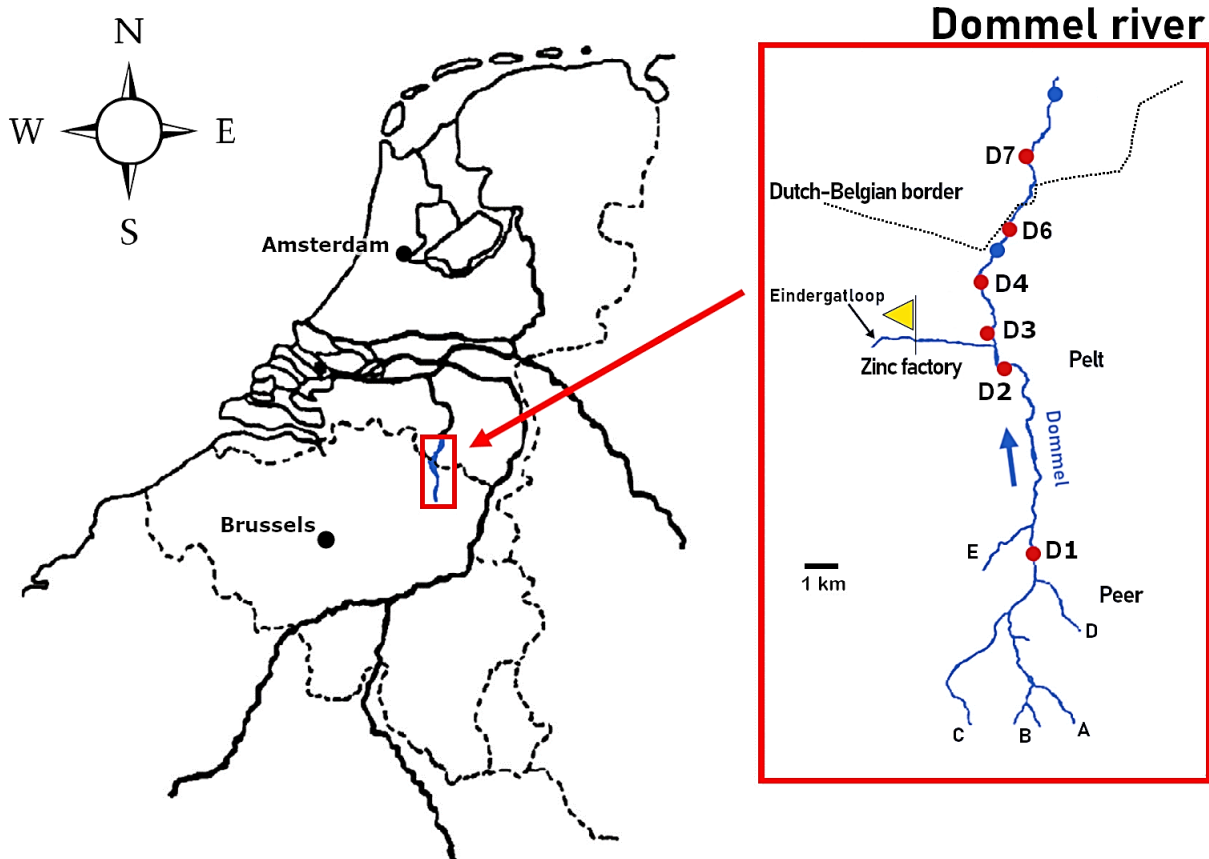


Figure 1: Map of study area. Enlarged view of the Dommel river investigated in the present study (red box), situated on the border of Belgium and The Netherlands, with measuring sites shown in red (D1 to D7). Yellow flag indicates location of zinc factory discharging into the Eindergatloop. Letters indicate tributaries of the Dommel (excl. Eindergatloop): Heidelossing (A), Kleinbeek (B), Bollisenbeek (C), Peerderloop (D) and Molenloop (E). Blue arrow illustrates stream direction. Blue dots indicate additional sites (D5, D8) used in De Jonge et al. (2008). Map adapted from Postma & Groenendijk (1999) and De Jonge et al. (2008). See Appendix 3 for more information on the study area and sites.

A total of six sampling points (D1, D2, D3, D4, D6 & D7), situated between Pelt (BE) and Valkenswaard (NL) – a few kilometres across the Belgian border – were selected for the present study, based on previous work by De Jonge et al. (2008). Additional information on these sampling locations can be found in Figure 1 and Appendix 3B. Previously, these sites were selected based on accessibility and for being part of a larger Flemish network of monitoring locations regularly evaluated by VMM (Flanders Environment Agency). Because of the known point source of contamination (the zinc factory), the sampling points located upstream of the

merge with the Eindergatloop (D1 & D2) are considered as reference sites and are located 8.25 and 1.20 km upstream, in that order. The other sites (D3, D4, D6 & D7; D5 and D8 were used in De Jonge et al. (2008) but were omitted here) are located downstream of the merge at approximately 0.20, 2.10, 4.40 and 7.60 km downstream, respectively. In total, three sampling campaigns were performed: 17 April 2019 (A), 21 August 2019 (B) and 24 January 2020 (C).

2.2. Physicochemical characterization of water

For each sampling campaign, a thoroughly pre-washed 10 L bucket (MQ, EMD Millipore, Billerica, USA) was rinsed several times with river water, after which new river water was collected and brought to the river bank. Temperature ($^{\circ}\text{C}$), acidity (pH), oxygen saturation ($\% \text{O}_2$), dissolved oxygen (mg/L) and electrical conductivity (EC; $\mu\text{S}/\text{cm}$) were measured in situ using a handheld multimeter (MultiLine P4, WTW GmbH, Germany). Water samples were collected from the river using three 50 mL polypropylene (PP) tubes (3×6 tubes) and stored in a portable cooling unit for further physico-chemical analysis. Two of these samples were destined for nutrient analysis while the remaining tube was used for metal analysis.

Water samples were analysed for NH_4^+ , NO_2^- , NO_3^- , PO_4^{3-} , sulphate (SO_4^{2-}) and chloride (Cl^-) concentrations using a SAN++ Continuous Flow Analyzer (Skalar Analytical B.V., The Netherlands). The analysis was preceded by filtration ($0.2 \mu\text{m}$ mesh) and acidification (0.002 mL HCl (37%) per mL sample) of the water samples used specifically for analysis of $\text{PO}_4^{3-}\text{-P}$, SO_4^{2-} and Cl^- .

For metal analysis, subsamples were created in 14 mL PP tubes from the remaining set of 50 mL samples (one for each sampling location); one series of filtered (Chromafil Xtra PES-20/25; $0.20 \mu\text{m}$ pore size, 25 mm diameter) and one series of unfiltered subsamples, both including a technical blank using MQ. Next, subsamples were acidified by adding 0.015 mL highly purified HNO_3 (69%; Nitric Acid – TraceMetal™ Grade, Fischer Scientific UK Ltd., UK) per mL sample and stored in a freezer at -20°C until further analysis.

2.3. Sampling and preparation of sediment

In January 2020 (campaign C), sediment was collected at each measuring site. Three randomly selected locations at each site were sampled to account for within-sample variation. Sediment was collected using a hand line-operated grab sampler (235 cm^3 , Petite Ponar, Wildco, USA). Next, sediment was sieved (mesh size of $1 \mu\text{m}$) to remove rocks and large organic material as well as homogenization of the samples. Finally, samples were collected in 50 mL PP tubes;

prior to further analysis, these samples were stored at -20°C. Sediment samples were defrosted in a water bath (25°C) for approximately 60 min. Following another step of homogenization (by means of shaking), sterile 10 mL pipette tips were used to scoop and transfer approximately 3 mL sediment to 14 mL PP tubes. Three reference samples (320 R Channel Sediment, European Union, Belgium) were also added using antistatic micro-scoops (140 mm, VWR International, USA), as well as three technical blanks. Following drying (96 hours, 60°C) and cooling down in a desiccator (2 hours), approximately 100 mg was weighed (Mettler AT261 DeltaRange, 0.0001g) using polystyrene weighing boats and transferred to a series of pre-dried 50 mL PP tubes. Subsequently, the samples were digested at room temperature (12 hours) by addition of 3 mL aqua regia (3 parts 37% HCl, 1 part 69% HNO₃). Next, sediment samples were digested in a hot block for 60 minutes (Environmental Express SC154). After heating, the samples were removed from the hot block and cooled down to approximately room temperature. Then, MQ water was added to the 40 mL mark and stored in a freezer at -20°C until further analysis.

2.4. Metal analysis of water and sediment

Concentrations of aluminium (Al), chromium (Cr), manganese (Mn), iron (Fe), cobalt (Co), (Cu), zinc (Zn), arsenic (As), cadmium (Cd) and lead (Pb) were measured using an inductively coupled plasma mass spectrometer (7700x ICP-MS, Agilent Technologies Inc., USA). Whenever a concentration was measured below the quantification limit (BMQL; Below Method Quantification Limit), all further calculations assumed a value of BMQL/2 for those particular measurements.

2.5. Sampling and identification of diatoms

Benthic diatoms were collected by selecting three equally sized pebbles at each sampling site. Only pebbles submerged in at least 10–15 cm deep water were used. Each pebble was brushed extensively on all sides exposed to light using a single-use toothbrush. The resulting material was stored in a 50 mL polyethylene (PE) square bottle (Graduated Square Bottle Series “600”, Kartell S.p.A. – LABWARE Division, Italy) filled with sparkling water (Wetzel et al., 2013). In case no submerged pebbles were found (D4 & D7), diatom samples were acquired by scraping a hard man-made substrate such as submerged concrete shore walls. While holding a 50 mL PE bottle horizontally and covering the bottle mouth with the thumb (only allowing space for scraped material to enter the container), scraping was performed in upstream direction. Samples were fixed by adding 95% ethanol until further preparation.

For diatom identification, samples were prepared following the method described in van der Werff (1953). Small parts of the samples were cleaned by adding 37% hydrogen peroxide (H₂O₂) (ROTIPURAN[®], Carl Roth GmbH, Germany) and heated to 80°C for about one hour. Here, H₂O₂ was used a strongly oxidizing agent to remove all organic cell contents, while preserving the silica valves, as specified by the European Committee for Standardization (European Standard: EN 13946:2014). The reaction was completed with the addition of saturated KMnO₄. Following digestion and centrifugation (3 × 10 minutes at 3700 rpm, Minicentrifuge CD-0412, Carl Roth GmbH), the resulting cleaned material was diluted with distilled water to avoid excessive concentrations of diatom valves. Cleaned diatom valves were mounted in Naphrax[®] (Brunel Microscopes Ltd., UK) with refractive index >1.6 (EN 13946:2014).

Identification of diatom valves was conducted according to European Standard EN 14407:2014 using an Olympus BX51 microscope equipped with differential interference contrast (Nomarski[®]) optics and an Olympus UC30 digital camera connected to the cellSens Standard Imaging Software (Olympus Belgium S.A./N.V., Belgium). In each sample, 400 diatom valves were identified and enumerated on random transects at x1000 magnification. Broken valves showing an intact central area and appropriate characteristics required for identification are also taken into account (Fig. 2). Taxonomic identification was mainly based on Lange-Bertalot et al. (2017) and several monographies discussing specific genera (see bibliography under *Specific taxonomic literature*). Furthermore, diatom valves exhibiting teratological forms were also enumerated to estimate the presence and magnitude of contaminant-related (e.g. metals) stress (Lavoie et al., 2017).

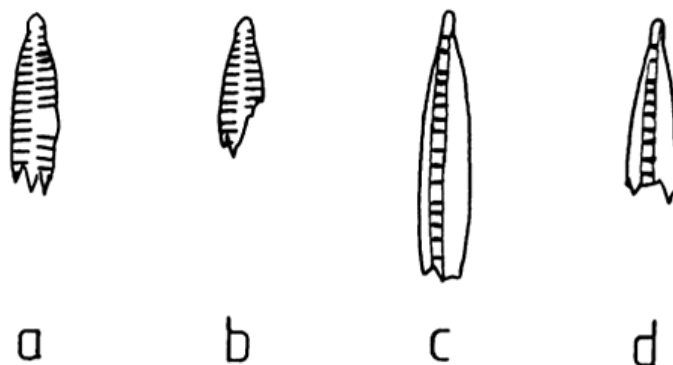


Figure 2: Broken valves showing appropriate characteristics for identification (**a**, **c**) and broken valves without the appropriate characteristics (**b**, **d**). *Fragilaria vaucheriae* with one pole and a central area shown in **a**, meaning it should be included in a count, while **b** shows only a pole and should not be included. *Nitzschia dissipata* does not have an obvious central area; **c** is sufficiently intact to be included as opposed to **d**. From Kelly et al. (2001).

2.6. Collection and classification macroinvertebrates

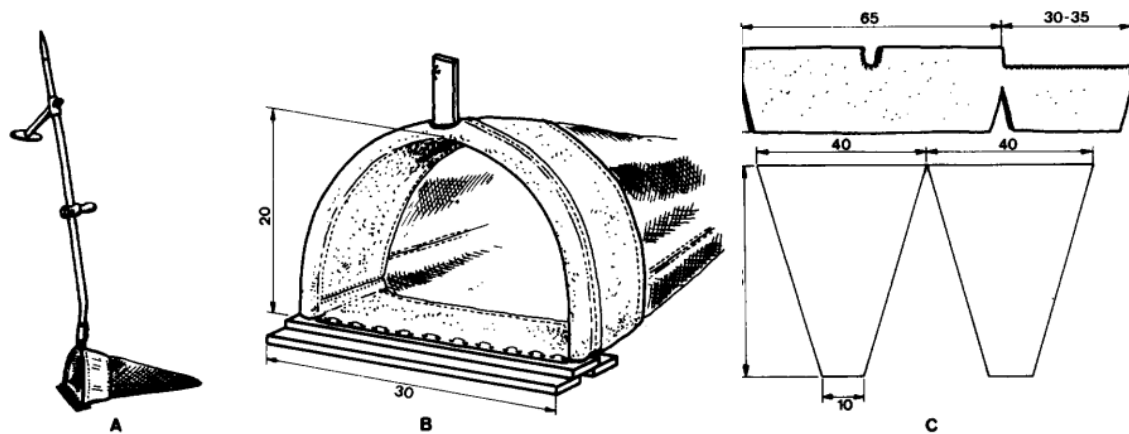


Figure 3: Structure of the standardized handnet, showing an overview of the handnet with handle (A), the metal frame holding the conical net (B) and the design of the net (C). Measurements are presented in cm. Adapted from De Pauw & Vanhooren (1983).

Macroinvertebrates were collected using a handnet following the method described in De Pauw & Vanhooren (1983) and Gabriels et al. (2010). The handnet (Fig. 3) consists of a metal frame of 200 mm by 300 mm to which a conical net is attached (depth of 500 mm with mesh size of 500 μm) with a 1 m shaft fitted to the frame. Using the handnet, a longitudinal stretch of ca. 10 m was sampled during approximately 5 minutes, taking into account all accessible (aquatic) habitats. Additionally, densely vegetated areas and rocks were manually shaken immediately upstream of the net and animals manually picked from stones and other material along the same stretch. The “kicksampling technique” was used to cover the sandy or muddy bed substrate. This technique involves holding the submerged net vertically while avoiding scraping of the river bed, as this may seriously increase the amount of sediment collected in the net (potentially hampering sorting later on). While kicksampling, bottom material is overturned directly upstream of the net by foot or hand (Gabriels et al., 2010). Following a zigzag pattern, the entire 10 m stretch was sampled to maximize diversity with respect to collected macroinvertebrates and their corresponding (micro-)habitats. Before collecting all material caught into pre-rinsed buckets (acid-washed and rinsed with MQ in case of August 2019, thoroughly washed with MQ in case of April 2019 and January 2020), the net was washed in river water to remove excess sediment (and thoroughly washed after sampled material had been collected to prevent contamination between sampling locations). In case of sampling D7 in April 2019 and August 2019, the 10 m stretch was kicksampled more extensively (at the right bank) given part of the river was too deep due to extremely high water levels.

All collected material was thoroughly examined for presence of macroinvertebrates. Upon return to the laboratory, contents of each bucket were emptied in a white sorting tray. Furthermore, in case of excessive amounts of material, samples were subdivided in two or four parts before counting (and counts multiplied accordingly afterwards). Macroinvertebrates were identified using a stereo microscope (Leica S8 APO, Leica Microsystems Belgium BVBA, Belgium) to either family, genus or an intermediate level for all taxa based on taxonomic levels defined by De Pauw & Vanhooren, 1983. All taxonomic identification levels are included in Appendix 2. In August 2019, sorting trays and other re-used pieces of equipment were acid-washed between sorting of different measuring sites to prevent cross-contamination. Specimens of three taxonomic groups were collected separately for metal analysis (see later).

To assess biological water quality, MMIF values were calculated for each sampling location and season, based on five parameters as described by Gabriels et al. (2010); see earlier.

2.7. Metal analysis of macroinvertebrates

Abundance analysis of the macroinvertebrates sampled in April 2019 (campaign A) showed that *Asellus aquaticus* (Ordo Crustacea), *Calopteryx virgo* (Ordo Odonata) and Chironomidae sF. Prodiamesinae (Ordo Diptera) were among the most consistently found taxa along all measuring sites, making them suitable for analysis of endogenous metal concentrations. As such, these three taxa were separated during the sorting procedure of the August 2019 samples. Once separated, each individual was blotted dry using sterile paper and collected in pre-weighed (Mettler AT216 DeltaRange, 0.0001g) and pre-dried Eppendorf tubes (48 hours, 60°C). Three replicates of three live specimens were collected per site and taxon, in addition to three reference samples (SRM-2976, NIST, USA) and three technical blanks and stored in a freezer at -20°C until further analysis.

Upon sample retrieval, wet weights of macroinvertebrates were determined. Subsequently, samples were dried for 48 hours at 60°C and cooled down in a desiccator (2 hours), after which the corresponding dry weights were determined. To verify and enhance accuracy of weight measurements, an additional weighing step was introduced using aluminium cups (VWR Round Weighing Dishes, 0.35 mL) and a precision scale (Sartorius SE2 Ultra-micro balance, 0.01 mg). In terms of weighing accuracy, Eppendorf (polypropylene) tubes may show high levels of variability with respect to their weights (e.g. electrostatic charge), while aluminium cups do not (B. Sloomackers, University of Antwerp, pers. comm.). After collecting all dried and weighed samples in pre-dried 14 mL PP tubes, samples were stored in a desiccator until

further sample preparation for metal analysis. To initiate sample digestion, 0.5 mL HNO₃ (69%) was added to each tube. After 12 hour digestion at room temperature (overnight), samples were placed in a Nalgene safety carrier box (36.8 × 18.4 × 17.0 cm) for microwave heating digestion (Blust et al., 1988). Samples are sequentially heated (3 × 3 min at 100 and 180W) and left to cool down approximately 10 min. Next, 50 µL H₂O₂ (30-32% w/w (Primar-Trace analysis grade), Fischer Scientific UK Limited, UK) was added. After waiting at least 30 min, samples are heated in the microwave (4 × 2 min at 300W), cooled down to approx. room temperature, after which MQ water is added to the 10 mL mark. Then, samples were stored at 8°C until further analysis, which was conducted using an inductively coupled plasma spectrometer (7700x ICP-MS).

2.8. Additional calculations and statistical analysis

2.8.1. Metals in water, in sediment and biota

For statistical analyses, only metal concentrations dissolved in water (filtered) were used (^wM), as total metal concentrations are poorly correlated with toxicity in natural waters and may even overestimate metal toxicity (Adams et al., 2020). Additionally, the Flemish ecological quality standards (VLAREM II) do not include threshold values for total metal concentrations.

Extraction recoveries of metals in sediment were within 15% of the certified values for Mn, Co, Zn and As, while suboptimal recoveries were observed for Al, Cr, Fe, Cd and Pb. At the same time, extraction recoveries for metals in biota were within 15% of the certified values for Mn, Co, Cu, Zn and As, while suboptimal recoveries were observed for Al, Cr, Fe, Cd and Pb. Given the inconsistent measurements for Cr between metals in sediment and metals in biota, this element was corrected according to the respective extraction efficiencies.

2.8.2. Toxic units (TU)

To gain a single and general impression of a sample's potential toxicity, toxic units (TU) can be calculated and compared between sites. The TU were calculated for metals measured in water (dissolved) and biota. For metals dissolved in water, the measured concentrations are divided by the available EQS (VLAREM II; WFD 2008). Only the mean of these TUs is used, which represents the average TU for a given sample. For metals in biota (for each of the three taxa), measured concentrations are divided by the lowest concentration found in each of the taxa. The biota under consideration comprised *Calopteryx virgo*, *Asellus aquaticus* and Chironomidae (sF. Prodiamesinae for all points except non-Prodiamesinae in D6).

2.8.3. *Diatom index calculations & autecology*

Diatom indices were calculated using OMNIDIA (version 5.5, 2014). This software package is designed for evaluation of water quality, management of diatomic inventories and calculation of diatomic indices (Lecointe et al., 1993). Indices used in the present report include IPS, TDI and IBD. Additionally, autecological attributes were calculated based on the updated data in Van Dam et al. (1994) (A.Mertens, Diatomella, pers. comm.) using the 20 most abundant species of each sample and using the most recent list of autecological scores (van Dam et al., 1994). Using ecological information on diatom species, information about the sites' ecology can be derived. This information includes attributes such as pH (R), salinity (H), oxygen requirements (O), saprobity (S) and trophic state (T). For each of these attributes, a weighted mean score is calculated which corresponds to a specific classification for said attribute (see Appendix 1). The score for a specific ecological indicator can be calculated by multiplication of a taxon's abundance N_i in a sample with its indicative class value v_i and calculating a weighted average across all taxa in the sample, with N_{tot} as the total number of valves used for the calculation.

2.8.4. *Multimetric Macroinvertebrate Index Flanders (MMIF)*

The MMIF is calculated using five metrics (see 1.3.2): TAX, EPT, NST, SWD and MTS. Because each metric is described by a different unit, they are rescaled to a score ranging from 0 ('bad ecological quality') to 4 ('high ecological quality'). These scores are based on a set of expert-reviewed reference values for each metric and type of water body; see Appendix 4 for more information (Gabriels et al., 2010). Once all metrics are assigned a score, these values are summed up and divided by 20 to obtain a single index value ranging from 0 (low ecological quality) to 1 (high ecological quality).

2.8.5. *Statistical analysis*

Statistical analyses were carried out in R (R Core Team, 2020). Significances were considered starting at the 95% confidence level ($p < 0.05$). In this report, (1) the differences between sites up- and downstream of the point source of contamination were evaluated, as well as the effect of sampling time (A vs B vs C; further referred to as 'season'). Next, (2) a correlation analysis on all physicochemical variables and all calculated indices was carried out. Lastly, (3) ordination (Principal Component Analysis) was applied to further investigate underlying relationships and to analyse community composition of diatoms and macroinvertebrates.

First, (1) the differences between sites up- and downstream of the putative point source of contamination were assessed. All variables were tested for normality using the Shapiro-Wilk Normality Test and base R diagnostic plots. The assumption of equal variances was evaluated using the F-test. Differences between variables were assessed using unpaired two-sample Student's t-tests or Welch's t-tests (for equal or unequal variances, respectively). Alternatively, non-parametric Mann-Whitney U-tests were conducted, which were also evaluated using t-tests (in case of unequal variances) to minimize erroneous conclusions (Kasuya, 2001). Further, the effect of sampling campaign on these variables was evaluated using a one-way ANOVA approach or Kruskal-Wallis rank sum tests (for normally or non-normally distributed variables, respectively). Post-hoc pairwise comparisons consisted of Tukey's honest significance tests or pairwise Wilcoxon tests (using Bonferroni correction for multiple testing).

For the correlation analysis (2), data included all in situ measurements, nutrient analyses, metal concentrations in water and sediment along with average TUs calculated for metals dissolved in water. To clarify, metals in sediment were only sampled in January 2020, of which the average values were used for all three sampling seasons. Further, all calculated indices were analysed for correlations with all physicochemical variables. Both Pearson and Spearman rank correlations were considered, as some variables showed deviations from normality.

Lastly (3), ordination techniques were used on the physicochemical data of water samples, the macroinvertebrate and diatom counts. Prior to the analysis of the macroinvertebrate and diatom counts, these datasets were screened to remove rare taxa. In case a given taxon was not present with a relative abundance of 2% in at least one sample (in the entire dataset), it was considered 'rare' and omitted from further analysis (Van de Vijver et al., 2004). Following $\log(x + 1)$ transformation (excl. pH) to normalize all three datasets (compressing the high level of variation present in ecological data; McCune & Grace (2002)), Detrended Correspondence Analysis (DCA) was carried out to decide whether a linear or unimodal ordination technique should be used. Because the first DCA axis (total gradient length) of all three datasets < 2 S.D. units, Principal Component Analysis (PCA; a linear unconstrained ordination method) was preferred to investigate underlying gradients of variation (Jongman et al., 1995). These PCAs are modelled for all three datasets in terms of their location from the point source of pollution (upstream vs downstream; 'contamination'), as well as the effect of sampling campaign ('season'). To visualize potential clustering or overlap of samples, polygons (convex hulls) are superimposed on either the 'contamination' or 'season' groupings.

3. Results

3.1. Physicochemical characterization of water and sediment samples

Physicochemical measurements of water and sediment are presented in Appendix 5. General characteristics of water samples are listed in Table 5A. Table 5B and 5C contain metal concentrations measured in water and sediment, respectively. The EQS for ^wCd is determined by CaCO₃ content, which was estimated using VMM data for dissolved Ca²⁺ and Mg²⁺ (Briggs & Ficke, 1977), see Table 5D. Average TU values were calculated *with* and *without* ^wCo. Because Co dissolved in water showed very large TUs (high Co concentrations compared to EQS), average TUs were also calculated *without* Co (TU*).

Table 3: All physicochemical variables measured in water and sediment that were significantly different between upstream (D1, D2) and downstream sites (D3, D4, D6, D7), including significance levels ($\cdot = 0.05 < p < 0.10$; $* = p < 0.05$; $** = p < 0.01$; $*** = p < 0.001$). Colours indicate the sites where the variable was significantly higher: **red** = upstream < downstream; **blue** = upstream > downstream. See Appendix 6 & 7 for more details.

UPSTREAM vs DOWNSTREAM			
\cdot	*	**	***
^w Fe	O ₂	^w Cu	EC
^w Zn	NO ₂ ⁻	^s Cd	SO ₄ ²⁻
^w Cd	NO ₃ ⁻	^s Pb	Cl ⁻
^s Cr	^w TU*		^w As
^s Mn	^s Co		^w Pb
^s Fe			

All variables that showed significant differences between sites upstream and downstream of the point source of pollution are presented in Table 3. In situ variables such as EC, SO₄²⁻ and Cl⁻ were significantly higher in downstream sites, while O₂ content and NO₃⁻ were significantly higher upstream of the Eindergatloop. For metals dissolved in water (^wM), Cu, As and Pb showed significantly higher concentrations in downstream sites. Additionally, TU* resulted in significantly higher values in sites downstream of the point source of pollution. All calculated TUs for each metal (and calculated averages) are presented in Appendix 5E. Finally, metals in sediment (^sM) showed significantly higher concentrations for Cd and Pb in sites downstream of the Eindergatloop. A complete list of the significances can be found in Appendix 6. Boxplots corresponding to all variables tested in sampling campaigns A, B and C are presented in Appendix 7. Bar plots for the variables mentioned above along all six sites are presented in Appendix 8, including an indication of the (available) EQS.

Table 4: In situ measurements and metals in water that were significantly different between campaign A, B and C, including significance levels (* = $p < 0.05$; ** = $p < 0.01$; *** = $p < 0.001$). Next to each variable, coloured letters indicate the sampling campaign in which significantly higher values were measured: **A** = 17/04/2019, **B** = 21/08/2019, **C** = 24/01/2020. See Appendix 9 & 10 for more details.

CAMPAIGN A vs B vs C					
*		**		***	
pH	A	NO ₃ ⁻	AC	Temp.	B
pc.O ₂	AB	Fe	AC	NH ₄ ⁺	AC
PO ₄ ³⁻	C			Al	C
NO ₂ ⁻	AC			Cr	C
Cd	A			Mn	C
TU*	AC			Co	AC
				Zn	AC
				TU	AC

All in situ measurements and metals in water that were significantly different between the three sampling campaigns are presented in Table 4. Most notably, many of these variables showed significantly higher values in campaign A and C. Metals dissolved in water often showed higher values in campaign C as opposed to the other campaigns. Campaign B often showed lower values for these measurements (see Appendix 9 & 10).

3.1.1. Correlation analysis of physicochemistry and metals in water

A correlation matrix for the general physicochemical variables and metals in water (along with average TU and TU*) is shown in Figure 4. Spearman rank correlation was applied due to some deviations from normality. See Appendix 11A for the corresponding correlation coefficients. Furthermore, a Pearson correlation matrix is also provided (see Appendix 11B) along with matching coefficients. Lastly, a Spearman correlation matrix for all variables (physicochemistry of water & sediment, indices) considered in this thesis is presented in 11C.

The correlation matrices are shown with a colour gradient ranging from red (negative correlation) to blue (positive correlation), with darker colours indicating stronger correlations.

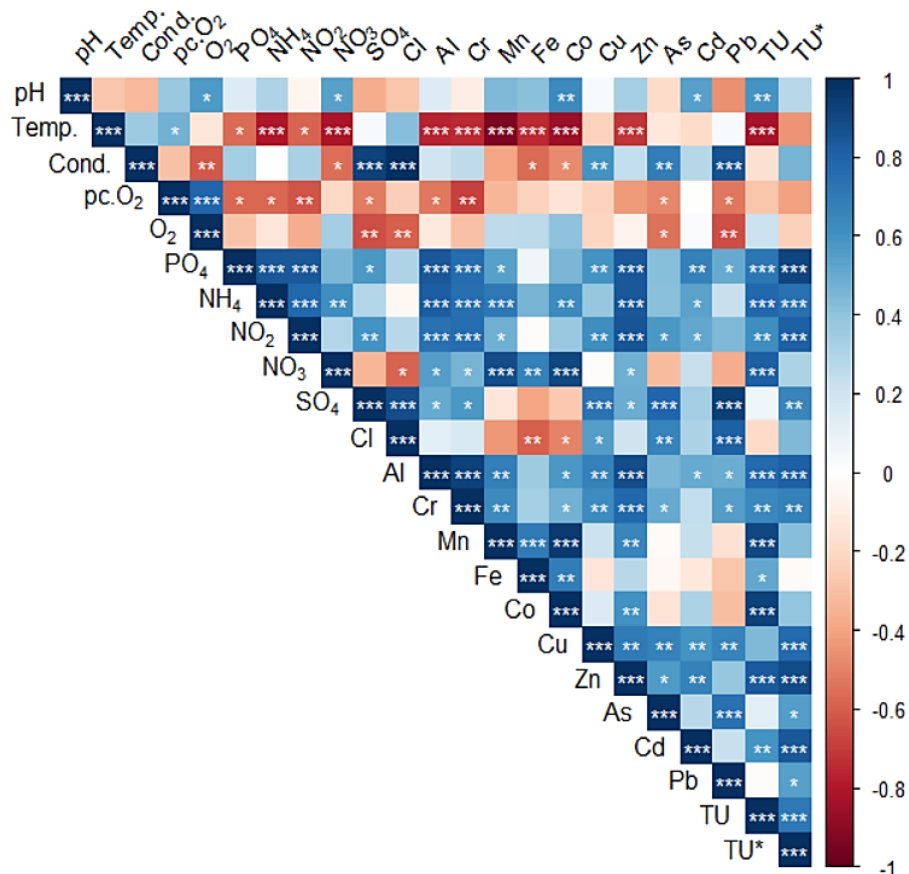


Figure 4: Spearman rank correlation matrix of all physicochemical variables, including metals dissolved in water and corresponding TUs (TU as average TU with ⁶⁰Co, TU* as average TU without ⁶⁰Co). Three significance levels are shown (* = $p < 0.05$; ** = $p < 0.01$; *** = $p < 0.001$). The colour gradient indicates the magnitude and sign (+/-) of a given correlation (blue = positive correlation; red = negative correlation).

3.1.2. Principal Component Analysis of physicochemistry

A PCA graph displaying all in situ measurements and metals dissolved in water is shown in Figure 5, with grouping based on upstream ('up'; blue) versus downstream sites ('down'; red). The PCA clearly separates D1 and D2 from all downstream sites across all three sampling campaigns. The largest separation occurs along the second axis (Dim2), while data points show overlap along the first axis (Dim1). Downstream sites appear to be characterized by higher EC (Cond), Pb, As and Cu, while upstream sites show higher O₂ values.

When data points are grouped according to sampling campaign, a different separation is shown (Appendix 12). Here, campaign B is clearly separated from both A and C, which – among one another – are not separated as strongly. The largest separation occurs along Dim1, while a lot of overlap can be observed with respect to Dim2. Campaign B mainly differs from the other campaigns due to higher water temperature, but also due to lower NO₂⁻ and NO₃⁻ concentrations. Additionally, B and C show separation from B based on higher concentrations for most metals dissolved in water (Cr, Cd, Zn, Al, Mn, Co, Fe).

Based on this dataset, Dim1 is responsible for explaining 45.1% of variation, while Dim2 is assigned 31.9%. More information on the contributing variables and explanatory power of the other principal components can be found in Appendix 12. Additionally, PCA diagrams and supporting graphs where physicochemistry and metals dissolved in water are presented separately can be found in Appendix 13-14.

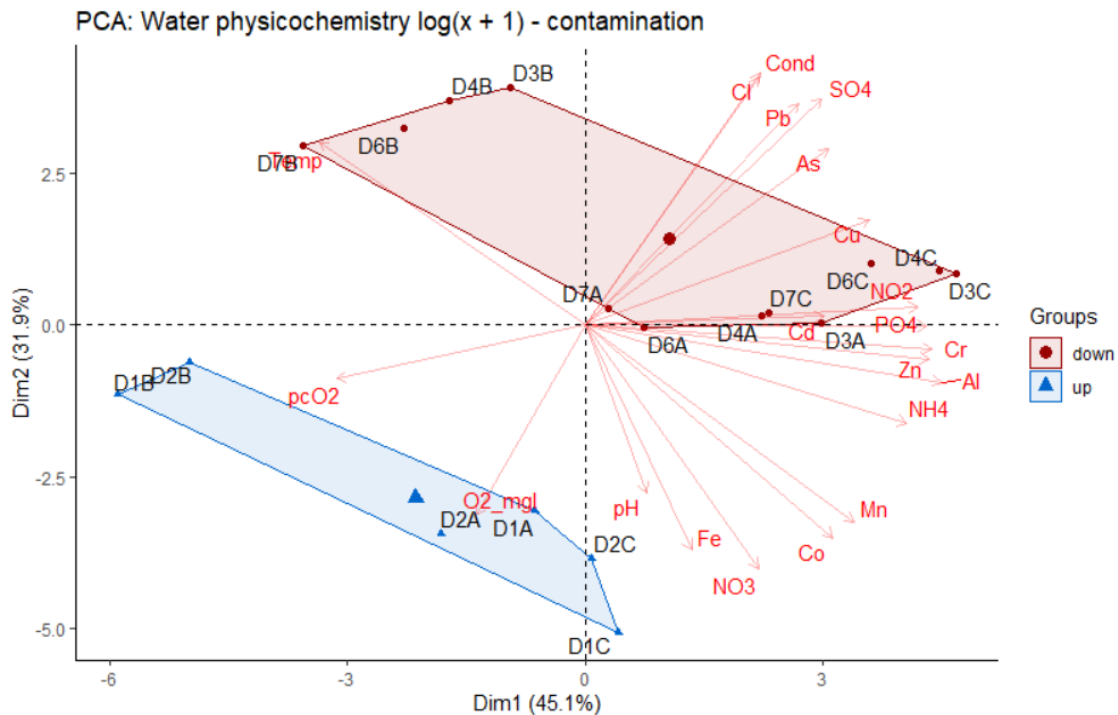


Figure 5: Principal Component Analysis (PCA) diagram of physicochemical characteristics of all water samples, as well as metal concentrations in water, $\log(x + 1)$ transformed. Including in situ measurements of acidity (pH), water temperature (Temp.), electrical conductivity (Cond), oxygen saturation (pcO₂), oxygen content (O₂). Additionally, concentrations of phosphate (PO₄), ammonia (NH₄), nitrite (NO₂), nitrate (NO₃), sulfate (SO₄) and chloride (Cl) are shown along with metals in water. Groups consist of ‘up’ (blue) and ‘down’ (red), referring to sites upstream or downstream of the Eindergatloop, respectively.

3.1. Diatoms

3.1.1. Abundance and diversity

A list of all counted diatoms including codes used for each species, as well as a systematic list of all identified diatom species are provided in Appendix 15A and 15B, respectively. A total of 202 diatom taxa (including species, varieties and forms) belonging to 54 genera were observed during the counts (total number of counted valves: 7200). Several taxa such as *Planothidium cf. engelbrechtii* and *Gomphonema cf. angustatum* could not be identified with 100% certainty up to species level. These taxa are listed as ‘cf.’ (*confer*) to indicate a possible taxonomic relation to an already described species. Further taxonomic analysis will be necessary to confirm their exact taxonomic identity and falls, at present, outside the scope of this thesis.

Table 5: A summary of diatom counts across all samples (six sites, sampled over three different sampling campaigns A, B & C). Total number of taxa (at species level) is shown along with the Shannon-Wiener Diversity index (SWD; higher values indicate a higher level of diversity in terms of species richness and species distribution) and Species Evenness (with values ranging from 0 to 1, indicating either unevenly or evenly distributed populations) derived from SWD, as calculated with OMNIDIA. For each site, a total of 400 valves were counted.

	D1A	D2A	D3A	D4A	D6A	D7A	Average
Taxa	67	43	41	39	40	47	46 ± 11
SWD	4.82	3.23	3.35	3.93	3.87	4.26	3.91 ± 0.59
Evenness	0.79	0.60	0.63	0.74	0.73	0.77	0.71 ± 0.08
	D1B	D2B	D3B	D4B	D6B	D7B	Average
Taxa	31	35	30	42	27	26	32 ± 6
SWD	3.21	2.67	3.08	3.57	3.11	3.38	3.17 ± 0.31
Evenness	0.65	0.52	0.63	0.66	0.65	0.72	0.64 ± 0.07
	D1C	D2C	D3C	D4C	D6C	D7C	Average
Taxa	43	43	28	47	37	71	45 ± 14
SWD	3.94	3.02	1.86	3.57	3.09	5.17	3.44 ± 1.10
Evenness	0.73	0.56	0.39	0.64	0.56	0.84	0.62 ± 0.16

The highest number of taxa was found in samples D7C (71) and D1A (67), whereas in samples D7B (26) and D6B (26) the lowest species richness was observed. Table 5 shows the species richness, Shannon-Wiener diversity and evenness of all samples. It is clear that samples from the second sampling campaign (B) had a lower species richness compared to the two other campaigns (32 ± 6 [B] vs. 46 ± 10 [A] and 45 ± 14 [C]). The 20 most abundant taxa accounted for more than 82 % of all counted valves (Table 6). *Platessa oblongella* (Østrup) C.E.Wetzel, Lange-Bertalot & Ector (almost 27%) and *Sellaphora nigri* (De Notaris) C.E.Wetzel & Ector (15%) dominated the flora.

Table 6: List of the 20 most abundant diatom species found during this project (total $N = 7200$ valves). Percentages calculated as a proportion of the total number of valves.

Taxon	Count	%	Taxon	Count	%
<i>Platessa oblongella</i>	1935	26.88%	<i>Sellaphora atomoides</i>	137	1.90%
<i>Sellaphora nigri</i>	1089	15.13%	<i>Ulnaria ulna</i>	111	1.54%
<i>Planothidium cf. engelbrechtii</i>	440	6.11%	<i>Gomphonema cf. angustatum</i>	86	1.19%
<i>Gomphonema parvulum</i>	439	6.10%	<i>Navicula rhynchocephala</i>	82	1.14%
<i>Achnantheidium microcephalum</i>	284	3.94%	<i>Stauroneis kriegeri</i>	81	1.13%
<i>Planothidium frequentissimum</i>	231	3.21%	<i>Navicula cryptocephala</i>	75	1.04%
<i>Nitzschia dissipata</i>	214	2.97%	<i>Prestauroneis protracta</i>	74	1.03%
<i>Nitzschia palea</i>	163	2.26%	<i>Fragilaria pectinalis</i>	72	1.00%
<i>Sellaphora saugerresii</i>	161	2.24%	<i>Frustulia vulgaris</i>	71	0.99%
<i>Planothidium lanceolatum</i>	160	2.22%	<i>Mayamaea permitis</i>	63	0.88%

3.1.2. *Diatom autecology*

The autecological characteristics for all samples were calculated based on the (updated) ecological scores according to van Dam et al. (1994) (Appendix 16A). Table 7 shows the average scores for all ecological attributes (see Appendix 16B for individual scores per sample).

Table 7: Average ($n = 6$, \pm S.D.) autecological attributes per sampling campaign (A, B and C), based on van Dam et al. (1994). See Appendix 16B for scores calculated per sample.

	pH (R)	Salinity (H)	O₂ (O)	Saprobity (S)	Trophic state (T)
A	3.2 \pm 0.2	2 \pm 0.1	2.5 \pm 0.3	3 \pm 0.2	4.5 \pm 0.3
B	3 \pm 0.4	1.8 \pm 0.3	2.4 \pm 0.7	2.9 \pm 0.6	4 \pm 0.8
C	3.2 \pm 0.2	2 \pm 0.1	2.4 \pm 0.2	2.9 \pm 0.4	4.3 \pm 0.3

No significant difference between the three sampling campaigns were found. Sampling campaign B shows lower values for salinity and trophic state. Analysis of the individual samples shows that these differences are mostly likely due to lower values for the samples D3B, D4B and D5B. No differences were observed between sampling campaigns A and C.

3.1.3. *Diatom indices: IBD, TDI & IPS*

Table 8: Calculated Trophic Diatom Index (TDI), Specific Polluosensitivity Index (IPS) and Diatom Biological Index (IBD) scores for each sample based on diatom counts. The TDI is scored as a percentage, while IPS and IBD are both converted to scores on 20.

	D1A	D2A	D3A	D4A	D6A	D7A
TDI (%)	51.8	40.8	45.0	57.0	48.7	67.9
IPS (/20)	14.6	14.8	14.3	13.2	14.7	10.6
IBD (/20)	14.7	15.4	15.0	13.7	14.8	11.7
	D1B	D2B	D3B	D4B	D6B	D7B
TDI (%)	38.2	41.5	75.4	55.5	62.8	74.7
IPS (/20)	18.0	13.0	10.8	13.5	11.5	7.6
IBD (/20)	16.3	14.7	12.0	14.3	12.8	10.3
	D1C	D2C	D3C	D4C	D6C	D7C
TDI (%)	61.9	38.5	31.3	45.0	46.8	69.7
IPS (/20)	15.6	14.5	16.2	14.5	12.9	13.1
IBD (/20)	14.6	15.3	16.8	15.3	14.1	12.9

Table 8 shows the results for three calculated diatom indices (IPS, TDI and IBD). No differences between the sampling campaigns were found (Appendix 17). The TDI scores varied between 31.3 and 75.4%. Next, IPS showed values ranging from 7.6 to 18. Lastly, scores ranging between 10.3 and 16.8 were found for IBD. Both IPS and IBD showed significantly

higher index scores in sites located upstream of the Eindergatloop. Furthermore, TDI showed higher scores in downstream sites, although only a trend was found ($0.05 < p < 0.10$).

Correlations between the diatom indices and the different physicochemical parameters measured during sampling are shown in Appendix 11C and 11D. Significant negative correlations were found between TDI and NO_3^- ($p < 0.05$) and a positive correlation with ^{65}Zn ($p < 0.05$). Other positive correlations were shown for IPS with ^{55}Mn , ^{60}Co , ^{51}Cr , ^{54}Mn , ^{56}Fe and ^{60}Co ($p < 0.05$) while negative correlations were found with water temperature, Cl^- and ^{65}Zn ($p < 0.05$). Lastly, positive correlations were observed for IBD and NO_3^- ($p < 0.01$), as well as a negative correlation with ^{65}Zn ($p < 0.05$).

3.1.4. Diatom community composition

Based on the Principal Component Analysis, different groupings of samples could be made, using either an ‘up- versus downstream’ or a ‘sampling campaign’ scenario.

Diatoms in sites downstream of the Eindergatloop were separated mostly along the first PC axis (Dim1), while a lot of overlap is observed on the second PC axis (Dim2). Additionally, clusters show a large degree of spread along both axes, especially in terms of D1 and D2 (see Appendix 18 for PCA graph). Some differences can be observed from the combination of the PCA and diatom abundance data. For instance, sites downstream of the Eindergatloop can be distinguished from upstream sites based on a lower abundance of *Platessa oblongella*, as well as higher abundances for *Gomphonema parvulum* (Kützing) Kützing, *Planothidium lanceolatum* (Brébisson ex Kützing) Lange-Bertalot, *Nitzschia palea* (Kützing) W.Smith and *Sellaphora saugerresii* (Desmazières) C.E.Wetzel & D.G.Mann.

On the other hand, the effect of the sampling campaign seemed to be larger (Fig. 6). A separation can be observed along the second PC axis (Dim2), despite a large degree of overlap along the first axis (Dim1). Diatom counts for campaign B and C are strongly grouped along Dim2, but show a large degree of spread along Dim1. Both axes cumulatively explain approximately 38% of all variation in the diatom count data. In terms of the most dominant taxa, all sampling campaigns showed high similarity. Looking at less dominant species, however, shows clearly higher numbers of species belonging to genera such as *Fragilaria* Lyngbye and *Ulnaria* (Kützing) Compère, with PCA arrows pointing strongly toward campaign A.

For more information on axis contributions, PC scores and enlarged graphs, see Appendix 18.

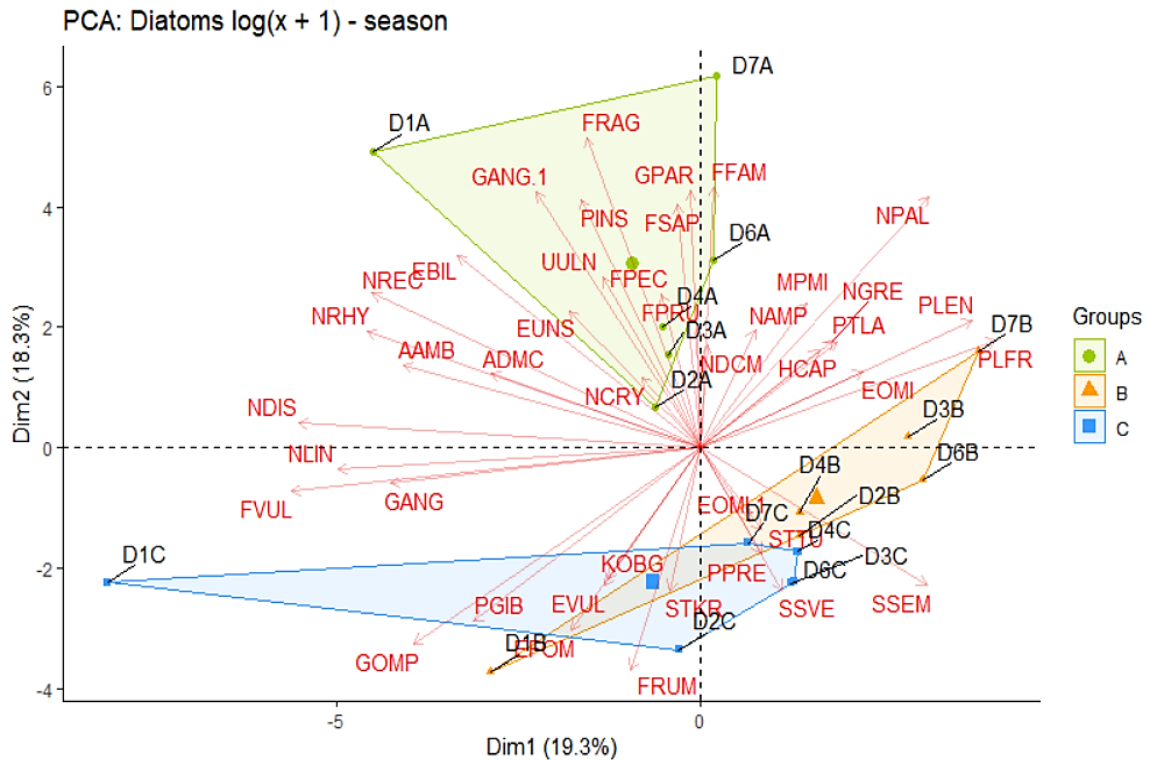


Figure 6: Principal Component Analysis (PCA) of diatom count data, $\log(x + 1)$ transformed. Groups consist of sampling campaigns A (green), B (orange) and C (blue). Variables shown in red represent diatom species of which the corresponding codes can be found in Appendix 15A. Enlarged graph in Appendix 18.

3.1. Macroinvertebrates

3.1.1. Abundance and diversity

A list of all counted/estimated macroinvertebrates, a list with codes used for each species (PCA; see later), as well as a systematic overview of all identified taxa are provided in Appendix 19. At total of 10960 macroinvertebrates were counted/estimated, involving 57 different taxa.

The highest number of taxa was found in samples D3B (29) and D6B (27), while samples D6A (13) and D1B (15) displayed the lowest taxa richness. These metrics are listed for all samples in Table 9 along with Shannon-Wiener diversity and evenness. Taxa richness appears to be highest in campaign B (24 ± 6) compared to the other campaigns. Furthermore, the 20 most abundant macroinvertebrate taxa identified during this project represent over 95% of all counted individuals. Chironomidae non *thummi-plumosus*, Simuliidae and Asellidae were the most abundant taxa and represent over 45% of all counted macroinvertebrates (Table 10).

Table 9: A summary of macroinvertebrate counts across all samples. Total number of counted/estimated macroinvertebrates, total number of taxa, Shannon-Wiener diversity index (SWD) and Species Evenness derived from SWD.

	D1A	D2A	D3A	D4A	D6A	D7A	Average
Total	1060	874	1401	700	335	372	790 ± 411
Taxa	25	22	23	19	13	20	20 ± 4
SWD	1.96	2.29	1.69	1.5	1.39	2.34	1.86 ± 0.4
Evenness	0.61	0.74	0.54	0.51	0.54	0.78	0.62 ± 0.11
	D1B	D2B	D3B	D4B	D6B	D7B	Average
Total	675	546	1027	326	699	339	602 ± 262
Taxa	15	28	29	19	27	23	24 ± 6
SWD	1.11	2.4	2.19	2.22	2.24	2.48	2.11 ± 0.5
Evenness	0.41	0.72	0.65	0.75	0.68	0.79	0.67 ± 0.14
	D1C	D2C	D3C	D4C	D6C	D7C	Average
Total	314	527	516	567	267	415	434 ± 123
Taxa	17	18	22	22	20	21	20 ± 2
SWD	1.96	1.85	2.14	2.02	2.28	2.02	2.05 ± 0.15
Evenness	0.69	0.64	0.69	0.65	0.76	0.66	0.68 ± 0.04

Table 10: List of the 20 most abundant macroinvertebrate species found during this project (total $N = 10960$ valves). Percentages calculated as a proportion of the total number of macroinvertebrates.

Taxon	Count	%	Taxon	Count	%
<i>Chir. non thummi-plumosus</i>	442	24.54%	<i>Sphaerium</i>	43	2.37%
Simuliidae	221	12.28%	<i>Calopteryx</i>	41	2.29%
Asellidae	200	11.14%	<i>Erpobdella</i>	38	2.10%
<i>Hydracarina</i> s.l.	123	6.86%	<i>Baetis</i>	28	1.57%
Gammaridae	112	6.24%	<i>Physa</i> s.s.	22	1.25%
Tubificidae	96	5.31%	Limnephilidae s.l.	14	0.78%
<i>Pisidium</i>	85	4.74%	<i>Dugesia</i> s.l.	13	0.71%
Lumbricidae	81	4.53%	Hydropsychidae	11	0.63%
<i>Helobdella</i>	74	4.13%	<i>Polycelis</i>	10	0.57%
<i>Lymnaea</i> s.l.	67	3.75%	<i>Chir. thummi-plumosus</i>	10	0.57%

3.1.2. Metals in macroinvertebrates

Metal concentrations were measured in three macroinvertebrate taxa collected during campaign B. Significant differences were found for metal concentrations in *Asellus aquaticus*, *Calopteryx virgo* and Chironomidae (sF. Prodiamesinae). In *Asellus*, metals such as Zn, As, Cd and Pb were significantly higher in sites downstream of the Eindergatloop. For *Calopteryx*, Al, As, Cd and Pb were significantly higher in downstream sites, although Mn and Co showed higher concentrations upstream of the point source of pollution. The only metals that showed significant difference in Chironomidae were As and Pb, both showing higher concentrations in downstream sites. See Table 11 for significant differences between up- and downstream sites

for metals dissolved in water, sediment and biota. Furthermore, all metal concentrations measured in these organisms, as well as the calculated TUs, are presented in Appendix 20. Statistical results and corresponding graphs are presented in Appendix 21, including box plots and bar graphs.

Table 11: Metal concentrations in biota (*Asellus aquaticus*, *Calopteryx virgo*, Chironomidae sF. Prodiamesinae) between sites up- and downstream of the Eindergatloop. Colours indicate the sites where the variable was significantly higher: **red** = upstream < downstream; **blue** = upstream > downstream. See Appendix 6, 7 & 21 for more details. Toxic units (TU) were not calculated for metals in sediment (sed.). Significance levels are included (· = 0.05 < p < 0.10; * = p < 0.05; ** = p < 0.01; *** = p < 0.001).

	Al	Cr	Mn	Fe	Co	Cu	Zn	As	Cd	Pb	TU	TU*
Metals (water)				·		**	·	***	·	***		*
Metals (sed.)		·	·	·	*				**	**		
<i>Asellus aquaticus</i>		*				*	***	**	***	***	**	
<i>Calopteryx virgo</i>	***	**	*	**	*			***	**	***	**	
Chironomidae (sF. Prodiamesinae)								**		*		

3.1.3. Multimetric Macroinvertebrate Index Flanders

All metrics used for calculating the MMIF are provided in Appendix 22. These calculations resulted in MMIF values (Table 12) ranging from 0.35 to 0.70, with an average of 0.57 ± 0.09 across all samples and sampling campaigns. Interestingly, both of the lowest and highest values were found in D6A (0.35) and D6B (0.70), respectively. No significant correlations were found for MMIF and other environmental variables (Appendix 11C, 11D). Furthermore, no significant differences were found for MMIF in upstream versus downstream sites, nor was there a significant difference between sampling campaigns.

Table 12: Calculated Multimetric Macroinvertebrate Index Flanders (MMIF) scores for all samples across all three campaigns (A, B, C) with average (\pm S.D.), see Appendix 22 for complete summary of MMIF metrics.

Campaign	D1	D2	D3	D4	D6	D7	Average
A	0.65	0.60	0.60	0.50	0.35	0.50	0.53 ± 0.11
B	0.45	0.65	0.65	0.50	0.70	0.60	0.59 ± 0.10
C	0.55	0.50	0.65	0.60	0.55	0.60	0.58 ± 0.05

3.1.4. Community composition

Principal Component Analysis was performed on macroinvertebrate proportionate count data. Grouping all datapoints according to their location relative to the Eindergatloop (upstream versus downstream), a large degree of spread and overlap can be observed for both groups and on both axes (Dim1 and Dim2). The same exercise was carried out by grouping according to sampling campaign (A, B, C). In this case, a large degree of overlap can be observed along Dim2, with some degree of separation of group A from B and C along Dim1.

Using the up- or downstream location of sites as a grouping factor (Fig. 7), a couple of taxa show differences in abundance between the up- and downstream groups. Based on the more dominant species (derived from abundance data), these differences consist of higher abundances for taxa such as Tubificidae, *Erpobdella*, *Lymnaea* s.l. and *Physa* s.s. in downstream sites along with lower abundances for *Hydracarina* s.l. and Hydropsychidae. Grouping based on sampling campaign (Appendix 23) also shows differences in abundance of the most dominant taxa. For instance, campaign B shows higher abundances for Tubificidae, *Helobdella*, *Erpobdella* and *Calopteryx*, as well as lower abundances for Chironomidae non *thummi-plumosus*.

Cumulatively, the two first PC axes explain less than 40% of all variation in the dataset. Both PCA diagrams and supporting graphs can be found in Appendix 23.

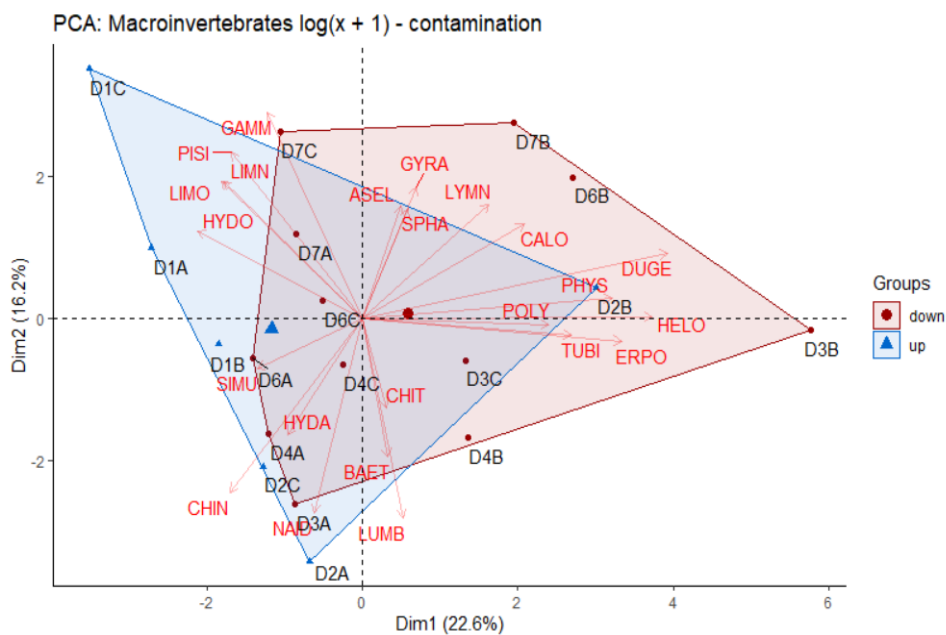


Figure 7: Principal Component Analysis (PCA) of diatom count data, $\log(x + 1)$ transformed. Groups consist of sites upstream (blue) and downstream (red) of the Eindergatloop. Variables shown with red arrows represent macroinvertebrate taxa of which the corresponding codes can be found in Appendix 19B. Enlarged graph in Appendix 23.

3.2. Comparison of diatom and macroinvertebrate indices

The MMIF did not show any significant correlations with any of the diatom indices (Table 13). However, TDI showed strongly negative correlations with both IPS and IBD. At the same time, IPS values displayed a strong and positive correlation with IBD. See Appendix 11C for the corresponding correlation matrix along with all other physicochemical variables. Furthermore, a bar graph of all biotic indices is shown in Figure 8 (all indices are normalized to a range between 0 and 1 to facilitate comparison). Both IPS and IBD show similar gradients, showing a decrease from D1 and D2 toward the downstream sites (D4 to D7). The gradient of TDI runs in the opposite direction (increasing from D1 and D2 toward D7). Lastly, MMIF scores appear highest in D3, while the other sites are relatively similar.

Table 13: Spearman rank correlation matrix using all calculated biotic indices. Lower left panel shows significances (* = $p < 0.05$; ** = $p < 0.01$; *** = $p < 0.001$), while the upper right panel shows correlation coefficients.

	MMIF	TDI	IPS	IBD
MMIF	/	+ 0.141	- 0.280	- 0.160
TDI	ns	/	- 0.759	- 0.916
IPS	ns	***	/	+ 0.940
IBD	ns	***	***	/

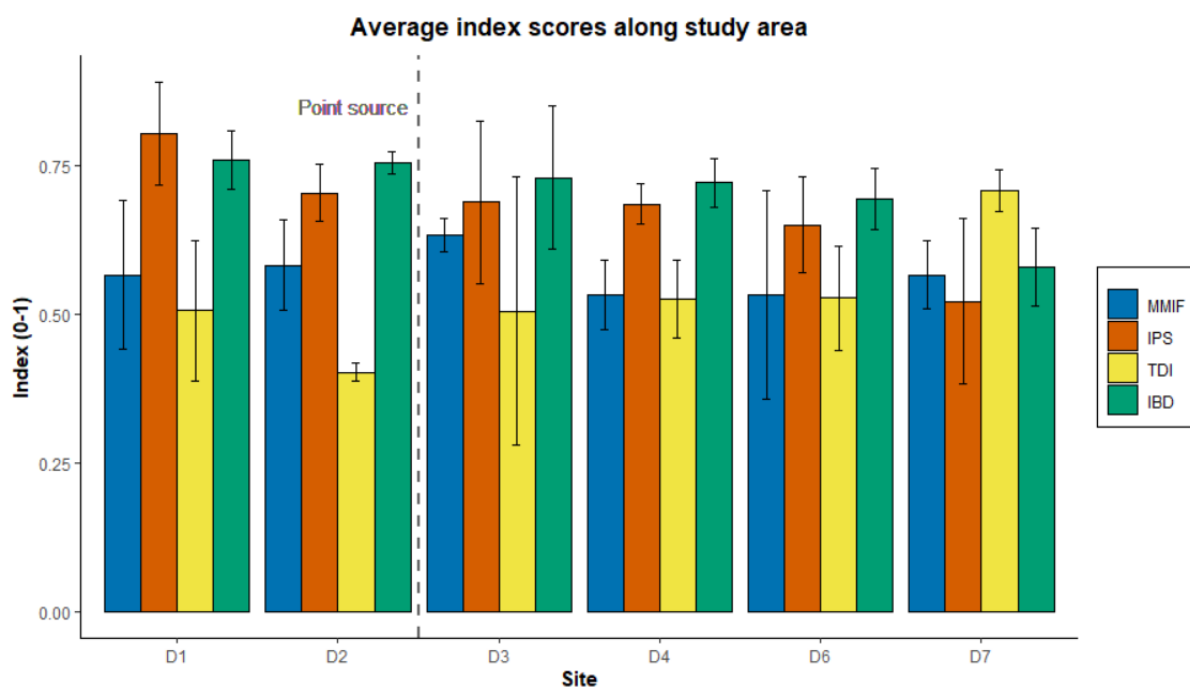


Figure 8: Bar graph showing all calculated indices (MMIF = blue; IPS = red; TDI = yellow; IBD = green) with S.D. (error bars). To allow comparison, all indices were normalized to a range of 0-1. Vertical line (dashed; - -) indicates location of point source of contamination.

4. Discussion

Physicochemistry of water and sediment

Electrical conductivity (EC), NO_2^- , SO_4^{2-} and Cl^- were significantly higher immediately downstream of entrance of the Eindergatloop (D3, D4, D6, D7) across all campaigns compared to the upstream sites (D1, D2). Apart from NO_2^- , these metrics showed values exceeding the Flemish EQS from sampling points D3 to D7. The sudden increase of SO_4^{2-} and Cl^- at site D3 followed by a gradual decrease is likely caused by metallurgic activity embanked on the Eindergatloop, as these are often generated as a secondary product (Nyrstar, 2019; Petelet-Giraud et al., 2009), which in turn affects EC.

Water samples downstream of the merge showed significantly higher dissolved metal concentrations for ^wCu (in $\mu\text{g L}^{-1}$, up: 1.7 ± 0.8 ; down: 2.8 ± 0.6), ^wAs (up: 1.8 ± 0.4 ; down: 3.8 ± 0.7) and ^wPb (up: 0.1 ± 0 ; down: 0.3 ± 0.1), along with trends for elevated ^wZn (up: 79 ± 45 ; down: 126 ± 50) and ^wCd (up: 0.2 ± 0.1 ; down: 0.3 ± 0.2). Of these elements, ^wZn and ^wCd exceeded Flemish EQS in virtually all samples, including at the upstream sites, while ^wAs consistently showed values exceeding the EQS starting from D3 onward. Additionally, a significantly higher $^w\text{TU}^*$ (up: 1.3 ± 0.8 ; down: 2.3 ± 1) was observed in downstream sites, indicating potentially elevated levels of toxicity. These observations largely agree with findings of De Jonge et al. (2008) and are most probably caused by discharge from the Eindergatloop into the Dommel. Further bolstering this statement is the gradient at which most of these metrics sharply increase at sampling point D3, followed by a gradual decrease toward D7.

The results also show a slight effect of sampling campaign. Notably, nutrients together with ^wZn , ^wCd and TU showed the lowest concentrations in campaign B. A possible explanation for these lower values could be found in the weather archives of meteoblue (meteoblue, 2020): Precipitation data indicate an increased amount of rain prior to sampling (12/08-20/08; approx. 15 mm). Possibly, this affected the physicochemistry of the Dommel by dilution and/or increased celerity of the river. Additionally, rain is typically characterized by increased acidity (André et al., 2007), which is also reflected by the significantly lower pH found during campaign B. Nonetheless, whether this volume of precipitation was sufficient to cause a physicochemical shift is another question entirely, which cannot be covered within the scope of this thesis.

In sediment, significantly higher concentrations of ^{65}Zn (in $\mu\text{g g}^{-1}$, up: 0.6 ± 0.3 ; down: 2.9 ± 2) and ^{210}Pb (up: 10 ± 2 ; down: 19 ± 10) were found in downstream sites as opposed to upstream, whereas on the other hand, a significant increase could not be observed for ^{65}Zn . Conversely, ^{60}Co (up: 12 ± 9 ; down: 2 ± 2) was shown to be significantly higher in upstream sites. Concentrations exceeding the Flemish standards were observed in several sites for ^{65}Zn (D1, D3, D4) and ^{75}As (D1, D6), while ^{109}Cd was found to exceed the EQS starting from D3. Additionally, D3 sediment showed ^{64}Cu concentrations exceeding the EQS. Given such ^{64}Cu concentrations were not found in any of the other sites, a local pollution source was likely responsible for this measurement. Metals such as ^{51}Cr , ^{56}Fe and ^{75}As showed high concentrations in D1 relative to D2 and the downstream sites. These elements were not statistically different between sites up- and downstream of the Eindergatloop and often did not concur with observations made for metals dissolved in water. Therefore, it is not completely clear why D1 showed such elevated levels of these metals. Possibly, other historical contamination upstream of D1 could explain this anomaly, as similar trends for these metals were not consistently found in water measurements. Additionally, similar patterns were not found at the same sites 15 years ago (De Jonge et al., 2008), indicating that another external factor may be the cause. An interesting observation was the lack of a significant increase of ^{65}Zn in downstream waters, given the historical metallurgic activity (e.g. Zn, Cd; Postma & Groenendijk (1999)) in the area. However, elevated concentrations at D1 (which was also observed for several other metals in sediment, e.g. Cr, Mn, As) likely ‘masked’ finding a difference between reference and downstream sites. To clarify, metals such as ^{65}Zn showed high concentrations in D1 which decreased in D2. In D3, ^{65}Zn concentrations sharply increased again, followed by a gradual decrease toward D7. In addition, sediment remediation (2007) was carried out along the course of D3 to D6 to alleviate some of the historical contamination (De Jonge et al., 2012; Van Thuyne et al., 2009). Compared to data from 1995 (VMM), sediment remediation of the Dommel resulted in lower ^{109}Cd and ^{65}Zn concentrations. This does not appear to be the case for ^{75}As or ^{210}Pb reported here. Important to note is that this comparison is far from conclusive and only serves as an indication, as recent data is not readily available.

Some of these results can be compared with De Jonge et al. (2008), who also performed in situ measurements of EC, SO_4^{2-} and Cl^- , as well as metals in water and sediment (Zn, Cd, As, Pb). Values reported here show similar EC, SO_4^{2-} and Cl^- values in upstream sites (D1, D2) as those reported by De Jonge et al. (2008), while we found higher values for EC and Cl^- in downstream sites (especially in D3 and D4). On the other hand, our Cl^- measurements show lower values

as those compared with De Jonge et al. (2008). As mentioned earlier, the significant elevation of these variables in downstream sites may be related to industrial discharge into the Eindergatloop. Comparisons for metals dissolved in water show increased Zn concentrations across all sampling sites compared to those reported in 2008. At the same time, Cd, As and Pb in water have decreased in downstream sites, although As shows higher concentrations in sites upstream of the Eindergatloop compared to De Jonge's findings. Metals in sediment showed lower concentrations in both up- and downstream sites for Zn and Pb compared to De Jonge's data. For As, we found lower concentrations downstream, but higher concentrations upstream of the Eindergatloop compared to 2008. For Cd, sediment concentrations have decreased in downstream sites and stayed similar in sediment collected upstream of the Eindergatloop.

Diatoms

Sampling methodology was chosen to avoid the presence of planktonic and epiphytic diatoms in the sample which may obscure a correct indication of the water quality of the sampling sites. Negligible numbers of *Cocconeis* valves (a typical, almost exclusive epiphytic species) or the almost complete absence of members of the genera *Stephanodiscus*, *Cyclotella* and *Cyclostephanos* (mostly planktonic genera) were observed, indicating that there was little influence of periphyton or planktonic diatoms (Håkansson & Bailey-Watts, 1993; Majewska et al., 2014). Planktonic diatoms could have drifted into the sampling site, but actually originated from much further upstream (Bolgovics et al., 2017). On the other hand, a higher proportion of epiphytic diatoms would only indicate the presence of submerged aquatic plants or helophytes and not reflect the real water quality value.

Diatom communities showed lower species richness in sampling campaign B. A possible reason might be the lower nutrient concentrations that favour the dominance of several species whereas many others did not seem to survive. This might have caused a shift in community composition (Orefice et al., 2019; Sgro et al., 2007).

In general, the observed diatom flora indicates that the water has an almost circumneutral pH ($R = 2.4\text{--}3.6$), a relatively low salinity ($H = 1.4\text{--}2.1$) and fairly high to moderate oxygen saturation ($O = 1.5\text{--}3.5$). Saprobity scores (S) ranged from β -mesosaprobous (2.2) to almost α -meso-/polysaprobous (3.8) pointing to moderate levels of organic pollution. The trophic state of the Dommel samples, as shown by the T scores (3.2–4.9) varied between a meso(-eu)trophic and almost eutrophic systems. It must be noted, however, that often less than 70%, (and in many cases even less than 50%) of the diatom flora was included in the analysis as most

diatoms were classified as being indifferent (score = 7). The latter had to be excluded from the analysis. These results of the calculated ecological scores (van Dam et al., 1994) did not show clear differences between up- and downstream sites. According to the most abundant diatom taxa, a lower salinity (H) was observed in campaign B, which could be linked to the increased precipitation in the week prior to the sampling. Such an effect of precipitation on autecological attributes was not observed for all other parameters, nor was H statistically different between sampling campaigns. The trophic state (T) of the Dommel in August 2019 was not statistically different from the other two sampling periods either, even though some lower values were reported. However, differences in T may have been masked due to high numbers of indifferent species. These indifferent taxa are excluded from the analysis as they lack a clear trophic preference (van Dam et al., 1994). Therefore, it is possible that a shift in species composition, favouring more indifferent species, did not reflect the lower nutrient levels that were measured in campaign B.

Diatoms are characterized by their outer silica cell wall. This cell wall is built after every cell division and can, therefore, give an indication of the environment in which the diatoms were living (Falasco et al., 2009; Round et al., 1990). Under the influence of increased levels of metals or pesticides, diatom frustules may show morphological deformations. These so-called teratological forms can be used as an indicator of increased metal or pesticide pollution (Falasco et al., 2009; Lavoie et al., 2017). In the present study, only a very low number of teratological valves was found in downstream sites but this number was certainly not higher when compared to the upstream sites. As this number is difficult to distinguish from naturally occurring malformations (background noise), there is no conclusive evidence for impact of metals on diatom metabolism in the Dommel. Perhaps concentrations were not high enough to instigate any morphological changes, or the diatom communities were able to resist elevated concentrations of metals. Diatoms seem to possess phenotypic and adaptive mechanisms to cope with elevated metal concentrations. For instance, diatoms show resistance by complexation and immobilization of metal complexes outside of the cell, can decrease the permeability of their cell membrane or simply excrete the toxicant (Morin et al., 2012). Alternatively, elevated metal concentrations could have caused inhibited growth or malformations of cells. In this case, the most sensitive taxa have already disappeared and the community has shifted to a more tolerant one (Falasco et al., 2009; Ivorra et al., 2002).

Based on the principal component analysis (PCA) two distinct patterns could be observed. The first seems to indicate differences between samples up- and downstream of the Eindergatloop,

as shown by a separation of the samples along the first axis. Nevertheless, apart from the spread, there is also quite some overlap, which illustrates a high level of similarity between the two groups. This observed similarity implies that sites upstream are also exposed to a certain level of pollution. Sites downstream of the Eindergatloop are primarily distinguished from those upstream based on somewhat lower abundances of *Platessa oblongella*, as well as higher abundances for other species such as *Gomphonema parvulum*. The ecological preferences of *P. oblongella* are unclear: The species has a tendency to occur in a wide range of ecological conditions and has a moderate tolerance to anthropogenic acidification, although it is often found in waters that are relatively clear of anthropogenic disturbance (Wetzel et al., 2017, Lange-Bertalot et al. 2017). In Sweden, for instance, *P. oblongella* is often found in more acid, mesotrophic conditions and disappears when nutrient levels exceed eutrophic levels (A. Jarlman, Jarlman Konsult, pers. comm.). At the same time, *G. parvulum* is a typical pollution-tolerant species, preferring high nutrient levels and tolerating increased metal pollution (Lange-Bertalot et al., 2017; Wetzel et al., 2017). Moreover, findings of Ivorra et al. (2002) suggest that *G. parvulum* may develop genetic metal adaptation resulting from chronic exposure in the field. Further, *P. lanceolatum* also has a very broad ecological amplitude. It appears in circumneutral to alkaline waters, is common in oligotrophic to polythropic waters, and favours conditions of low organic pollution and high concentrations of dissolved oxygen (Lange-Bertalot et al., 2017; Moreno & Ramirez, 2013). Additionally, *P. lanceolatum* is of interest in wastewater treatment for its ability to bind metals such as Cd, Cu and Zn to its cellular structures in a process called ‘biosorption’ (Sbihi et al., 2014). Finally, *S. saugerresii* and *N. palea* are species that are often found in pollution-tolerant assemblages, often together, however, with *P. oblongella* (Wetzel et al., 2017). Together with *S. nigri*, *N. palea* and *S. saugerresii* make up a group of eutrophic species that show higher abundances from D3 onward. The higher abundances of these species clearly indicate more anthropogenic disturbance downstream of the Eindergatloop. One notable observation is the relatively high abundance of *Planothidium* cf. *engelbrechtii* found in downstream sites. Unfortunately, it was impossible to identify this taxon up to species level. It shows a similarity to several other *Planothidium* species such as *P. pericavum* (Carter) Lange-Bertalot or *P. engelbrechtii* (Cholnoky) Round & Bukhtiyarova (Krammer & Lange-Bertalot, 1991). Due to this lack of a positive identification, it is impossible to explain this high abundance, other than using the ecological characteristics found in the present study. The description of this taxon is currently ongoing (Van de Vijver et al., unpubl. res.) and one of the samples from this study will be used as type material, determining its environmental preferences based on the results of this study.

The second pattern shows slight differences between sampling campaigns, separating samples from campaign A with all samples from campaign B and C. However, clear differences in diatom composition could not be detected when looking only at the dominant species. Therefore, a possible explanation should be sought in the lesser dominant species. The diatom flora of campaign A has a clearly higher number of species belonging to the genera *Fragilaria* and *Ulnaria*. This can also be seen in the PCA diagram with arrows of almost all *Fragilaria* and *Ulnaria* species pointing upwards (i.e. group of campaign A – 17/04/2019). *Fragilaria* and *Ulnaria* are typical pioneer species that rapidly respond to temperature changes of their environment. Therefore, they are typically characterized by a strong ‘spring bloom’ effect at the onset of seasonal increase of water temperature, followed by exponential growth (Gamier et al., 1995; Zhang et al., 2019). Over two decades ago, this phenomenon was also reported in another Belgian lowland stream, the Kleine Nete, where large numbers of *U. ulna* were found in early May (Van de Vijver & Beyens, 1998). A similar change in timing of spring diatom bloom has also been reported by Winder & Schindler (2004). However, further analysis will be necessary to fully explore and substantiate this statement.

An important implication for the high interseasonal similarity is that water quality evaluation may not require frequent sampling of diatoms to obtain a representative monitoring of the water quality of our rivers. This could be beneficial, given the process of collection, preparation and identification of diatoms is very resource- and time-consuming. On the other hand, several variables did show significant differences between sampling campaigns (e.g. water temperature, N-containing molecules, potential toxicity). Moreover, diatom communities typically show a seasonal succession (Gamier et al., 1995). Perhaps, seasonal shifts took place in conjunction with changing environmental variables. For instance, temperature – an important factor in driving diatom community composition (Dalu et al., 2017) – was highest in August 2019, while many pollutants showed low concentrations in this campaign (relative to A and C). Several interseasonal differences were observed, but these may have been ‘evened out’ by other variables that were significantly different between sampling campaigns. Nevertheless, diatom assemblages in rivers are affected by complex environmental gradients and often poorly understood spatial patterns of species distribution (Kelly et al., 1998; Potapova & Charles, 2002). Due to this complexity, a straight-forward explanation for the high interseasonal similarity of diatom communities was not found within the scope of this thesis.

The slight differences in the abundance of certain diatom species, such as *G. parvulum* and *N. palea* (see above), also influenced the results observed for IPS, TDI and IBD between sites up-

and downstream of the Eindergatloop. However, significant differences were not found for any of the three diatom indices between the sampling campaigns. Both IPS and IBD showed significantly higher index scores in upstream sites, while TDI showed a trend for higher scores in downstream sites. These findings indicate lower water quality and higher levels of organic pollution in sites downstream of the Eindergatloop. At the same time, some correlations were found between these indices and the physicochemical environment. Positive correlations were found for metals in water and IPS (Mn, Co), which was also the case for metals found in sediment (Cr, Mn, Fe, Co). Arguably, these observations may be accredited to long-term exposure effects to metal and tolerance build-up (Sabater, 2000). Moreover, the lack of any significant degree of teratological valves already indicates low levels of metal-induced stress on the diatom populations presented here. All three indices showed a correlation with ^{107}Cd : TDI was positively correlated, IPS and IBD were negatively correlated. One possible scenario is that higher ^{107}Cd implies less Cd being released into the water column. In any case, IPS shows the most correlations with metals concentrations in water and sediment as opposed to TDI and IBD.

However, Sabater (2000) only found a handful of (negative) correlations between indices and metals in the environment, while Corcoll et al. (2012) concluded that indices such as IPS are actually limited in the assessment of metal pollution. This is not unlikely as IPS was originally developed to assess trophic pollution and may therefore not be suitable to evaluate metal contamination (Corcoll et al., 2012; Morin et al., 2008). De Jonge et al., (2008) also found a limited number of significant correlations between diatom indices and the physicochemical characteristics of the environment. These statements imply that correlations in the present report may not provide an accurate representation. As diatom-metal interactions are rather complex and subject to many different factors, they are considered beyond the scope of this thesis.

Furthermore, the TDI is negatively correlated with both IBD and IPS, while IPS and IBD are positively correlated. These correlations make sense, as TDI and the other two diatom indices are inversely related; lower TDI scores indicate higher levels of pollution, while higher scores of IPS and TDI indicate lower levels of pollution.

Both IBD and IPS scores found in the present report are higher in both up- and downstream sites than those reported by De Jonge et al. (2008). Additionally, TDI scores are lower across all six sampling sites than those reported in 2008. In other words, water quality evaluation

based on diatoms implies that the ecological quality of the Dommel has improved compared to De Jonge's work.

Macroinvertebrates

Two patterns could be observed based on the principal component analysis. The first shows a difference between samples up- and downstream of the Eindergatloop along the first axis. This axis is characterized by a large degree of spread and overlap between the two groups, which signifies a high level of similarity between up- and downstream samples. Downstream sites are mostly differentiated from those upstream based on higher abundances for Tubificidae, *Erpobdella*, *Lymnaea* s.l. and *Physa* s.s., as well as lower abundances for *Hydracarina* s.l. and Hydropsychidae. Tubificidae are sediment-dwelling, oligochaeta worms that tolerate low levels of oxygen (Bervoets et al., 2016). These worms are tolerant to environmental pollution and have been shown to be good accumulators of metals, making them suitable in biomonitoring practices (Bervoets et al., 2016; Mosleh et al., 2006). Next, *Erpobdella* is a predatory freshwater leech commonly found in running waters throughout Europe. In case of organic pollution, this species may occur in very high densities as they feed on *Tubifex* (F. Tubificidae) and *Chironomus* (F. Chironomidae) (Kutschera, 2003; K. H. Mann, 1955). Further, *Lymnaea* s.l. and *Physa* s.s. are freshwater pulmonate snails that show sensitivity to pollution such as sulphates and metals. These organisms have been argued to be an indicator of anthropogenic stress (Croteau & Luoma, 2008; Lewin, 2006; Reátegui-Zirena et al., 2017). Finally, lower abundances of Hydropsychidae were reported in downstream sites. The distribution of these species suggests slightly more tolerant species in downstream sites as opposed to upstream, even though the more abundant taxa are highly similar between the two groups (Asellidae, Simuliidae, Chironomidae).

The second PCA pattern shows a difference between sampling campaigns. Samples of campaign B are separated from those collected in campaign A and C. Looking at the dominant species, higher abundances are found in B for Tubificidae, *Helobdella*, *Erpobdella* and *Calopteryx*, while lower abundances were observed for Chironomidae non *thummi-plumosus*. As was the case for *Erpobdella*, *Helobdella* are predatory freshwater leeches that show slightly lower tolerance to pollution than *Erpobdella*. The damselfly (*Calopteryx*) has already been covered earlier and is sensitive to environmental pollution (Gabriels et al., 2010). Furthermore, Chironomidae non *thummi-plumosus* are a 'form' of chironomids that are distinguished from their *thummi-plumosus* counterparts by the absence of external respiratory tubes. These

organisms show high tolerance to pollution (Bervoets et al., 2016; De Pauw & Heylen, 2001). It is likely that there is an effect of seasonality, as *Calopteryx* display the highest abundances in summer (Conrad & Herman, 1990). Other than that, there is no clear indication for seasonal differences based on the most dominant and distinct taxa between samples. Looking at the less dominant taxa, *Dugesia* s.l. shows higher abundances than those found in campaign A and C. This species, too, shows a certain degree of seasonality – offspring develops and hatches in spring and reaches maturity in summer (Stocchino & Manconi, 2013).

Many of the tested bioaccumulated metals (Cr, As, Cd, Pb) showed increased concentrations in downstream sites in both *Asellus aquaticus* and *Calopteryx virgo*. For Chironomidae only As and Pb showed elevated levels in sites downstream of the Eindergatloop.

Differences in accumulated metal concentrations between up- and downstream sites were represented most accurately by *A. aquaticus*: a detritivorous isopod that lives in various bottom substrates and top layers, being in close contact with both sediment and the water column (van Hattum et al., 1989). Similar concentrations as those reported here were found for Cd, Cu, Zn and Pb in *Asellus* collected in the Dommel by van Hattum et al. (1991). As their measurements were conducted close to three decades ago, the similar concentrations found in our measurements may indicate the prevalence and longevity of metal contamination in the Dommel river. In the present report, *Asellus* matched differences in water more than those in sediment. For instance, while sediment samples showed increased concentrations of ^{54}Cr in upstream sites, the opposite was true in *Asellus*. Furthermore, sediment samples did not show significantly different concentrations for ^{65}Cu , ^{66}Zn or ^{75}As , but *Asellus* showed elevated levels of these metals in downstream sites ($\mu\text{g/g}^{-1}$, on average: Cu +93; Zn +91; As +10). This indicates that these metals may be more bioavailable in the contaminated sites for these organisms to assimilate. As such, *Asellus* showed significant differences even when these were not picked up during statistical analysis of sediment and water samples. Nevertheless, water may be the predominant pathway through which *Asellus* accumulates metals. This has already been shown for Cd uptake which mainly occurred via aqueous uptake, while uptake via food mainly occurred at enhanced dietary Cd levels (van Hattum et al., 1989). Additionally, synergistic interactions (i.e. total effect of multiple toxicants combined is greater than the total sum of the individual effects) have been reported in *Asellus* for Cd and Pb (Van Ginneken et al., 2015). The potential toxicity of metals in *Asellus* in downstream sites was significantly higher, as indicated by a higher TU in *Asellus* (TU_{asl}). Furthermore, Zn concentrations found in *Asellus* can be compared with the critical concentration of metabolically available Zn (i.e. the

maximum tolerable concentration of metal in metabolically available form before toxic effects ensue) in a crustacean ($> 150 \mu\text{g g}^{-1}$; Rainbow & Luoma (2011)). Applying this threshold, *Asellus* Zn concentrations showed values exceeding this threshold in all downstream sites by 50 to $150 \mu\text{g g}^{-1}$, signifying the potential Zn toxicity these organisms are exposed to. As literature on bioaccumulated metal concentrations in *A. aquaticus* is sparse, direct comparisons with analogous studies cannot be discussed here. Nevertheless, comparison of concentrations in upstream (in $\mu\text{g g}^{-1}$ dry weight (DW); Cu 115 ± 7 ; Zn 119 ± 8 ; As 7.52 ± 2.43 ; Cd 0.92 ± 0.7 ; Pb 1.23 ± 0.07) and downstream sites (in $\mu\text{g g}^{-1}$ DW; Cu 208 ± 100 ; Zn 210 ± 42 ; As 17.68 ± 8.06 ; Cd 5.78 ± 2.01 ; Pb 10.88 ± 6.36) indicates a clear increase in metal assimilation of *Asellus* found in sites exposed to discharge of the Eindergatloop. In case of non-essential metals such as As, Cd and Pb, even low concentrations have been shown to cause toxicity, which is not necessarily the case for essential metals such as Cu and Zn (Rainbow, 2002). Even so, very low concentrations of essential metals may cause other side effects caused by e.g. deficiency, rather than effects caused by excessive concentrations (Quintaneiro et al., 2015).

The nymphs of *Calopteryx virgo* are obligate predators. They are largely restricted to running waters such as streams and rivers, where they are often found in between water plants (Brooks & Cham, 2014; Dobson et al., 2012; Johnson, 1991). Elevated metal concentrations (Al, Cr, Fe, As, Cd, Pb) within these organisms were observed in downstream sites, though no differences were found for Zn. Elevated concentrations for As, Cd and Pb correspond to our findings in water, as well as for Cd and Pb in sediment. Different from *Asellus*, *Calopteryx* shows elevated concentrations of Mn and Co in upstream sites, which is also found in the sediment. Other differences include *Calopteryx* showing higher concentrations for Al, Cr and Fe downstream of the Eindergatloop, while concentrations in sediment or water showed the opposite, or none at all. Notably, *Calopteryx* shows higher Fe downstream, while water and sediment samples show the opposite. A straight-forward explanation is not readily available, although inverse relationships between environment and concentrations in tissue have already been shown before, indicating the complexity of trace metal bioavailability and assimilation (DeForest et al., 2007). As for the damselfly larvae showing differences which were not detected in either water or sediment analysis, an explanation may be related to the organism's position in the foodweb. If a predator's diet consists of bottom-dwelling prey that assimilated metals over time, trophic transfer to the predator may take place. Even so, variation exists depending on the species or metal (Rainbow et al., 2006; Rainbow, 2002), or on the size of the macroinvertebrate (Frag et al., 1998). As *Calopteryx* mostly spends time within the canopy of

water plants (or on hard substrates), it is likely that it accumulated metals over time primarily through prey consumption (Cui et al., 2011). Regardless, as hypothesized, most metals found in *Calopteryx* show higher values downstream of the Eindergatloop. Similar to findings in *Asellus*, the TU in *Calopteryx* (TU_{clx}) was also higher in downstream sites, signifying the differences in absolute dissolved or bioavailable metal concentrations. As was the case for *A. aquaticus*, endogenous concentrations in *Calopteryx* are sparse. Therefore, a direct comparison with such analogous reports cannot be explored here. However, elevated levels of several non-essential metals were found in downstream sites (in $\mu\text{g g}^{-1}$ DW; Al: 167 ± 56 ; As: 22.9 ± 22.23 ; Cd: 2.15 ± 0.94 ; Pb: 7.28 ± 4.5) as opposed to sites upstream of the Eindergatloop (in $\mu\text{g g}^{-1}$ DW; Al: 38 ± 0 ; As: 3.52 ± 0.99 ; Cd: 0.58 ± 0.26 ; Pb: 0.55 ± 0.33). Although the actual toxicity exerted on these organisms is not completely clear, there are obvious and often large differences in endogenous metal concentrations in *Calopteryx* reported here. As was the case for *Asellus*, non-essential metals present potential toxicity at low endogenous concentrations, indicating the potential metal-induced stress (here: Al, As, Cd, Pb) in *Calopteryx* in downstream sites (Rainbow, 2002).

Chironomidae are sediment-dwelling organisms that tolerate low oxygen levels (Bervoets et al., 2016) and are quite tolerant to chemically contaminated sites (Di Veroli et al., 2014). Because they live in close contact with freshwater sediments, they are exposed to concentrations of toxicants contained therein (Di Veroli et al., 2014). In our data, only As and Pb showed increased concentrations in chironomids, which contrasts the multiple significances found in water and sediment. Additionally, chironomids display sudden and strong changes rather than a clear metal gradient. Some of this variation is likely due to not having sufficient amounts of material to generate decent replicates of Prodiamesinae for metal analysis. For instance, only D1 and D2 contained enough chironomids (F. Prodiamesinae, specifically) for three replicates of three specimens each, while this was not the case in the other sites (often only one or two specimens per replicate, or other taxa than F. Prodiamesinae). Moreover, chironomids are relatively small compared to most of the collected *Asellus* and *Calopteryx*. As such, any variation may be inflated because of the low chironomid dry masses. For instance, there appear to be increases of Al, Cu and Zn starting from D4, but no significant differences were found. Nevertheless, even though As and Pb were significantly higher in downstream sites, these did not exceed threshold values determined by Bervoets et al. (2016). These observations can be compared with measurements by De Jonge et al. (2012), who evaluated endogenous concentrations of Cd, Zn and Pb at D2, D3 and D6 (identical to sites in the present

report) in Chironomidae. Notably, similar observations regarding differences between D2, D3 and D6 can be made in both our and De Jonge's results. For instance, D6 shows the highest concentrations in D6 for Zn, Cd and Pb in both our results and De Jonge's. However, this observation cannot be made for our measurements of metals in sediment or dissolved in water (i.e. D6 does not show higher metal concentrations as opposed to D2 and D3). Most interestingly, the present study shows decreased concentrations in chironomids for accumulated Zn, Cd and Pb compared to De Jonge et al. (2012), with the biggest differences in terms of downstream sites D3 and D6.

As several metals in water and sediment showed different patterns than those found in macroinvertebrates, a couple of other factors may be at play. For instance, other than the life history and ecology of the three taxa above, it is possible that *Asellus* are more resistant to pollution than the other two species (O'Callaghan et al., 2019). As reported in literature, these organisms have a wide ecological range: they can tolerate episodes of oxygen deficiency, low pH and have an intermediate tolerance to metals (Moldovan et al., 2001; O'Callaghan et al., 2019). At the same time, chironomids are reported to be suitable indicators of metal pollution by evaluating chironomid deformities as toxicity endpoints (Di Veroli et al., 2014), which may be an option for future research. Also, the level of metal adaptation in chironomids is highly dynamic (Groenendijk et al., 1999b). Further, differences in structural and functional organisation of a macroinvertebrate community are also important factors in determining metal bioavailability (Bervoets et al., 1997; Casas & Crecelius, 1994; Toro et al., 2001). Additional factors that determine metal bioavailability and community response include metal complexation (in the environment or to metal-binding proteins) or adaptation by chronic exposure to pollutants (Clements, 2004; Nahmani & Rossi, 2003; Rosabal et al., 2012).

However, the relationship between bioaccumulation and the onset of toxic effects is not as clear-cut, considering metals can often – to some extent – be stored in a detoxified form. In other words, metal toxicity is more dependent on the concentration of accumulated metal that is metabolically available, rather than the total accumulated metal concentration, i.e. when metal accumulation exceeds the rate of detoxification and/or excretion (Rainbow & Luoma, 2011).

No statistically different MMIF scores were found between up- and downstream sites or between sampling campaigns. According to the MMIF, the Dommel (or at least the part that was sampled in this report) is of 'moderate' water quality. This comes as no surprise, as there

was no strong distinction of pollution sensitive or tolerant species between up- and downstream sites. Distributions often showed high abundances for Asellidae and Chironomidae in sites up- and downstream of the Eindergatloop, indicating some degree of pollution in both groups. Additionally, no correlations were found between MMIF and any of the environmental variables. The lack of correlations contrasts with findings of Gabriels et al. (2010), who reported a positive correlation with dissolved oxygen and negative correlations with ammonium, nitrite, total phosphorous BOD and COD. De Jonge et al. (2008) also reported negative correlations with SO_4^{2-} and Zn in both water and sediment. Possibly, the lack of correlations may be related to adaptation (see earlier) or to the intrinsic ability of organisms to integrate environmental conditions over a longer timespan (Metcalf, 1989). As the present study only collected physicochemical data in three single point measurements (across three campaigns), these may display a high level of variability (as they are instantaneous in nature; ‘snapshots’) which was not the case for our MMIF results. Lastly, because physicochemical conditions have improved compared to those reported by De Jonge et al. (2008), there may not be enough environmental stress for macroinvertebrates to show distinct communities in up- and downstream sites.

Diatom indices show significant differences between sites up- and downstream of the Eindergatloop, while the MMIF does not. No differences between sampling campaigns were found for any of the indices. It is not entirely clear as to why the diatom indices responded to the gradient of metal pollution, while the MMIF did not. Perhaps it is related to the shorter life cycles of diatoms compared to macroinvertebrates. In other words, the faster diatom community turnover may be translated into faster responses to environmental changes (He et al., 2020). On the other hand, it is also possible that an adaptational response of macroinvertebrates obscured a distinctive pollution gradient along the six sites, which is indicated by the minor differences between macroinvertebrate communities.

Past and present

Regarding physicochemistry, comparisons for both in situ measurements and dissolved metal concentrations indicate that human activity in the area is still strongly affecting the downstream waters of the Dommel. Moreover, dissolved Zn and As concentrations in water have increased in both up- and downstream sites as compared with De Jonge (2008). This may indicate that other sources of pollution (other than the metallurgic industry) are also exerting pressure on the Dommel river, as upstream sites are not fed by the Eindergatloop. At the same time,

decreased concentrations of dissolved Cd and Pb in downstream sites are promising with respect to the river's water quality. Regarding sediment characteristics, there are indications that soil remediation in 2007 was relatively successful, given the decreased values for Zn, As, Cd and Pb reported here. Even so, downstream sites (as well as D1 for Zn and As) still show metal concentrations in sediment exceeding the EQS and it is not entirely clear whether other anthropogenic input has taken place between 2007 and 2019. As such, it cannot be stated for certain whether these elevated sediment concentrations (compared to De Jonge et al. (2008)) are completely attributed to historical metal contamination in the area or to other sources. For instance, we also reported elevated concentrations for ^sZn and ^sAs at site D1, indicating that there is another pollution source upstream of the Eindergatloop.

Comparing diatom index scores to findings of De Jonge et al. (2008), water quality in the Dommel today is higher than in 2006. Presently, TDI and IPS show distinctly higher scores, indicating an improvement of biological water quality. However, as taxonomy has changed strongly in the past 15 years, index calculations can not necessarily be compared as is. Re-evaluating samples collected by De Jonge would be advised to compare diatom indices. For MMIF, De Jonge et al. (2008) reported no significant difference between sites up- and downstream of the Eindergatloop, which falls in line with our findings. However, on average, MMIF has increased compared to the situation in 2006. Additionally, some differences were observed between De Jonge's sampling seasons, while no seasonal differences were found in the present study. Additionally, lower concentrations of accumulated Zn and Cd in Chironomidae were shown compared to values of 2006 (De Jonge et al., 2012). As for Pb, bioaccumulated concentrations have decreased only in D6, while remaining similar in D2 and D3. Overall, these observations imply that the Dommel's ecological quality has improved since 2006 in both upstream and downstream sites.

As such, even though biological conditions have improved, sites downstream of the Eindergatloop still appear to be exposed to elevated levels of pollution, which can be related to both historical contamination, as well as anthropogenic pressure in the present. Tackling pollution discharged by metallurgic industry embanked on the Eindergatloop (even though these are within the ecological quality standards) could alleviate some of the anthropogenic pressure on the Dommel. However, it is clear that the heavily populated area and other industrial activity ought to be responsible for other discharges into the Dommel, as elevated concentrations of metals were also reported in upstream sites.

Caveats and recommendations

The different sites were tested based on their up- or downstream location, but no samples were collected from the Eindergatloop itself, which could have been an interesting venture in an attempt to find correlations between physicochemical variables in the tributary and in the Dommel. Additionally, incorporating more climatological information (e.g. air temperature, precipitation) may provide more insight in physicochemical fluctuations in the river. Investigating reference sites that are located more closely together would also be advised. In this report, D1 was located further upstream from D3 than D7 was located downstream of the Eindergatloop. Additionally, having at least three (rather than two) reference sites could also alleviate some of the potential bias causing data and results to be skewed to one of the sampling sites. Furthermore, gathering more sediment samples during a single sampling would be preferable, as spatial variation at a given site may obscure patterns that would otherwise be quite distinct (De Cooman et al., 1995). Next, not having quantified bioavailability (e.g. through estimations via Organic Carbon (OC)) made interpretation of patterns in metal concentrations all the more challenging. If such data would be collected, more bolstered statements could be made on the presence or lack of metal pollution and metal-induced stress. Finally, re-evaluating samples collected by De Jonge et al. (2008) is advised to recalculate the index scores of IPS, IBD and TDI. Given the changes in diatom taxonomy and ecology, it would be interesting to explore how this would affect water quality assessment of 2006 samples using state-of-the-art diatom taxonomy.

5. Conclusion

In this report, sites downstream of the Eindergatloop showed different physicochemical conditions as opposed to upstream sites. Downstream waters showed elevated metal concentrations in both sediment and water for metals such as Cd and Pb. Downstream of the Eindergatloop, elevated concentrations were also found in water for Cu, Zn and As, as well as high levels of electrical conductivity, SO_4^{2-} and Cl^- . Additionally, macroinvertebrates showed higher metal concentrations for metals such as Zn, As, Cd and Pb in downstream sites compared to those collected upstream of the Eindergatloop. However, teratological diatom valves were not found to a degree that would signify a high(er) degree of metal pollution in downstream sites. Based on community analysis, diatoms reflected the metal pollution better than was the case for macroinvertebrates. The latter did show some differences between up- and downstream sites, but the high similarity of dominant taxa implied a certain degree of pollution across all sites. No distinctive effect of sampling season was found in either diatom or macroinvertebrate communities, opposed to physicochemical variation between sampling campaigns. Based on biotic indices, diatoms showed a better response to the metal pollution gradient along the Dommel. However, as diatom taxonomy has drastically changed over the past decade, a comparison is not straightforward with former studies in this area. Nevertheless, the IPS reflected the difference in metal concentrations between up- and downstream better than any of the other indices. The MMIF also showed an overall increase, which implies – combined with improvements in diatom indices (though limited due to changes in taxonomy), bioaccumulated metals in biota and physicochemistry of the Dommel – that the biological water quality has improved since De Jonge's work in 2006.

In summary, a combination of historical and present-day pollution in the Dommel appears to have an effect on both diatom and macroinvertebrate communities. Diatoms displayed decreased water quality in downstream sites based mostly on IPS, while macroinvertebrates mainly displayed the prevalence of metals in the Dommel based on internal metal concentrations. All in all, the Dommel's water quality has improved, but has not yet achieved the WFD goal of being of 'good ecological quality'.

6. Bibliography

Specific taxonomic literature

- Krammer, K., & Lange-Bertalot, H. (1991). Süßwasserflora von Mitteleuropa 2: Bacillariophyceae 4. Teil: Achnantheaceae Kritische Ergänzungen zu Navicula (Lineolatae) und Gomphonema. Gustav Fischer.
- Lange-Bertalot, H. (Ed.). (2001). Navicula sensu stricto: 10 genera separated from Navicula sensu lato Frustulia (Vol. 2). Koeltz Scientific Books.
- Lange-Bertalot, H., Båk, M., & Witkowski, A. (Eds.). (2011). Eunotia and some related genera (Vol. 6). Koeltz Scientific Books.
- Lange-Bertalot, H., Hofmann, G., Werum, M., & Cantonati, M. (2017). Freshwater benthic diatoms of Central Europe: Over 800 common species used in ecological assessment. (English edition with updated taxonomy and added species). Koeltz Botanical Books, Schmittens-Oberreifenberg.
- Wetzel, C. E., Lange-Bertalot, H., & Ector, L. (2017). Type analysis of Achnanthes oblongella Østrup and resurrection of Achnanthes saxonica Krasske (Bacillariophyta). Nova Hedwigia, Beihefte, 146, 209–227. <https://doi.org/10.1127/1438-9134/2017/209>
- Wetzel, Carlos E., Ector, L., Van de Vijver, B., Compère, P., & Mann, D. G. (2015). Morphology, typification and critical analysis of some ecologically important small naviculoid species (Bacillariophyta). Fottea, 15(2), 203–234. <https://doi.org/10.5507/fot.2015.020>

List of references

- Adams, W., Blust, R., Dwyer, R., Mount, D., Nordheim, E., Rodriguez, P. H., & Spry, D. (2020). Bioavailability Assessment of Metals in Freshwater Environments: A Historical Review. *Environmental Toxicology and Chemistry*, 39(1), 48–59. <https://doi.org/10.1002/etc.4558>
- AFNOR. (2000). Norme française NF T90-354 Juin 2000, Qualité de l'eau. Détermination de l'Indice Biologique Diatomées (IBD). (p. 63).
- André, F., Jonard, M., & Ponette, Q. (2007). Influence of meteorological factors and polluting environment on rain chemistry and wet deposition in a rural area near Chimay, Belgium. *Atmospheric Environment*, 41(7), 1426–1439. <https://doi.org/10.1016/j.atmosenv.2006.10.013>
- Bahls, L. L. (2009). A Checklist of Diatoms from Inland Waters of the Northwestern United States. *Proceedings of the Academy of Natural Sciences of Philadelphia*, 158(1), 1–35. <https://doi.org/10.1635/053.158.0101>
- Battarbee, R. W., Jones, V. J., Flower, R. J., Cameron, N. G., Bennion, H., Carvalho, L., & Juggins, S. (2001). Diatoms. In John P. Smol, H. J. B. Birks, W. M. Last, R. S. Bradley, & K. Alverson (Eds.), *Tracking Environmental Change Using Lake Sediments: Terrestrial, Algal, and Siliceous Indicators* (pp. 155–202). Springer Netherlands. https://doi.org/10.1007/0-306-47668-1_8
- Beasley, G., & Kneale, P. E. (2003). Investigating the influence of heavy metals on macro-invertebrate assemblages using Partial Cononical Correspondence Analysis (pCCA). *Hydrology and Earth System Sciences Discussions*, 7(2), 221–233.
- Begon, M., Townsend, C. R., & Harper, J. L. (2006). *Ecology: From Individuals to Ecosystems* (4th edition). Blackwell Publishing Ltd.
- Beltman, D. J., Clements, W. H., Lipton, J., & Cacela, D. (1999). Benthic invertebrate metals exposure, accumulation, and community-level effects downstream from a hard-rock mine site. *Environmental Toxicology and Chemistry*, 18(2), 299–307. <https://doi.org/10.1002/etc.5620180229>
- Bentaalla-Kaced, S., Aïfa, T., & Deramchi, K. (2017). Organic-rich Albian deposits as the origin of hydrocarbon-contaminated phosphates, southeastern Constantine Basin, Algeria. *Journal of Petroleum Science and Engineering*, 157, 680–695. <https://doi.org/10.1016/j.petrol.2017.07.064>
- Bervoets, L., & Blust, R. (2003). Metal concentrations in water, sediment and gudgeon (Gobio gobio) from a pollution gradient: Relationship with fish condition factor. *Environmental Pollution*, 126(1), 9–19. [https://doi.org/10.1016/S0269-7491\(03\)00173-8](https://doi.org/10.1016/S0269-7491(03)00173-8)
- Bervoets, L., Blust, R., de Wit, M., & Verheyen, R. (1997). Relationships between river sediment characteristics and trace metal concentrations in tubificid worms and chironomid larvae. *Environmental Pollution*, 95(3), 345–356. [https://doi.org/10.1016/S0269-7491\(96\)00134-0](https://doi.org/10.1016/S0269-7491(96)00134-0)
- Bervoets, L., De Jonge, M., & Blust, R. (2016). Identification of threshold body burdens of metals for the protection of the aquatic ecological status using two benthic invertebrates. *Environmental Pollution*, 210, 76–84. <https://doi.org/10.1016/j.envpol.2015.12.005>
- Besse-Lototskaya, A., Verdonschot, P. F. M., Coste, M., & Van de Vijver, B. (2011). Evaluation of European diatom trophic indices. *Ecological Indicators*, 11(2), 456–467. <https://doi.org/10.1016/j.ecolind.2010.06.017>
- Birk, S., Bonne, W., Borja, A., Brucet, S., Courrat, A., Poikane, S., Solimini, A., van de Bund, W., Zampoukas, N., & Hering, D. (2012). Three hundred ways to assess Europe's surface waters: An almost complete overview of biological methods to implement the Water Framework Directive. *Ecological Indicators*, 18, 31–41. <https://doi.org/10.1016/j.ecolind.2011.10.009>

- Bleeker, E. A. J., & van Gestel, C. A. M. (2007). Effects of spatial and temporal variation in metal availability on earthworms in floodplain soils of the river Dommel, The Netherlands. *Environmental Pollution*, **148**(3), 824–832. <https://doi.org/10.1016/j.envpol.2007.01.034>
- Blust, R., Linden, A. van der, Verheyen, E., & Decler, W. (1988). Evaluation of microwave heating digestion and graphite furnace atomic absorption spectrometry with continuum source background correction for the determination of iron, copper and cadmium in brine shrimp. *Journal of Analytical Atomic Spectrometry*, **3**(2), 387–393. <https://doi.org/10.1039/JA9880300387>
- Bolgovics, Á., Várbiro, G., Ács, É., Trábert, Z., Kiss, K. T., Pozderka, V., Görgényi, J., Boda, P., Lukács, B.-A., Nagy-László, Z., Abonyi, A., & Borics, G. (2017). Phytoplankton of rhithral rivers: Its origin, diversity and possible use for quality-assessment. *Ecological Indicators*, **81**, 587–596. <https://doi.org/10.1016/j.ecolind.2017.04.052>
- Bottjer, D. J. (2016). *Paleoecology: Past, present, and future*. Wiley-Blackwell.
- Briggs, J. C., & Ficke, J. F. (1977). *Quality of rivers of the United States, 1975 water year—Based on the National Stream Quality Accounting Network (NASQAN)*. (pp. 78–200). U.S. Geological Survey.
- Brooks, S., & Cham, S. (2014). *Field Guide to the Dragonflies & Damselflies of Great Britain and Ireland | NHBS Field Guides & Natural History* (5th ed.). British Wildlife Publishing. <https://www.nhbs.com/field-guide-to-the-dragonflies-damselflies-of-great-britain-and-ireland-book>
- Casas, A. M., & Crecelius, E. A. (1994). Relationship between acid volatile sulfide and the toxicity of zinc, lead and copper in marine sediments. *Environmental Toxicology and Chemistry*, **13**(3), 529–536. <https://doi.org/10.1002/etc.5620130325>
- Cemagref. (1982). *Etude des méthodes biologiques d'appréciation quantitative de la qualité des eaux. Rapport Division Qualité des Eux Lyon-A.F. in Bassin Rhône-Méditerranée-Corse [A study on the biological methods of qualitative assessment of water quality. A report of the Water Division Lyon-Outflow Rhône River section Catchment]* (p. 218). CEMAGREF.
- Cid, N., Ibáñez, C., Palanques, A., & Prat, N. (2010). Patterns of metal bioaccumulation in two filter-feeding macroinvertebrates: Exposure distribution, inter-species differences and variability across developmental stages. *Science of The Total Environment*, **408**(14), 2795–2806. <https://doi.org/10.1016/j.scitotenv.2010.03.030>
- CIW. (2016). *Summary of the Management Plan for the Flemish part of the International Scheldt/Meuse River Basin Districts* (p. 21). Coordination Committee on Integrated Water Policy. <https://www.integraalwaterbeleid.be/nl/stroomgebiedbeheerplannen/stroomgebiedbeheerplannen-2016-2021/documenten/engelse-vertaling-samenvatting-stroomgebiedbeheerplannen>
- Clements, W. H. (1994). Benthic Invertebrate Community Responses to Heavy Metals in the Upper Arkansas River Basin, Colorado. *Journal of the North American Benthological Society*, **13**(1), 30–44. JSTOR. <https://doi.org/10.2307/1467263>
- Clements, W. H. (2004). Small-Scale Experiments Support Causal Relationships Between Metal Contamination and Macroinvertebrate Community Responses. *Ecological Applications*, **14**(3), 954–967. <https://doi.org/10.1890/03-5009>
- Collier, K. J. (1995). Environmental factors affecting the taxonomic composition of aquatic macroinvertebrate communities in lowland waterways of Northland, New Zealand. *New Zealand Journal of Marine and Freshwater Research*, **29**(4), 453–465. <https://doi.org/10.1080/00288330.1995.9516679>
- Conrad, K. F., & Herman, T. B. (1990). Seasonal dynamics, movements and the effects of experimentally increased female densities on a population of imaginal Calopteryx aequabilis (Odonata: Calopterygidae). *Ecological Entomology*, **15**(2), 119–129. <https://doi.org/10.1111/j.1365-2311.1990.tb00792.x>
- Corcoll, N., Bonet, B., Morin, S., Tlili, A., Leira, M., & Guasch, H. (2012). The effect of metals on photosynthesis processes and diatom metrics of biofilm from a metal-contaminated river: A translocation experiment. *Ecological Indicators*, **18**, 620–631. <https://doi.org/10.1016/j.ecolind.2012.01.026>
- Coste, M., Boutry, S., Tison-Rosebery, J., & Delmas, F. (2009). Improvements of the Biological Diatom Index (BDI): Description and efficiency of the new version (BDI-2006). *Ecological Indicators*, **9**(4), 621–650. <https://doi.org/10.1016/j.ecolind.2008.06.003>
- Coste, Michel, & Ector, L. (2000). Diatomées invasives exotiques ou rares en France: Principales Observations effectuées au cours des dernières décennies. *Systematics and Geography of Plants*, **70**(2), 373–400. JSTOR. <https://doi.org/10.2307/3668651>
- Croteau, M.-N., & Luoma, S. N. (2008). A Biodynamic Understanding of Dietborne Metal Uptake by a Freshwater Invertebrate. *Environmental Science & Technology*, **42**(5), 1801–1806. <https://doi.org/10.1021/es7022913>
- Cui, B., Zhang, Q., Zhang, K., Liu, X., & Zhang, H. (2011). Analyzing trophic transfer of heavy metals for food webs in the newly-formed wetlands of the Yellow River Delta, China. *Environmental Pollution*, **159**(5), 1297–1306. <https://doi.org/10.1016/j.envpol.2011.01.024>
- Dalu, T., Wasserman, R. J., Magoro, M. L., Mwedzi, T., Froneman, P. W., & Weyl, O. L. F. (2017). Variation partitioning of benthic diatom community matrices: Effects of multiple variables on benthic diatom communities in an Austral temperate river system. *Science of The Total Environment*, **601–602**, 73–82. <https://doi.org/10.1016/j.scitotenv.2017.05.162>
- De Cooman, W., Seuntjens, P., Bervoets, L., Panis, L. I., De Wit, M., & Verheyen, R. F. (1995). Research on the Spatial Variability of Three Sediment Types in Flanders. In W. J. Van Den Brink, R. Bosman, & F. Arendt (Eds.), *Contaminated Soil '95* (pp. 191–192). Springer Netherlands. https://doi.org/10.1007/978-94-011-0415-9_31
- De Jonge, M., Belpaire, C., Geeraerts, C., De Cooman, W., Blust, R., & Bervoets, L. (2012). Ecological impact assessment of sediment remediation in a metal-contaminated lowland river using translocated zebra mussels and resident macroinvertebrates. *Environmental Pollution*, **171**, 99–108. <https://doi.org/10.1016/j.envpol.2012.07.038>

- De Jonge, Maarten, Van de Vijver, B., Blust, R., & Bervoets, L.** (2008). Responses of aquatic organisms to metal pollution in a lowland river in Flanders: A comparison of diatoms and macroinvertebrates. *Science of The Total Environment*, **407**(1), 615–629. <https://doi.org/10.1016/j.scitotenv.2008.07.020>
- de Paiva Magalhães, D., da Costa Marques, M. R., Baptista, D. F., & Buss, D. F.** (2015). Metal bioavailability and toxicity in freshwaters. *Environmental Chemistry Letters*, **13**(1), 69–87. <https://doi.org/10.1007/s10311-015-0491-9>
- De Pauw, N., Gabriels, W., & Goethals, P. L. M.** (2006). River Monitoring and Assessment Methods Based on Macroinvertebrates. In *Biological Monitoring of Rivers* (pp. 111–134). John Wiley & Sons, Ltd. <https://doi.org/10.1002/0470863781.ch7>
- De Pauw, N., & Heylen, S.** (2001). Biotic index for sediment quality assessment of watercourses in Flanders, Belgium. *Aquatic Ecology*, **35**(2), 121–133. <https://doi.org/10.1023/A:1011478427152>
- De Pauw, N., & Vanhooren, G.** (1983). Method for biological quality assessment of watercourses in Belgium. *Hydrobiologia*, **100**(1), 153–168. <https://doi.org/10.1007/BF00027428>
- De Pauw, N., & Vannevel, R.** (1991). *Macroinvertebraten en waterkwaliteit. Determineersleutels van macroin-vertebraten en beoordelingsmethoden van de waterkwaliteit*. Stichting Leefmilieu. <http://hdl.handle.net/1854/LU-228333>
- De Wolf, H.** (1982). *Method of coding of ecological data from diatoms for computer utilization*. **63**(2), 95–98.
- DeForest, D. K., Brix, K. V., & Adams, W. J.** (2007). Assessing metal bioaccumulation in aquatic environments: The inverse relationship between bioaccumulation factors, trophic transfer factors and exposure concentration. *Aquatic Toxicology*, **84**(2), 236–246. <https://doi.org/10.1016/j.aquatox.2007.02.022>
- Denys, L., & Lodeijckx, E.** (1984). *An improved method of coding diatom data for computer utilisation*. **93**(3), 297–299.
- Descy, J.-P., & Micha, J.-C.** (1988). Use of biological indices of water quality. *Statistical Journal of the United Nations Economic Commission for Europe*, **5**(3), 249–261. <https://doi.org/10.3233/SJU-1988-5305>
- Desrosiers, C., Leflaive, J., Eulin, A., & Ten-Hage, L.** (2013). Bioindicators in marine waters: Benthic diatoms as a tool to assess water quality from eutrophic to oligotrophic coastal ecosystems. *Ecological Indicators*, **32**, 25–34. <https://doi.org/10.1016/j.ecolind.2013.02.021>
- Di Veroli, A., Santoro, F., Pallottini, M., Selvaggi, R., Scardazza, F., Cappelletti, D., & Goretti, E.** (2014). Deformities of chironomid larvae and heavy metal pollution: From laboratory to field studies. *Chemosphere*, **112**, 9–17. <https://doi.org/10.1016/j.chemosphere.2014.03.053>
- Dobson, M., Pawley, S., Fletcher, M., & Powell, A.** (2012). *Guide to freshwater invertebrates* (A. Crowden, Ed.). Freshwater Biological Association.
- Dugdale, R. C., & Wilkerson, F. P.** (1998). Silicate regulation of new production in the equatorial Pacific upwelling. *Nature*, **391**(6664), 270–273. <https://doi.org/10.1038/34630>
- EauFrance.** (1994). *Diatoms: Specific Polluosensitivity Index (IPS) | MDM of Pike perch*. <http://mdm.sandre.eaufrance.fr/node/192739>
- European Commission.** (2000). *Directive 2000/60/EC of the European parliament and of the council of 23 October 2000: Establishing a framework for Community action in the field of water policy (Water Framework Directive)*. <https://eur-lex.europa.eu/eli/dir/2000/60/2014-11-20>
- Falasco, E., Bona, F., Badino, G., Hoffmann, L., & Ector, L.** (2009). Diatom teratological forms and environmental alterations: A review. *Hydrobiologia*, **623**(1), 1–35. <https://doi.org/10.1007/s10750-008-9687-3>
- Falkowski, P. G., Katz, M. E., Knoll, A. H., Quigg, A., Raven, J. A., Schofield, O., & Taylor, F. J. R.** (2004). The Evolution of Modern Eukaryotic Phytoplankton. *Science*, **305**(5682), 354–360. <https://doi.org/10.1126/science.1095964>
- Frag, A. M., Woodward, D. F., Goldstein, J. N., Brumbaugh, W., & Meyer, J. S.** (1998). Concentrations of metals associated with mining waste in sediments, biofilm, benthic macroinvertebrates, and fish from the Coeur d'Alene River basin, Idaho. *Archives of Environmental Contamination and Toxicology*, **34**(2), 119–127. <https://doi.org/10.1007/s002449900295>
- Ferreira da Silva, E., Almeida, S. F. P., Nunes, M. L., Luís, A. T., Borg, F., Hedlund, M., de Sá, C. M., Patinha, C., & Teixeira, P.** (2009). Heavy metal pollution downstream the abandoned Coval da Mó mine (Portugal) and associated effects on epilithic diatom communities. *Science of The Total Environment*, **407**(21), 5620–5636. <https://doi.org/10.1016/j.scitotenv.2009.06.047>
- Fore, L. S., & Grafe, C.** (2002). Using diatoms to assess the biological condition of large rivers in Idaho (U.S.A.). *Freshwater Biology*, **47**(10), 2015–2037. <https://doi.org/10.1046/j.1365-2427.2002.00948.x>
- Friberg, N., Bonada, N., Bradley, D. C., Dunbar, M. J., Edwards, F. K., Grey, J., Hayes, R. B., Hildrew, A. G., Lamouroux, N., Trimmer, M., & Woodward, G.** (2011). Biomonitoring of Human Impacts in Freshwater Ecosystems: The Good, the Bad and the Ugly. In G. Woodward (Ed.), *Advances in Ecological Research* (Vol. 44, pp. 1–68). Academic Press. <https://doi.org/10.1016/B978-0-12-374794-5.00001-8>
- Gabriels, W., Lock, K., De Pauw, N., & Goethals, P. L. M.** (2010). Multimetric Macroinvertebrate Index Flanders (MMIF) for biological assessment of rivers and lakes in Flanders (Belgium). *Limnologia - Ecology and Management of Inland Waters*, **40**(3), 199–207. <https://doi.org/10.1016/j.limno.2009.10.001>
- Gamier, J., Billen, G., & Coste, M.** (1995). Seasonal succession of diatoms and Chlorophyceae in the drainage network of the Seine River: Observation and modeling. *Limnology and Oceanography*, **40**(4), 750–765. <https://doi.org/10.4319/lo.1995.40.4.0750>
- Groenendijk, D., Kraak, M. H. S., & Admiraal, W.** (1999a). Efficient shedding of accumulated metals during metamorphosis in metal-adapted populations of the midge Chironomus riparius. *Environmental Toxicology and Chemistry*, **18**(6), 1225–1231. <https://doi.org/10.1002/etc.5620180622>
- Groenendijk, D., van Opzeeland, B., Dionisio Pires, L. M., & Postma, J. F.** (1999b). Fluctuating Life-History Parameters Indicating Temporal Variability in Metal Adaptation in Riverine Chironomids. *Archives of Environmental Contamination and Toxicology*, **37**(2), 175–181. <https://doi.org/10.1007/s002449900503>

- Groenendijk, D., Zeinstra, L. W. M., & Postma, J. F. (1998). Fluctuating asymmetry and mentum gaps in populations of the midge *Chironomus riparius* (diptera: Chironomidae) from a metal-contaminated river. *Environmental Toxicology and Chemistry*, **17**(10), 1999–2005. <https://doi.org/10.1002/etc.5620171016>
- Håkansson, H., & Bailey-Watts, A. E. (1993). A Contribution to the Taxonomy of *Stephanodiscus Hantzschii* Grunow, a Common Freshwater Planktonic Diatom. *Diatom Research*, **8**(2), 317–332. <https://doi.org/10.1080/0269249X.1993.9705265>
- Hare, L. (1992). Aquatic Insects and Trace Metals: Bioavailability, Bioaccumulation, and Toxicity. *Critical Reviews in Toxicology*, **22**(5–6), 327–369. <https://doi.org/10.3109/10408449209146312>
- Hawkes, H. A. (1979). Invertebrates as Indicators of River Water Quality. In James & Evison (Eds.), *Biological Indicators of Water Quality*.
- He, S., Chen, K., Soininen, J., Heino, J., Ding, N., & Wang, B. (2020). Elements of metacommunity structure of diatoms and macroinvertebrates within stream networks differing in environmental heterogeneity. *Journal of Biogeography*, **47**(8), 1755–1764. <https://doi.org/10.1111/jbi.13859>
- Herr, C., De Becker, P., Leyssen, A., & Van Thuyne, G. (2014). *Advies betreffende de impact van lozingen in het brongebied van de Bolisserbeek* (INBO.A.2013.135; p. 23). INBO. <https://purews.inbo.be/ws/files/2237006/INBO.A.2013.135.pdf>
- Ivorra, N., Barranguet, C., Jonker, M., Kraak, M. H. S., & Admiraal, W. (2002). Metal-induced tolerance in the freshwater microbenthic diatom *Gomphonema parvulum*. *Environmental Pollution*, **116**(1), 147–157. [https://doi.org/10.1016/S0269-7491\(01\)00152-X](https://doi.org/10.1016/S0269-7491(01)00152-X)
- Jochems, H., Schneiders, A., Denys, L., & Van den Bergh, E. (2002). *Typologie van de oppervlaktewateren in Vlaanderen*.
- Johnson, D. M. (1991). Behavioral ecology of larval dragonflies and damselflies. *Trends in Ecology & Evolution*, **6**(1), 8–13. [https://doi.org/10.1016/0169-5347\(91\)90140-S](https://doi.org/10.1016/0169-5347(91)90140-S)
- Jongman, R. H. G., Ter Braak, C. J. F., & Van Tongeren, O. F. R. (Eds.). (1995). *Data analysis in community and landscape ecology*. Cambridge University Press.
- Kasuya, E. (2001). Mann–Whitney U test when variances are unequal. *Animal Behaviour*, **61**(6), 1247–1249. <https://doi.org/10.1006/anbe.2001.1691>
- Kelly, M. G. (1998). Use of the trophic diatom index to monitor eutrophication in rivers. *Water Research*, **32**(1), 236–242. [https://doi.org/10.1016/S0043-1354\(97\)00157-7](https://doi.org/10.1016/S0043-1354(97)00157-7)
- Kelly, M. G., Adams, C., Graves, A. C., Jamieson, J., Krokowski, J., Lycett, E. B., Murray-Bligh, J., Pritchard, S., & Wilkins, C. (2001). *The Trophic Diatom Index: A User's Manual—R&D Technical Report E2/TR2* (p. 146). Environment Agency.
- Kelly, M. G., Cazaubon, A., Coring, E., Dell'Uomo, A., Ector, L., Goldsmith, B., Guasch, H., Hürlimann, J., Jarlman, A., Kawecka, B., Kwadrans, J., Laugaste, R., Lindstrøm, E.-A., Leitao, M., Marvan, P., Padisák, J., Pipp, E., Prygiel, J., Rott, E., ... Vizinet, J. (1998). Recommendations for the routine sampling of diatoms for water quality assessments in Europe. *Journal of Applied Phycology*, **10**(2), 215. <https://doi.org/10.1023/A:1008033201227>
- Kelly, M. G., & Whitton, B. A. (1995). The Trophic Diatom Index: A new index for monitoring eutrophication in rivers. *Journal of Applied Phycology*, **7**(4), 433–444. <https://doi.org/10.1007/BF00003802>
- Kelly, M., Juggins, S., Guthrie, R., Pritchard, S., Jamieson, J., Rippey, B., Hirst, H., & Yallop, M. (2008). Assessment of ecological status in U.K. rivers using diatoms. *Freshwater Biology*, **53**(2), 403–422. <https://doi.org/10.1111/j.1365-2427.2007.01903.x>
- Kelly, M. K., & Yallop, M. (2012). *A streamlined taxonomy for the Trophic Diatom Index*. Environment Agency.
- Klemm, D. J., Blocksom, K. A., Fulk, F. A., Herlihy, A. T., Hughes, R. M., Kaufmann, P. R., Peck, D. V., Stoddard, J. L., Thoeny, W. T., Griffith, M. B., & Davis, W. S. (2003). Development and Evaluation of a Macroinvertebrate Biotic Integrity Index (MBII) for Regionally Assessing Mid-Atlantic Highlands Streams. *Environmental Management*, **31**(5), 0656–0669. <https://doi.org/10.1007/s00267-002-2945-7>
- Kociolek, J. P. (2005). *A checklist and preliminary bibliography of the recent freshwater diatoms of inland environments of the continental United States*. **56**(27), 395–525.
- Kociolek, J. P. (2006). *Some thoughts on the development of a diatom flora for freshwater ecosystems in the continental United States and a listing of recent taxa described from U.S. freshwaters*. **57**(21), 561–586.
- Kolkwitz, R., & Marsson, M. (1908). Ökologie der pflanzlichen Saprobien. *Berichte Der Deutschen Botanischen Gesellschaft*, **26**(7), 505–519. <https://doi.org/10.1111/j.1438-8677.1908.tb06722.x>
- Krammer, K., & Lange-Bertalot, H. (1991). *Süßwasserflora von Mitteleuropa 2: Bacillariophyceae 4. Teil: Achnantheaceae Kritische Ergänzungen zu Navicula (Lineolatae) und Gomphonema* (Vol. 2). Gustav Fischer.
- Kröger, N., & Poulsen, N. (2008). Diatoms—From Cell Wall Biogenesis to Nanotechnology. *Annual Review of Genetics*, **42**(1), 83–107. <https://doi.org/10.1146/annurev.genet.41.110306.130109>
- Kutschera, U. (2003). The Feeding Strategies of the Leech *Erpobdella octoculata* (L.): A Laboratory Study. *International Review of Hydrobiology*, **88**(1), 94–101. <https://doi.org/10.1002/iroh.200390008>
- Lange-Bertalot, H., Hofmann, G., Werum, M., & Cantonati, M. (2017). *Freshwater benthic diatoms of Central Europe: Over 800 common species used in ecological assessment*. (English edition with updated taxonomy and added species). Koeltz Botanical Books, Schmittens-Oberreifenberg.
- Lavoie, I., Hamilton, P. B., Morin, S., Kim Tiam, S., Kahlert, M., Gonçalves, S., Falasco, E., Fortin, C., Gontero, B., Heudre, D., Kojadinovic-Sirinelli, M., Manoylov, K., Pandey, L. K., & Taylor, J. C. (2017). Diatom teratologies as biomarkers of contamination: Are all deformities ecologically meaningful? *Ecological Indicators*, **82**, 539–550. <https://doi.org/10.1016/j.ecolind.2017.06.048>
- Lecoointe, C., Coste, M., & Prygiel, J. (1993). “Omnidia”: Software for taxonomy, calculation of diatom indices and inventories management. *Hydrobiologia*, **269**(1), 509–513. <https://doi.org/10.1007/BF00028048>

- Lecointe, C., Coste, M., Prygiel, J., & Ector, L. (2008). *OMNIDIA version 5.2 software for diatom-based water quality assessment*.
- Lenoir, A., & Coste, M. (1996). *Development of a practical diatom index of overall water quality applicable to the French National Water Board Network*. (Use of Algae in Monitoring Rivers II, pp. 29–43). Institut für Botanik.
- Lewin, I. (2006). The gastropod communities in the lowland rivers of agricultural areas - their biodiversity and bioindicative value in the ciechanowska upland, Central Poland. *Malacologia*, **49**(1), 7–23. <https://doi.org/10.4002/1543-8120-49.1.7>
- Li, R., Carter, J. A., Xie, S., Zou, S., Gu, Y., Zhu, J., & Xiong, B. (2010). Phytoliths and microcharcoal at Jinluojia archeological site in middle reaches of Yangtze River indicative of paleoclimate and human activity during the last 3000 years. *Journal of Archaeological Science*, **37**(1), 124–132. <https://doi.org/10.1016/j.jas.2009.09.022>
- Loria, A., Cristescu, M. E., & Gonzalez, A. (2019). Mixed evidence for adaptation to environmental pollution. *Evolutionary Applications*, **12**(7), 1259–1273. <https://doi.org/10.1111/eva.12782>
- Luís, A. T., Teixeira, P., Almeida, S. F. P., Ector, L., Matos, J. X., & Ferreira da Silva, E. A. (2009). Impact of Acid Mine Drainage (AMD) on Water Quality, Stream Sediments and Periphytic Diatom Communities in the Surrounding Streams of Aljustrel Mining Area (Portugal). *Water, Air, and Soil Pollution*, **200**(1), 147–167. <https://doi.org/10.1007/s11270-008-9900-z>
- Luoma, S. N., & Rainbow, P. S. (2005). Why Is Metal Bioaccumulation So Variable? Biodynamics as a Unifying Concept. *Environmental Science & Technology*, **39**(7), 1921–1931. <https://doi.org/10.1021/es048947e>
- Majewska, R., D'Alelio, D., & De Stefano, M. (2014). *Cocconeis Ehrenberg* (Bacillariophyta), a genus dominating diatom communities associated with *Posidonia oceanica* Delile (monocotyledons) in the Mediterranean Sea. *Aquatic Botany*, **112**, 48–56. <https://doi.org/10.1016/j.aquabot.2013.07.008>
- Mann, D. G., & Droop, S. J. M. (1996). 3. Biodiversity, biogeography and conservation of diatoms. *Hydrobiologia*, **336**(1), 19–32. <https://doi.org/10.1007/BF00010816>
- Mann, K. H. (1955). The ecology of the British freshwater leeches. *Journal of Animal Ecology*, **24**(1), 98–119.
- McCune, B., & Grace, J. B. (2002). Chapter 9: Data Transformations. In *Analysis of Ecological Communities* (pp. 67–79). MjM Software Design.
- Medley, C. N., & Clements, W. H. (1998). Responses of Diatom Communities to Heavy Metals in Streams: The Influence of Longitudinal Variation. *Ecological Applications*, **8**(3), 631–644. JSTOR. <https://doi.org/10.2307/2641255>
- Medlin, L. K. (2016). Evolution of the diatoms: Major steps in their evolution and a review of the supporting molecular and morphological evidence. *Phycologia*, **55**(1), 79–103. <https://doi.org/10.2216/15-105.1>
- Metcalfe, J. L. (1989). Biological water quality assessment of running waters based on macroinvertebrate communities: History and present status in Europe. *Environmental Pollution*, **60**(1), 101–139. [https://doi.org/10.1016/0269-7491\(89\)90223-6](https://doi.org/10.1016/0269-7491(89)90223-6)
- meteoblue. (2020). *Weerarchie Neerpelt: 2019-08-01—2019-08-31*. https://www.meteoblue.com/nl/weer/historyclimate/weatherarchive/neerpelt_belgi%c3%ab_2790357?fcstlength=1m&year=2019&month=8
- Moldovan, M., Rauch, S., Gómez, M., Antonia Palacios, M., & Morrison, G. M. (2001). Bioaccumulation of palladium, platinum and rhodium from urban particulates and sediments by the freshwater isopod *Asellus aquaticus*. *Water Research*, **35**(17), 4175–4183. [https://doi.org/10.1016/S0043-1354\(01\)00136-1](https://doi.org/10.1016/S0043-1354(01)00136-1)
- Montoya-Moreno, Y., & Aguirre-Ramirez, N. (2013). Knowledge to Ecological Preferences in a Tropical Epiphytic Algae to Use with Eutrophication Indicators. *Journal of Environmental Protection*, **2013**. <https://doi.org/10.4236/jep.2013.411A004>
- Morin, S., Duong, T. T., Dabrin, A., Coynel, A., Herlory, O., Baudrimont, M., Delmas, F., Durrieu, G., Schäfer, J., Winterton, P., Blanc, G., & Coste, M. (2008). Long-term survey of heavy-metal pollution, biofilm contamination and diatom community structure in the Riou Mort watershed, South-West France. *Environmental Pollution*, **151**(3), 532–542. <https://doi.org/10.1016/j.envpol.2007.04.023>
- Morin, Soizic, Cordonier, A., Lavoie, I., Arini, A., Blanco, S., Duong, T. T., Tornés, E., Bonet, B., Corcoll, N., Faggiano, L., Laviale, M., Pérès, F., Becares, E., Coste, M., Feurtet-Mazel, A., Fortin, C., Guasch, H., & Sabater, S. (2012). Consistency in Diatom Response to Metal-Contaminated Environments. In H. Guasch, A. Ginebreda, & A. Geiszinger (Eds.), *Emerging and Priority Pollutants in Rivers: Bringing Science into River Management Plans* (pp. 117–146). Springer. https://doi.org/10.1007/978-3-642-25722-3_5
- Morin, Soizic, Duong, T. T., Herlory, O., Feurtet-Mazel, A., & Coste, M. (2008). Cadmium Toxicity and Bioaccumulation in Freshwater Biofilms. *Archives of Environmental Contamination and Toxicology*, **54**(2), 173–186. <https://doi.org/10.1007/s00244-007-9022-4>
- Mosleh, Y. Y., Paris-Palacios, S., & Biagiatti-Risbourg, S. (2006). Metallothioneins induction and antioxidative response in aquatic worms *Tubifex tubifex* (Oligochaeta, Tubificidae) exposed to copper. *Chemosphere*, **64**(1), 121–128. <https://doi.org/10.1016/j.chemosphere.2005.10.045>
- Moss, B. (2008). The Water Framework Directive: Total environment or political compromise? *Science of The Total Environment*, **400**(1), 32–41. <https://doi.org/10.1016/j.scitotenv.2008.04.029>
- Nahmani, J., & Rossi, J.-P. (2003). Soil macroinvertebrates as indicators of pollution by heavy metals. *Comptes Rendus Biologies*, **326**(3), 295–303. [https://doi.org/10.1016/S1631-0691\(03\)00070-2](https://doi.org/10.1016/S1631-0691(03)00070-2)
- Nordberg, G., Fowler, B., & Nordberg, M. (Eds.). (2015). *Handbook on the Toxicology of Metals—4th Edition* (4th Edition). Academic Press/Elsevier. <https://www.elsevier.com/books/handbook-on-the-toxicology-of-metals/nordberg/978-0-444-59453-2>
- Nyrstar. (2019). *Balen/Pelt fact sheet*. Nyrstar. <https://www.nyrstar.com/~media/Files/N/Nyrstar/operations/melting/2019%20Fact%20Sheet%20-Balen.pdf>

- O'Callaghan, I., Harrison, S., Fitzpatrick, D., & Sullivan, T. (2019). The freshwater isopod *Asellus aquaticus* as a model biomonitor of environmental pollution: A review. *Chemosphere*, *235*, 498–509. <https://doi.org/10.1016/j.chemosphere.2019.06.217>
- Orefice, I., Musella, M., Smerilli, A., Sansone, C., Chandrasekaran, R., Corato, F., & Brunet, C. (2019). Role of nutrient concentrations and water movement on diatom's productivity in culture. *Scientific Reports*, *9*(1), 1479. <https://doi.org/10.1038/s41598-018-37611-6>
- Palma, P., Ledo, L., & Alvarenga, P. (2015). Assessment of trace element pollution and its environmental risk to freshwater sediments influenced by anthropogenic contributions: The case study of Alqueva reservoir (Guadiana Basin). *CATENA*, *128*, 174–184. <https://doi.org/10.1016/j.catena.2015.02.002>
- Pan, Y., Stevenson, R. J., Hill, B. H., & Herlihy, A. T. (2000). Ecoregions and benthic diatom assemblages in Mid-Atlantic Highlands streams, USA. *Journal of the North American Benthological Society*, *19*(3), 518–540. <https://doi.org/10.2307/1468112>
- Passy, S. I. (2007). Diatom ecological guilds display distinct and predictable behavior along nutrient and disturbance gradients in running waters. *Aquatic Botany*, *86*(2), 171–178. <https://doi.org/10.1016/j.aquabot.2006.09.018>
- Pawlowski, J., Kelly-Quinn, M., Altermatt, F., Apothéloz-Perret-Gentil, L., Beja, P., Boggero, A., Borja, A., Bouchez, A., Cordier, T., Domaizon, I., Feio, M. J., Filipe, A. F., Fornaroli, R., Graf, W., Herder, J., van der Hoorn, B., Iwan Jones, J., Sagova-Mareckova, M., Moritz, C., ... Kahlert, M. (2018). The future of biotic indices in the ecogenomic era: Integrating (e)DNA metabarcoding in biological assessment of aquatic ecosystems. *Science of The Total Environment*, *637–638*, 1295–1310. <https://doi.org/10.1016/j.scitotenv.2018.05.002>
- Petelet-Giraud, E., Klaver, G., & Negrel, P. (2009). Natural versus anthropogenic sources in the surface- and groundwater dissolved load of the Dommel river (Meuse basin): Constraints by boron and strontium isotopes and gadolinium anomaly. *Journal of Hydrology*, *369*(3), 336–349. <https://doi.org/10.1016/j.jhydrol.2009.02.029>
- Pienkos, P. T., & Darzins, A. (2009). The promise and challenges of microalgal-derived biofuels. *Biofuels, Bioproducts and Biorefining*, *3*(4), 431–440. <https://doi.org/10.1002/bbb.159>
- Piette, M. H. A., & De Letter, E. A. (2006). Drowning: Still a difficult autopsy diagnosis. *Forensic Science International*, *163*(1), 1–9. <https://doi.org/10.1016/j.forsciint.2004.10.027>
- Postma, J. F., & Groenendijk, D. (1999). Adaptation to metals in the midge *Chironomus riparius*: A case study in the River Dommel. In V. E. Forbes, *Genetics and Ecotoxicology* (pp. 79–101). Taylor and Francis. https://books.google.be/books?id=vU4rEqu8_7UC&pg=PA81&dq=Dommel+characterization+river&hl=en&sa=X&ved=2ahUKEWjCmu7intXqAhXCGewKHUbnDmkQ6wEWAHoECAMQAQ#v=onepage&q&f=false
- Potapova, M. G., & Charles, D. F. (2002). Benthic diatoms in USA rivers: Distributions along spatial and environmental gradients. *Journal of Biogeography*, *29*(2), 167–187. <https://doi.org/10.1046/j.1365-2699.2002.00668.x>
- Potapova, M. G., Charles, D. F., Ponader, K. C., & Winter, D. M. (2004). Quantifying species indicator values for trophic diatom indices: A comparison of approaches. *Hydrobiologia*, *517*(1), 25–41. <https://doi.org/10.1023/B:HYDR.0000027335.73651.ea>
- Prygiel, J., & Coste, M. (1993). Utilisation des indices diatomiques pour la mesure de la qualité des eaux du bassin Artois-Picardie: Bilan et perspectives. *Annales de Limnologie - International Journal of Limnology*, *29*(3), 255–267. <https://doi.org/10.1051/limn/1993021>
- Prygiel, J., & Coste, M. (1995). Les diatomées et le diagnostic de la qualité des eaux courantes continentales: Les principales méthodes indiciaires. *Vie Milieu*, *45*, 179–186.
- Prygiel, Jean, Carpentier, P., Almeida, S., Coste, M., Druart, J.-C., Ector, L., Guillard, D., Honoré, M.-A., Iserentant, R., Ledeganck, P., Lalanne-Cassou, C., Lesniak, C., Mercier, L., Moncaut, P., Nazart, M., Nouchet, N., Peres, F., Peeters, V., Rimet, F., ... Zydek, N. (2002). Determination of the biological diatom index (IBD NF T 90–354): Results of an intercomparison exercise. *Journal of Applied Phycology*, *14*(1), 27–39. <https://doi.org/10.1023/A:1015277207328>
- Prygiel, L., Leveque, L., & Iserentant, R. (1996). *Un nouvel Indice Diatomique Pratique pour l'évaluation de la qualité des eaux en réseau de surveillance*.
- Quintaneiro, C., Ranville, J., & Nogueira, A. J. A. (2015). Effects of the essential metals copper and zinc in two freshwater detritivores species: Biochemical approach. *Ecotoxicology and Environmental Safety*, *118*, 37–46. <https://doi.org/10.1016/j.ecoenv.2015.04.006>
- Rainbow, P. S., & Luoma, S. N. (2011). Metal toxicity, uptake and bioaccumulation in aquatic invertebrates—Modelling zinc in crustaceans. *Aquatic Toxicology (Amsterdam, Netherlands)*, *105*(3–4), 455–465. <https://doi.org/10.1016/j.aquatox.2011.08.001>
- Rainbow, P. S., Poirier, L., Smith, B. D., Brix, K. V., & Luoma, S. N. (2006). Trophic transfer of trace metals from the polychaete worm *Nereis diversicolor* to the polychaete *N. virens* and the decapod crustacean *Palaemonetes varians*. *Marine Ecology Progress Series*, *321*, 167–181. <https://doi.org/10.3354/meps321167>
- Rainbow, Philip S. (2002). Trace metal concentrations in aquatic invertebrates: Why and so what? *Environmental Pollution*, *120*(3), 497–507. [https://doi.org/10.1016/S0269-7491\(02\)00238-5](https://doi.org/10.1016/S0269-7491(02)00238-5)
- Reátegui-Zirena, E. G., French, A. D., Klein, D. M., & Salice, C. J. (2017). Cadmium Compartmentalization in the Pulmonate Snail *Lymnaea stagnalis*: Improving Our Understanding of Exposure. *Archives of Environmental Contamination and Toxicology*, *72*(4), 575–585. <https://doi.org/10.1007/s00244-017-0407-8>
- Rosabal, M., Hare, L., & Campbell, P. G. C. (2012). Subcellular metal partitioning in larvae of the insect *Chaoborus* collected along an environmental metal exposure gradient (Cd, Cu, Ni and Zn). *Aquatic Toxicology*, *120–121*, 67–78. <https://doi.org/10.1016/j.aquatox.2012.05.001>
- Rott, E., Duthie, H. C., & Pipp, E. (1998). Monitoring organic pollution and eutrophication in the Grand River, Ontario, by means of diatoms. *Canadian Journal of Fisheries and Aquatic Sciences*, *55*(6), 1443–1453. <https://doi.org/10.1139/f98-038>

- Round, F. E., Crawford, R. M., & Mann, D. G. (1990). *The Diatoms. Biology and Morphology of the Genera*. (1 edition). Cambridge University Press.
- Sabater, S. (2000). Diatom communities as indicators of environmental stress in the Guadiamar River, S-W. Spain, following a major mine tailings spill. *Journal of Applied Phycology*, **12**(2), 113–124. <https://doi.org/10.1023/A:1008197411815>
- Sarkar, B. (2002). *Heavy metals in the environment*. CRC Press.
- Sbihi, K., Cherifi, O., Bertrand, M., & Gharmali, A. E. (2014). Biosorption of metals (Cd, Cu and Zn) by the freshwater diatom *Planorhynchium lanceolatum*: A laboratory study. *Diatom Research*, **29**(1), 55–63. <https://doi.org/10.1080/0269249X.2013.872193>
- Schmidt, T. S., Clements, W. H., Mitchell, K. A., Church, S. E., Wanty, R. B., Fey, D. L., Verplanck, P. L., & Juan, C. A. S. (2010). Development of a new toxic-unit model for the bioassessment of metals in streams. *Environmental Toxicology and Chemistry*, **29**(11), 2432–2442. <https://doi.org/10.1002/etc.302>
- Sekiranda, S. B. K., Okot-Okumu, J., Bugenyi, F. W. B., Ndawula, L. M., & Gandhi, P. (2004). Variation in composition of macro-benthic invertebrates as an indication of water quality status in three bays in Lake Victoria. *Uganda Journal of Agricultural Sciences*, **9**(1), 396–411. <https://doi.org/10.4314/ujas.v9i1>
- Sgro, G. V., Poole, J. B., & Johansen, J. R. (2007). Diatom species composition and ecology of the Animas river watershed, Colorado, USA. *Western North American Naturalist*, **67**(4), 510–519. [https://doi.org/10.3398/1527-0904\(2007\)67\[510:DSCAEO\]2.0.CO;2](https://doi.org/10.3398/1527-0904(2007)67[510:DSCAEO]2.0.CO;2)
- Shannon, C. E. (1948). *A Mathematical Theory of Communication*. **27**, 379–423, 623–656.
- Shikhova, L. N. (2017). Heavy Metals in Soils And Parent Rocks Of Natural Lands in North-East Of European Russia. In *Heavy Metals and Other Pollutants in the Environment* (pp. 3–30). Apple Academic Press. <https://doi.org/10.1201/9781315366029-1>
- Sládeček, V. (1973). *System of water quality from the biological point of view*. **7**, 1–218.
- Sládeček, V. (1986). Diatoms as Indicators of Organic Pollution. *Acta Hydrochimica et Hydrobiologica*, **14**(5), 555–566. <https://doi.org/10.1002/aheh.19860140519>
- Smol, J. P., & Stoermer, E. F. (2010). *The Diatoms: Applications for the Environmental and Earth Sciences* (2nd edition). Cambridge University Press.
- Šporka, F., Vlek, H. E., Bulánková, E., & Krno, I. (2006). Influence of seasonal variation on bioassessment of streams using macroinvertebrates. In M. T. Furse, D. Hering, K. Brabec, A. Buffagni, L. Sandin, & P. F. M. Verdonchot (Eds.), *The Ecological Status of European Rivers: Evaluation and Intercalibration of Assessment Methods* (pp. 543–555). Springer Netherlands. https://doi.org/10.1007/978-1-4020-5493-8_36
- Stocchino, G. A., & Manconi, R. (2013). Overview of life cycles in model species of the genus *Dugesia* (Platyhelminthes: Tricladida). *Italian Journal of Zoology*, **80**(3), 319–328. <https://doi.org/10.1080/11250003.2013.822025>
- Stockdale, A., Tipping, E., Lofts, S., Ormerod, S. J., Clements, W. H., & Blust, R. (2010). Toxicity of proton–metal mixtures in the field: Linking stream macroinvertebrate species diversity to chemical speciation and bioavailability. *Aquatic Toxicology*, **100**(1), 112–119. <https://doi.org/10.1016/j.aquatox.2010.07.018>
- Stone, J. R., Westover, K. S., & Cohen, A. S. (2011). Late Pleistocene paleohydrography and diatom paleoecology of the central basin of Lake Malawi, Africa. *Palaeogeography, Palaeoclimatology, Palaeoecology*, **303**(1), 51–70. <https://doi.org/10.1016/j.palaeo.2010.01.012>
- Toro, D. M. D., Allen, H. E., Bergman, H. L., Meyer, J. S., Paquin, P. R., & Santore, R. C. (2001). Biotic ligand model of the acute toxicity of metals. 1. Technical Basis. *Environmental Toxicology and Chemistry*, **20**(10), 2383–2396. <https://doi.org/10.1002/etc.5620201034>
- Uchida, N., Kubota, K., Aita, S., & Kazama, S. (2020). Aquatic insect community structure revealed by eDNA metabarcoding derives indices for environmental assessment. *PeerJ*, **8**. <https://doi.org/10.7717/peerj.9176>
- van Dam, H., Mertens, A., & Sinkeldam, J. (1994). A coded checklist and ecological indicator values of freshwater diatoms from The Netherlands. *Netherlands Journal of Aquatic Ecology*, **28**(1), 117–133. <https://doi.org/10.1007/BF02334251>
- Van de Vijver, B., & Beyens, L. (1998). Diatoms and water quality in the Kleine Nete, a Belgian lowland stream. *Limnologia*, **28**(2), 145–152.
- Van de Vijver, Bart, Beyens, L., Vincke, S., & Gremmen, N. J. M. (2004). Moss-inhabiting diatom communities from Heard Island, sub-Antarctic. *Polar Biology*, **27**(9), 532–543. <https://doi.org/10.1007/s00300-004-0629-x>
- van der Werff, A. (1953). A new method of concentrating and cleaning diatoms and other organisms. *SIL Proceedings*, **12**(1), 276–277. <https://doi.org/10.1080/03680770.1950.11895297>
- Van Ginneken, M., De Jonge, M., Bervoets, L., & Blust, R. (2015). Uptake and toxicity of Cd, Cu and Pb mixtures in the isopod *Asellus aquaticus* from waterborne exposure. *Science of The Total Environment*, **537**, 170–179. <https://doi.org/10.1016/j.scitotenv.2015.07.153>
- van Hattum, B., de Voogt, P., van den Bosch, L., van Straalen, N. M., Joosse, E. N. G., & Govers, H. (1989). Bioaccumulation of cadmium by the freshwater isopod *Asellus aquaticus* (L.) from aqueous and dietary sources. *Environmental Pollution*, **62**(2), 129–151. [https://doi.org/10.1016/0269-7491\(89\)90183-8](https://doi.org/10.1016/0269-7491(89)90183-8)
- van Hattum, B., Timmermans, K. R., & Govers, H. A. (1991). Abiotic and biotic factors influencing in situ trace metal levels in macroinvertebrates in freshwater ecosystems. *Environmental Toxicology and Chemistry*, **10**(2), 275–292. <https://doi.org/10.1002/etc.5620100217>
- Van Thuyne, G., Breine, J., & Belpaire, C. (2009). *Visbestanden op de Dommel in het kader van de sanering van de bodem ...* (p. 59). INBO. <https://issuu.com/vlaanderen-be/docs/c2eabbfc-34af-44d8-b42c-ba5d350824a7/10?ff>
- Vasselon, V., Rimet, F., Tapolczai, K., & Bouchez, A. (2017). Assessing ecological status with diatoms DNA metabarcoding: Scaling-up on a WFD monitoring network (Mayotte island, France). *Ecological Indicators*, **82**, 1–12. <https://doi.org/10.1016/j.ecolind.2017.06.024>

- VMM. (2014). *Druk en impact analyse in afstroomzone (VL05_136)*. Vlaamse Milieumaatschappij.
- VMM. (2020). *Geoloket*. Geoloket Water. <http://geoloket.vmm.be/>
- Waite, I. R., Herlihy, A. T., Larsen, D. P., Urquhart, N. S., & Klemm, D. J. (2004). The effects of macroinvertebrate taxonomic resolution in large landscape bioassessments: An example from the Mid-Atlantic Highlands, U.S.A. *Freshwater Biology*, **49**(4), 474–489. <https://doi.org/10.1111/j.1365-2427.2004.01197.x>
- Wallace, J. B., & Webster, J. R. (1996). The Role of Macroinvertebrates in Stream Ecosystem Function. *Annual Review of Entomology*, **41**(1), 115–139. <https://doi.org/10.1146/annurev.en.41.010196.000555>
- Waterschap De Dommel. (2019). *Factsheet waterlichaam Boven Dommel (NL27_BO_1_2)*. Waterschap De Dommel.
- Waterschap De Dommel. (2020). *Werkgebied* [Pagina]. Waterschap De Dommel; Waterschap De Dommel. /werkgebied
- Weckström, K., & Juggins, S. (2006). Coastal Diatom–Environment Relationships from the Gulf of Finland, Baltic Sea. *Journal of Phycology*, **42**(1), 21–35. <https://doi.org/10.1111/j.1529-8817.2006.00166.x>
- Weigand, H., Weiss, M., Cai, H., Li, Y., Yu, L., Zhang, C., & Leese, F. (2018). Fishing in troubled waters: Revealing genomic signatures of local adaptation in response to freshwater pollutants in two macroinvertebrates. *Science of The Total Environment*, **633**, 875–891. <https://doi.org/10.1016/j.scitotenv.2018.03.109>
- Wetzel, C. E., Lange-Bertalot, H., & Ector, L. (2017). Type analysis of *Achnanthes oblongella* Østrup and resurrection of *Achnanthes saxonica* Krasske (Bacillariophyta). *Nova Hedwigia, Beihefte*, **146**, 209–227. <https://doi.org/10.1127/1438-9134/2017/209>
- Wetzel, Carlos E., Martínez-Carreras, N., Hlúbíková, D., Hoffmann, L., Pfister, L., & Ector, L. (2013). New Combinations and Type Analysis of Chamaepinnularia Species (Bacillariophyceae) from Aerial Habitats. *Cryptogamie, Algologie*, **34**(2), 149–168. <https://doi.org/10.7872/crya.v34.iss2.2013.149>
- Winder, M., & Schindler, D. E. (2004). Climate Change Uncouples Trophic Interactions in an Aquatic Ecosystem. *Ecology*, **85**(8), 2100–2106. <https://doi.org/10.1890/04-0151>
- Witkowski, A., Cedro, B., Kierzek, A., & Baranowski, D. (2009). Diatoms as a proxy in reconstructing the Holocene environmental changes in the south-western Baltic Sea: The lower Rega River Valley sedimentary record. In K. Buczkó, J. Korponai, J. Padišák, & S. W. Starratt (Eds.), *Palaeolimnological Proxies as Tools of Environmental Reconstruction in Fresh Water* (pp. 155–172). Springer Netherlands. https://doi.org/10.1007/978-90-481-3387-1_9
- Wu, X., Cobbina, S. J., Mao, G., Xu, H., Zhang, Z., & Yang, L. (2016). A review of toxicity and mechanisms of individual and mixtures of heavy metals in the environment. *Environmental Science and Pollution Research*, **23**(9), 8244–8259. <https://doi.org/10.1007/s11356-016-6333-x>
- Zaikov, G. E., Weisfeld, L. I., Lisitsyn, E. M., & Bekuzarova, S. A. (Eds.). (2017). *Heavy metals and other pollutants in the environment*. Apple Academic Press.
- Zelinka, M., & Marvan, P. (1961). *Zur Präzisierung der biologischen Klassifikation des Rheinhet fliessender Gewässer*. **57**, 389–407.
- Zhang, Y., Peng, C., Wang, J., Huang, S., Hu, Y., Zhang, J., & Li, D. (2019). Temperature and silicate are significant driving factors for the seasonal shift of dominant diatoms in a drinking water reservoir. *Journal of Oceanology and Limnology*, **37**(2), 568–579. <https://doi.org/10.1007/s00343-019-8040-1>
- Zurzolo, C., & Bowler, C. (2001). Exploring Bioinorganic Pattern Formation in Diatoms. A Story of Polarized Trafficking. *Plant Physiology*, **127**(4), 1339–1345. <https://doi.org/10.1104/pp.010709>

7. Appendix

Appendix 1: Classification of ecological attributes

Table 1A: Classification of ecological indicator values according to Van Dam et al. (1994).

(R) pH				
1	acidobiontic	optimal occurrence at pH <5.5		
2	acidophilous	mainly occurring at pH <7		
3	circumneutral	mainly occurring at pH-values about 7		
4	alkaliphilous	mainly occurring at pH > 7		
5	alkalibiontic	exclusively occurring at pH >7		
6	indifferent	no apparent optimum		
(H) Salinity		Cl⁻ (mg l⁻¹)	Salinity ‰	
1	fresh	<100	<0.2	
2	fresh brackish	<500	<0.9	
3	brackish fresh	500-1000	0.9 - 1.8	
4	brackish fresh	1000-500	1.8 - 9.0	
(O) Oxygen requirements				
1	continuously high (about 100% saturation)			
2	fairly high (above 75% saturation)			
3	moderate (above 50% saturation)			
4	low (above 30% saturation)			
5	very low (about 10% saturation)			
(S) Saprobity		H₂O quality class	O₂ (%)	BOD₅²⁰ (mg l⁻¹)
1	oligosaprobous	I, I-II	>85	<2
2	β-mesosaprobous	II	70 - 85	2 - 4
3	α-mesosaprobous	III	25 - 70	4 - 13
4	α -meso-/polysaprobous	III-IV	10 - 25	13 - 22
5	polysaprobous	IV	< 10	>22
(T) Trophic state				
1	oligotraphentic			
2	oligo-mesotraphentic			
3	mesotraphentic			
4	meso-eutraphentic			
5	eutraphentic			
6	hypereutraphentic			
7	oligo- to eutraphentic (hypereutraphentic)			

Appendix 2: Macroinvertebrate tolerance scores (TS)

Table 2A: List with macroinvertebrate taxa and corresponding tolerance scores (TS) used for calculating Multimetric Macroinvertebrate Index Flanders (MMIF) metrics. From Gabriels et al. (2010).

Taxon	TS	Taxon	TS
Platyhelminthes		Hemiptera	
<i>Bdellocephala</i>	5	<i>Aphelocheirus</i>	8
<i>Crenobia</i>	7	<i>Arctocorisa</i>	5
<i>Dendrocoelum</i>	5	<i>Callicorixa</i>	5
<i>Dugesia</i> s.l.	5	<i>Corixa</i>	5
<i>Phagocata</i>	5	<i>Cymatia</i>	6
<i>Planaria</i>	6	<i>Gerris</i> s.l.	6
<i>Polycelis</i>	6	<i>Glaenocorisa</i>	5
Polychaeta		<i>Hebrus</i>	6
Ampharetidae	3	<i>Hesperocorixa</i>	5
Oligochaeta		<i>Hydrometra</i>	6
Aelosomatidae	2	<i>Ilyocoris</i>	5
Branchiobdellidae	2	<i>Mesovelgia</i>	6
Enchytraeidae	2	<i>Micronecta</i>	6
Haplotaxidae	4	<i>Microvelia</i>	7
Lumbricidae	2	<i>Naucoris</i>	6
Lumbriculidae	2	<i>Nepa</i>	6
Naididae s.s.	5	<i>Notonecta</i>	5
Tubificidae	1	<i>Paracorixa</i>	5
Hirudinea		<i>Plea</i>	6
<i>Cystobranchus</i>	4	<i>Ranatra</i>	6
<i>Dina</i>	4	<i>Sigara</i>	5
<i>Erpobdella</i>	3	<i>Velia</i>	7
<i>Glossiphonia</i>	4	Odonata	
<i>Haementeria</i>	4	<i>Aeshna</i>	6
<i>Haemopis</i>	4	<i>Anax</i>	6
<i>Helobdella</i>	4	<i>Brachytron</i>	7
<i>Hemiclepsis</i>	4	<i>Calopteryx</i>	8
<i>Hirudo</i>	4	<i>Cercion</i>	7
<i>Piscicola</i>	5	<i>Ceriagrion</i>	7
<i>Theromyzon</i>	4	<i>Coenagrion</i>	6
<i>Trocheta</i>	4	<i>Cordulegaster</i>	9
Mollusca		<i>Cordulia</i>	7
<i>Acroloxus</i>	6	<i>Crocothemis</i>	7
<i>Ancylus</i>	7	<i>Enallagma</i>	7
<i>Anisus</i>	5	<i>Epitheca</i>	7
<i>Anodonta</i>	6	<i>Erythromma</i> s.s.	7
<i>Aplexa</i>	6	<i>Gomphus</i>	7
<i>Armiger</i>	6	<i>Ischnura</i>	6
<i>Bathyomphalus</i>	5	<i>Lestes</i>	7
<i>Bithynia</i>	5	<i>Leucorrhinia</i>	7
<i>Bythinella</i>	8	<i>Libellula</i>	7

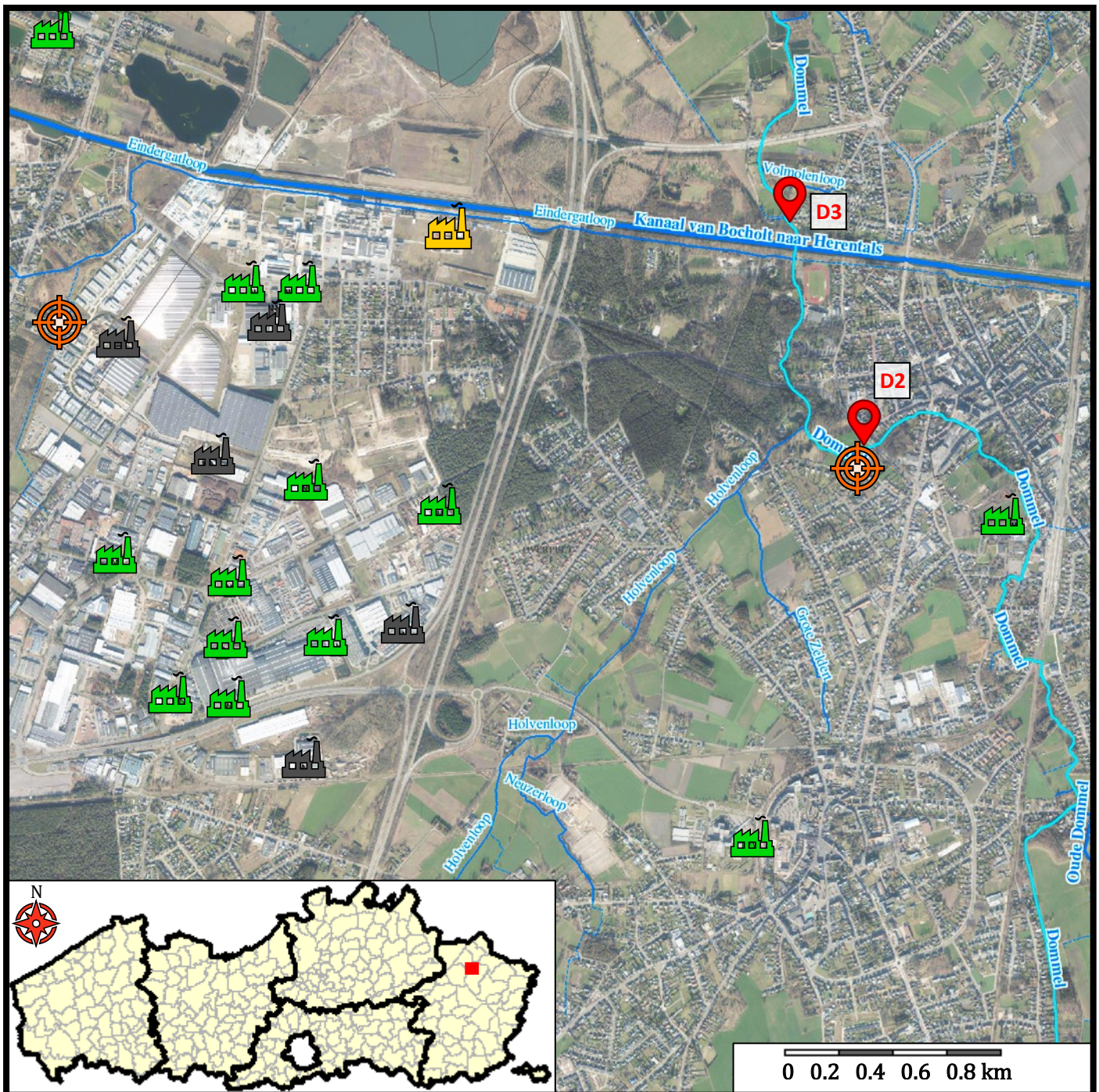
Appendix 2: Macroinvertebrate tolerance scores (TS) – continued (1)

Taxon	TS	Taxon	TS
<i>Corbicula</i>	5	<i>Nehalennia</i>	7
<i>Dreissena</i>	5	<i>Onychogomphus</i>	7
<i>Ferrissia</i>	7	<i>Ophiogomphus</i>	7
<i>Gyraulus</i>	6	<i>Orthetrum</i>	7
<i>Hippeutis</i>	6	<i>Oxygastra</i>	7
<i>Lithoglyphus</i>	6	<i>Platycnemis</i>	7
<i>Lymnaea</i> s.l.	5	<i>Pyrrhosoma</i>	7
<i>Margaritifera</i>	10	<i>Somatochlora</i>	7
<i>Marstoniopsis</i>	5	<i>Sympetma</i>	7
<i>Menetus</i>	5	<i>Sympetrum</i>	7
<i>Myxas</i>	7	Ephemeroptera	
<i>Physa</i> s.s.	5	<i>Baetis</i>	6
<i>Physella</i>	3	<i>Brachycercus</i>	7
<i>Pisidium</i>	4	<i>Caenis</i>	6
<i>Planorbarius</i>	5	<i>Centroptilum</i>	7
<i>Planorbis</i>	6	<i>Cloeon</i>	6
<i>Potamopyrgus</i>	6	<i>Ecyonurus</i>	9
<i>Pseudamnicola</i> s.l.	5	<i>Epeorus</i>	10
<i>Pseudanodonta</i>	6	<i>Ephemera</i>	8
<i>Segmentina</i>	6	<i>Ephemerella</i> s.l.	8
<i>Sphaerium</i>	4	<i>Ephoron</i>	9
<i>Theodoxus</i>	7	<i>Habroleptoides</i>	8
<i>Unio</i>	6	<i>Habrophlebia</i>	8
<i>Valvata</i>	6	<i>Heptagenia</i> s.l.	10
<i>Viviparus</i>	6	<i>Isonychia</i>	7
Acari		<i>Leptophlebia</i> s.s.	8
<i>Hydracarina</i> s.l.	5	<i>Metreletus</i>	7
Crustacea		<i>Oligoneuriella</i>	7
Argulidae	5	<i>Paraleptophlebia</i>	8
Asellidae	4	<i>Potamanthus</i>	8
Astacidae	8	<i>Procloeon</i>	7
Atyidae	7	<i>Rhitrogena</i>	10
Cambaridae	6	<i>Siphonurus</i>	7
Chirocephalidae	6	Trichoptera	
Corophiidae	5	Beraeidae	9
Crangonyctidae	4	Brachycentridae	9
Gammaridae	5	Ecnomidae	6
Janiridae	5	Glossosomatidae	9
Leptestheriidae	6	Goeridae	9
Limnadiidae	6	Hydropsychidae	6
Mysidae	5	Hydroptilidae	8
Palaemonidae	5	Lepidostomatidae	9
Panopeidae	4	Leptoceridae	8
Sphaeromatidae	4	Limnephilidae s.l.	8

Appendix 2: Macroinvertebrate tolerance scores (TS) – continued (2)

Taxon	TS	Taxon	TS
Talitridae	5	Molannidae	9
Triopsidae	6	Odontoceridae	9
Varunidae	4	Philopotamidae	6
Diptera		Phryganeidae	9
Athericidae	7	Polycentropodidae	6
Blephariceridae	7	Psychomyiidae	7
Ceratopogonidae	3	Rhyacophilidae	8
Chaoboridae	3	Sericostomatidae	8
Chironomidae (Chir).		Plecoptera	
Chir. non <i>thummi-plumosus</i>	3	<i>Amphinemura</i>	9
Chir. <i>thummi-plumosus</i>	2	<i>Brachyptera</i>	10
Culicidae	3	<i>Capnia</i> s.l.	10
Cylindrotomidae	3	<i>Chloroperia</i> s.l.	10
Dixidae	6	<i>Dinocras</i>	10
Dolichopodidae	3	<i>Isogenus</i>	10
Empididae	3	<i>Isoperla</i>	10
Ephydriidae	3	<i>Leuctra</i>	9
Limoniidae	4	<i>Marthamea</i>	10
Muscidae	3	<i>Nemoura</i>	8
Psychodidae	3	<i>Nemurella</i>	8
Ptychopteridae	3	<i>Perla</i>	10
Rhagionidae	3	<i>Perlodes</i>	10
Scatophagidae	3	<i>Protonemura</i>	9
Sciomyzidae	3	<i>Rhabdiopteryx</i>	10
Simuliidae	5	<i>Taeniopteryx</i>	10
Stratiomyidae	4		
Syrphidae	1		
Tabanidae	3		
Thaumaleidae	3		
Tipulidae	3		
Megaloptera			
<i>Sialis</i>	5		
Coleoptera			
Dryopidae	6		
Dytiscidae	5		
elminthidae	7		
Gyrinidae	7		
Haliplidae	6		
Hydraenidae	6		
Hydrophilidae	5		
Hygrobiidae	5		
Noteridae	5		
Pesephenidae	6		
Scirtidae	7		

Appendix 3A: Industrial activity and wastewater treatment in study area (1)







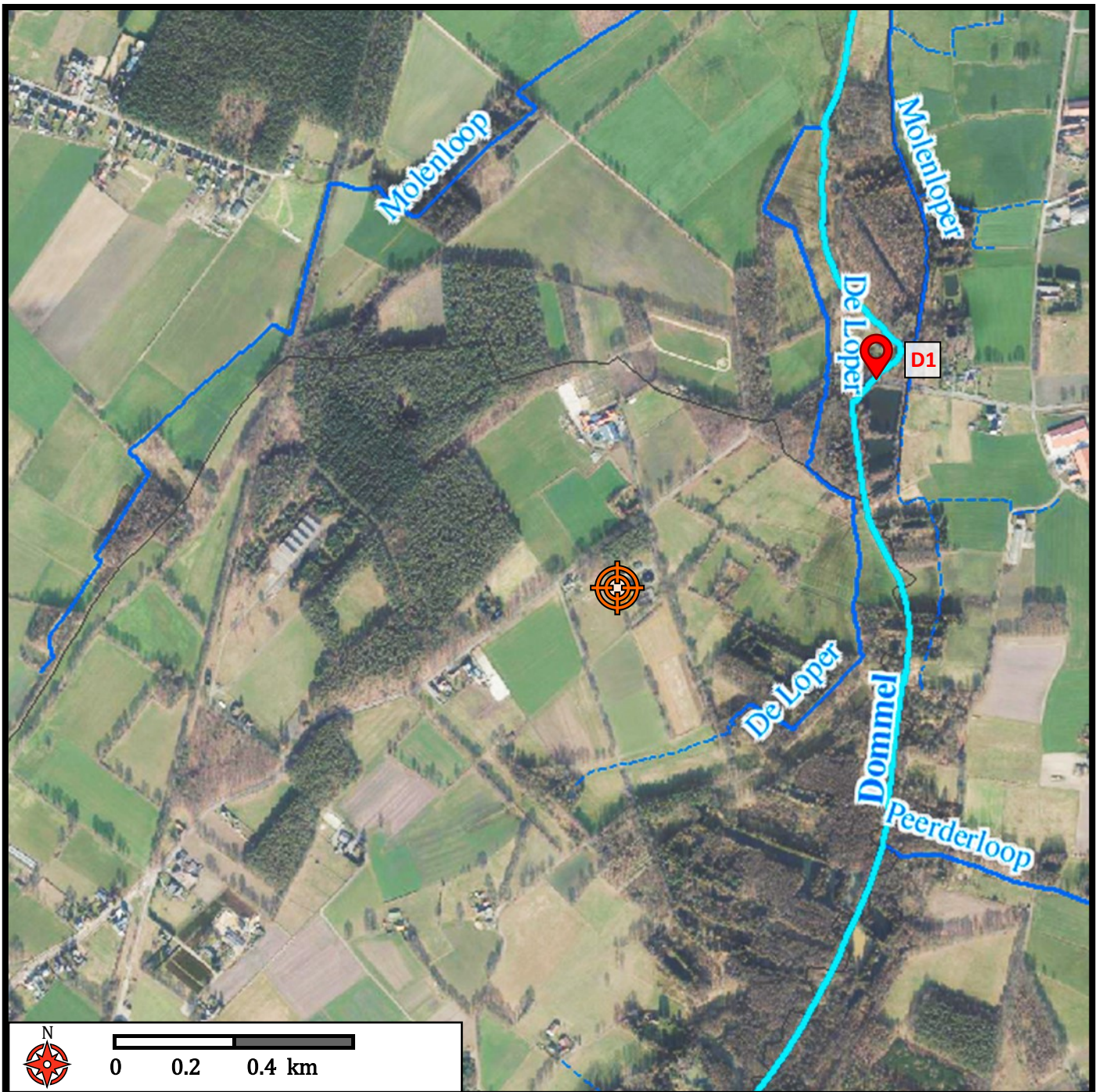
-  Site of active industrial discharge
-  Site of non-active industrial discharge
-  Sewage treatment plant
-  Measuring site - Dommel

Figure 3A: Map of the area near the Eindergatloop tributary of the Dommel river – locality in Flanders indicated with a red box (bottom left). The course of the Dommel river is shown in cyan, while tributaries and other waterways are shown in dark blue. Additionally, sewage treatment plants (orange) and sites of industrial discharge (active – green; inactive – grey) are shown along with some of the measuring sites assessed in this thesis. Metallurgic industry presently discharging into the Eindergatloop indicated in yellow. Map adapted from VMM GeoViews.

Appendix 3A: Industrial activity and wastewater treatment in study area (2)



Sewage treatment plant



Measuring site - Dommel

Figure 3B: Map of the area near the Eindergatloop tributary of the Dommel river – locality in Flanders indicated with a red box (Figure 3A). Sewage treatment plant (orange) is shown near site D1 covered in this thesis.

Appendix 3B: General information of study sites

Table 3A: General information of all study sites covered in this thesis. Site numbers, VMM code (VMM nr.), coordinates, additional information (sampling location, diatom substrate) and index values of De Jonge et al. (2008) are included. Multimetric Macroinvertebrate Index Flanders or MMIF (2008) show means of samples taken on 09/08/2006 and 12/12/2006. Diatom indices Specific Polluosensitivity Index (IPS), Trophic Diatom Index (TDI) and Diatom Biological Index (IBD) (2008) show averages of samples taken on 09/08/2006 and 09/11/2006.

Site	D1	D2	D3	D4	D6	D7
VMM nr.	93000	92100	91700	E001523	91000	E003575
Position	upstream	upstream	downstream	downstream	downstream	downstream
Coordinates (Lambert; x,y)	224672, 207495	223907, 213568	223523, 214512	223148, 216099	233950, 218100	225272, 221621
Coordinates (WGS 84)	51°10'21.4"N 5°26'11.4"E	51°13'37.5"N 5°25'35.9"E	51°14'10.0"N 5°25'17.3"E	51°15'0.5"N 5°24'59.2"E	51°16'4.9"N 5°25'42.0"E	51°17'29.0"N 5°26'18.7"E
Sampling location	upstream of bridge	downstream of bridge + overflow	downstream of bridge	upstream of bridge	upstream of bridge	downstream of bridge
Diatom substrate	pebbles	pebbles	pebbles	scraped (shore wall)	pebbles	scraped (shore wall)
IPS (2008) (n = 2)	10.8 ± 0.6	11.2 ± 3.2	8.5 ± 0.3	8.2 ± 1.3	9.9 ± 1.6	9.6 ± 0.9
TDI (2008) (n = 2)	88.7 ± 8.3	78.1 ± 15.1	82 ± 5.3	80.5 ± 9.3	77.6 ± 3.7	77.3 ± 4
IBD (2008) (n = 2)	12.1 ± 2.6	13.9 ± 2.4	12.5 ± 0.2	11 ± 1.2	11.9 ± 0.1	11.6 ± 0.3
MMIF (2008) (n = 2)	0.5 ± 0.0	0.5 ± 0.1	0.4 ± 0.1	0.3 ± 0.1	0.4 ± 0.1	0.5 ± 0.1

Appendix 4: Macroinvertebrate tolerance scores (TS)

Table 4A: Table with score conversions from MMIF metrics (Taxa richness = TAX; number of Ephemeroptera, Plecoptera and Trichoptera = EPT; number of non-sensitive taxa = NST; Shannon-Wiener diversity index = SWD; mean tolerance score = MTS) to scores ranging from 0 to 4. Only score conversions for river type 'Grote beek Kempen/Large brook Kempen' (BgK) are shown. For a full list, see Gabriels et al. (2010).

River Type: BgK							
Score	TAX	EPT	NST	SWD	MTS	MMIF score	Evaluation of quality
0	≤ 5	0	0	≤ 0.2	≤ 2	0.90 - 1.00	High
1	≤ 13.25	≤ 2.25	≤ 2.5	≤ 1.025	≤ 3.125	0.70 - 0.89	Good
2	≤ 21.5	≤ 4.5	≤ 5	≤ 1.85	≤ 4.25	0.50 - 0.69	Moderate
3	≤ 29.75	≤ 6.75	≤ 7.5	≤ 2.675	≤ 5.375	0.30 - 0.49	Poor
4	> 29.75	> 6.75	> 7.5	> 2.675	> 5.375	0.00 - 0.29	Bad

Appendix 5A

Table 5A: General physicochemical characteristics of all water samples (A: 17/04/2019; B: 21/08/2019; C: 24/01/2020). Including in situ measurements of acidity (pH), water temperature (Temp.), electrical conductivity (EC), oxygen saturation (pc.O2), oxygen content (O₂). Additionally, concentrations of phosphate (PO₄³⁻-P), ammonia (NH₄⁺-N), nitrite (NO₂⁻-N), nitrate (NO₃⁻-N), sulfate (SO₄²⁻) and chloride (Cl⁻) are shown. Whenever ecological quality standards (EQS; VLAREM II) were available, these were included at the bottom of the table. Values exceeding the EOS are indicated in red.

Sample	pH	Temp. (T) °C	EC/Cond. μS cm ⁻¹	pc.O ₂ %	O ₂ (O) mg L ⁻¹	PO ₄ ³⁻ -P mg P L ⁻¹	NH ₄ ⁺ -N mg N L ⁻¹	NO ₂ ⁻ -N mg N L ⁻¹	NO ₃ ⁻ -N mg N L ⁻¹	SO ₄ ²⁻ (S) mg L ⁻¹	Cl ⁻ (Cl) mg L ⁻¹
D1A	7.68	11.1	312	80.3	8.39	0.041	0.37	0.08	4.27	49	33
D2A	7.82	12.2	334	91.1	9.76	0.041	0.27	0.07	4.31	55	37
D3A	8.20	12.8	1111	83.4	8.55	0.111	0.79	0.11	3.80	131	223
D4A	7.99	12.8	1048	80.2	8.14	0.080	0.71	0.11	3.58	124	198
D6A	7.89	12.7	945	79.0	8.27	0.053	0.55	0.10	3.22	112	179
D7A	7.21	12.4	900	80.2	8.50	0.053	0.62	0.10	3.04	109	166
D1B	6.80	15.4	305	83.9	8.46	0.019	0.19	0.05	3.47	41	31
D2B	6.63	16	311	80.7	8.04	0.037	0.40	0.06	2.74	45	31
D3B	6.81	18.2	1564	72.4	6.88	0.071	0.29	0.08	2.63	153	313
D4B	6.87	17.8	1579	72.9	7.00	0.044	0.22	0.07	2.38	150	317
D6B	6.96	17.4	1207	80.2	7.50	0.026	0.13	0.05	1.96	130	234
D7B	7.21	18.9	1268	104.4	9.79	0.025	0.06	0.04	1.91	120	236
D1C	8.82	9.1	346	80.4	9.21	0.065	0.80	0.05	5.52	48	38
D2C	7.25	8.3	361	78.0	9.13	0.067	0.54	0.09	4.59	53	41
D3C	6.80	9.3	1255	66.3	7.58	0.110	0.82	0.13	4.28	186	213
D4C	6.76	9.5	1209	65.7	7.47	0.095	0.77	0.12	4.06	175	204
D6C	6.82	9.5	1153	63.9	7.29	0.080	0.77	0.11	3.42	162	198
D7C	6.89	9.2	927	68.2	7.81	0.064	0.66	0.09	3.26	127	158
D1-D2	7.5 ± 0.8	12 ± 3.2	328 ± 22	82.4 ± 4.7	8.83 ± 0.64	0.045 ± 0.018	0.43 ± 0.22	0.07 ± 0.01	4.15 ± 0.96	49 ± 5	35 ± 4
D3-D7	7.2 ± 0.52	13.4 ± 3.8	1181 ± 222	76.4 ± 11.1	7.9 ± 0.81	0.068 ± 0.029	0.53 ± 0.28	0.09 ± 0.03	3.13 ± 0.78	140 ± 25	220 ± 51
EQS	5.5 ≤ pH ≤ 8.5	T ≤ 25	EC ≤ 600	% < 120	O > 6	P ≤ 0.14	/	/	N < 10	S < 90	Cl < 120

Appendix 5B(1)

Table 5B.1: Metal concentrations measured in filtered water (denoted by ^wM) samples (A: 17/04/2019; B: 21/08/2019; C: 24/01/2020). Aluminium (Al), chromium (Cr), manganese (Mn), iron (Fe), cobalt (Co), copper (Cu), zinc (Zn), arsenic (As), cadmium (Cd) and lead (Pb) are shown. The ecological quality standards (EQS) for lead is based on WFD 2008/105/EC, while other EQS are according to Flemish regulation (VLAREM II) and are shown at the bottom. The EQS for ^wCd depends on CaCO₃ concentration and is shown in Appendix 5D. Values exceeding the EQS are indicated in red. The average values in upstream and downstream sites are included (upstream: D1, D2; downstream: D3, D4, D6, D7).

Sample	^w Al	^w Cr	^w Mn	^w Fe	^w Co	^w Cu	^w Zn	^w As	^w Cd	^w Pb
	µg/L	µg/L	µg/L	µg/L	µg/L	µg/L	µg/L	µg/L	µg/L	µg/L
D1A	10	0.6	201.5	243	14.3	3.0	95	2.2	0.3	0.1
D2A	10	0.6	187.9	187	14.9	1.9	99	1.5	0.2	0.1
D3A	20	0.7	160.3	120	11.3	3.3	179	3.0	0.9	0.3
D4A	14	0.7	156.1	154	10.7	3.2	166	4.6	0.5	0.2
D6A	11	0.6	140.9	193	9.0	2.3	148	4.0	0.3	0.2
D7A	8	0.6	132.1	142	9.0	2.2	128	3.5	0.3	0.2
D1B	2	0.3	59.2	157	2.8	0.8	28	1.2	0.05*	0.1
D2B	2	0.3	90.2	141	4.0	0.9	15	2.1	0.05*	0.1
D3B	6	0.5	76.2	70	3.8	2.2	67	3.0	0.2	0.4
D4B	4	0.5	73.6	96	3.3	2.1	59	3.4	0.2	0.3
D6B	6	0.5	73.9	121	3.0	2.6	63	3.5	0.2	0.3
D7B	7	0.4	51.9	96	2.2	3.2	62	3.2	0.2	0.3
D1C	17	0.8	239.3	355	17.4	1.6	116	2.0	0.3	0.1
D2C	13	0.8	260.4	233	15.7	1.7	118	1.7	0.1	0.1
D3C	28	1.4	193.6	129	10.9	3.6	176	3.3	0.4	0.4
D4C	27	1.4	202.1	168	11.1	3.6	180	4.4	0.3	0.4
D6C	19	1.3	172.6	254	9.1	3.2	150	5.0	0.2	0.4
D7C	20	0.9	175.2	300	9.9	2.5	139	4.5	0.2	0.4
D1-D2	9 ± 6	0.6 ± 0.2	173 ± 81	219 ± 78	11.5 ± 6.4	1.7 ± 0.8	79 ± 45	1.8 ± 0.4	0.2 ± 0.1	0.1 ± 0
D3-D7	14 ± 8	0.8 ± 0.4	134 ± 52	154 ± 67	7.8 ± 3.6	2.8 ± 0.6	126 ± 50	3.8 ± 0.7	0.3 ± 0.2	0.3 ± 0.1
EQS	/	Cr<5	/	/	Co<0.5	Cu<7	Zn<20	As<3	~CaCO ₃	Pb<7.2

Appendix 5B(2)

Table 5B.2: Total metal concentrations measured in unfiltered water (denoted by ^{w*}M) samples (A: 17/04/2019; B: 21/08/2019; C: 24/01/2020). Aluminium (Al), chromium (Cr), manganese (Mn), iron (Fe), cobalt (Co), copper (Cu), zinc (Zn), arsenic (As), cadmium (Cd) and lead (Pb) are shown. Ecological quality standards are not shown, as these are only provided for dissolved metal concentrations (VLAREM II).

Sample	^{w*} Al	^{w*} Cr	^{w*} Mn	^{w*} Fe	^{w*} Co	^{w*} Cu	^{w*} Zn	^{w*} As	^{w*} Cd	^{w*} Pb
	<i>µg/L</i>	<i>µg/L</i>	<i>µg/L</i>	<i>µg/L</i>	<i>µg/L</i>	<i>µg/L</i>	<i>µg/L</i>	<i>µg/L</i>	<i>µg/L</i>	<i>µg/L</i>
D1A	121	1.0	241.0	3872	18.0	4.3	133	6.3	0.5	0.7
D2A	51	0.7	177.7	1548	14.2	2.5	104	2.9	0.3	0.5
D3A	91	0.8	157.2	982	11.2	4.1	186	4.3	1.0	1.1
D4A	102	1.0	193.6	1418	13.1	5.4	216	7.2	1.1	1.3
D6A	101	2.3	167.2	1641	10.6	4.9	196	7.7	1.0	1.9
D7A	53	0.8	155.0	1222	10.5	3.3	166	6.5	0.7	1.0
D1B	14	0.3	63.3	1157	3.0	0.9	34	2.4	0.1	0.2
D2B	21	0.4	93.9	1035	4.2	1.3	21	3.2	0.1	0.4
D3B	124	1.0	85.0	1409	4.4	4.3	102	5.5	0.8	3.6
D4B	44	0.7	75.1	834	3.5	3.0	73	5.1	0.4	1.7
D6B	18	0.5	71.6	584	2.8	2.8	67	5.2	0.3	0.8
D7B	19	0.5	54.4	442	2.4	3.5	68	4.6	0.3	0.8
D1C	233	1.6	273.1	8116	21.7	3.7	165	9.5	0.7	1.6
D2C	381	2.0	327.0	7763	21.9	8.0	249	10.8	1.0	7.9
D3C	437	3.0	220.3	4623	13.0	10.6	270	12.0	2.0	13.0
D4C	515	3.2	218.3	5371	13.0	12.7	287	15.6	2.4	15.6
D6C	590	3.3	196.9	5837	11.2	13.9	304	21.6	3.0	20.4
D7C	404	2.2	189.5	4559	11.2	9.3	233	17.0	2.2	11.2

Appendix 5C

Table 5C: Metal concentrations measured in sediment (denoted by ^sM), sampled during campaign C (24/01/2020). Aluminium (Al), chromium (Cr), manganese (Mn), iron (Fe), cobalt (Co), copper (Cu), zinc (Zn), arsenic (As), cadmium (Cd) and lead (Pb) are shown. Values shown are averages ± S.D. based on multiple sediment samples (*n* = 3) taken at each site. Whenever ecological quality standards (EQS; VLAREM II) were available, these were included at the bottom of the table. Values exceeding the ecological quality standards are indicated in red. The average values in upstream and downstream sites are included (upstream: D1, D2; downstream: D3, D4, D6, D7).

Site	^s Al	^s Cr	^s Mn	^s Fe	^s Co	^s Cu	^s Zn	^s As	^s Cd	^s Pb
	<i>μg/g</i>	<i>μg/g</i>	<i>μg/g</i>	<i>μg/g</i>	<i>μg/g</i>	<i>μg/g</i>	<i>μg/g</i>	<i>μg/g</i>	<i>μg/g</i>	<i>μg/g</i>
D1	1248 ± 116	21 ± 0	207 ± 36	32464 ± 1873	21 ± 3	1 ± 0	205 ± 10	54 ± 3	0.8 ± 0	10 ± 1
D2	973 ± 108	7 ± 2	25 ± 15	5265 ± 2680	4 ± 2	4 ± 2	76 ± 20	9 ± 3	0.4 ± 0.2	9 ± 2
D3	1199 ± 295	9 ± 5	22 ± 13	4780 ± 2772	4 ± 2	65 ± 94	161 ± 81	10 ± 4	2.1 ± 1.2	21 ± 12
D4	1042 ± 332	7 ± 3	12 ± 12	2861 ± 1734	2 ± 2	7 ± 3	131 ± 56	12 ± 5	3.9 ± 3	28 ± 7
D6	700 ± 266	8 ± 5	10 ± 4	4080 ± 1136	1 ± 0	3 ± 2	59 ± 39	21 ± 6	1.6 ± 1.1	11 ± 7
D7	1074 ± 469	6 ± 4	13 ± 12	3343 ± 2289	2 ± 1	4 ± 3	95 ± 72	13 ± 10	3.8 ± 2.2	16 ± 9
D1-D2	1111 ± 181	14 ± 8	116 ± 103	18865 ± 15040	12 ± 9	3 ± 2	140 ± 72	31 ± 25	0.6 ± 0.3	10 ± 2
D3-D7	1004 ± 355	8 ± 4	14 ± 10	3766 ± 1926	2 ± 2	20 ± 49	111 ± 68	14 ± 7	2.9 ± 2	19 ± 10
EQS	/	Cr<37	/	/	/	Cu<17	Zn<147	As<19	Cd<1	Pb<40

Appendix 5D

Table 5D: Tables showing magnesium (Mg^{2+}) and calcium (Ca^{2+}) concentrations obtained from VMM (Geoloket); VMM site codes are provided. Data of Ca^{2+} and Mg^{2+} concentrations were retrieved for sites D1, D3 and D6 as these were consistently available. In terms of date, information was retrieved to match sampling dates of the present report as closely as possible. The $CaCO_3$ content was calculated according to formula: $CaCO_3 \frac{mg}{L} = 2.497 \left[Ca \frac{mg}{L} \right] + 4.118 \left[Mg \frac{mg}{L} \right]$ (Briggs et al., 1997). Information of D1 was used for D1 and D2; D3 for D3 and D4; D6 for D6 and D7. This information is used to determine the ecological quality standard (EQS; VLAREM II) for cadmium dissolved in water (wCd).

Site	VMM	Date	Ca^{2+}	Mg^{2+}	$CaCO_3$	Site	$CaCO_3$	wCd EQS
			$\mu g/L$	$\mu g/L$	mg/L		mg/L	$Cd (\mu g/L)$
D1	93000	24/04/2019	28000	6200	95	D1	93 ± 3	0.09
D1	93000	27/08/2019	28000	5800	94	D2	93 ± 3	0.09
D1	93000	29/01/2020	26000	6200	90	D3	99 ± 27	0.09
D3	91700	24/04/2019	35000	5800	111	D4	99 ± 27	0.09
D3	91700	27/08/2019	39000	5000	118	D6	116 ± 17	0.15
D3	91700	26/02/2020	21000	3700	68	D7	116 ± 17	0.15
D6	91000	24/04/2019	36000	5900	114			
D6	91000	27/08/2019	44000	5700	133			
D6	91000	29/01/2020	32000	4800	100			

Appendix 5E

Table 5E: All calculated toxic units (TU) for each metal in water along with average TUs (^wTU with Co, ^wTU* without Co) ± S.D. These TUs are calculated according to formula: $TU = \frac{[M]}{EQS}$, where [M] is the measured concentration of a given metal and EQS the ecological quality standard according to Flemish regulation (VLAREM II). The average values in upstream and downstream sites are included (upstream: D1, D2; downstream: D3, D4, D6, D7).

Sample	^w Cr	^w Co	^w Cu	^w Zn	^w As	^w Cd	^w Pb	^w TU	^w TU*
D1A	0.1	28.6	0.4	4.8	0.7	3.3	1.1	5.6 ± 10.3	1.7 ± 1.9
D2A	0.1	29.8	0.3	5.0	0.5	2.2	1.1	5.6 ± 10.8	1.5 ± 1.8
D3A	0.1	22.6	0.5	9.0	1.0	10.0	3.3	6.6 ± 8.1	4.0 ± 4.4
D4A	0.1	21.4	0.5	8.3	1.5	5.6	2.2	5.7 ± 7.5	3.0 ± 3.2
D6A	0.1	18.0	0.3	7.4	1.3	2.0	1.3	4.4 ± 6.5	2.1 ± 2.7
D7A	0.1	18.0	0.3	6.4	1.2	2.0	1.3	4.2 ± 6.4	1.9 ± 2.3
D1B	0.1	5.6	0.1	1.4	0.4	0.6	1.1	1.3 ± 2.0	0.6 ± 0.5
D2B	0.1	8.0	0.1	0.8	0.7	0.6	1.1	1.6 ± 2.8	0.6 ± 0.4
D3B	0.1	7.6	0.3	3.4	1.0	2.2	4.4	2.7 ± 2.7	1.9 ± 1.7
D4B	0.1	6.6	0.3	3.0	1.1	2.2	3.3	2.4 ± 2.2	1.7 ± 1.4
D6B	0.1	6.0	0.4	3.2	1.2	1.3	2.0	2.0 ± 2.0	1.4 ± 1.1
D7B	0.1	4.4	0.5	3.1	1.1	1.3	2.0	1.8 ± 1.5	1.3 ± 1.1
D1C	0.2	34.8	0.2	5.8	0.7	3.3	1.1	6.6 ± 12.6	1.9 ± 2.2
D2C	0.2	31.4	0.2	5.9	0.6	1.1	1.1	5.8 ± 11.5	1.5 ± 2.2
D3C	0.3	21.8	0.5	8.8	1.1	4.4	4.4	5.9 ± 7.6	3.3 ± 3.3
D4C	0.3	22.2	0.5	9.0	1.5	3.3	4.4	5.9 ± 7.8	3.2 ± 3.3
D6C	0.3	18.2	0.5	7.5	1.7	1.3	2.7	4.6 ± 6.5	2.3 ± 2.7
D7C	0.2	19.8	0.4	7.0	1.5	1.3	2.7	4.7 ± 7.0	2.2 ± 2.5
D1-D2	0.1 + 0.0	23.0 + 12.8	0.2 + 0.1	3.9 + 2.3	0.6 + 0.1	1.9 + 1.3	1.1 + 0.0	4.4 + 4.7	1.3 + 0.8
D3-D7	0.2 + 0.1	15.6 + 7.2	0.4 + 0.1	6.3 + 2.5	1.3 + 0.2	3.1 + 2.6	2.9 + 1.2	4.2 + 2.6	2.3 + 1.0

Appendix 6

Table 6A: A summary of Student's and Welch's *t*-tests (*t*) and Mann-Whitney *U*-tests (*w*) conducted on physicochemical variables and metals dissolved in water, as well as metals in sediment, including significance levels (* = $p < 0.05$; ** = $p < 0.01$; *** = $p < 0.001$; ns = not significant). Normality (*N*) and homogeneity of variance (σ^2) assumptions were tested using the Shapiro-Wilk test and the *F*-test, respectively. In case of statistical significance, the difference between up- and downstream sites is indicated by either 'up < down' or 'up > down'.

	pH	Temp.	EC	pc.O ₂	O ₂	PO ₄ ³⁻ -P	NH ₄ ⁺ -N	NO ₂ ⁻ -N	NO ₃ ⁻ -N	SO ₄ ²⁻	Cl ⁻
<i>N</i>	0	0	0	1	1	1	0	1	1	0	0
σ^2	1	1	0	1	1	1	1	1	1	0	0
Test	<i>w</i>	<i>w</i>	<i>t</i>	<i>t</i>	<i>t</i>	<i>t</i>	<i>w</i>	<i>t</i>	<i>t</i>	<i>t</i>	<i>t</i>
<i>p</i>	ns	ns	***	ns	*	ns	ns	*	*	***	***
	up < down			up > down			up < down		up > down	up < down	up < down
	^w Al	^w Cr	^w Mn	^w Fe	^w Co	^w Cu	^w Zn	^w As	^w Cd	^w Pb	^w TU
<i>N</i>	1	0	1	1	1	1	1	1	0	0	0
σ^2	1	1	1	1	1	1	1	1	1	0	1
Test	<i>t</i>	<i>w</i>	<i>t</i>	<i>t</i>	<i>t</i>	<i>t</i>	<i>t</i>	<i>t</i>	<i>w</i>	<i>t</i>	<i>w</i>
<i>p</i>	ns	ns	ns	.	ns	**	.	***	.	***	ns
	up > down			up < down		up < down	up < down	up < down	up < down	up < down	
	^s TU*	^s Al	^s Cr	^s Mn	^s Fe	^s Co	^s Cu	^s Zn	^s As	^s Cd	^s Pb
<i>N</i>	1	1	0	0	0	0	0	1	0	0	0
σ^2	1	1	0	0	0	0	0	1	0	0	0
Test	<i>t</i>	<i>t</i>	<i>t</i>	<i>t</i>	<i>t</i>	<i>t</i>	<i>t</i>	<i>t</i>	<i>t</i>	<i>t</i>	<i>t</i>
<i>p</i>	*	ns	.	.	.	*	ns	ns	ns	**	**
	up < down	up > down		up > down	up > down	up > down				up < down	up < down

Appendix 7A

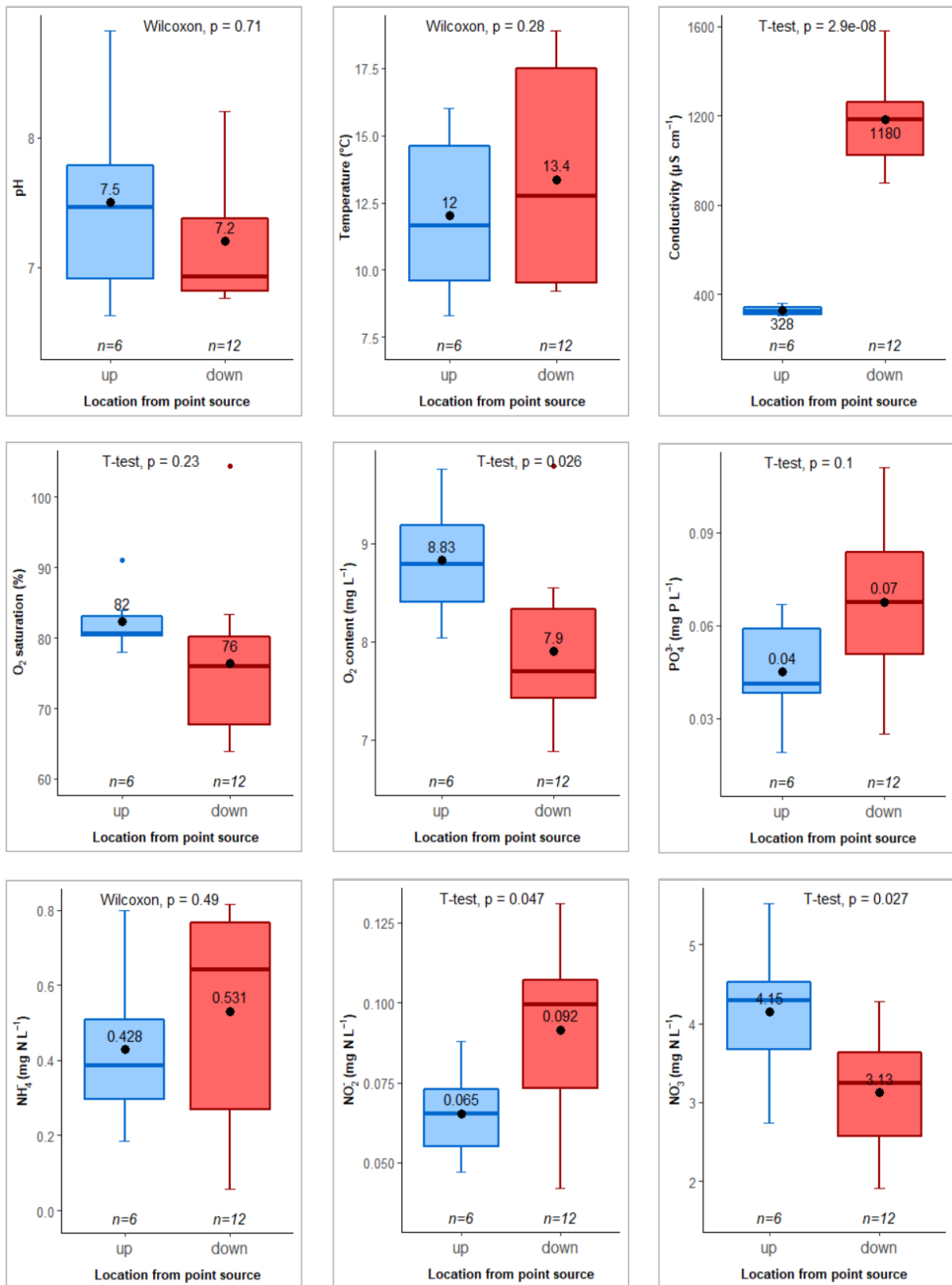


Figure 7A: Boxplots of all variables measured in water (incl. metals dissolved in water) when compared between reference (D1, D2; upstream - blue) and contaminated (D3, D4, D6, D7; downstream - red) sites. Additionally, the statistical test is shown at the top of each graph along with the statistical significance. Furthermore, the average values are indicated with a black dot, corresponding to its location on the Y-axis. Respective sample sizes are shown above the X-axis for each of the two groups under consideration.

Appendix 7B

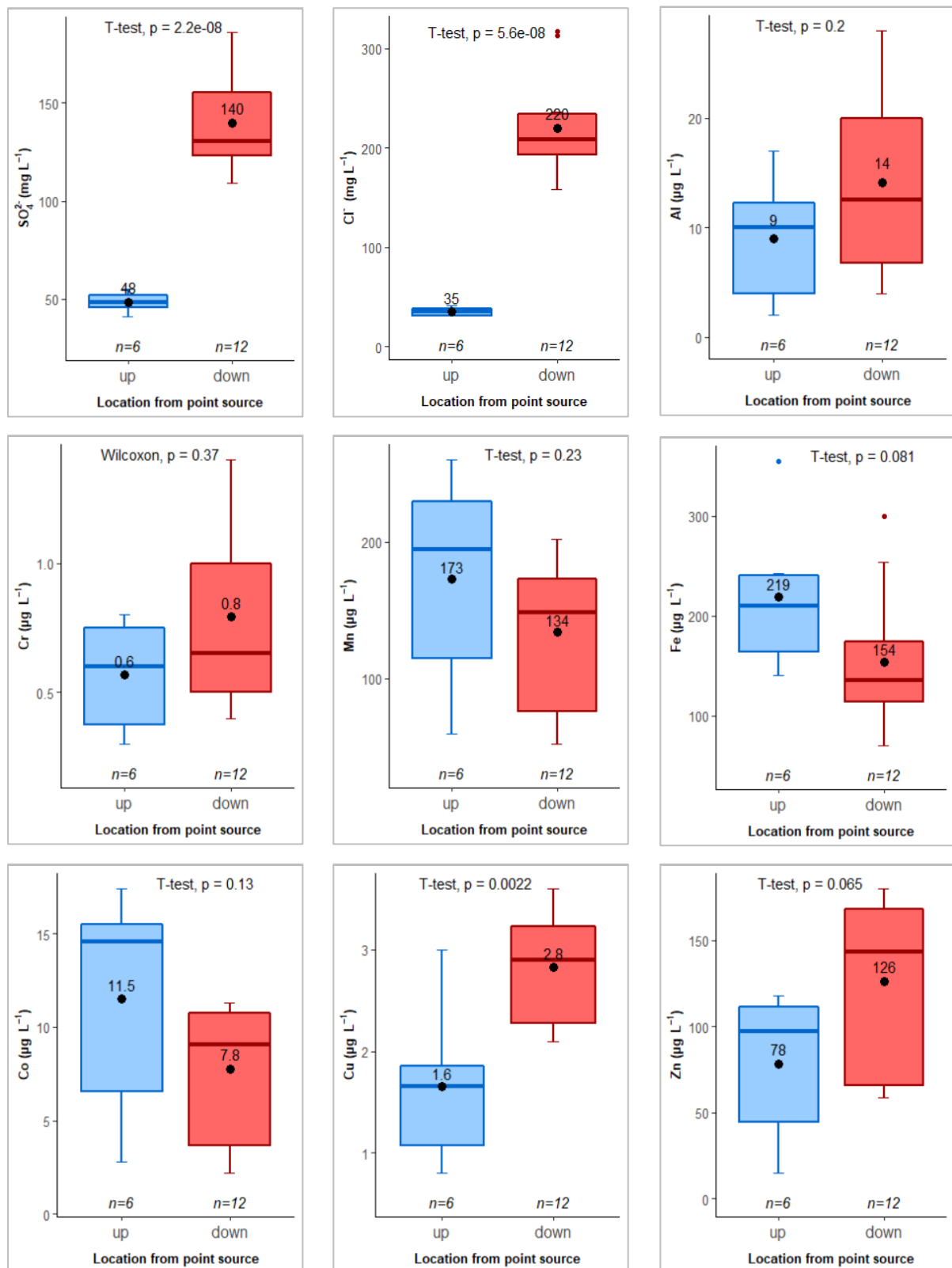


Figure 7B: Boxplots of all variables measured in water (incl. metals dissolved in water) when compared between reference (D1, D2; upstream - blue) and contaminated (D3, D4, D6, D7; downstream - red) sites. Additionally, the statistical test is shown at the top of each graph along with the statistical significance. Furthermore, the average values are indicated with a black dot, corresponding to its location on the Y-axis. Respective sample sizes are shown above the X-axis for each of the two groups under consideration.

Appendix 7C

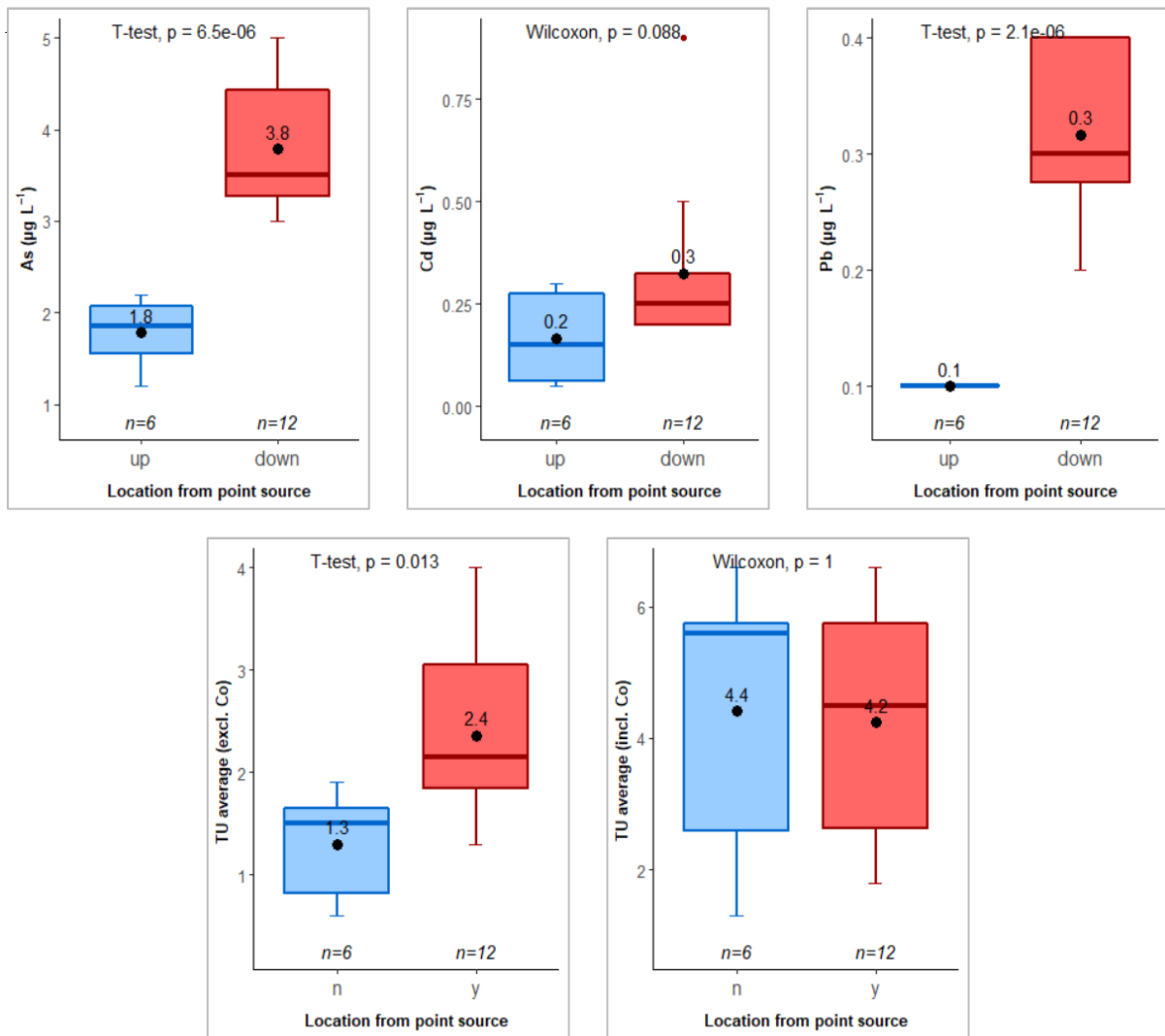


Figure 7C: Boxplots of all variables measured in water (incl. metals dissolved in water) when compared between reference (D1, D2; upstream - blue) and contaminated (D3, D4, D6, D7; downstream - red) sites. Additionally, the statistical test is shown at the top of each graph along with the statistical significance. Furthermore, the average values are indicated with a black dot, corresponding to its location on the Y-axis. Respective sample sizes are shown above the X-axis for each of the two groups under consideration.

Appendix 8A: Water physicochemistry

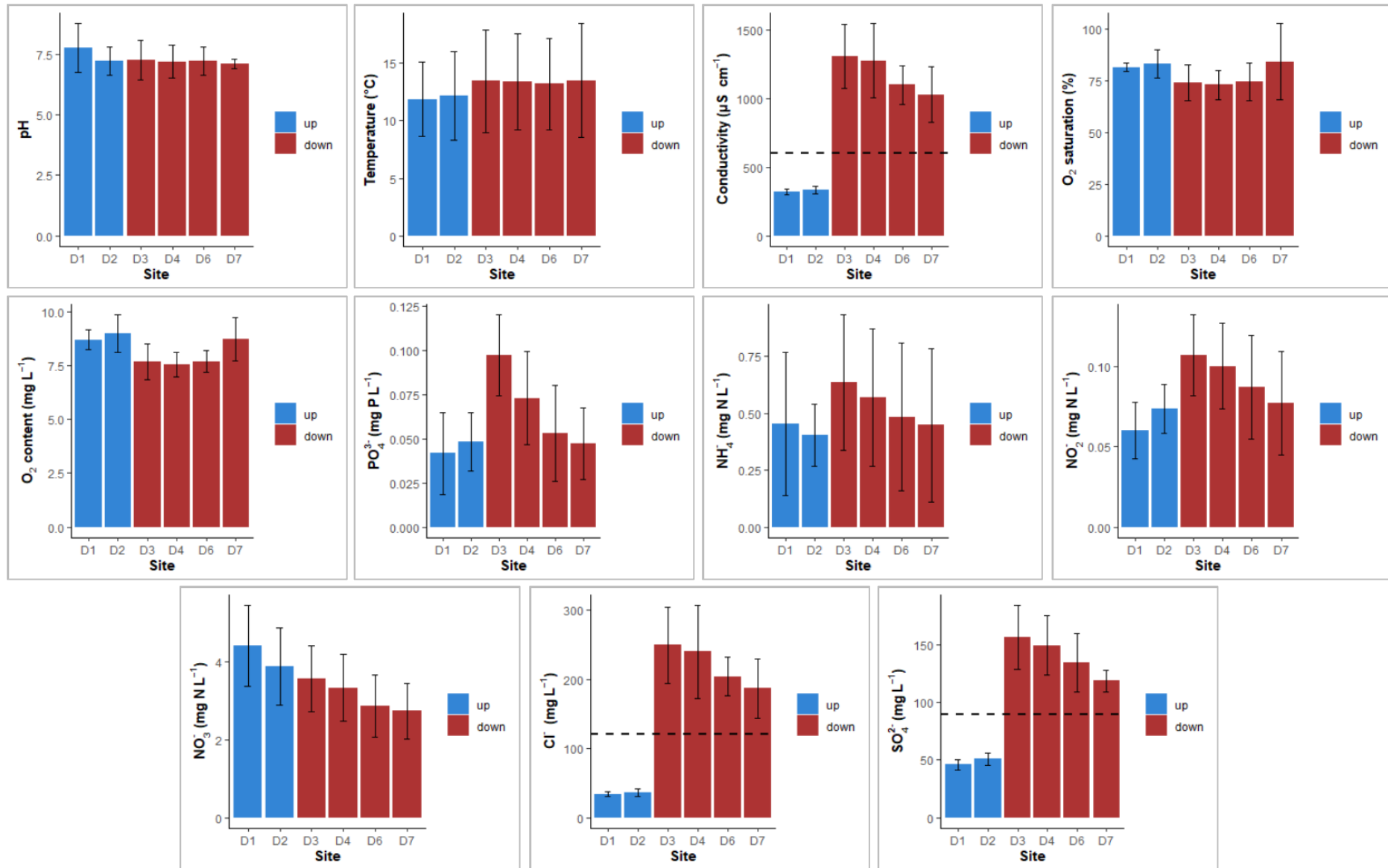


Figure 8A: Bar graphs for all abiotic variables tested along all six sites, with S.D. (error bars). Groupings are shown for reference ('up'; blue) and contaminated sites ('down'; red). For measurements derived from water samples, averages are presented along sampling campaigns A, B and C. For metal concentrations obtained from sediment samples, averages are shown based on three (separately analysed) subsamples at each site. Whenever available, horizontal lines indicate the maximum EQS (VLAREM II). 77

Appendix 8B: Metals in water

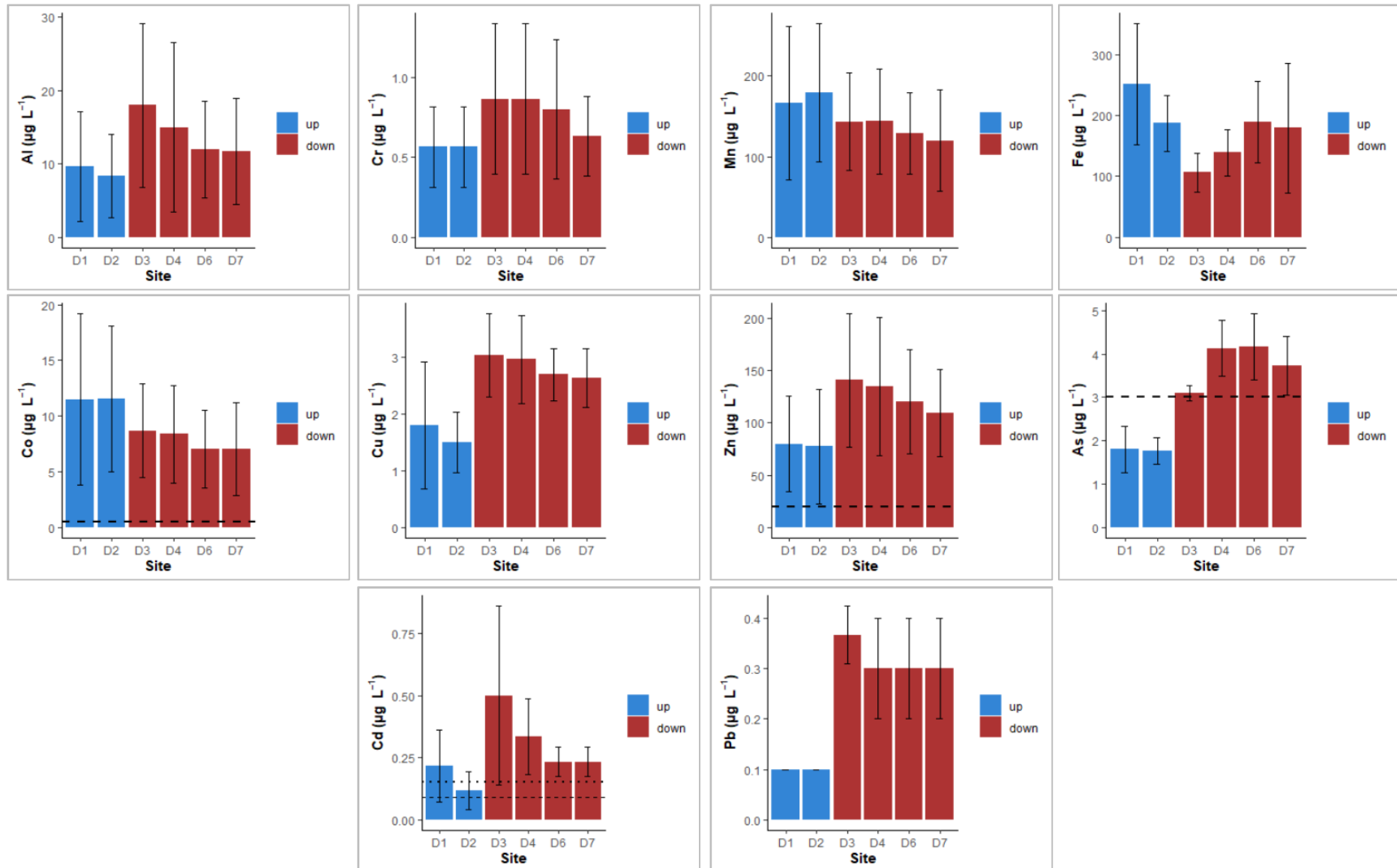


Figure 8B: Bar graphs for all abiotic variables tested along all six sites, with S.D. (error bars). Groupings are shown for reference ('up'; blue) and contaminated sites ('down'; red). For measurements derived from water samples, averages are presented along sampling campaigns A, B and C. For metal concentrations obtained from sediment samples, averages are shown based on three (separately analysed) subsamples at each site. Whenever available, horizontal lines indicate the maximum EQS (VLAREM II). Two horizontal lines are shown for Cd; the bottom line (dashed; - -) indicates the EQS in case of water hardness 50-100 $\text{mg CaCO}_3 \text{ L}^{-1}$, while the top (dotted; · · ·) indicates the EQS in case of water hardness 100-200 $\text{mg CaCO}_3 \text{ L}^{-1}$. More specifically, the former applies to D1-D4, while the latter applies to D6 and D7.

Appendix 8C: Metals in sediment

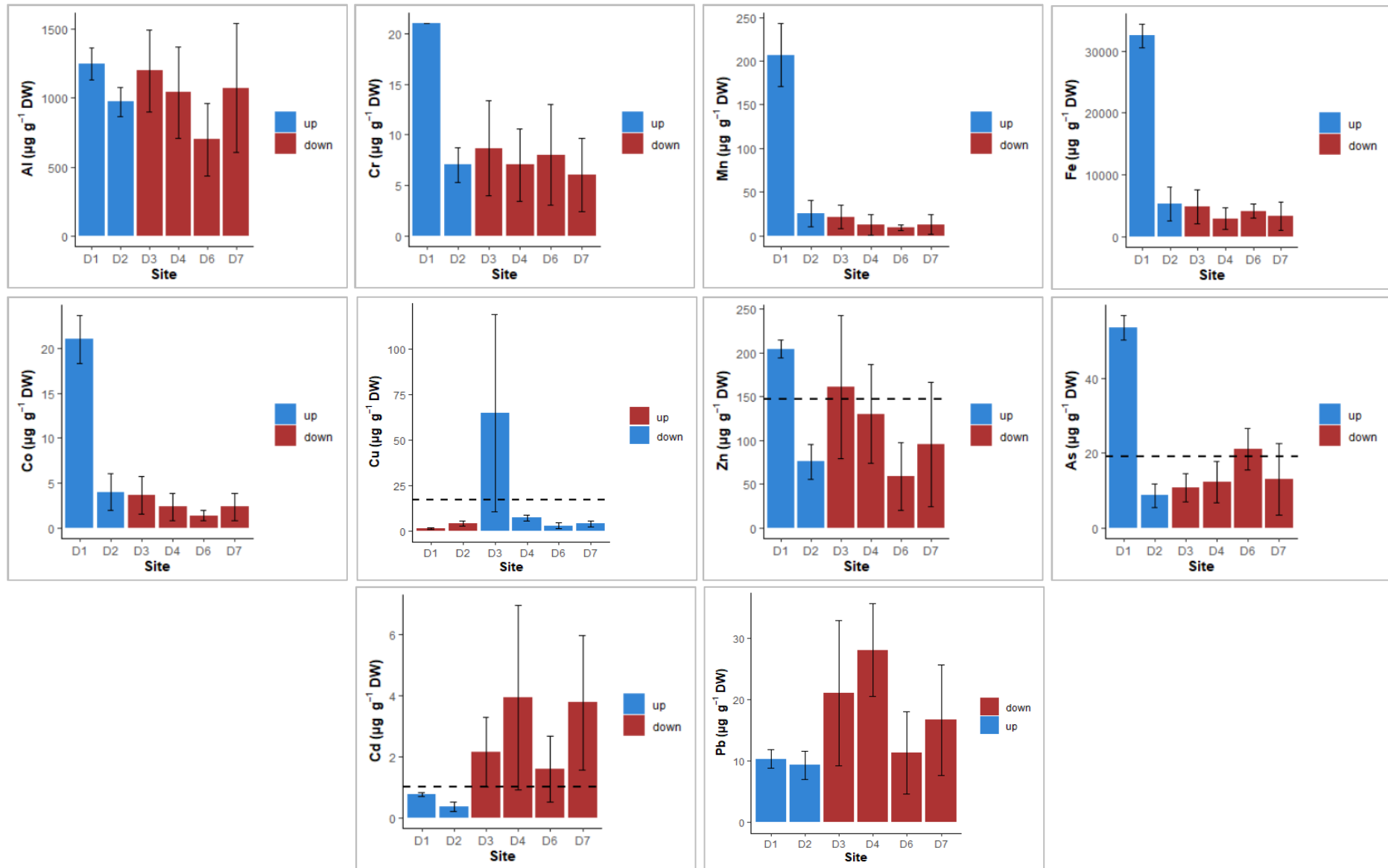


Figure 8C: Bar graphs for all abiotic variables tested along all six sites, with S.D. (error bars). Groupings are shown for reference ('up'; blue) and contaminated sites ('down'; red). For measurements derived from water samples, averages are presented along sampling campaigns A, B and C. For metal concentrations obtained from sediment samples, averages are shown based on three (separately analysed) subsamples at each site.

Appendix 9A

Table 9A: A summary of one-way ANOVA (*A*) and Kruskal-Wallis rank sum tests (*K*) conducted on all variables measured along all three sampling campaigns (A: 17/04/2019; B: 21/08/2019; C: 24/01/2020), including significance levels (* = $p < 0.05$; ** = $p < 0.01$; *** = $p < 0.001$; ns = not significant). Normality (*N*) and homogeneity of variance (σ^2) assumptions were tested using the Shapiro-Wilk test and Levene's test, respectively. Post hoc pairwise comparisons (*pairwise*) were carried out using TukeyHSD or pairwise Wilcoxon tests (using Bonferroni correction for multiple testing) depending on the assumption of normality.

	pH	Temp.	EC/Cond.	pc.O ₂	O ₂	PO ₄ ³⁻	NH ₄ ⁺	NO ₂ ⁻	NO ₃ ²⁻	SO ₄ ²⁻	Cl ⁻	
<i>N</i> (μ, σ^2)	0	1	0	0	1	0	1	1	1	0	0	
σ^2	1	1	1	1	1	1	1	1	1	1	1	
Test	<i>K</i>	<i>A</i>	<i>K</i>	<i>K</i>	<i>A</i>	<i>K</i>	<i>A</i>	<i>A</i>	<i>A</i>	<i>K</i>	<i>K</i>	
<i>p</i>	*	***	ns	*	ns	*	***	*	**	ns	ns	
<i>pairwise</i>	A > B	B > A > C		A & B > C		C > B	A & C > B	A & C > B	A & C > B			
	^w Al	^w Cr	^w Mn	^w Fe	^w Co	^w Cu	^w Zn	^w As	^w Cd	^w Pb	TU	TU*
<i>N</i> (μ, σ^2)	1	1	1	1	1	1	1	1	0	0	0	1
σ^2	1	0	1	1	1	1	1	1	1	1	1	1
Test	<i>A</i>	<i>A</i>	<i>A</i>	<i>A</i>	<i>A</i>	<i>A</i>	<i>A</i>	<i>A</i>	<i>K</i>	<i>K</i>	<i>K</i>	<i>A</i>
<i>p</i>	***	***	***	**	***	ns	***	ns	*	ns	***	*
<i>pairwise</i>	C > A > B	C > A > B	C > A > B	A & C > B	A & C > B		A & C > B		A > B		A & C > B	A & C > B

Appendix 10A

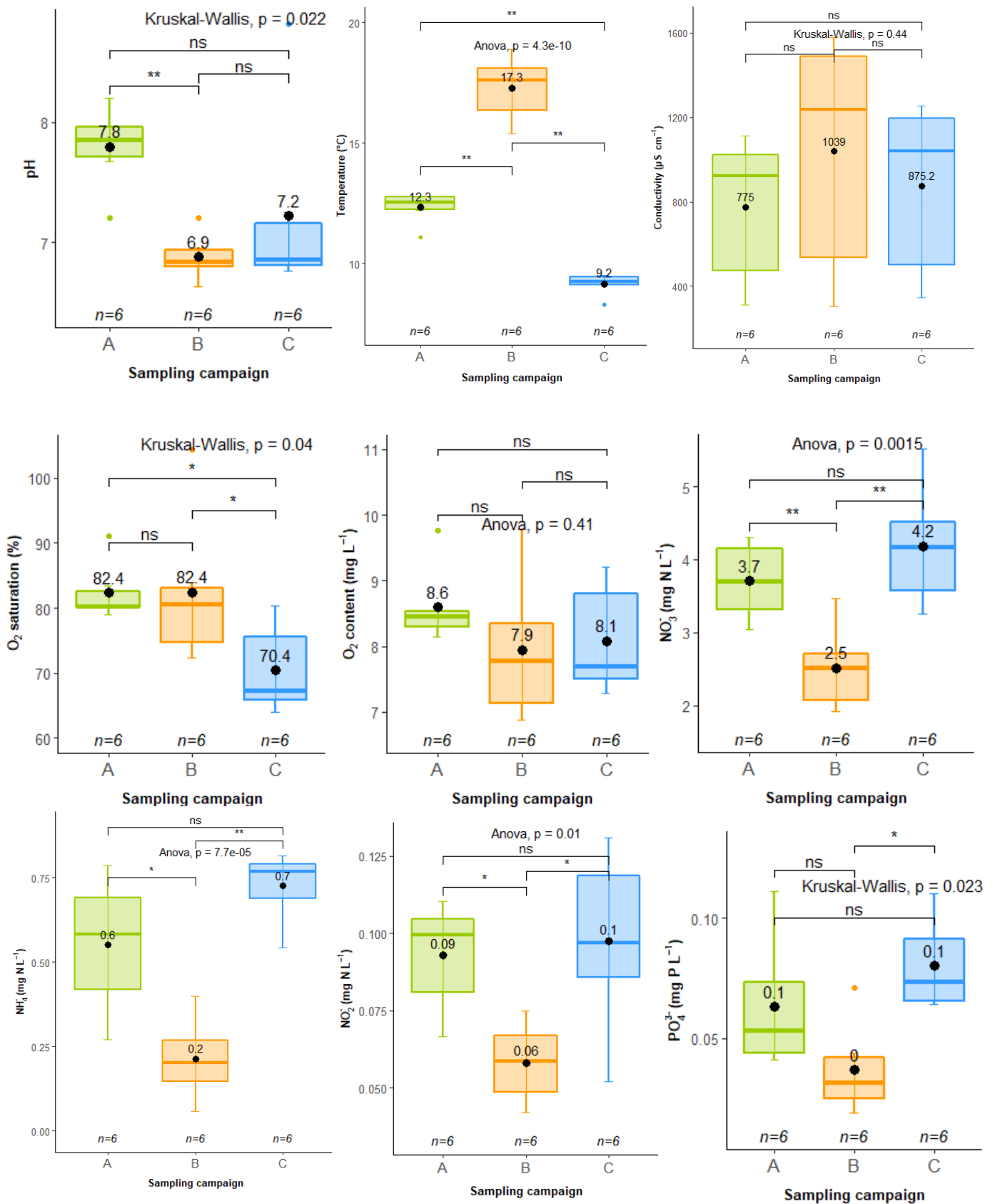


Figure 10A: Boxplots of all variables measured in water (incl. metals dissolved in water) when compared between sampling campaigns (A, B, C). Additionally, the statistical test is shown at the top of each graph along with the statistical significance and pairwise comparisons. Furthermore, the average values are indicated with a black dot, corresponding to its location on the Y-axis. Respective sample sizes are shown above the X-axis for each of the two groups under consideration.

Appendix 10B

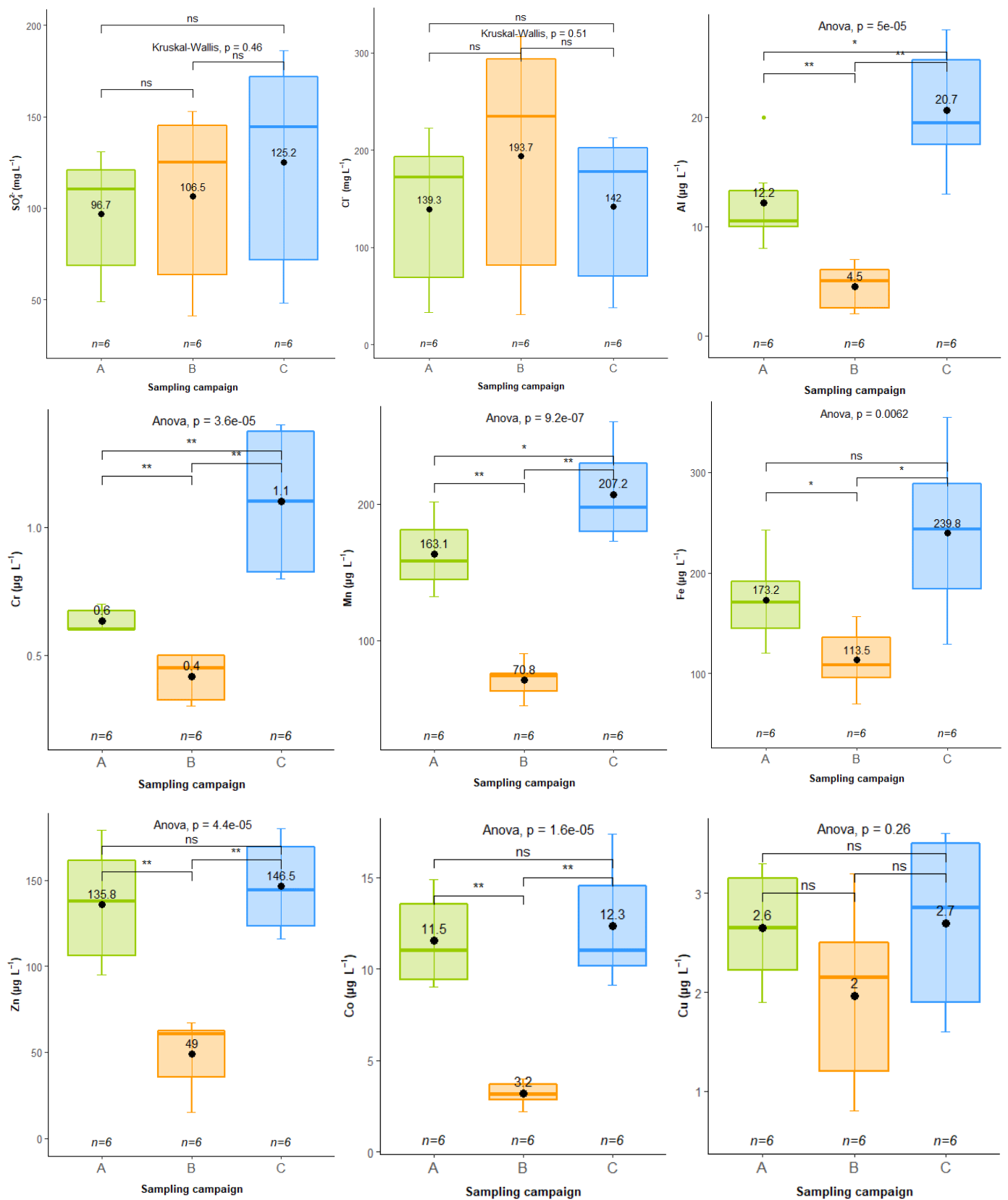


Figure 10B: Boxplots of all variables measured in water (incl. metals dissolved in water) when compared between sampling campaigns (A, B, C). Additionally, the statistical test is shown at the top of each graph along with the statistical significance and pairwise comparisons. Furthermore, the average values are indicated with a black dot, corresponding to its location on the Y-axis. Respective sample sizes are shown above the X-axis for each of the two groups under consideration.

Appendix 10C

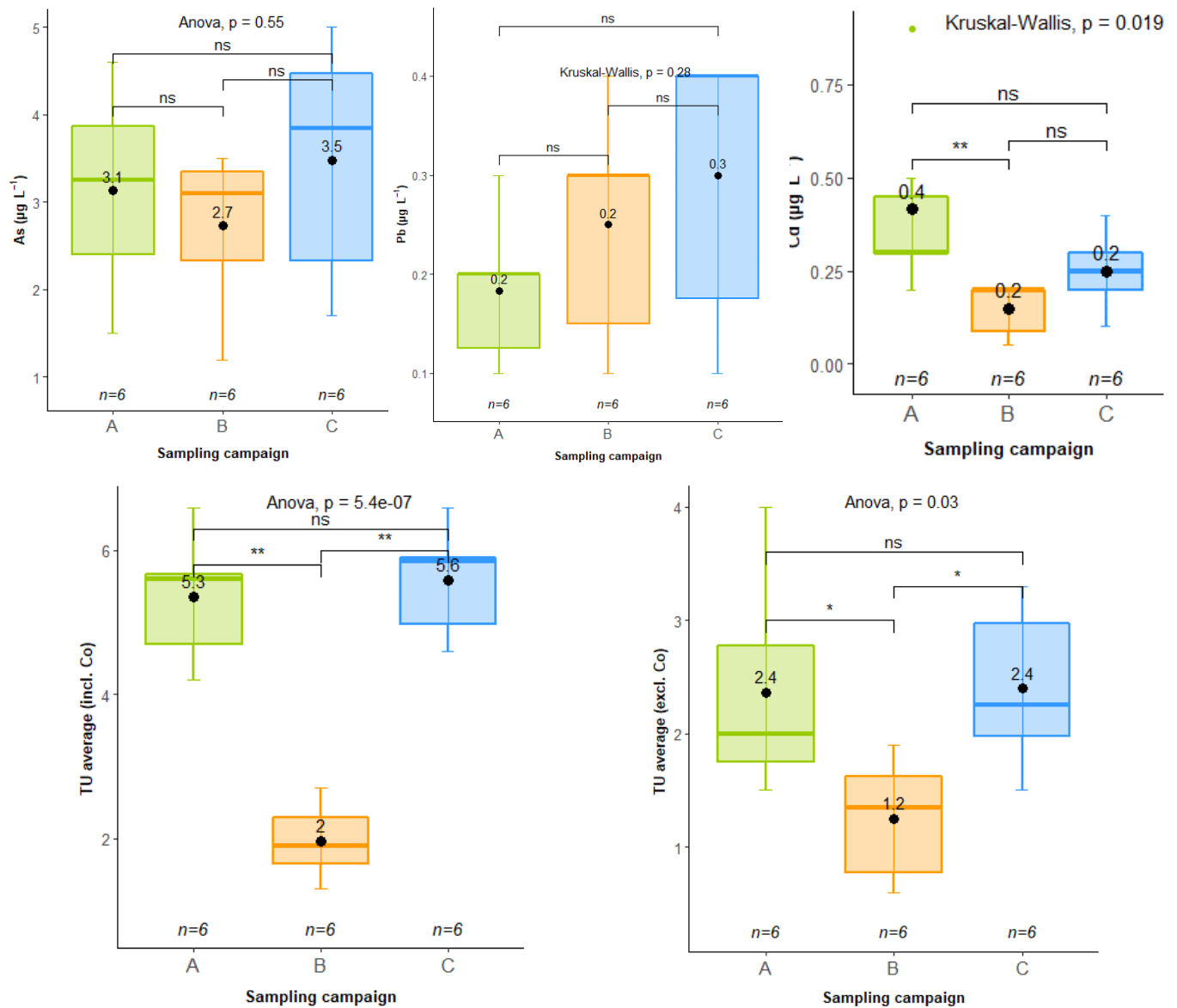


Figure 10C: Boxplots of all variables measured in water (incl. metals dissolved in water) when compared between sampling campaigns (A, B, C). Additionally, the statistical test is shown at the top of each graph along with the statistical significance and pairwise comparisons. Furthermore, the average values are indicated with a black dot, corresponding to its location on the Y-axis. Respective sample sizes are shown above the X-axis for each of the two groups under consideration.

Appendix 11A – Spearman correlation (coefficients)

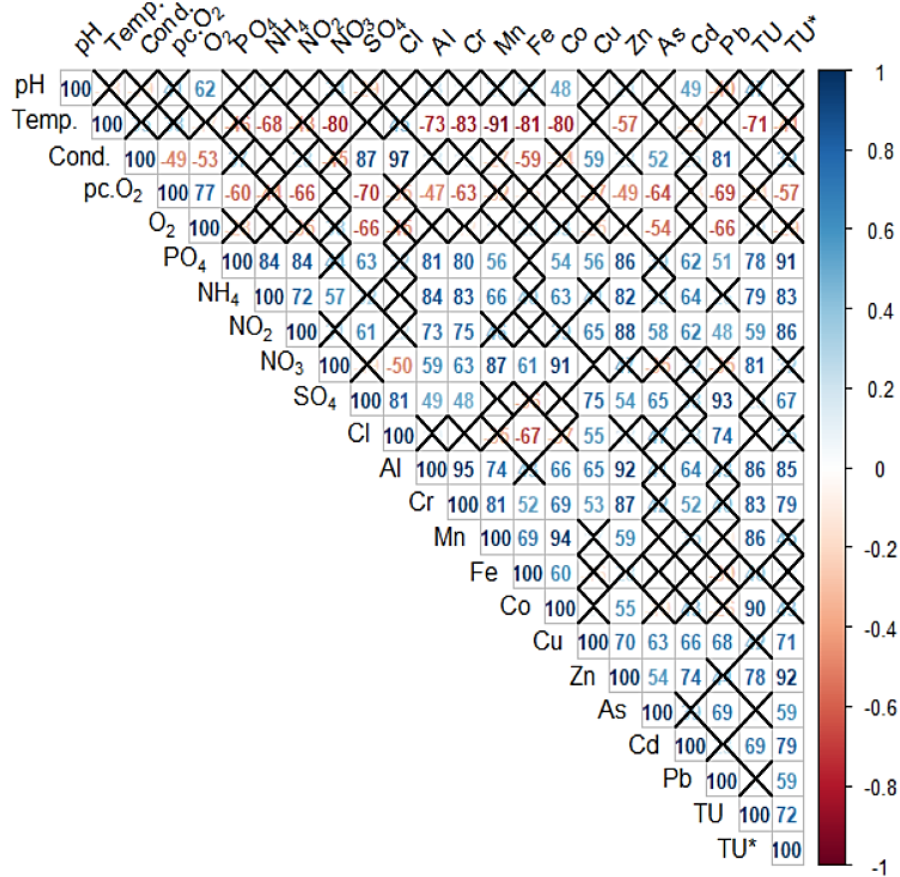


Figure 11A: Spearman rank correlation matrix for general water characteristics and metals dissolved in water. Correlation coefficients are shown as percentages for increased readability (i.e. coefficients multiplied by 100). All non-significant values are crossed out (at significance level $p < 0.05$).

Appendix 11B – Pearson correlation (matrix + coefficients)

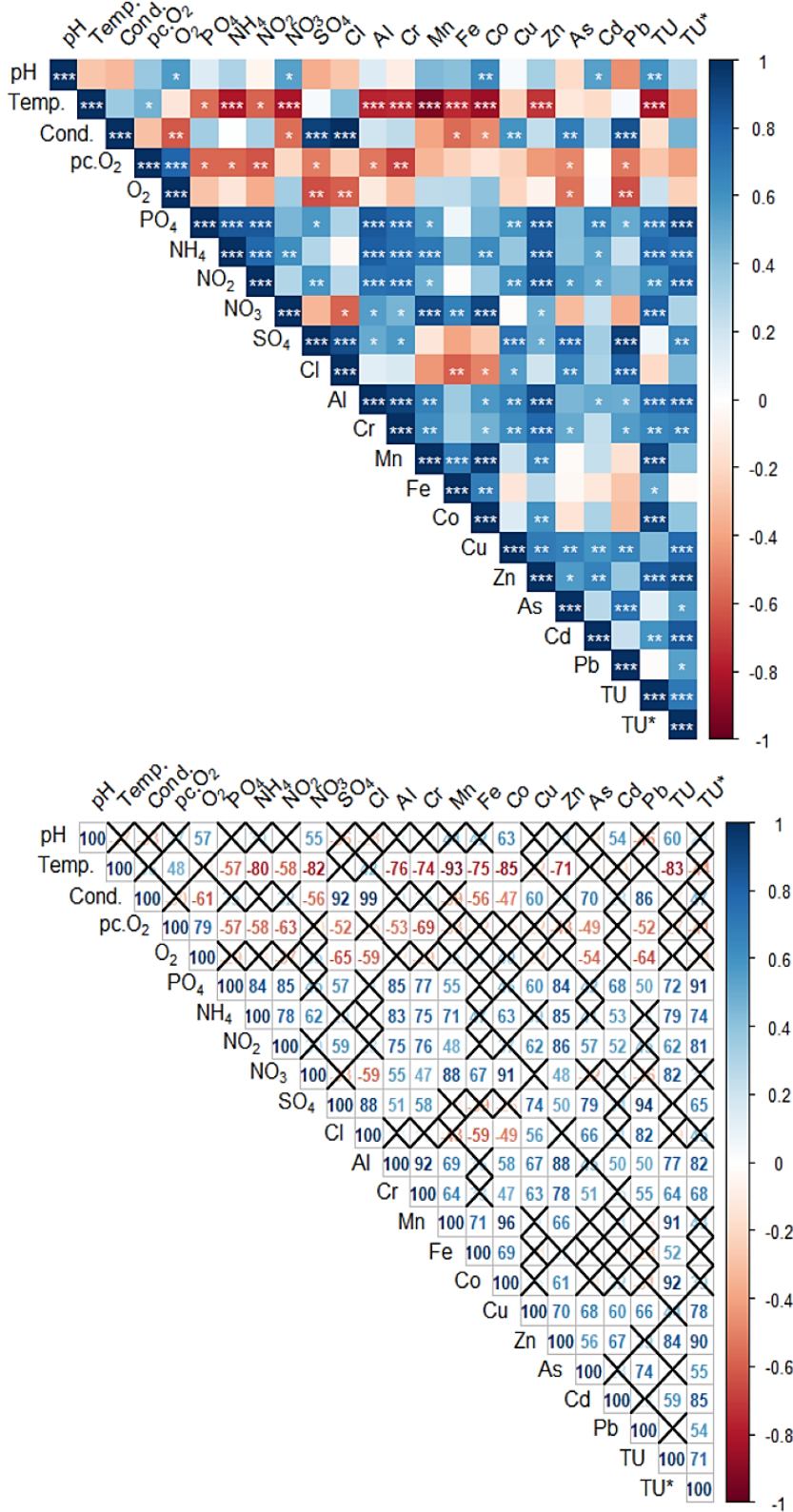


Figure 11B: Pearson correlation matrix for general water characteristics and metals dissolved in water. Top graph shows colour gradients corresponding to positive (blue) and negative (red) correlations, with three significance levels (* = $p < 0.05$; ** = $p < 0.01$; *** = $p < 0.001$). Bottom graph shows correlation coefficients as percentages for increased readability (i.e. coefficients multiplied by 100). All non-significant values are crossed out (at significance level $p < 0.05$).

Appendix 11C – Correlation matrix of all variables and calculated indices

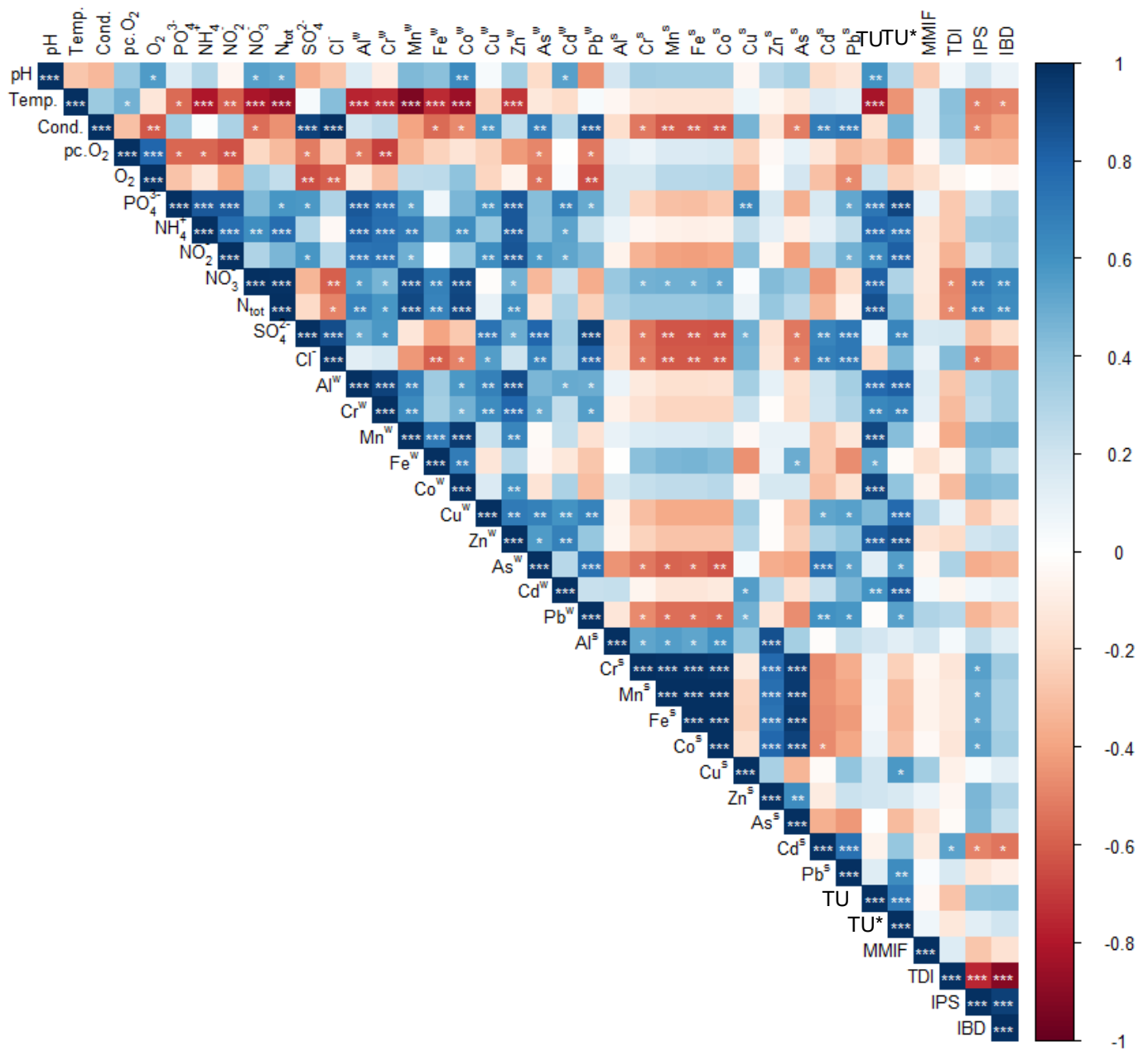


Figure 11C: Spearman correlation matrix for general water characteristics, metals dissolved in water, metals in sediment, corresponding toxic units (TU and TU*) and all biotic indices (MMIF, TDI, IPS, IBD), with three significance levels (* = $p < 0.05$; ** = $p < 0.01$; *** = $p < 0.001$). Colour gradients indicate sign (+/-) and magnitude of the correlation.

Appendix 11D – Correlation matrix of all variables with biotic indices

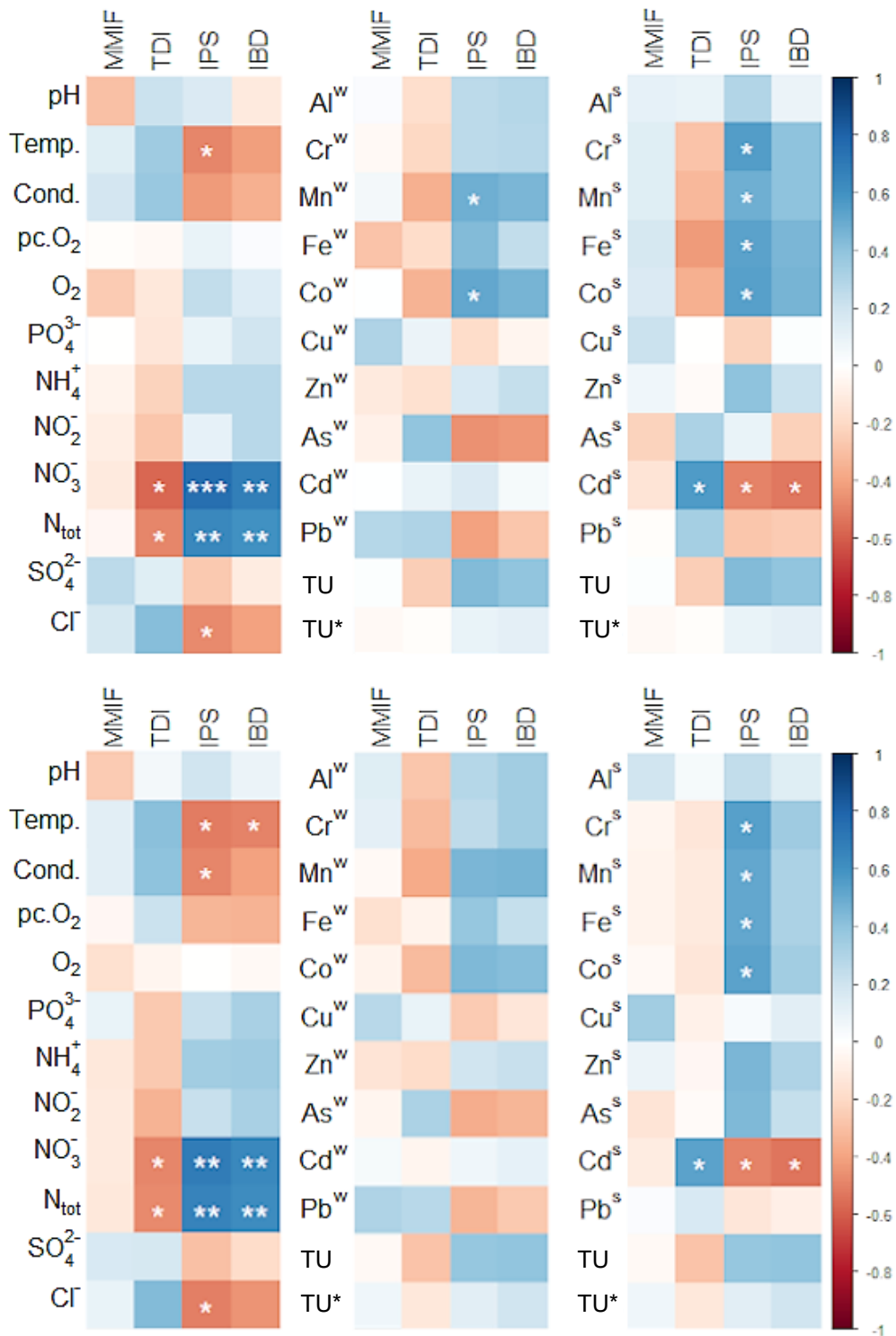


Figure 11D: Spearman (**top**) and Pearson (**bottom**) correlation matrix for biotic indices with general water characteristics, metals in water and in sediment. Graphs shows colour gradients corresponding to positive (blue) and negative (red) correlations, with three significance levels (* = $p < 0.05$; ** = $p < 0.01$; *** = $p < 0.001$).

Appendix 12A – PCA: water physicochemistry incl. metals in water

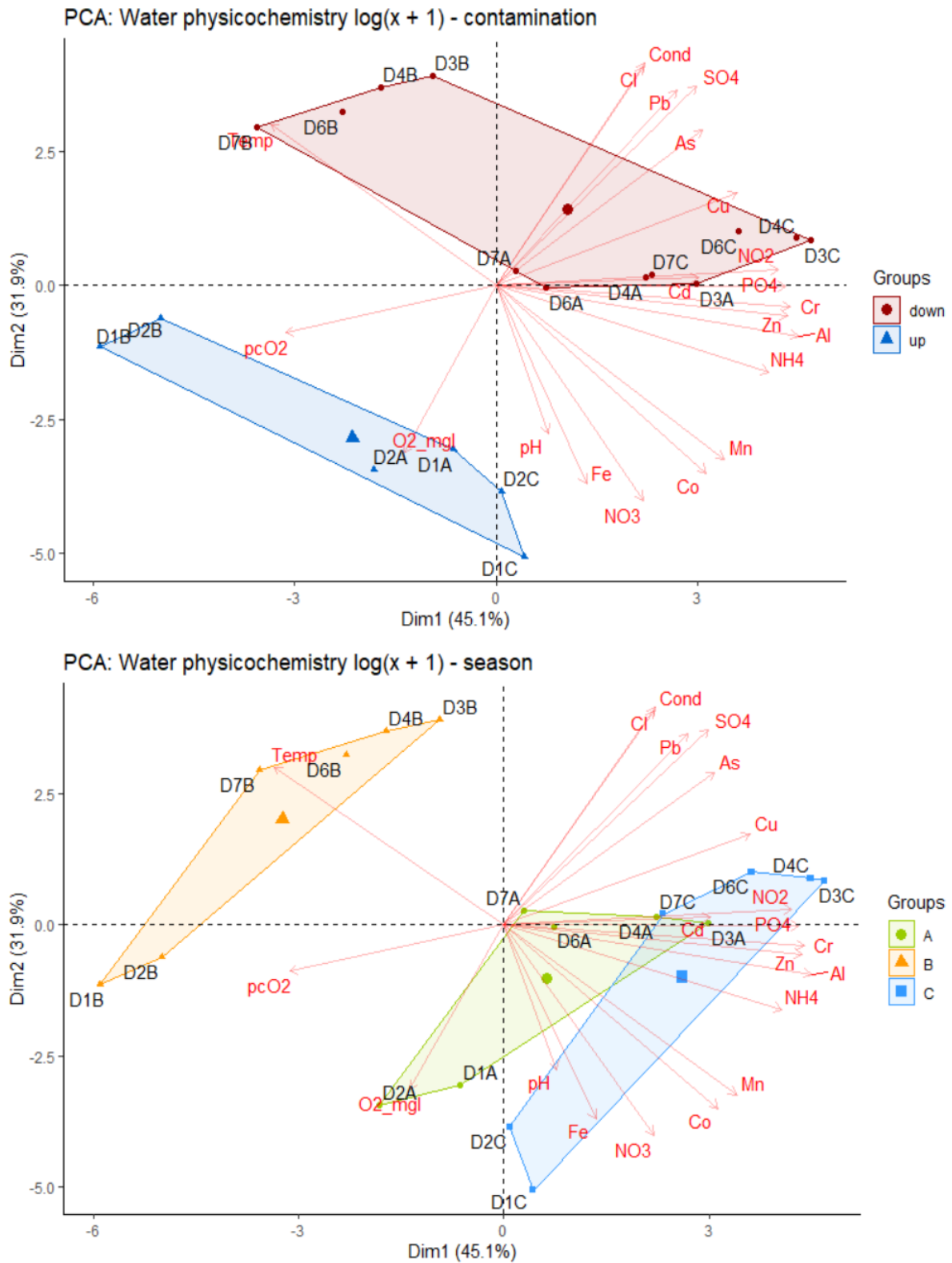


Figure 12A: Principal Component Analysis diagram for all variables measured in water with grouping based on ‘contamination (up- versus downstream; **top**) and sampling campaign (**bottom**; A: 17/04/2019; B: 21/08/2019; C: 24/01/2020), data $\log(x + 1)$ transformed. Variables under investigation are indicated with red arrows. Top graph provided in text (Fig. 5) but shown enlarged here. Additional information on the different PC axes can be found in Appendix 12B.

Appendix 12B – PCA: water physicochemistry incl. metals in water

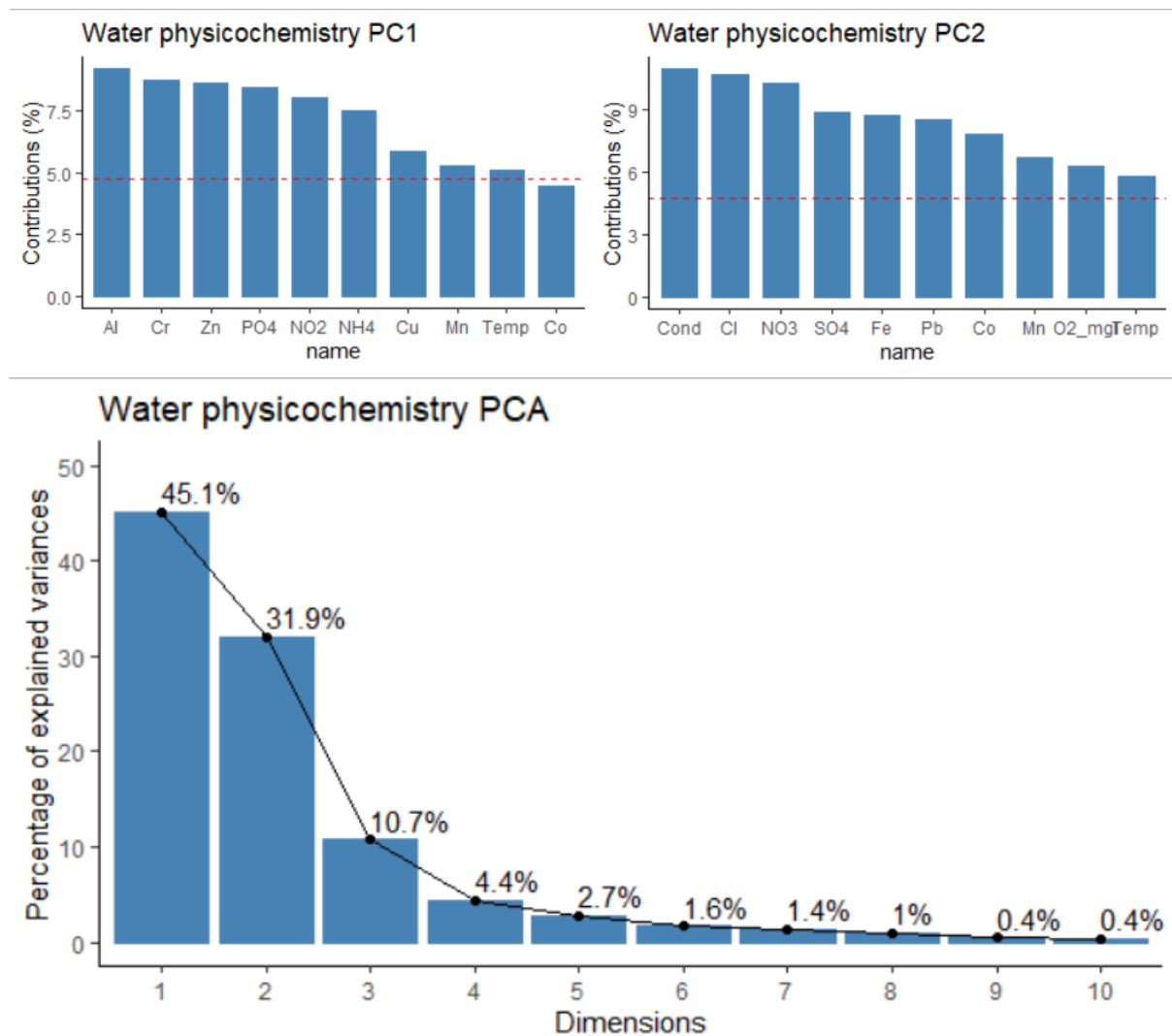


Figure 12B: Graphs supporting the PCA diagrams of Figure 5 and Appendix 12A. Graphs on top show the top 10 of variables contributing to either PC1 (Dim1; left) or PC2 (Dim2; right). The red dashed line serves as a reference which corresponds to the expected value if the contribution were uniform. The bottom graph shows the percentage of variance explained by the different PC dimensions.

Appendix 13A – PCA: water physicochemistry excl. metals in water

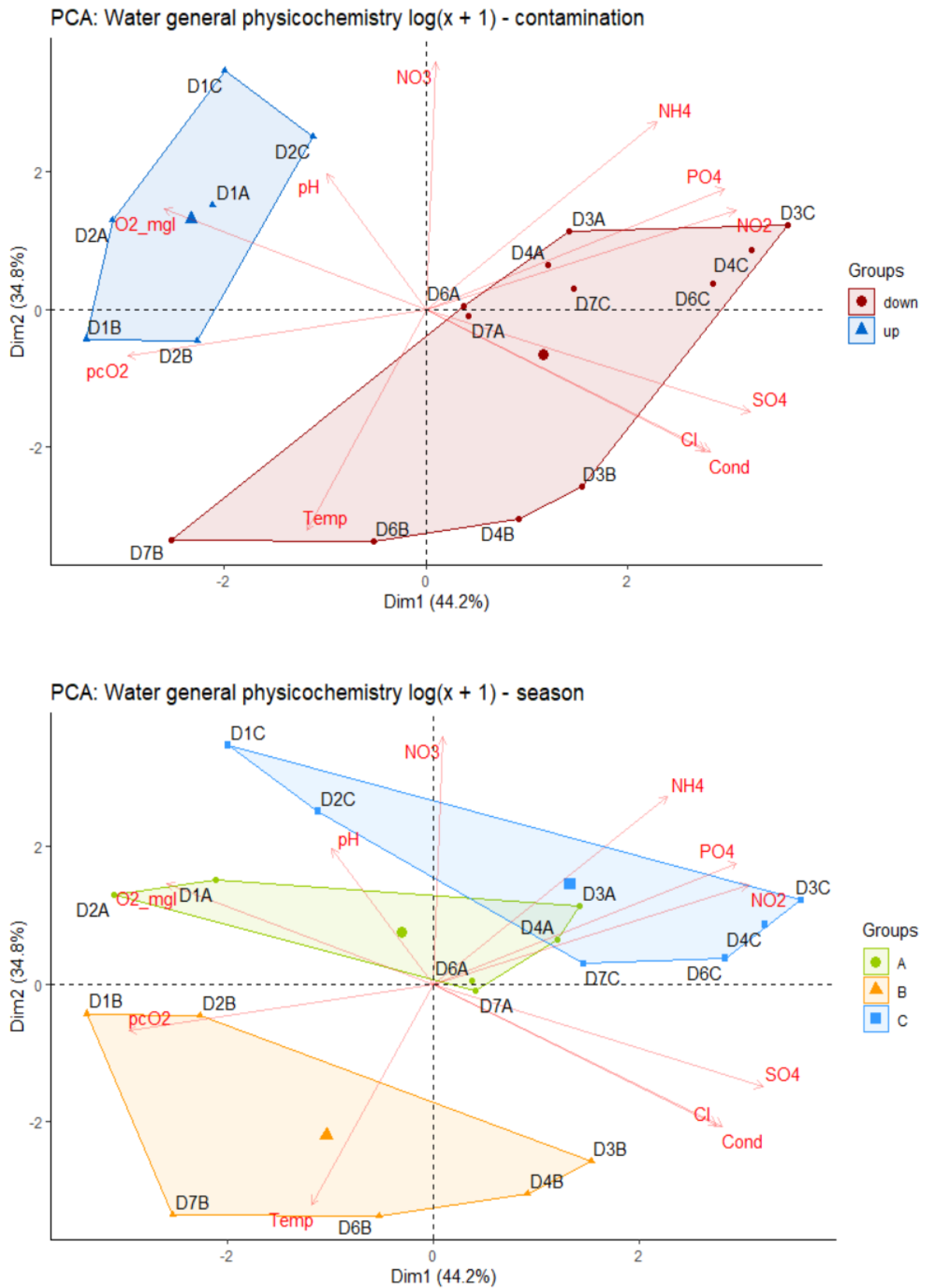


Figure 13A: Principal Component Analysis diagram for general water characteristics with grouping based on ‘contamination’ (up vs downstream; **top**), and based on sampling campaign (‘season’: A: 17/04/2019; B: 21/08/2019; C: 24/01/2020; **bottom**), data log(x + 1) transformed. Variables under investigation are indicated with red arrows. Additional information on the different PC axes can be found in Appendix 13B.

Appendix 13B – PCA: water physicochemistry excl. metals in water

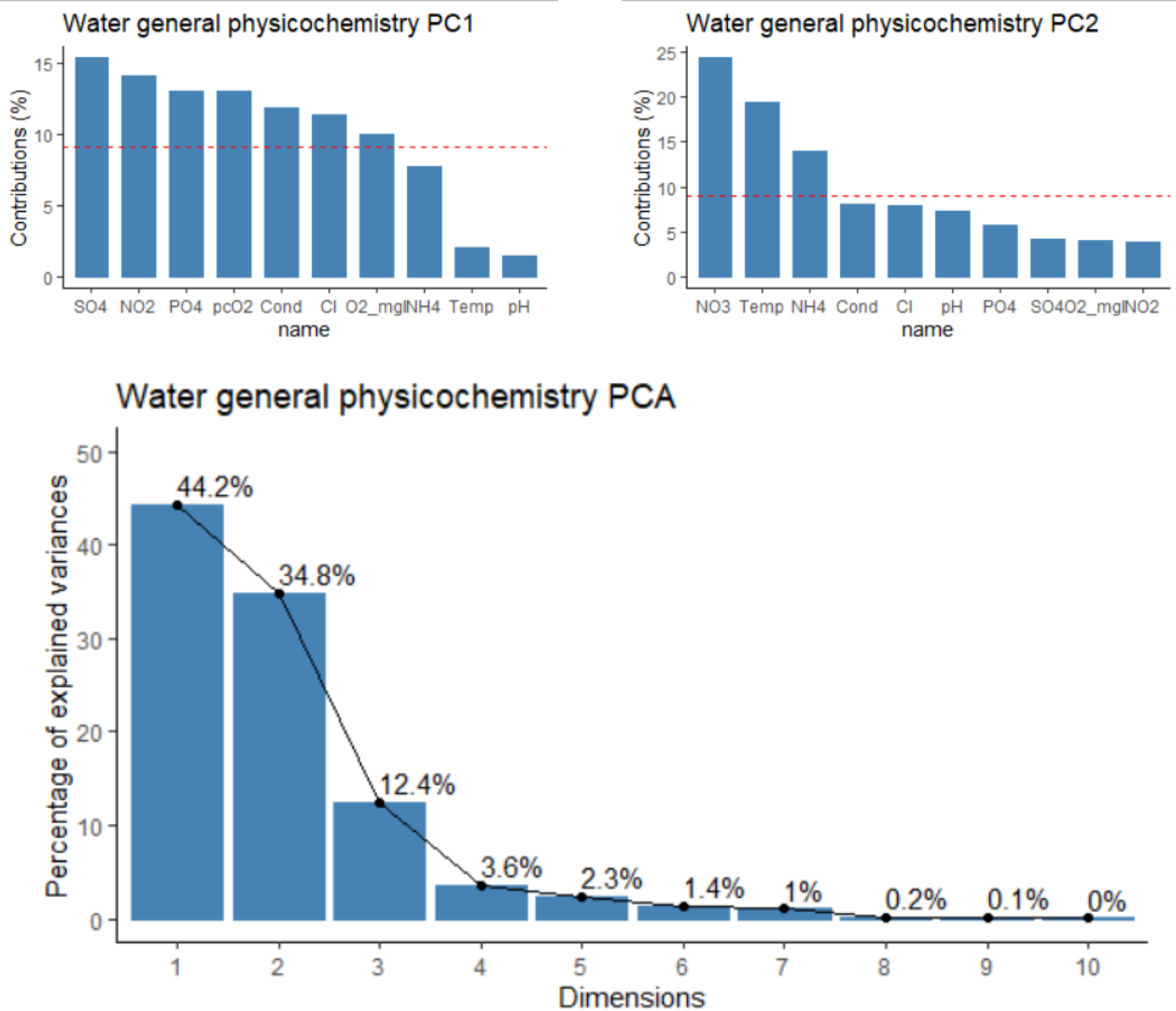


Table 13B: Graphs supporting the PCA diagrams in Appendix 13A. Graphs on top show the top 10 of variables contributing to either PC1 (Dim1; left) or PC2 (Dim2; right). The red dashed line serves as a reference which corresponds to the expected value if the contribution were uniform. The bottom graph shows the percentage of variance explained by the different PC dimensions.

Appendix 14A – PCA: metals in water

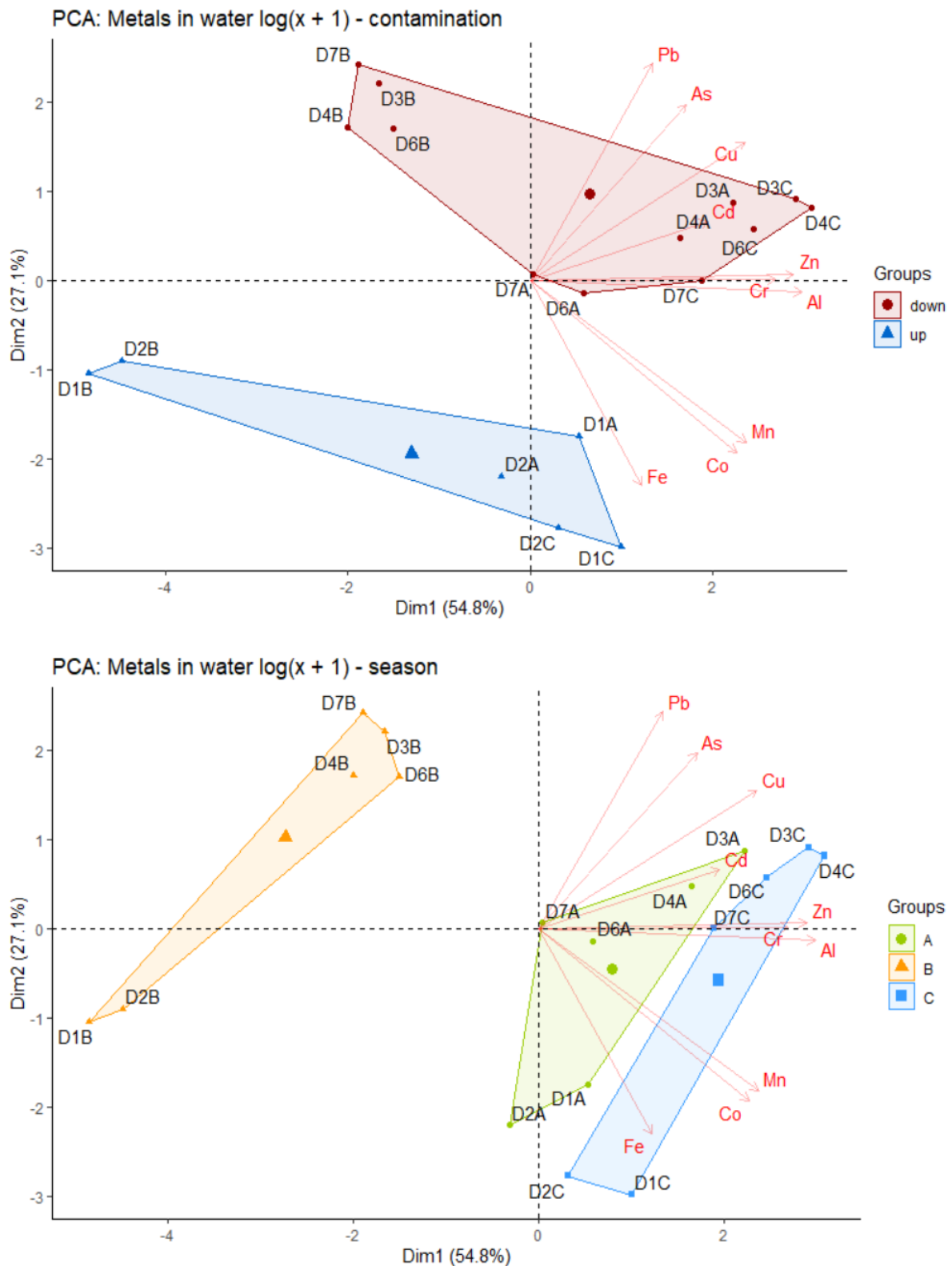


Figure 14A: Principal Component Analysis diagram for metals in water with grouping based on ‘contamination’ (up vs downstream; **top**), and based on sampling campaign (‘season’; A: 17/04/2019; B: 21/08/2019; C: 24/01/2020; **bottom**), data log(x + 1) transformed. Variables under investigation are indicated with red arrows. Additional information on the different PC axes can be found in Appendix 13B.

Appendix 14B – water physicochemistry excl. metals in water

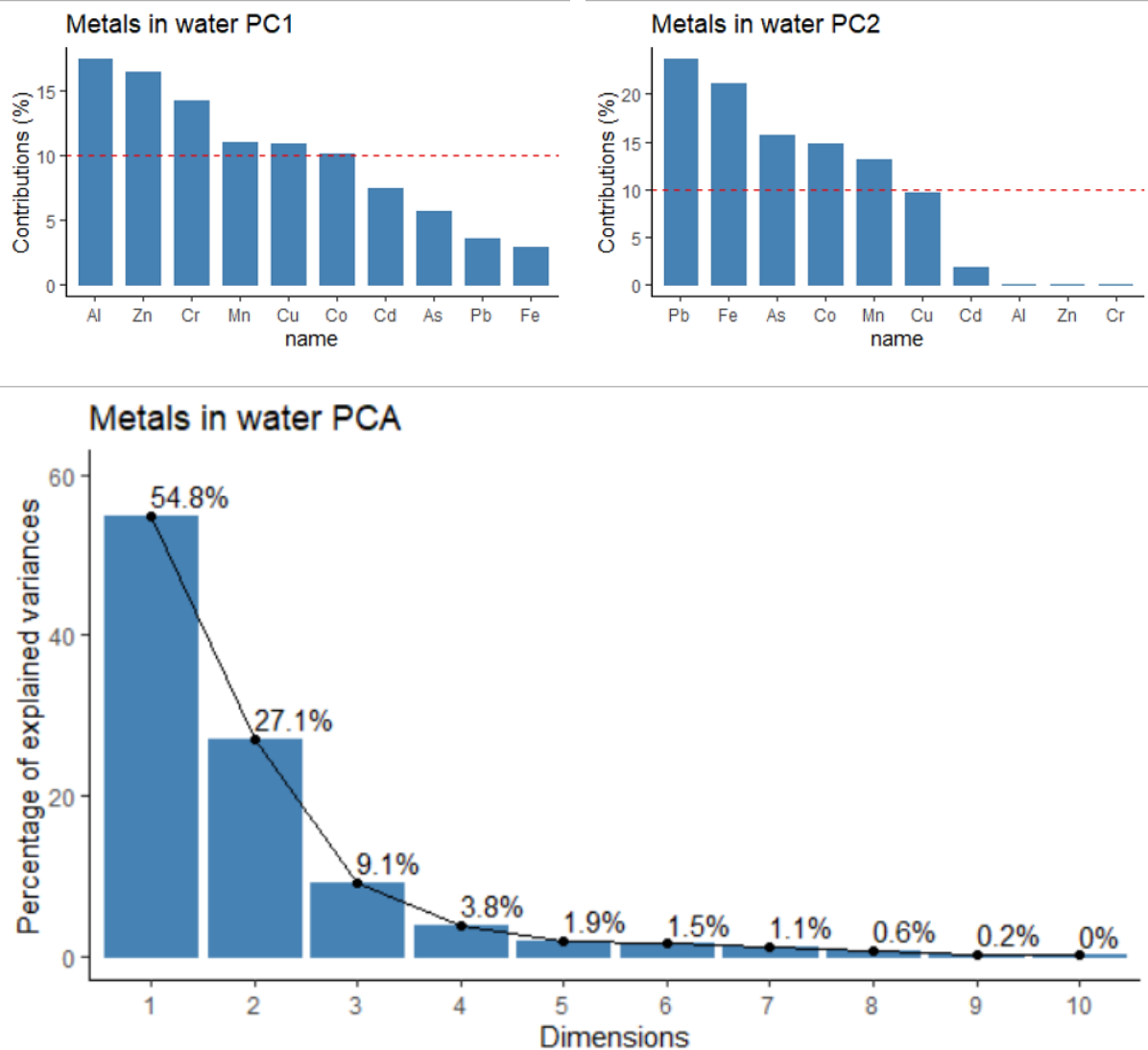


Table 14B: Graphs supporting the PCA diagrams in Appendix 14A. Graphs on top show the top 10 of variables contributing to either PC1 (Dim1; left) or PC2 (Dim2; right). The red dashed line serves as a reference which corresponds to the expected value if the contribution were uniform. The bottom graph shows the percentage of variance explained by the different PC dimensions.

Appendix 15A: Diatom count list

 Table 19A: Count data of all diatom samples across all sampling campaigns (A, B, C) with total $N = 400$ valves per sample.

Taxon	CODE	D1A	D2A	D3A	D4A	D6A	D7A	D1B	D2B	D3B	D4B	D6B	D7B	D1C	D2C	D3C	D4C	D6C	D7C
<i>Achnantheidium catenatum</i>	ADCT										2	4		2					
<i>Achnantheidium jackii</i>	ADJK															2			
<i>Achnantheidium microcephalum</i>	ADMC	12	5	5	3	39	22	159	2	2	3	9	1	1	4			2	6
<i>Achnantheidium minutissimum</i>	ADMI																		3
<i>Achnantheidium peetersianum</i>	ADMI							1							3			4	
<i>Adlafia brockmannii</i>	ABKM					1													
<i>Amphora copulata</i>	ACOP										2						2		2
<i>Amphora indistincta</i>	AMID																	1	
<i>Amphora normannii</i>	ANOR														1				
<i>Amphora pediculus</i>	APED																		2
<i>Aulacoseira ambigua</i>	AAMB	11									2			4					
<i>Aulacoseira muzzanensis</i>	AMUZ													2					
<i>Aulacoseira sp.</i>	AULA																4		
<i>Aulacoseira tenella</i>	AUTL													3					
<i>Caloneis lancettula</i>	CLCT																		2
<i>Caloneis sp.</i>	CALO					3													
<i>Cavinula variostrata</i>	CVVA																		1
<i>Chamaepinnularia soehrensii</i>	CHSO																4		
<i>Cocconeis euglypta</i>	CEUG								1	1						1		2	
<i>Cocconeis lineata</i>	CPLI		3						1						3				1
<i>Cocconeis pediculus</i>	CPED																2		
<i>Cocconeis sp.</i>	COCS		4	2	1														
<i>Craticula sp.</i>	CRAT				1														
<i>Ctenophora pulchella</i>	CTPU																1		1
<i>Cyclotella meneghiniana</i>	CMEN										4						1	1	3
<i>Cyclotella sp.</i>	CYCL				2		1												
<i>Cymbopleura naviculiformis</i>	CBNA	2		1	1									2					
<i>Diadesmis confervaceae</i>	DCTG																		2

Appendix 15A: Diatom count list – continued (1)

Taxon	CODE	D1A	D2A	D3A	D4A	D6A	D7A	D1B	D2B	D3B	D4B	D6B	D7B	D1C	D2C	D3C	D4C	D6C	D7C
<i>Diatoma tenuis</i>	DITE	1																	
<i>Discostella pseudostelligera</i>	DPST																1		
<i>Discostella stelligera</i>	DSTE																	1	
<i>Encyonema minutum</i>	ENMI						1												
<i>Encyonema ventricosum</i>	ENVE		2	1		1	1		1						1				
<i>Encyonema vulgare</i>	EVUL							26											3
<i>Eunotia bilunaris</i>	EBIL	5	8	1	2	1	1				1			2					
<i>Eunotia cf. botuliformis</i>	EBOT		1																
<i>Eunotia formicina</i>	EFOM		1					2			1			2	8				9
<i>Eunotia intermedia</i>	EUIN						2												
<i>Eunotia minor</i>	EMIN	2		1		1		4		6				1	1		2		4
<i>Eunotia soleirolii</i>	ESOL															4	4		
<i>Eunotia sp.</i>	EUNS	1	3	1	1												4		
<i>Eunotia tenella</i>	ETEN								1										
<i>Fistulifera saprophila</i>	FSAP	5					27			4									1
<i>Fragilaria capucina</i>	FRCA																		1
<i>Fragilaria famelica</i>	FFAM	5	1	1		1	13					6	1						2
<i>Fragilaria gracilis</i>	FGRA											4							
<i>Fragilaria longifusiformis</i>	FLFU																		1
<i>Fragilaria microvaucheriae</i>	FRAG				2		1												
<i>Fragilaria pararumpens</i>	FPRU	2		1		1	2						9	1	2			1	3
<i>Fragilaria pectinalis</i>	FPEC	12	2	9	7	6	4	2			4		2		2		11	11	
<i>Fragilaria rinoi</i>	FRIO			2	1		7												
<i>Fragilaria rumpens</i>	FRUM			1				12	3		1		2	2	2		1	2	9
<i>Fragilaria sp.</i>	FRAG1	6	2	5	4	1	1												
<i>Fragilaria tenera</i>	FTEN																		5
<i>Fragilaria vaucheriae</i>	FVAU										1								

Appendix 15A: Diatom count list – continued (2)

Taxon	CODE	D1A	D2A	D3A	D4A	D6A	D7A	D1B	D2B	D3B	D4B	D6B	D7B	D1C	D2C	D3C	D4C	D6C	D7C
<i>Fragilariforma bicapitata</i>	FFBI													1	1			2	
<i>Fragilariforma virescens</i>	FFVS																		2
<i>Frustulia vulgaris</i>	FVUL	7	1	1	3	1		4						49	2	1		2	
<i>Frustulia weinholdii</i>	FWEI													1					
<i>Geissleria decussis</i>	GDEC																	2	
<i>Gomphonema angustatum</i>	GANG1	5				2	21		1					2					
<i>Gomphonema cf. angustatum</i>	GANG	16	4	3	1		3	8	7	1	5	2		22	3		6		5
<i>Gomphonema exilissimum</i>	GEXL				1														
<i>Gomphonema graciledictum</i>	GGRA									2							1		1
<i>Gomphonema hebridense</i>	GHEB															2			
<i>Gomphonema innocens</i>	GINN						1												
<i>Gomphonema parvulus</i>	GPVL				5														
<i>Gomphonema parvulum</i>	GPAR	41	1	26	39	1	9	5	1	26	11	9	58	19	5	8	1	4	58
<i>Gomphonema pseudoaugur</i>	GPSA									2									
<i>Gomphonema pumilum</i>	GPUM	2						4											
<i>Gomphonema sp.</i>	GOMP							14						12	4				2
<i>Halamphora veneta</i>	HVEN																		3
<i>Hantzschia amphioxys</i>	HAMP		1			2													
<i>Hippodonta capitata</i>	HCAP	1	1		1	3	2			1	2		2			2		2	1
<i>Humidophila contenta</i>	HUCO									2							2		
<i>Humidophila perpusilla</i>	HPEP													1					
<i>Lemnicola cf. hungarica</i>	LHUN						1												
<i>Lemnicola hungarica</i>	LHUN	1	1										1						1
<i>Luticola frequentissima</i>	LUTI	1															1		
<i>Luticola goeppertiana</i>	LGOE	1																	
<i>Luticola saprophila</i>	LSAP										2			2	5		5	1	
<i>Mayamaea agrestis</i>	MAGR								2			2		4	2				6

Appendix 15A: Diatom count list – continued (3)

Taxon	CODE	D1A	D2A	D3A	D4A	D6A	D7A	D1B	D2B	D3B	D4B	D6B	D7B	D1C	D2C	D3C	D4C	D6C	D7C
<i>Mayamaea atomus</i>	MAAT																		1
<i>Mayamaea exelsa</i>	MAEX										1								
<i>Mayamaea fossalis</i>	MAFO													1					
<i>Mayamaea permitis</i>	MPMI	3				5	1	1	1			2	5						
<i>Melosira varians</i>	MVAR							1	1	1	1		1		3		1	1	1
<i>Meridion circulare</i>	MCIR	2																	1
<i>Meridion constrictum</i>	MCCO	1				2													
<i>Navicula antverpiensis</i>	NATV							4						2					
<i>Navicula arvensis</i>	NARV									2		1							1
<i>Navicula cincta</i>	NCIN													2					
<i>Navicula cryptocephala</i>	NCRY	7	2	5	2	1	5	12	5	2	1		16	2	1		2	4	8
<i>Navicula exilis</i>	NEXI		1												2	2			
<i>Navicula gregaria</i>	NGRE					12	2		2		1		8						8
<i>Navicula lanceolata</i>	NLAN		2		4	3	3		1		3				3		3	1	1
<i>Navicula reichardtiana</i>	NRCH											2	3					2	
<i>Navicula rhynchocephala</i>	NRHY	13	2	4	13	7	4	2						24	1		6	3	3
<i>Navicula sp.</i>	NAVI	3			2	1	1						6						
<i>Navicula subrhynchocephala</i>	NSRH		1																
<i>Navicula tenelloides</i>	NTEN	1					1												
<i>Navicula trivialis</i>	NTRV															2			
<i>Navicula veneta</i>	NVEN									2			2						
<i>Navicula vilaplantii</i>	NVIP						1												1
<i>Neidium ampliatum</i>	NEAM			1															
<i>Nitzschia acidoclinata</i>	NACD												1						3
<i>Nitzschia adamata</i>	NZAD						1								1				
<i>Nitzschia amphibia</i>	NAMP	2		1		5	2			21									14
<i>Nitzschia archibaldii</i>	NIAR											2					1		3

Appendix 15A: Diatom count list – continued (4)

Taxon	CODE	D1A	D2A	D3A	D4A	D6A	D7A	D1B	D2B	D3B	D4B	D6B	D7B	D1C	D2C	D3C	D4C	D6C	D7C
<i>Nitzschia capitellata</i>	NCPL						2							1					
<i>Nitzschia dissipata</i>	NDIS	11	9	7	16	11	6	27	2		1			112	3	1	1	5	2
<i>Nitzschia fonticola</i>	NFON											1							2
<i>Nitzschia frustulum</i>	NIFR																2	1	
<i>Nitzschia intermedia</i>	NINT	4		1									1						
<i>Nitzschia linearis</i>	NLIN	1												8					
<i>Nitzschia palea</i>	NPAL	5	1	4	13	5	36	1	4	8	4	6	66			2	4	2	2
<i>Nitzschia palea debilis</i>	NPAD									2							2		
<i>Nitzschia perminuta</i>	NIPM	1										1	3				1		
<i>Nitzschia pura</i>	NIPR		1																
<i>Nitzschia pusilla</i>	NIPU									2			2						1
<i>Nitzschia recta</i>	NREC	5	1	3	3	2	2				1			12					3
<i>Nitzschia sp.</i>	NITZ	4	4																
<i>Nitzschia subacicularis</i>	NSUA																1		
<i>Pinnularia anglica</i>	PIAN																		1
<i>Pinnularia appendiculata</i>	PAMJ													2					
<i>Pinnularia cf. subgibba/parvulissima</i>	PPVS				1		3												
<i>Pinnularia gibba</i>	PGIB	1						2		2	2			8	2	3			3
<i>Pinnularia microstauron</i>	PMIC	1		1			1	1	1					4		3	2		
<i>Pinnularia parvulissima</i>	PPVS			3	1														
<i>Pinnularia rupestris</i>	PRUP	1				3								2					
<i>Pinnularia schoenfelderi</i>	PSHO	1																	
<i>Pinnularia silvatica</i>	PSIL										3					2			
<i>Pinnularia sinistra</i>	PSIN										3	1						1	
<i>Pinnularia sp.</i>	PINS	9			1	11	1												
<i>Pinnularia subcapitata</i>	PSCA	2																	
<i>Pinnularia subrupestris</i>	PSRU	1																	

Appendix 15A: Diatom count list – continued (5)

Taxon	CODE	D1A	D2A	D3A	D4A	D6A	D7A	D1B	D2B	D3B	D4B	D6B	D7B	D1C	D2C	D3C	D4C	D6C	D7C
<i>Pinnularia viridiformis</i>	PVIF													1					
<i>Placoneis clementioides</i>	PCLD	2					2												
<i>Placoneis clementis</i>	PCLT														1				2
<i>Placoneis ignorata</i>	PLIG	2																	
<i>Planothidium alekseevae</i>	PLFR															4			
<i>Planothidium biporumum</i>	PLBI			1															
<i>Planothidium cf. engelbrechtii</i>	PLEN	7	11	1	13	16	15			125	75	84	2			12	13	9	3
<i>Planothidium cf. lanceolatum</i>	PLAN		7	2	2														
<i>Planothidium dau</i>	PDAU															2		1	
<i>Planothidium frequentissimum</i>	PLFR	4	2	19	16	13	25	4	13	12	21	18	1		19	3	5	15	14
<i>Planothidium granum</i>	PGRN		2						2			1			1		1		
<i>Planothidium lanceolatum</i>	PTLA	5	2	12	38	7	17	2	5	1	16	8			6	2	17	5	8
<i>Planothidium minutissimum</i>	PLMN			7	5	7	3												
<i>Planothidium potapovae</i>	PLFR		1			2													
<i>Planothidium reichardtii</i>	PLRC													3		1			
<i>Planothidium robustius</i>	PRBU														1				
<i>Planothidium rostratoholarcticum</i>	PRST							2	1	2					2				
<i>Platessa conspicua</i>	PTCO		1																
<i>Platessa hustedtii</i>	PLHU	1												1	1				
<i>Platessa oblongella</i>	KOBG	98	178	166	77	117	7	76	157	33	125	65		46	172	295	179	125	19
<i>Prestauroneis integra</i>	PITE		1																
<i>Prestauroneis protracta</i>	PPRE	1	1	1	9	5		2	11		12				3	4	13	1	11
<i>Psammothidium helveticum</i>	PHEL																		2
<i>Psammothidium rechtense</i>	PSRE				2														
<i>Psammothidium rosenstockii</i>	PRSK																		2
<i>Psammothidium sp.</i>	PLTD													2					
<i>Psammothidium subatomoides</i>	PSAT							2	1		7	3			1	3	1		1

Appendix 15A: Diatom count list – continued (6)

Taxon	CODE	D1A	D2A	D3A	D4A	D6A	D7A	D1B	D2B	D3B	D4B	D6B	D7B	D1C	D2C	D3C	D4C	D6C	D7C
<i>Pseudostaurosira brevistriata</i>	PSBR							2											
<i>Pseudostaurosira trainorii</i>	PTRN									2				1					
<i>Sellaphora atomoides</i>	EOMI1																	137	
<i>Sellaphora cosmopolitana</i>	NDCM					1													
<i>Sellaphora lundii</i>	NHFM	2																	
<i>Sellaphora nigri</i>	EOMI	14	7	67	8	69	37	9	144	117	56	123	92	14	17	31	45		14
<i>Sellaphora pupula</i>	SPUP	3																	
<i>Sellaphora pupula</i> s.l.	SPUP			1					4	1	1		2						
<i>Sellaphora rhombelliptica</i>	EORH									1	2					2	2		
<i>Sellaphora saugerresii</i>	SSEM	2	4					7	3	8	4	39	4		7		11	24	12
<i>Sellaphora</i> sp.	SELS	2	4	1															
<i>Stauroforma exiguiformis</i>	SEXG	4															2		
<i>Stauroneis amphicephala</i>	SAAP									1									
<i>Stauroneis gracilis</i>	SGRC	2												2					
<i>Stauroneis kriegeri</i>	STKR		1	2	5	4					4	2		6	6	4	8	3	36
<i>Stauroneis reichardtii</i>	SRCH						1												
<i>Stauroneis</i> sp.	STAS	1			1														
<i>Stauroneis thermicola</i>	STHE								2			2				1			2
<i>Staurosira binodis</i>	SBND								1										
<i>Staurosira</i> sp.	SSPE										7								
<i>Staurosira venter</i>	SSVE								1						1		2	14	6
<i>Staurosirella berolinensis</i>	STSB	4																2	
<i>Staurosirella martyi</i>	SLMA	1		4					2		2	2					6		
<i>Staurosirella pinnata</i>	SPIN	1		1							1								2
<i>Staurosirella</i> sp.	SSSP											1							
<i>Stephanodiscus hantzschii</i>	SHAN													2			3		7
<i>Stephanodiscus parvus</i>	SPAV																		2

Appendix 15A: Diatom count list – continued (7)

Taxon	CODE	D1A	D2A	D3A	D4A	D6A	D7A	D1B	D2B	D3B	D4B	D6B	D7B	D1C	D2C	D3C	D4C	D6C	D7C
<i>Stephanodiscus</i> sp.	STSP	2					1												
<i>Stephanodiscus tenuis</i>	STTU										1						2		9
<i>Surirella amphioxys</i>	SAPH	1																	
<i>Surirella angusta</i>	SANG														1				1
<i>Surirella brebissonii</i>	SBKU					1	1												
<i>Surirella brebissonii kuetzingii</i>	SBKU																		1
<i>Surirella minuta</i>	SUMI																	1	
<i>Tabellaria flocculosa</i>	TFLO	6						1	1										1
<i>Ulnaria acus</i>	UACU																		2
<i>Ulnaria</i> sp.	ULNS	1	1																
<i>Ulnaria ulna</i>	UULN	7	22	15	21	8	9	3	4	1	2		1	1	3	1		5	8
<i>Ulnaria vitrea</i>	UVIT																2		

Appendix 15B: Diatoms systematic overview: *Melosira varians* – *Stephanodiscus parvus*

Classification after AlgaeBase.org

- D. (divisio, phylum)
 - sD. (subdivisio, subphylum)
 - Cl. (classis, class)
 - sCl. (subclassis, subclass)
 - O. (ordo, order)
 - sO. (subordo, suborder)
 - F. (familia, family)
 - Genus species*

Empire Eukaryota
Kingdom Chromista

- D.
Bacillariophyta
 - sD. Coscinodiscophytina
 - Cl. Coscinodiscophyceae
 - sCl. Melosirophycidae
 - O. Melosirales
 - F. Melosiraceae
 - Melosira varians* C.Agardh
-
- O. Aulacoseirales
 - F. Aulacoseiraceae
 - Aulacoseira ambigua* (Grunow) Simonsen
 - Aulacoseira muzzanensis* (F.Meister) Krammer
 - Aulacoseira tenella* (Nygaard) Simonsen

- sD. Bacillariophytina
 - Cl. Mediophyceae
 - sCl. Thalassiosirophycidae
 - O. Stephanodiscales
 - F. Stephanodiscaceae
 - Cyclotella meneghiniana* Kützing
 - Discostella pseudostelligera* (Hustedt) Houk & Klee
 - Discostella stelligera* (Cleve & Grunow) Houk & Klee
 - Stephanodiscus hantzschii* f. *tenuis* (Hustedt) Håkansson & Stoermer
 - Stephanodiscus hantzschii* Grunow
 - Stephanodiscus parvus* Stoermer & Håkansson

- Cl. Bacillariophyceae
 - sCl. Fragilariophycidae
 - O. Fragilariales

Appendix 15B: *Fragilaria capucina* – *Eunotia soleirolii*

F. Fragilariaceae

- Fragilaria capucina* Desmazières
- Fragilaria famelica* (Kützing) Lange-Bertalot
- Fragilaria gracilis* Østrup
- Fragilaria longifusiformis* (Hains & Sebring) Siver et al. - unchecked
- Fragilaria microvaucheriae* C.E.Wetzel & Ector
- Fragilaria pararumpens* Lange-Bertalot, G.Hofmann & Werum
- Fragilaria pectinalis* (O.F.Müller) Lyngbye
- Fragilaria rinoi* Almeida & C.Delgado
- Fragilaria rumpens* (Kützing) G.W.F.Carlson
- Fragilaria tenera* (W.Smith) Lange-Bertalot
- Fragilaria vaucheriae* (Kützing) J.B.Petersen
- Fragilariforma bicapitata* (A.Mayer) D.M.Williams & Round
- Fragilariforma virescens* (Ralfs) D.M.Williams & Round

F. Staurosiraceae

- Nanofrustulum trainorii* (E.A.Morales) E.A.Morales
- Pseudostaurosira brevistriata* (Grunow) D.M.Williams & Round
- Stauroforma exiguiformis* (Lange-Bertalot) R.J.Flower, V.J.Jones & Round
- Staurosira binodis* (Ehrenberg) Lange-Bertalot
- Staurosira venter* (Ehrenberg) Cleve & J.D.Möller
- Staurosirella martyi* (Héribaud-Joseph) E.A.Morales & K.M.Manoylov
- Staurosirella pinnata* (Ehrenberg) D.M.Williams & Round

O. Licmophorales

F. Ulnariaceae

- Ctenophora pulchella* (Ralfs ex Kützing) D.M.Williams & Round
- Ulnaria acus* (Kützing) Aboal
- Ulnaria ulna* (Nitzsch) Compère
- Ulnaria vitrea* (Kützing) E.Reichardt

O. Tabellariales

F. Tabellariaceae

- Diatoma tenuis* C.Agardh
- Meridion circulare* (Greville) C.Agardh
- Meridion constrictum* Ralfs
- Tabellaria flocculosa* (Roth) Kützing

sCl. Eunotiophycidae

O. Eunotiales

F. Eunotiaceae

- Eunotia bilunaris* (Ehrenberg) Schaarschmidt
- Eunotia* cf. *botuliformis* F.Wild, Nörpel & Lange-Bertalot
- Eunotia formicina* Lange-Bertalot
- Eunotia intermedia* (Krasske ex Hustedt) Nörpel & Lange-Bertalot
- Eunotia minor* (Kützing) Grunow

Appendix 15B: *Eunotia tenella* – *Planothidium rostratoholarcticum*

Eunotia soleirolii (Kützing) Rabenhorst

Eunotia tenella (Grunow) Hustedt

sCl. Bacillariophycidae

O. Bacillariales

F. Bacillariaceae

Hantzschia amphioxys (Ehrenberg) Grunow

Nitzschia acidoclinata Lange-Bertalot

Nitzschia adamata Hustedt

Nitzschia amphibia Grunow

Nitzschia archibaldii Lange-Bertalot

Nitzschia capitellata Hustedt

Nitzschia dissipata (Kützing) Rabenhorst

Nitzschia fonticola (Grunow) Grunow

Nitzschia frustulum (Kützing) Grunow

Nitzschia intermedia Hantzsch

Nitzschia linearis W.Smith

Nitzschia palea (Kützing) W.Smith

Nitzschia palea var. *debilis* (Kützing) Grunow

Nitzschia perminuta Grunow

Nitzschia pura Hustedt

Nitzschia pusilla Grunow

Nitzschia recta Hantzsch ex Rabenhorst

Nitzschia subacicularis Hustedt, nom. inval.

O. Cocconeidales

F. Achnanthidiaceae

Achnanthidium catenatum (Bily & Marvan) Lange-Bertalot

Achnanthidium jackii Rabenhorst

Achnanthidium microcephalum Kützing

Achnanthidium minutissimum (Kützing) Czarnecki

Achnanthidium peetersianum C.E. Wetzel, I. Juttner & L. Ector

Achnanthidium rosenstockii (Lange-Bertalot) Lange-Bertalot

Lemnicola cf. *hungarica* (Grunow) Round & Basson

Planothidium alekseevae Gogorev & Lange

Planothidium biporum (M.H. Hohn & Hellerman) Lange-Bertalot

Planothidium dau (Foged) Lange-Bertalot

Planothidium cf. *engelbrechtii* (Cholnoky) Round & Bukhtiyarova

Planothidium frequentissimum (Lange-Bertalot) Lange-Bertalot

Planothidium granum (M.H. Hohn & Hellerman) Lange-Bertalot

Planothidium lanceolatum (Brébisson ex Kützing) Lange-Bertalot

Planothidium cf. *lanceolatum* (Brébisson ex Kützing) Lange-Bertalot

Planothidium minutissimum (Krasske) E.A. Morales

Planothidium potapovae C.E. Wetzel & L. Ector

Planothidium reichardtii Lange-Bertalot & Werum

Planothidium robustum (Hustedt) Lange-Bertalot

Appendix 15B: *Psammothidium helveticum* – *Mayamaea atomus*

Planothidium rostratoholarcticum Lange-Bertalot & Bak
Psammothidium helveticum (Hustedt) Bukhtiyarova & Round
Psammothidium hustedtii (Krasske) S.Mayama
Psammothidium rechtense (Leclercq) Lange-Bertalot
Psammothidium subatomoides (Hustedt) Bukhtiyarova & Round

F. Cocconeidaceae

Cocconeis euglypta Ehrenberg
Cocconeis lineata Ehrenberg
Cocconeis pediculus Ehrenberg

O. Cymbellales

F. Anomoeoneidaceae

Adlafia brockmannii (Hustedt) Bruder & Hinz

F. Cymbellaceae

Cymbopleura naviculiformis (Auerswald ex Heiberg) Krammer
Geissleria decussis (Østrup) Lange-Bertalot & Metzeltin

F. Gomphonemataceae

Encyonema minutum (Hilse) D.G.Mann
Encyonema ventricosum (C.Agardh) Grunow
Encyonema vulgare Krammer
Gomphonema angustatum (Kützing) Rabenhorst
Gomphonema cf. *angustatum* (Kützing) Rabenhorst
Gomphonema exilissimum (Grunow) Lange-Bertalot & E.Reichardt
Gomphonema graciledictum E.Reichardt
Gomphonema hebridense W.Gregory
Gomphonema innocens E.Reichardt
Gomphonema parvulus (Lange-Bertalot & E.Reichardt) Lange-Bertalot & E.Reichardt
Gomphonema parvulum (Kützing) Kützing
Gomphonema pseudoaugur Lange-Bertalot
Gomphonema pumilum (Grunow) E.Reichardt & Lange-Bertalot
Placoneis clementioides (Hustedt) E.J.Cox
Placoneis clementis (Grunow) E.J.Cox
Placoneis ignorata (Schimanski) Lange-Bertalot

O. Mastogloiales

F. Achnanthaceae

Platessa conspicua (Ant.Mayer) Lange-Bertalot
Platessa oblongella (Østrup) C.E.Wetzel, Lange-Bertalot & Ector

O. Naviculales

F. Naviculales incertae sedis

Chamaepinnularia soehrensensis (Krasske) Lange-Bertalot & Krammer
Mayamaea agrestis (Hustedt) Lange-Bertalot

Appendix 15B: *Mayamaea excelsa* – *Diadesmis confervacea*

Mayamaea atomus (Kützing) Lange-Bertalot
Mayamaea excelsa (Krasske) Lange-Bertalot
Mayamaea fossalis (Krasske) Lange-Bertalot
Mayamaea permitis (Hustedt) K.Bruder & Medlin

sO. Naviculineae

F. Naviculaceae

Caloneis lancettula (Schulz) Lange-Bertalot & Witkowski
Hippodonta capitata (Ehrenberg) Lange-Bertalot, Metzeltin & Witkowski
Navicula antverpiensis B.Van de Vijver & Lange-Bertalot
Navicula arvensis Hustedt
Navicula cincta (Ehrenberg) Ralfs
Navicula cryptocephala (Kützing)
Navicula exilis Kützing
Navicula gregaria Donkin
Navicula lanceolata Ehrenberg
Navicula metareichardtiana Lange-Bertalot & Kusber
Navicula rhynchocephala Kützing
Navicula subrhynchocephala Hustedt
Navicula tenellodes Hustedt
Navicula trivialis Lange-Bertalot
Navicula veneta Kützing
Navicula vilaplani (Lange-Bertalot & Sabater) Lange-Bertalot & Sabater

F. Stauroneidaceae

Craticula sp. Grunow
Fistulifera saprophila (Lange-Bertalot & Bonik) Lange-Bertalot
Prestauroneis integra (W.Smith) Bruder
Prestauroneis protracta (Grunow) Kulikovskiy & Glushchenko
Stauroneis amphicephala Kützing
Stauroneis gracilis Ehrenberg
Stauroneis kriegeri R.M.Patrick
Stauroneis reichardtii Lange-Bertalot, Cavacini, Tagliaventi & Alfinito
Stauroneis thermicola (J.B.Petersen) J.W.G.Lund

sO. Neidiineae

F. Amphipleuraceae

Frustulia vulgaris (Thwaites) De Toni
Frustulia weinholdii Hustedt
Halamphora veneta (Kützing) Levkov

F. Cavinulaceae

Cavinula variostrata (Krasske) D.G.Mann & A.J.Stickle

F. Diadesmidaceae

Diadesmis confervacea Kützing

Appendix 15B: *Humidophila contenta* – *Surirella minuta*

Humidophila contenta (Grunow) Lowe, Kociolek, J.R.Johansen, Van de Vijver, Lange-Bertalot & Kopalová

Humidophila perpusilla (Grunow) Lowe, Kociolek, J.R.Johansen, Van de Vijver, Lange-Bertalot & Kopalová

Luticola frequentissima Levkov, Metzeltin & A.Pavlov

Luticola goeppertiana (Bleisch) D.G.Mann ex J.Rarick, S.Wu, S.S.Lee & Edlund

Luticola saprophila Levkov, Metzeltin & A.Pavlov

F. Neidiaceae

Neidium ampliatum (Ehrenberg) Krammer

sO. Sellaphorineae

F. Pinnulariaceae

Pinnularia anglica Krammer

Pinnularia appendiculata (C.Agardh) Schaarschmidt

Pinnularia gibba (Ehrenberg) Ehrenberg

Pinnularia microstauron (Ehrenberg) Cleve

Pinnularia parvulissima Krammer

Pinnularia parvulissima Krammer

Pinnularia rupestris Hantzsch

Pinnularia schoenfelderi Krammer

Pinnularia silvatica J.B.Petersen

Pinnularia sinistra Krammer

Pinnularia subcapitata W.Gregory

Pinnularia subrupestris Krammer

Pinnularia viridiformis Krammer

F. Sellaphoraceae

Sellaphora atomoides (Grunow) Wetzel & Van de Vijver

Sellaphora cosmopolitana (Lange-Bertalot) C.E.Wetzel & L.Ector

Sellaphora lundii C.E.Wetzel, Barragán & Ector

Sellaphora nigri (De Notaris) C.E.Wetzel & L.Ector

Sellaphora pupula (Kützing) Mereschkovsky

Sellaphora pupula (Kützing) Mereschkovsky

Sellaphora rhombelliptica (G.Moser, Lange-Bertalot & Metzeltin) C.E.Wetzel & L.Ector

Sellaphora saugerresii (Desmazières) C.E.Wetzel & D.G.Mann

O. Surirellales

F. Surirellaceae

Iconella amphioxys (W.Smith) D.Kapustin & O.Kryvosheia

Surirella angusta Kützing

Surirella brebissonii Krammer & Lange-Bertalot

Surirella brebissonii var. *kuetzingii* Krammer & Lange-Bertalot

Surirella minuta Brébisson ex Kützing, nom. illeg.

O. Thalassiophysales

F. Catenulaceae

Appendix 15B: *Amphora copulata* – *Belonastrum berolinense*

Amphora copulata (Kützing) Schoeman & R.E.M. Archibald

Amphora indistincta Levkov

Amphora normanii Rabenhorst

Amphora pediculus (Kützing) Grunow

Cl. Bacillariophyta classis incertae sedis

O. Bacillariophyta ordo incertae sedis

F. Bacillariophyta familia incertae sedis

Belonastrum berolinense (Lemmerman) Round & Maidana

Appendix 16A

Table 16A: List based on 20 most abundant taxa of each sample. With pH (R), salinity (H), oxygen requirements (O), saprobity (S) and trophic state (T). Scores R=6 and T=7 indicated in red represent 'indifferent' taxa to a specific ecological classification and were not included in calculating the ecological scores.

TAXON	R	H	O	S	T
<i>Achnanthydium microcephalum</i>	4	2	1	2	5
<i>Aulacoseira ambigua</i>	4	2	3	2	5
<i>Encyonema vulgare</i>	2	1	1	1	1
<i>Eunotia bilunaris</i>	6	2	2	2	7
<i>Eunotia formicina</i>	2	2	1	1	3
<i>Eunotia</i> sp.	0	0	0	0	0
<i>Fistulifera saprophila</i>	3	2	4	4	5
<i>Fragilaria famelica</i>	3	2	4	4	5
<i>Fragilaria microvaucheriae</i>	0	2	0	2	5
<i>Fragilaria pararumpens</i>	3	2	0	2	7
<i>Fragilaria pectinalis</i>	3	2	0	2	5
<i>Fragilaria rumpens</i>	3	2	0	2	3
<i>Frustulia vulgaris</i>	4	2	1	2	4
<i>Gomphonema angustatum</i>	3	2	2	3	4
<i>Gomphonema parvulum</i>	3	2	4	4	5
<i>Gomphonema</i> sp.	0	0	0	0	0
<i>Hippodonta capitata</i>	4	2	3	3	4
<i>Mayamaea permitis</i>	4	2	4	4	5
<i>Navicula cryptocephala</i>	3	2	3	3	7
<i>Navicula gregaria</i>	4	3	4	3	5
<i>Navicula rhychocephala</i>	4	2	4	2	7
<i>Nitzschia amphibia</i>	4	2	3	3	5
<i>Nitzschia dissipata</i>	4	2	2	2	4
<i>Nitzschia linearis</i>	4	2	2	2	4
<i>Nitzschia palea</i>	3	2	4	5	6
<i>Nitzschia recta</i>	4	2	2	2	7
<i>Pinnularia gibba</i>	3	2	3	3	7
<i>Pinnularia</i> sp.	0	0	0	0	0
<i>Planothidium alekseevae</i>	4	3	0	3	5
<i>Planothidium</i> cf. <i>engelbrechtii</i>	0	0	0	0	0
<i>Planothidium lanceolatum</i>	4	2	3	3	5
<i>Platessa oblongella</i>	3	2	2	3	7
<i>Prestauroneis protracta</i>	3	3	3	2	5
<i>Sellaphora atomoides</i>	4	2	4	4	5
<i>Sellaphora cosmopolitana</i>	0	2	0	3	5
<i>Sellaphora saugerresii</i>	3	2	4	4	5
<i>Stauroneis kriegeri</i>	3	2	2	2	4
<i>Staurosira venter</i>	4	2	1	2	4
<i>Stephanodiscus tenuis</i>	5	2	4	4	6
<i>Ulnaria ulna</i>	4	2	3	3	5

Appendix 16B

Table 16B: Ecological scores calculated based on diatom abundances, as well as ecological attribute scores in Appendix 16A, including pH (R), salinity (H), oxygen requirements (O), saprobity (S) and trophic state (T). Each weighted mean score is shown alongside a % (in *italics*) indicating the proportion of the total number of valves used in calculating the respective score (total $N = 400$ valves per sample). These percentages are colour coded: **brown** = < 75%, **red** indicates < 50% of 20 most abundant taxa represented.

Sample	R		H		O		S		T	
D1A	2.9	<i>74%</i>	1.8	<i>75%</i>	2.3	<i>75%</i>	2.7	<i>75%</i>	4.1	<i>45%</i>
D2A	3.4	<i>87%</i>	2.0	<i>89%</i>	2.3	<i>89%</i>	3.0	<i>89%</i>	4.5	<i>42%</i>
D3A	3.2	<i>91%</i>	2.0	<i>91%</i>	2.4	<i>91%</i>	3.1	<i>91%</i>	4.7	<i>47%</i>
D4A	3.4	<i>91%</i>	2.0	<i>91%</i>	2.8	<i>91%</i>	3.1	<i>91%</i>	4.7	<i>67%</i>
D6A	3.2	<i>91%</i>	1.9	<i>91%</i>	2.3	<i>91%</i>	2.8	<i>91%</i>	4.4	<i>60%</i>
D7A	3.1	<i>89%</i>	2.0	<i>89%</i>	2.9	<i>89%</i>	3.4	<i>89%</i>	4.8	<i>85%</i>
D1B	3.4	<i>95%</i>	1.9	<i>95%</i>	1.5	<i>95%</i>	2.2	<i>95%</i>	4.2	<i>72%</i>
D2B	3.5	<i>94%</i>	2.1	<i>94%</i>	2.8	<i>94%</i>	3.4	<i>94%</i>	4.9	<i>53%</i>
D3B	2.4	<i>93%</i>	1.4	<i>93%</i>	2.2	<i>93%</i>	2.4	<i>93%</i>	3.2	<i>84%</i>
D4B	2.7	<i>88%</i>	1.7	<i>88%</i>	2.0	<i>88%</i>	2.5	<i>88%</i>	3.3	<i>56%</i>
D6B	2.8	<i>93%</i>	1.6	<i>93%</i>	2.4	<i>93%</i>	2.8	<i>93%</i>	3.6	<i>77%</i>
D7B	3.3	<i>95%</i>	1.9	<i>95%</i>	3.5	<i>95%</i>	3.8	<i>95%</i>	4.9	<i>88%</i>
D1C	3.6	<i>89%</i>	1.9	<i>89%</i>	2.1	<i>89%</i>	2.3	<i>89%</i>	4.0	<i>66%</i>
D2C	3.3	<i>90%</i>	2.0	<i>90%</i>	2.5	<i>90%</i>	3.2	<i>90%</i>	4.7	<i>46%</i>
D3C	3.0	<i>92%</i>	2.0	<i>92%</i>	2.2	<i>92%</i>	3.0	<i>92%</i>	4.1	<i>18%</i>
D4C	3.1	<i>85%</i>	2.0	<i>85%</i>	2.3	<i>85%</i>	3.0	<i>85%</i>	4.4	<i>38%</i>
D6C	3.4	<i>94%</i>	2.0	<i>94%</i>	2.7	<i>94%</i>	3.3	<i>94%</i>	4.7	<i>61%</i>
D7C	3.0	<i>74%</i>	1.9	<i>74%</i>	2.5	<i>74%</i>	2.7	<i>74%</i>	4.1	<i>67%</i>

Appendix 17

Table 17A: Summary of statistical tests conducted with diatom indices TDI (Trophic Diatom Index), IPS (Specific Polluosensitivity Index) and IBD (Diatom Biological Index). **Left:** comparison of index values between up- and downstream sites using Student's t -test. Assumptions were tested using the Shapiro-Wilk test and the F -test. **Right:** comparison of index values between sampling campaigns (A, B, C) using a one-way ANOVA approach. Assumptions were tested using the Shapiro-Wilk test and Levene's test. Significance levels: * = $p < 0.05$; ** = $p < 0.01$; *** = $p < 0.001$; ns = not significant.

	UP vs DOWNSTREAM			SEASON		
	TDI	IPS	IBD	TDI	IPS	IBD
$N(\mu, \sigma^2)$	1	1	1	1	1	1
σ^2	1	1	0	1	1	1
Test	t	t	t	a	a	a
p	.	*	*	ns	ns	ns
	up < down	up > down	up > down			

Appendix 18A - PCA: diatom counts

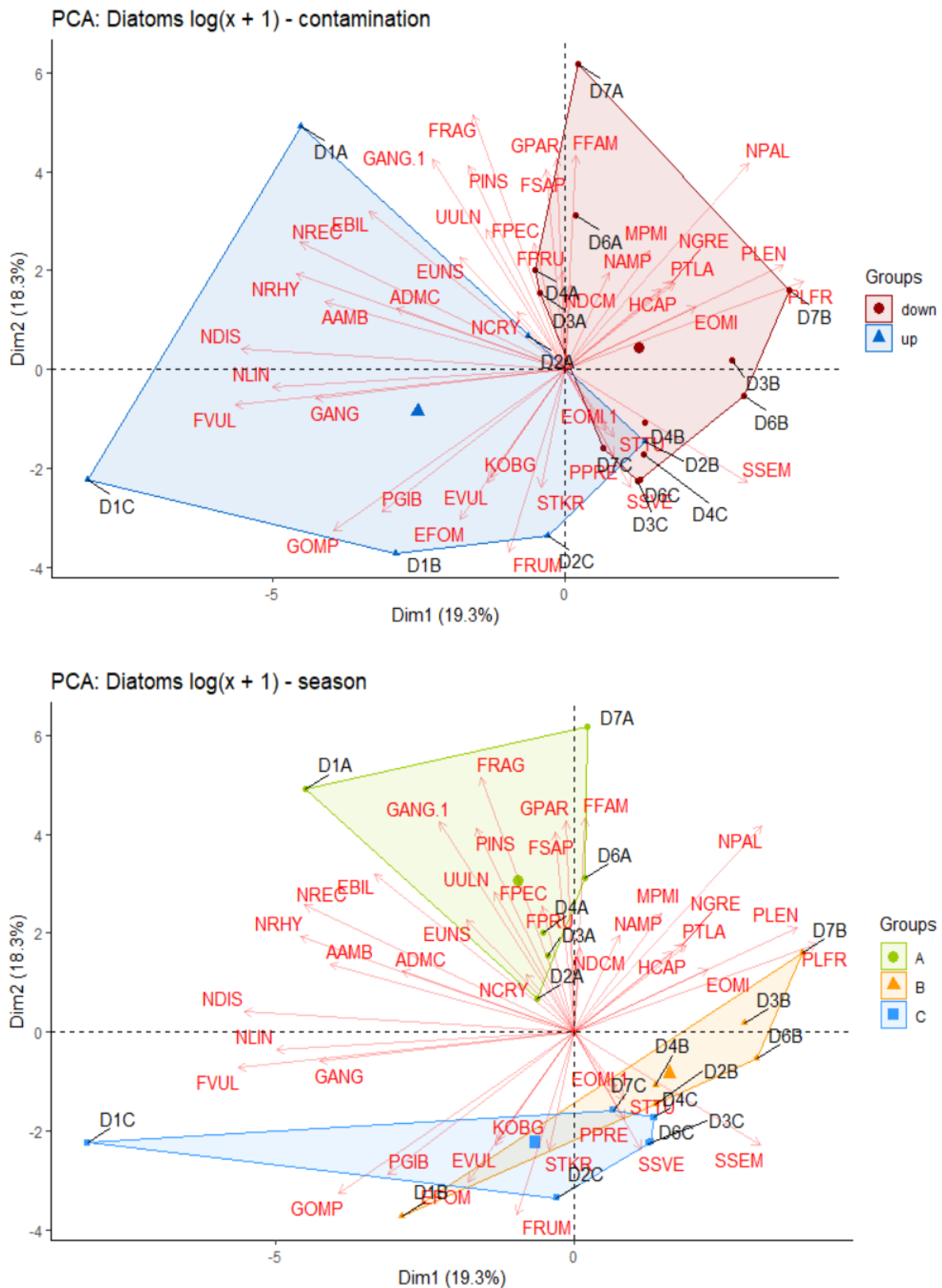


Figure 18A: Principal Component Analysis diagram for diatom counts with grouping based on ‘contamination’ (up vs downstream; **top**) and based on sampling campaign (‘season’; A: 17/04/2019; B: 21/08/2019; C: 24/01/2020; **bottom**), data $\log(x + 1)$ transformed. Bottom graph provided in text (Fig. 6) but shown enlarged here. Variables under investigation are indicated with red arrows. Additional information on the different PC axes can be found in Appendix 18B. Diatom codes can be found in Appendix 15.

Appendix 18B - PCA: diatom counts

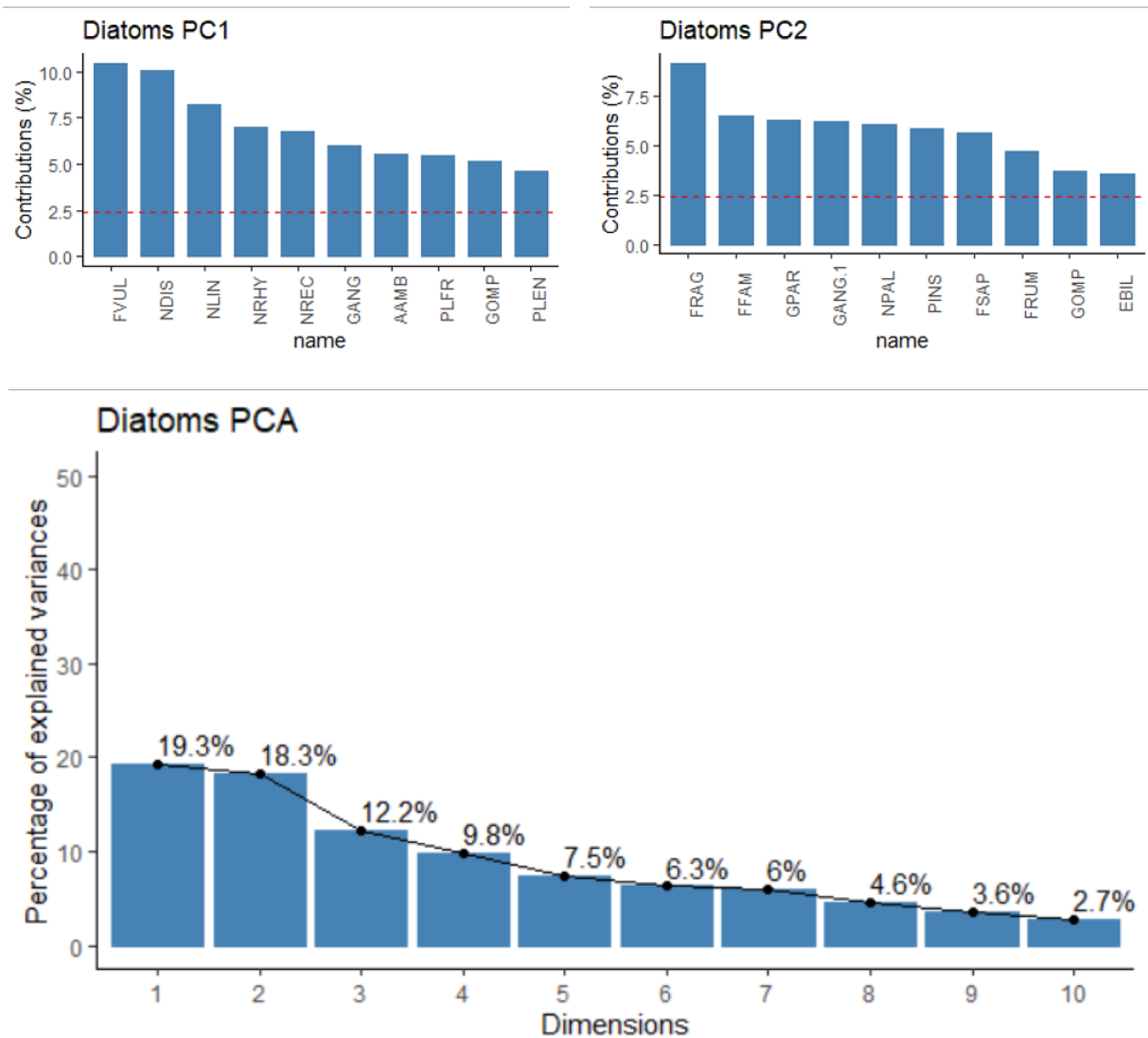


Figure 18B: Graphs supporting the PCA diagrams in Figure 6 and Appendix 18A. Graphs on top show the top 10 of variables contributing to either PC1 (Dim1; left) or PC2 (Dim2; right). The red dashed line serves as a reference which corresponds to the expected value if the contribution were uniform. The bottom graph shows the percentage of variance explained by the different PC dimensions. Diatom codes can be found in Appendix 15.

Appendix 19A: Macroinvertebrates count list

Table 19A: Count data of all macroinvertebrate samples across all sampling campaigns (A, B, C).

Taxon	D1A	D2A	D3A	D4A	D6A	D7A	D1B	D2B	D3B	D4B	D6B	D7B	D1C	D2C	D3C	D4C	D6C	D7C
Platyhelminthes																		
<i>Dendrocoelum</i>		5									8				1		1	
<i>Dugesia</i> s.l.	2	1	5			1		14	27	3	15	4			5	3	1	2
<i>Polycelis</i>		9	5					11	23		1			1	8	5		8
Oligochaeta																		
Lumbricidae	67	80	153	48	4			11	83	39	5	7	5	25	15	26	21	2
Naididae s.s.		20	25			2	10	3	2					9	5			
Tubificidae	2	16	30	12	8	25		21	357		2	11		22	62	53	27	12
Hirudinea																		
<i>Erpobdella</i>		10	9	8	1	1	3	11	105	14	31	7		3	48	1	2	
<i>Glossiphonia</i>		4	1					1										
<i>Helobdella</i>	1	20	13	4	3			99	166	34	46	27		11	20	25		
<i>Hemiclepsis</i>									2							1		
<i>Piscicola</i>								8	2									
<i>Theromyzon</i>		1	2								1						1	1
Mollusca																		
<i>Bathyomphalus</i>																		1
<i>Gyraulus</i>	2					5			2			11					2	1
<i>Hippeutis</i>				4			1	5			7							
<i>Lymnaea</i> s.l.	3			8	11	34		5	18	18	220	40				5	2	2
<i>Physa</i> s.s.		1				4		2	83	18	29	5			1	3		4
<i>Pisidium</i>	48	8	4	4	4	58		1	16	27		13	115	3		13	3	32
<i>Planorbarius</i>										1	11							
<i>Planorbis</i>								1	4		1							
<i>Sphaerium</i>	5			20	16	12			1	2	115	8	6	2		1	20	8
Acari																		
<i>Hydracarina</i> s.l.	68	142	66	40	4	21	7	16	14	22	41	20	21	155	28	39	23	11

Appendix 19A: Macroinvertebrates count list – continued (1)

Taxon	D1A	D2A	D3A	D4A	D6A	D7A	D1B	D2B	D3B	D4B	D6B	D7B	D1C	D2C	D3C	D4C	D6C	D7C
Crustacea																		
Asellidae	141	39	95			23	65	168	4	3	105	81	37	124	115	9	40	62
Crangonyctidae	1						1	1					4	9				
Gammaridae	74	23	6	4		33	31	29	4		3	44	73	5	26	1	2	162
Ephemeroptera																		
<i>Baetis</i>		124	33	16			5	43	4						2			
<i>Caenis</i>												1						
<i>Ephemera</i>	1																	
Odonata																		
<i>Aeshna</i>									3			1						
<i>Calopteryx</i>	25	11	32	12	4	8	10	28	33	4	13	26	2		7	18	9	5
<i>Coenagrion</i>				4														
Coenagrionidae									1									
<i>Libellula</i>											5	1						
<i>Platycnemis</i>			4					5	4	3	2	2			1	1		1
<i>Somatochlora</i>													1					
Hemiptera																		
<i>Arctocorisa</i>														1				
<i>Corixa</i>								3			2							
<i>Micronecta</i>				4														
<i>Microvelia</i>																1		
<i>Plea</i>											1							
Megaloptera																		
<i>Sialis</i>											1							
Coleoptera																		
Dytiscidae		2				2	5	4	1	1		1						
Gyrinidae								1			1							

Appendix 19A: Macroinvertebrates count list – continued (2)

Taxon	D1A	D2A	D3A	D4A	D6A	D7A	D1B	D2B	D3B	D4B	D6B	D7B	D1C	D2C	D3C	D4C	D6C	D7C
Haliplidae										4		2						
Trichoptera																		
Hydropsychidae	35		4	4	2		8	2	5				7		2	7	1	1
Hydroptilidae		10	4															
Leptoceridae	17	10	8			3						2	2	1	1	5	1	3
Limnephilidae s.l.	45					6					1		4	2	3		6	15
Polycentropodidae	1																	
Sericostomatidae	1																	
Diptera																		
Ceratopogonidae	3		3	12		4						1	1		1	6		1
Chironomidae (Ch.)	485	199	797	460	151	107	33	45	8	111	30	24	17	139	155	165	60	17
Ch. non <i>thummi-plumosus</i>																		
Ch. <i>thummi-plumosus</i>	1		8	4	1	5				19				6	2			
Limoniidae	7						2		1	1			11					
Psychodidae								2										
Simuliidae	24	139	94	32	126	18	493	6	53	2	2		6	9	8	179	44	65
Tipulidae	1						1		1				2					

Appendix 19B – List of macroinvertebrate PCA codes

Table 19B: Macroinvertebrate codes used in PCA. Selection of taxa was obtained from filtering the count list for all species with a proportionate abundance of >2% in at least one sample.

TAXON	CODE
<i>Asellidae</i>	ASEL
<i>Baetis</i>	BAET
<i>Calopteryx</i>	CALO
<i>Chironomidae non thummi-plumosus</i>	CHIN
<i>Chironomidae thummi-plumosus</i>	CHIT
<i>Dugesia</i> s.l.	DUGE
<i>Erpobdella</i>	ERPO
<i>Gammaridae</i>	GAMM
<i>Gyraulus</i>	GYRA
<i>Helobdella</i>	HELO
<i>Hydracarina</i> s.l.	HYDA
<i>Hydropsychidae</i>	HYDO
<i>Limnephilidae</i> s.l.	LIMN
<i>Limoniidae</i>	LIMO
<i>Lumbricidae</i>	LUMB
<i>Lymnaea</i> s.l.	LYMN
<i>Naididae</i> s.s.	NAID
<i>Physa</i> s.s.	PHYS
<i>Pisidium</i>	PISI
<i>Polycelis</i>	POLY
<i>Simuliidae</i>	SIMU
<i>Sphaerium</i>	SPHA
<i>Tubificidae</i>	TUBI

Appendix 19C: Macroinvertebrates systematic overview

Classification after De Pauw en Vannevel (1991)

Ph. (phylum)

sPh. (subphylum)

Cl. (classis, class)

sCl. (subclassis, subclass)

Coh. (cohort)

SO. (superordo, superorder)

O. (ordo, order)

sO. (subordo, suborder)

iO. (infraordo, infraorder)

SF. (superfamilia, superfamily)

F. (familia, family)

sF. (subfamilia, subfamily)

Genus species

Empire Eukaryota

Kingdom Animalia

Ph. Plathelminthes (syn. Platyhelminthes)

Cl. Turbellaria

O. Seriata

sO. Tricladida

F. Planariidae

Polycelis

F. Dugesiidae

Dugesia

F. Dendrocoelidae

Dendrocoelum lacteum

Ph. Annelida

Cl. Oligochaeta

F. Tubificidae

F. Naeididae

F. Lumbricidae

Cl. Hirudinea (syn. Achaeta)

O. Rhynchobdellae

F. Piscicolidae

Piscicola geometra

F. Glossiphonidae

Glossiphonia

Appendix 19C: Macroinvertebrates systematic overview – continued (1)

Hemiclepsis marginatum

Helobdella stagnalis

Theromyzon tessulatum

O. Pharyngobdellae

F. Erpobdellidae

Erpobdella

Ph. Mollusca

Cl. Gastropoda

sCl. Pulmonata

O. Basommatophora

F. Physidae

Physa

F. Lymnaeidae

Lymnaea

F. Planorbidae

Planorbis

Gyraulus

Bathyomphalus contortus

Hippeutis complanatus

Planorbarius corneus

Cl. Bivalvia

sCl. Heterodonta

O. Veneroida

F. Sphaeriidae

Sphaerium

Pisidium

Ph. Arthropoda

sPh. Chelicerata

Cl. Arachnida

sCl. Acari

Coh. Acariformes

O. Actinedida (syn. Hydracarina)

sPh. Crustacea

Cl. Malacostraca

SO. Peracarida

O. Amphipoda

F. Gammaridae

F. Crangonyctidae

Appendix 19C: Macroinvertebrates systematic overview – continued (2)

O. Isopoda

sO. Asellota

F. Asellidae

sPh. Uniramia

Cl. Insecta, Hexapoda

sCl. Pterygota

O. Ephemeroptera

F. Baetidae

Baetis

F. Ephemeridae

Ephemera

F. Caenidae

Caenis

O. Odonata

sO. Zygoptera

F. Calopterygidae

Calopteryx

F. Platycnemidae

Platycnemis pennipes

F. Coenagrionidae

Coenagrion

sO. Anisoptera

F. Aeschnidae

Aeschna

F. Corduliidae

Somatochlora

F. Libellulidae

Libellula

O. Hemiptera

iO. Gerromorpha

F. Veliidae

Microvelia

iO. Nepomorpha

F. Pleidae

Plea minutissima

Appendix 19C: Macroinvertebrates systematic overview – continued (3)

F. Corixidae
Micronecta
Corixa
Arctocorisa

O. Megaloptera

F. Sialidae
Sialis

O. Coleoptera

sO. Adephaga
SF. Caraboidea
F. Haliplidae
F. Dytiscidae
F. Gyrinidae

O. Trichoptera

F. Hydroptilidae
F. Hydropsychidae
F. Polycentropodidae
F. Limnephilidae
F. Leptoceridae
F. Sericostomatidae

O. Diptera

sO. Nematocera
F. Psychodidae

F. Chironomidae (syn. Tendipedidae)
Chironomidae thummi-plumosus
Chironomidae non thummi-
plumosus

F. Ceratopogonidae

F. Simuliidae

F. Limoniidae

F. Tipulidae

Appendix 20A: Metal concentrations measured in macroinvertebrates

Table 20A: Metal concentrations as measured in three macroinvertebrate taxa (^bM): *Asellus aquaticus*, *Calopteryx virgo* and Chironomidae (consisting of sF. Prodiamesinae and non-Prodiamesinae). All measurements are presented in $\mu\text{g } ^b\text{M g}^{-1}$ macroinvertebrate dry weight (DW). Additionally, the number of individual organisms in each sample are shown.

Sample	Species	Number	Al $\mu\text{g/g DW}$	Cr $\mu\text{g/g DW}$	Mn $\mu\text{g/g DW}$	Fe $\mu\text{g/g DW}$	Co $\mu\text{g/g DW}$	Cu $\mu\text{g/g DW}$	Zn $\mu\text{g/g DW}$	As $\mu\text{g/g DW}$	Cd $\mu\text{g/g DW}$	Pb $\mu\text{g/g DW}$
D1	<i>Calopteryx virgo</i>	3	37	0.40	348	1517	20.72	80	157	2.75	0.99	0.30
D1	<i>Calopteryx virgo</i>	3	36	0.42	614	1630	35.56	90	141	2.66	0.51	0.31
D1	<i>Calopteryx virgo</i>	3	41	0.46	816	1843	48.12	118	163	3.05	0.78	0.35
D2	<i>Calopteryx virgo</i>	3	18	0.47	279	1308	12.05	32	121	1.81	0.55	0.55
D2	<i>Calopteryx virgo</i>	3	50	0.54	743	2962	30.56	33	162	4.74	0.31	0.86
D2	<i>Calopteryx virgo</i>	3	44	0.45	817	3522	31.70	35	135	6.13	0.33	0.94
D3	<i>Calopteryx virgo</i>	3	127	0.59	83	3124	6.04	34	148	6.20	0.83	4.44
D3	<i>Calopteryx virgo</i>	3	136	0.89	92	3858	6.36	37	154	8.21	0.78	5.34
D3	<i>Calopteryx virgo</i>	3	210	0.71	130	3813	10.00	38	186	8.21	0.99	6.20
D4	<i>Calopteryx virgo</i>	1	103	0.33	129	3554	4.67	25	128	9.99	0.89	5.21
D4	<i>Calopteryx virgo</i>	1	333	1.59	630	8048	18.91	38	177	24.09	4.32	4.32
D4	<i>Calopteryx virgo</i>	1	131	0.83	271	6678	8.80	29	144	23.83	2.26	7.49
D6	<i>Calopteryx virgo</i>	3	258	0.80	357	9785	22.64	41	241	61.36	3.50	16.66
D6	<i>Calopteryx virgo</i>	3	232	1.73	275	8523	16.65	51	238	49.53	3.04	14.69
D6	<i>Calopteryx virgo</i>	3	189	0.68	490	10100	30.65	47	206	55.14	2.72	10.54
D7	<i>Calopteryx virgo</i>	3	92	0.63	359	1877	11.54	39	144	7.35	1.81	3.92
D7	<i>Calopteryx virgo</i>	3	96	1.08	489	2437	16.98	59	254	11.25	3.10	4.16
D7	<i>Calopteryx virgo</i>	3	94	0.58	622	2236	28.57	40	146	9.70	1.54	4.34
D1	<i>Asellus aquaticus</i>	3	98	0.38	188	3217	10.18	106	99	6.38	1.22	0.66
D1	<i>Asellus aquaticus</i>	3	157	0.49	227	5054	11.65	128	128	7.52	1.38	1.15
D1	<i>Asellus aquaticus</i>	3	273	0.63	473	8848	23.96	126	147	13.81	1.66	1.74
D2	<i>Asellus aquaticus</i>	3	140	0.58	140	3026	7.26	115	114	6.58	0.27	1.45
D2	<i>Asellus aquaticus</i>	3	44	0.34	90	1414	4.21	90	99	3.53	0.36	0.36
D2	<i>Asellus aquaticus</i>	3	134	0.47	565	3419	24.85	125	125	7.30	0.67	2.04

Appendix 20A: Metal concentrations measured in macroinvertebrates – continued (1)

D3	<i>Asellus aquaticus</i>	1	100	0.71	55	2766	3.21	185	145	9.69	1.82	3.09
D3	<i>Asellus aquaticus</i>	1	337	0.81	152	3655	6.13	101	252	8.59	2.19	10.91
D3	<i>Asellus aquaticus</i>	1	356	1.96	1216	10051	52.66	23	219	17.45	5.32	11.49
D4	<i>Asellus aquaticus</i>	1	537	1.71	258	12617	11.53	243	299	27.24	4.66	24.64
D4	<i>Asellus aquaticus</i>	1	414	0.72	246	11139	12.24	541	223	31.51	6.61	18.96
D4	<i>Asellus aquaticus</i>	1	442	1.14	288	9173	10.75	247	275	29.81	5.67	17.21
D6	<i>Asellus aquaticus</i>	3	53	0.33	73	1494	3.66	177	143	10.48	8.72	4.15
D6	<i>Asellus aquaticus</i>	3	70	0.61	91	1696	3.87	155	144	10.89	4.75	3.95
D6	<i>Asellus aquaticus</i>	3	191	0.62	193	5307	9.85	243	202	26.08	10.19	10.28
D7	<i>Asellus aquaticus</i>	3	260	0.65	278	3369	12.07	238	200	15.60	6.91	9.09
D7	<i>Asellus aquaticus</i>	3	146	0.50	163	1770	7.04	192	200	10.49	6.17	5.81
D7	<i>Asellus aquaticus</i>	3	320	0.83	201	2890	9.25	156	218	14.30	6.35	11.02
D1	Prodiamesinae	3	33	0.39	71	1384	2.65	19	189	1.06	2.20	1.06
D1	Prodiamesinae	3	212	0.58	121	3569	6.24	21	146	3.82	1.57	1.57
D1	Prodiamesinae	3	113	0.36	206	3321	9.63	17	205	4.69	0.97	0.97
D2	Prodiamesinae	3	27	0.45	34	681	0.53	6	75	2.01	0.53	0.53
D2	Prodiamesinae	3	24	0.48	33	981	0.40	8	73	1.57	0.40	5.14
D2	Prodiamesinae	3	42	0.49	40	1349	0.51	9	79	2.32	0.51	0.51
D3	Prodiamesinae	1	17	0.61	27	250	1.67	20	89	4.77	1.67	1.67
D3	Prodiamesinae	1	161	0.60	34	2612	1.63	10	135	7.93	1.63	4.27
D3	Prodiamesinae	1	13	0.49	11	183	1.34	6	72	1.34	1.34	1.34
D4	Prodiamesinae	2	272	0.66	69	4286	1.80	23	170	14.30	1.80	13.22
D4	Prodiamesinae	2	301	0.88	72	3572	2.39	18	185	14.03	2.39	10.11
D4	Prodiamesinae	1	280	1.10	56	4169	3.00	18	149	17.05	3.00	10.08
D6	non-Prodiamesinae	1	152	5.58	371	-517	15.15	89	698	15.15	15.15	15.15
D6	non-Prodiamesinae	1	105	3.88	75	-360	10.55	11	105	10.55	10.55	10.55
D7	Prodiamesinae	2	109	0.50	56	1131	1.35	20	111	6.19	3.54	4.30
D7	Prodiamesinae	2	159	0.46	50	745	1.24	26	125	5.93	1.24	1.24
D7	Prodiamesinae	1	45	0.49	34	453	1.32	25	114	3.65	1.32	1.32

Appendix 20B: Metals in macroinvertebrates: Toxic Units (TU)

Table 20B: Table containing Toxic Units (TU) based on metal concentrations found in Appendix 20A. For each species and metal, the lowest average concentration (i.e. calculating the mean of metal concentrations per species \times sample combination) was calculated. This lowest average served as a reference to compute the TUs shown here. The average TU is calculated based on all the separate TU values. For average TU in Chironomidae, Fe was not taken into consideration because of unreliable results.

Site	Species	TU Al	TU Cr	TU Mn	TU Fe	TU Co	TU Cu	TU Zn	TU As	TU Cd	TU Pb	TU
D1	<i>Calopteryx virgo</i>	0.98	0.93	3.41	0.91	2.78	2.59	1.13	0.98	2.51	0.93	1.71
D1	<i>Calopteryx virgo</i>	0.96	0.98	6.02	0.98	4.76	2.91	1.01	0.94	1.30	0.96	2.08
D1	<i>Calopteryx virgo</i>	1.10	1.08	8.00	1.11	6.44	3.82	1.17	1.08	1.98	1.11	2.69
D2	<i>Calopteryx virgo</i>	0.49	1.10	2.74	0.79	1.61	1.05	0.87	0.64	1.38	1.71	1.24
D2	<i>Calopteryx virgo</i>	1.34	1.27	7.28	1.78	4.09	1.08	1.16	1.68	0.78	2.72	2.32
D2	<i>Calopteryx virgo</i>	1.17	1.07	8.01	2.12	4.25	1.14	0.97	2.17	0.84	2.94	2.47
D3	<i>Calopteryx virgo</i>	3.39	1.39	0.82	1.88	0.81	1.09	1.06	2.20	2.10	13.93	2.87
D3	<i>Calopteryx virgo</i>	3.63	2.11	0.90	2.32	0.85	1.20	1.11	2.91	1.98	16.77	3.38
D3	<i>Calopteryx virgo</i>	5.59	1.68	1.28	2.29	1.34	1.24	1.33	2.91	2.52	19.47	3.96
D4	<i>Calopteryx virgo</i>	2.74	0.78	1.27	2.14	0.63	0.81	0.92	3.54	2.27	16.35	3.14
D4	<i>Calopteryx virgo</i>	8.88	3.75	6.18	4.84	2.53	1.24	1.27	8.54	10.96	13.56	6.17
D4	<i>Calopteryx virgo</i>	3.50	1.96	2.66	4.02	1.18	0.95	1.03	8.45	5.73	23.52	5.30
D6	<i>Calopteryx virgo</i>	6.86	1.88	3.50	5.88	3.03	1.34	1.73	21.75	8.89	52.31	10.72
D6	<i>Calopteryx virgo</i>	6.18	4.08	2.70	5.12	2.23	1.64	1.71	17.56	7.71	46.11	9.50
D6	<i>Calopteryx virgo</i>	5.02	1.60	4.81	6.07	4.11	1.54	1.48	19.55	6.91	33.09	8.42
D7	<i>Calopteryx virgo</i>	2.46	1.48	3.52	1.13	1.55	1.26	1.03	2.60	4.61	12.32	3.20
D7	<i>Calopteryx virgo</i>	2.55	2.54	4.80	1.47	2.27	1.92	1.82	3.99	7.86	13.07	4.23
D7	<i>Calopteryx virgo</i>	2.50	1.38	6.09	1.34	3.83	1.29	1.04	3.44	3.90	13.64	3.85
D1	<i>Asellus aquaticus</i>	0.94	0.83	1.57	1.23	1.76	1.03	0.87	1.10	2.83	0.56	1.27
D1	<i>Asellus aquaticus</i>	1.50	1.06	1.90	1.93	2.01	1.24	1.14	1.30	3.19	0.97	1.62
D1	<i>Asellus aquaticus</i>	2.60	1.36	3.97	3.38	4.14	1.23	1.31	2.38	3.84	1.47	2.57
D2	<i>Asellus aquaticus</i>	1.33	1.25	1.17	1.16	1.25	1.12	1.01	1.13	0.62	1.22	1.13
D2	<i>Asellus aquaticus</i>	0.42	0.74	0.75	0.54	0.73	0.88	0.88	0.61	0.83	0.30	0.67
D2	<i>Asellus aquaticus</i>	1.28	1.01	4.74	1.30	4.29	1.21	1.11	1.26	1.55	1.72	1.95
D3	<i>Asellus aquaticus</i>	0.95	1.54	0.46	1.06	0.55	1.79	1.28	1.67	4.22	2.61	1.61
D3	<i>Asellus aquaticus</i>	3.22	1.75	1.28	1.40	1.06	0.98	2.24	1.48	5.08	9.22	2.77

Appendix 20B: Metals in macroinvertebrates: Toxic Units (TU) – continued (1)

Asellus aquaticus

Site	<i>Asellus aquaticus</i>	TU Al	TU Cr	TU Mn	TU Fe	TU Co	TU Cu	TU Zn	TU As	TU Cd	TU Pb	TU
D3	<i>Asellus aquaticus</i>	3.40	4.25	10.20	3.84	9.09	0.22	1.94	3.01	12.33	9.70	5.80
D4	<i>Asellus aquaticus</i>	5.13	3.72	2.17	4.82	1.99	2.36	2.65	4.69	10.80	20.82	5.91
D4	<i>Asellus aquaticus</i>	3.95	1.56	2.07	4.25	2.11	5.25	1.98	5.43	15.32	16.02	5.79
D4	<i>Asellus aquaticus</i>	4.22	2.47	2.42	3.50	1.86	2.39	2.44	5.14	13.14	14.53	5.21
D6	<i>Asellus aquaticus</i>	0.51	0.71	0.62	0.57	0.63	1.72	1.27	1.81	20.22	3.50	3.16
D6	<i>Asellus aquaticus</i>	0.67	1.32	0.77	0.65	0.67	1.51	1.28	1.88	11.02	3.33	2.31
D6	<i>Asellus aquaticus</i>	1.82	1.34	1.62	2.03	1.70	2.36	1.79	4.49	23.61	8.68	4.94
D7	<i>Asellus aquaticus</i>	2.48	1.41	2.33	1.29	2.08	2.31	1.77	2.69	16.01	7.67	4.00
D7	<i>Asellus aquaticus</i>	1.39	1.08	1.37	0.68	1.21	1.86	1.78	1.81	14.30	4.91	3.04
D7	<i>Asellus aquaticus</i>	3.05	1.80	1.69	1.10	1.60	1.51	1.93	2.46	14.73	9.31	3.92
D1	Prodiamesinae	1.05	0.88	2.97		5.51	2.47	2.49	0.54	4.58	0.88	2.38
D1	Prodiamesinae	6.81	1.31	5.07		12.97	0.45	1.93	1.95	3.26	1.31	3.90
D1	Prodiamesinae	3.64	0.81	8.66		20.01	0.37	2.71	2.38	2.02	0.81	4.60
D2	Prodiamesinae	0.88	1.02	1.44		1.11	0.14	0.99	1.02	1.11	0.44	0.91
D2	Prodiamesinae	0.76	1.09	1.37		0.84	0.17	0.97	0.80	0.84	4.29	1.23
D2	Prodiamesinae	1.36	1.12	1.69		1.05	0.19	1.04	1.18	1.05	0.42	1.01
D3	Prodiamesinae	0.54	1.39	1.12		3.47	0.43	1.18	2.43	3.47	1.39	1.71
D3	Prodiamesinae	5.18	1.36	1.42		3.39	0.21	1.79	4.03	3.39	3.56	2.70
D3	Prodiamesinae	0.43	1.12	0.46		2.79	0.13	0.96	0.68	2.79	1.12	1.16
D4	Prodiamesinae	8.75	1.50	2.90		3.73	0.49	2.25	7.27	3.73	11.02	4.63
D4	Prodiamesinae	9.68	1.99	3.00		4.96	0.40	2.44	7.13	4.96	8.43	4.78
D4	Prodiamesinae	8.99	2.50	2.35		6.24	0.40	1.96	8.67	6.24	8.40	5.08
D6	non-Prodiamesinae	4.87	12.63	15.58		31.50	1.92	9.23	7.71	31.50	12.63	14.17
D6	non-Prodiamesinae	3.39	8.79	3.14		21.93	0.23	1.40	5.37	21.93	8.79	8.33
D7	Prodiamesinae	3.51	1.13	2.35		2.81	0.42	1.47	3.15	7.36	3.58	2.86
D7	Prodiamesinae	5.10	1.03	2.11		2.57	0.57	1.65	3.02	2.57	1.03	2.18
D7	Prodiamesinae	1.44	1.10	1.44		2.75	0.53	1.50	1.85	2.75	1.10	1.61

Appendix 21A: Statistical results of metals in biota

Table 21A: A summary of Student's and Welch's *t*-tests (*t*) and Mann-Whitney *U*-tests (*w*) conducted on metal concentrations in biota, as well as calculated average TUs (for *Asellus aquaticus*, *Calopteryx virgo* and Chironomidae: TU_{asl}, TU_{clx} and TU_{chr}, respectively. Concentrations per species are compared between sites upstream ('up') and downstream ('down'). Assumptions were tested using the Shapiro-Wilk test and the *F*-test. Significance levels: * = *p* < 0.05; ** = *p* < 0.01; *** = *p* < 0.001; ns = not significant. Graphical representations are presented in Appendix 21B.

		Al	Cr	Mn	Fe	Co	Cu	Zn	As	Cd	Pb	TU _{asl}
Asellus	<i>N</i>	1	0	0	0	0	0	1	0	1	0	1
	σ^2	1	0	1	1	1	0	0	1	0	0	1
	Test	<i>t</i>	<i>t</i>	<i>w</i>	<i>w</i>	<i>w</i>	<i>t</i>	<i>t</i>	<i>w</i>	<i>t</i>	<i>t</i>	<i>t</i>
	<i>p</i>	ns	*	ns	ns	ns	*	***	**	***	***	**
		up < down				up < down		up < down	up < down	up < down	up < down	up < down
		Al	Cr	Mn	Fe	Co	Cu	Zn	As	Cd	Pb	TU _{clx}
Calopteryx	<i>N</i>	1	0	1	0	1	0	0	0	0	0	0
	σ^2	1	1	0	1	0	1	1	1	1	1	0
	Test	<i>t</i>	<i>w</i>	<i>t</i>	<i>w</i>	<i>t</i>	<i>w</i>	<i>w</i>	<i>w</i>	<i>w</i>	<i>w</i>	<i>t</i>
	<i>p</i>	***	**	*	**	*	ns	ns	***	**	***	**
		up < down	up < down	up > down	up < down	up > down			up < down	up < down	up < down	up < down
		Al	Cr	Mn	Fe	Co	Cu	Zn	As	Cd	Pb	TU _{chr}
Chironomidae	<i>N</i>	0	0	0	0	0	0	0	0	0	0	0
	σ^2	1	0	1	1	1	0	0	0	0	0	1
	Test	<i>w</i>	<i>t</i>	<i>w</i>	<i>w</i>	<i>w</i>	<i>t</i>	<i>t</i>	<i>t</i>	<i>t</i>	<i>t</i>	<i>w</i>
	<i>p</i>	ns	ns	ns	ns	ns	ns	ns	**	ns	*	ns
								up < down		up < down		

Appendix 21B: Boxplots of metals in biota

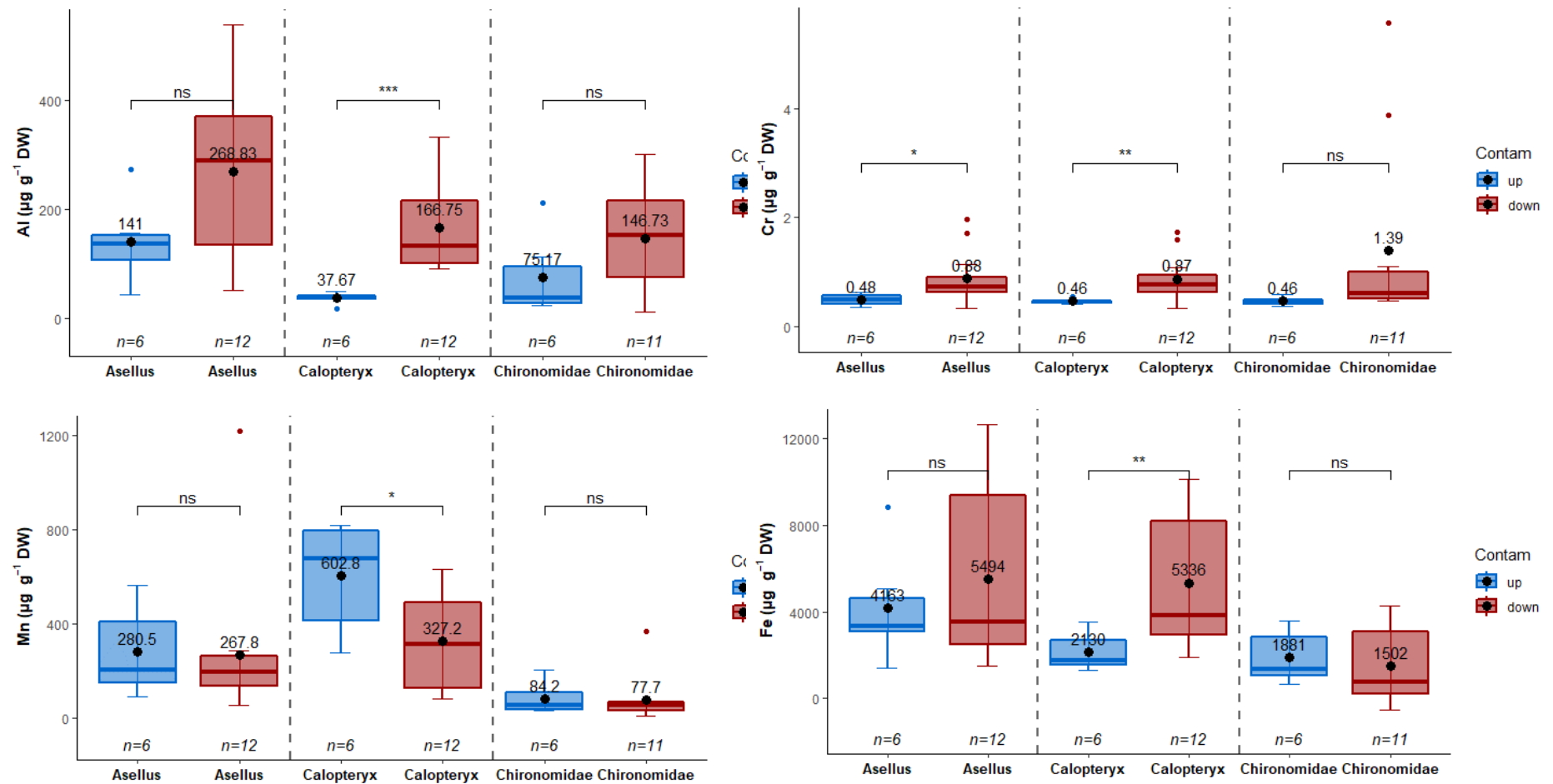


Figure 21B: Boxplots of metals in biota (*Asellus*, *Calopteryx*, *Chironomidae*) comparing between reference (D1, D2; upstream - blue) and contaminated (D3, D4, D6, D7; downstream - red) sites. Statistical results are shown as significance levels (* = $p < 0.05$; ** = $p < 0.01$; *** = $p < 0.001$; ns = not significant.). Furthermore, the average values are indicated with a black dot, corresponding to its location on the Y-axis. Respective sample sizes are shown above the X-axis. A summary of these results can be found in Appendix 21A.

Appendix 21B: Boxplots of metals in biota – continued (1)

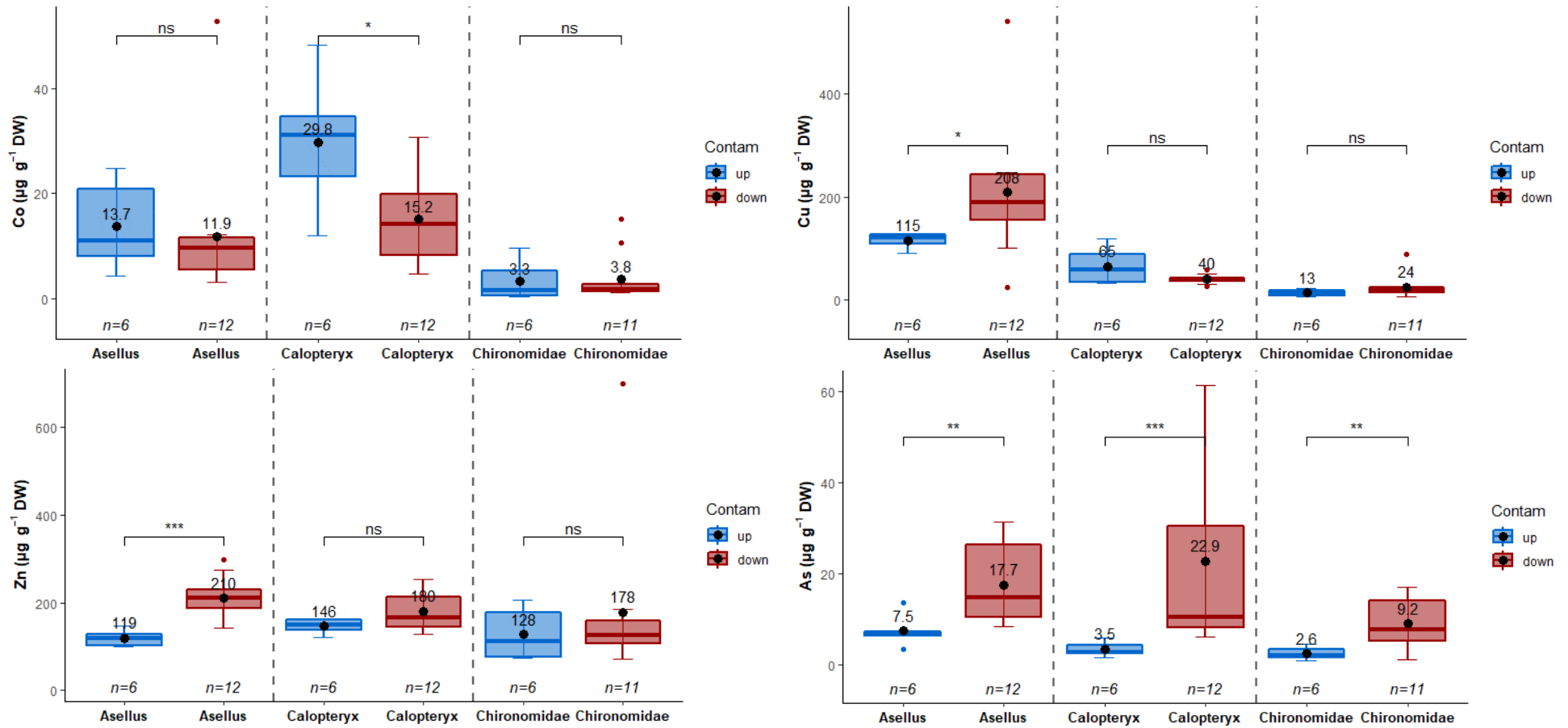


Figure 21B: Boxplots of metals in biota (*Asellus*, *Calopteryx*, *Chironomidae*) comparing between reference (D1, D2; upstream - blue) and contaminated (D3, D4, D6, D7; downstream - red) sites. Statistical results are shown as significance levels (* = $p < 0.05$; ** = $p < 0.01$; *** = $p < 0.001$; ns = not significant.). Furthermore, the average values are indicated with a black dot, corresponding to its location on the Y-axis. Respective sample sizes are shown above the X-axis. A summary of these results can be found in Appendix 21A.

Appendix 21B: Boxplots of metals in biota – continued (2)

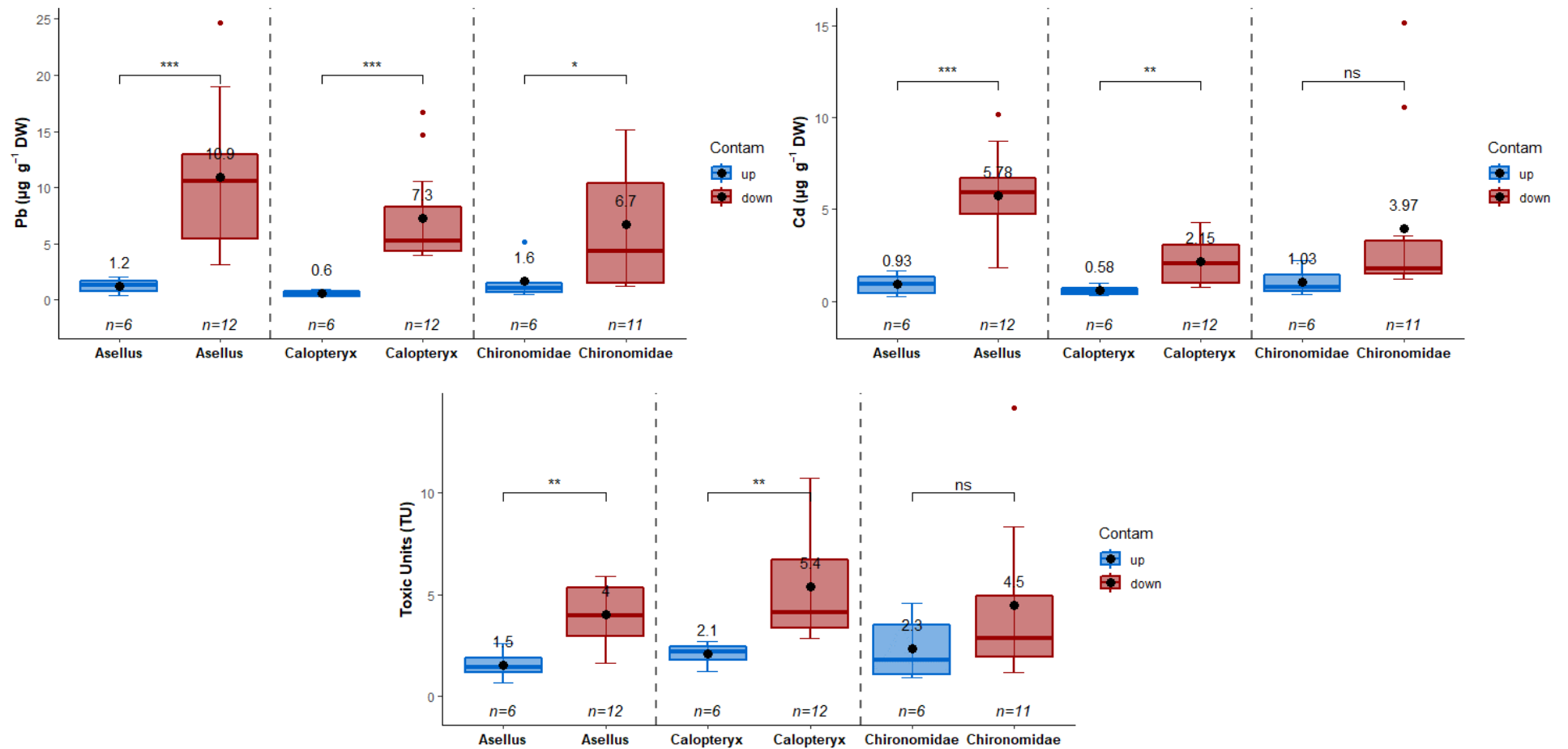


Figure 21B: Boxplots of metals in biota (Asellus = *Asellus aquaticus*, Calopteryx = *Calopteryx virgo*, Chironomidae) comparing between reference (D1, D2; upstream - blue) and contaminated (D3, D4, D6, D7; downstream - red) sites. Statistical results are shown as significance levels (* = $p < 0.05$; ** = $p < 0.01$; *** = $p < 0.001$; ns = not significant.). Furthermore, the average values are indicated with a black dot, corresponding to its location on the Y-axis. Respective sample sizes are shown above the X-axis. A summary of these results can be found in Appendix 21A.

Appendix 21C: Bar plots of metals in biota

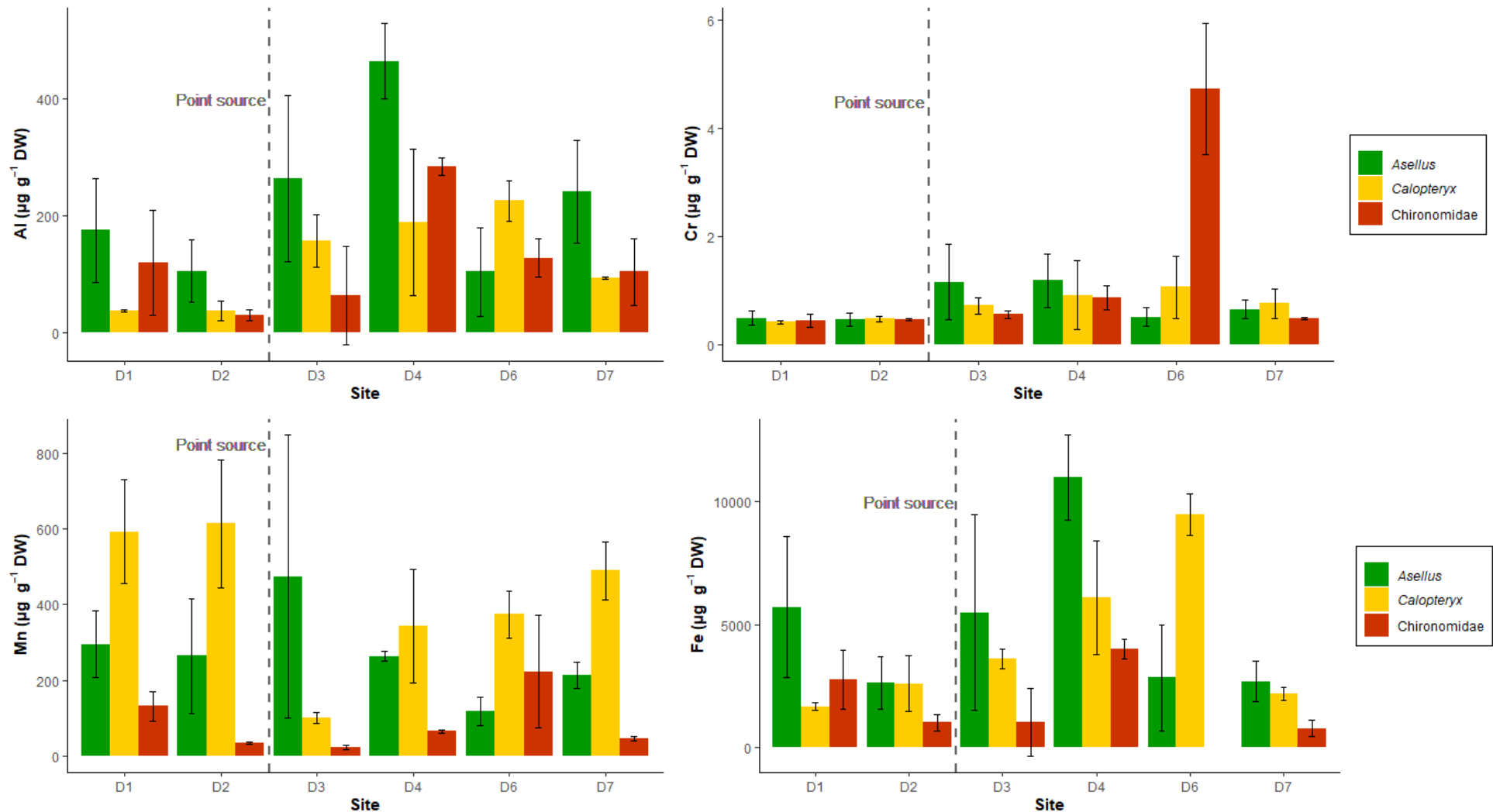


Figure 21C: Bar graphs for all metal concentrations (in $\mu\text{g metal g}^{-1}$ dry weight (DW)) in three macroinvertebrate taxa (*Asellus* = green; *Calopteryx* = yellow; Chironomidae = red), with S.D. (error bars). A vertical line (dashed; - -) indicates the location of the point source of contamination (the merge of the Dommel river with a tributary river; the Eindergatloop). Samples were obtained during sampling campaign B. Chironomidae Fe was omitted for site D6 as it was characterized by a lot of outlying data.

Appendix 21C: Bar plots of metals in biota – continued (1)

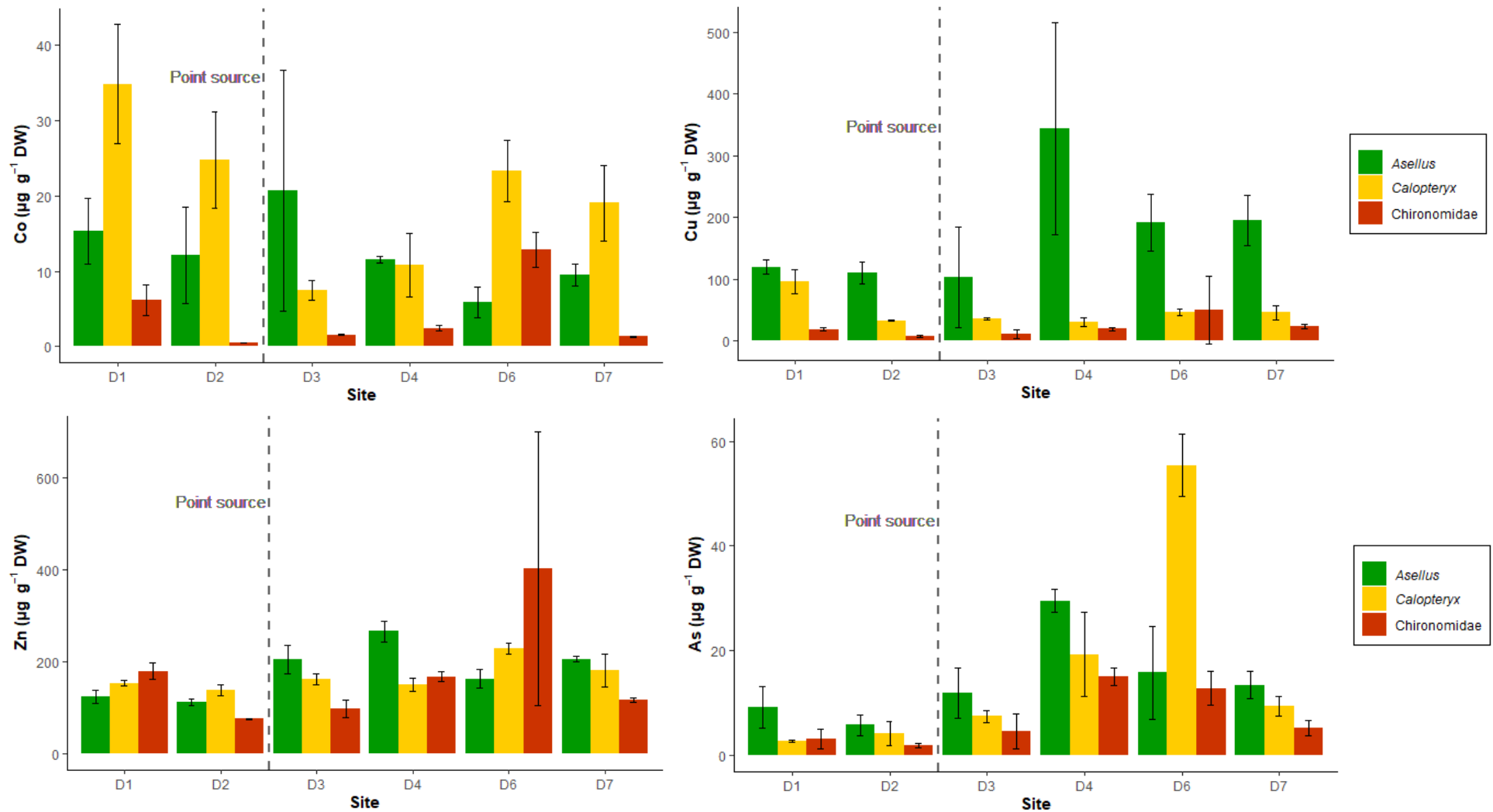


Figure 21C: Bar graphs for all metal concentrations (in $\mu\text{g metal g}^{-1}$ dry weight (DW)) in three macroinvertebrate taxa (*Asellus* = green; *Calopteryx* = yellow; Chironomidae = red), with S.D. (error bars). A vertical line (dashed; - - -) indicates the location of the point source of contamination (the merge of the Dommel river with a tributary river; the Eindergatloop). Samples were obtained during sampling campaign B.

Appendix 21C: Bar plots of metals in biota – continued (2)

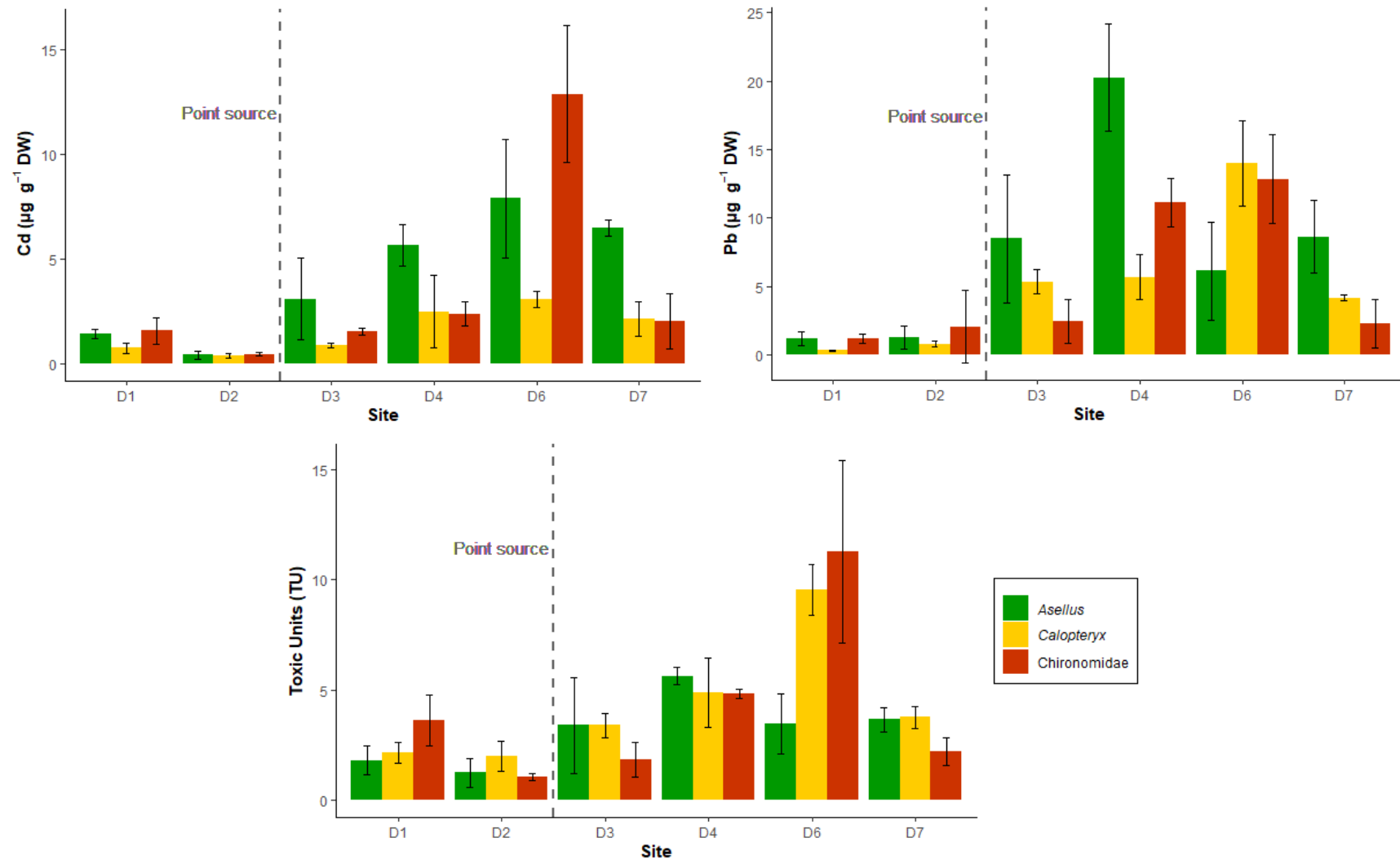


Figure 21C: Bar graphs for all metal concentrations (in $\mu\text{g metal g}^{-1}$ dry weight (DW)) in three macroinvertebrate taxa (*Asellus aquaticus* = green; *Calopteryx virgo* = yellow; Chironomidae = red), with S.D. (error bars). A vertical line (dashed; - - -) indicates the location of the point source of contamination (the merge of the Dommel river with a tributary river; the Eindergatloop). Samples were obtained during sampling campaign B.

Appendix 21D: Average concentrations of metals in biota

Figure 21D: Average concentrations of metals in biota in up- (D1, D2) and downstream sites (D3, D4, D6, D7) for *Calopteryx virgo*, *Asellus aquaticus* and Chironomidae. For ease of comparison, upstream (blue) and downstream (red) sites are colour-coded. All concentrations are presented in $\mu\text{g metal g}^{-1}$ dry weight (DW).

Sample	Species	Al	Cr	Mn	Fe	Co	Cu	Zn	As	Cd	Pb
		$\mu\text{g/g DW}$	$\mu\text{g/g DW}$	$\mu\text{g/g DW}$	$\mu\text{g/g DW}$	$\mu\text{g/g DW}$	$\mu\text{g/g DW}$	$\mu\text{g/g DW}$	$\mu\text{g/g DW}$	$\mu\text{g/g DW}$	$\mu\text{g/g DW}$
D1-D2	Calopteryx	38 ± 0	0.46 ± 0.04	603 ± 14	2130 ± 661	29.79 ± 7.09	65 ± 44	147 ± 10	3.52 ± 0.99	0.58 ± 0.26	0.55 ± 0.33
D3-D7	Calopteryx	167 ± 56	0.87 ± 0.15	327 ± 163	5336 ± 3195	15.15 ± 7.3	40 ± 8	180 ± 35	22.9 ± 22.23	2.15 ± 0.94	7.28 ± 4.5
D1-D2	Asellus	141 ± 50	0.48 ± 0.03	280 ± 22	4163 ± 2183	13.68 ± 2.23	115 ± 7	119 ± 8	7.52 ± 2.43	0.92 ± 0.7	1.23 ± 0.07
D3-D7	Asellus	269 ± 148	0.88 ± 0.34	268 ± 150	5494 ± 3876	11.86 ± 6.33	208 ± 100	210 ± 42	17.68 ± 8.06	5.78 ± 2.01	10.88 ± 6.36
D1-D2	Chironomidae	75 ± 62	0.46 ± 0.02	84 ± 69	1881 ± 1240	3.33 ± 4.02	13 ± 8	128 ± 74	2.58 ± 0.87	1.03 ± 0.78	1.63 ± 0.61
D3-D7	Chironomidae	145 ± 97	1.67 ± 2.05	90 ± 90	1340 ± 1890	4.52 ± 5.57	26 ± 16	196 ± 140	9.48 ± 5.29	4.71 ± 5.44	7.18 ± 5.61

Appendix 22: Summary of MI counts, including metrics used for calculating MMIF

Table 22A: A summary of macroinvertebrate counts across all samples (six sites, sampled over three sampling campaigns). Number of taxa (TAX) mostly at Family or Genus level; see Appendix 3. Including the number of Ephemeroptera, Plecoptera and Trichoptera (EPT), number sensitive species (tolerance scores > 5; see Appendix 3) without counting EPT (NST), the Shannon-Wiener Diversity index (SWD), the mean tolerance score (MTS) and the calculated MMIF (based on TAX, EPT, NST, SWD and MTS; see Appendix 2 and 3).

	D1A	D2A	D3A	D4A	D6A	D7A
Total N	1060	874	1401	700	335	372
TAX	25	22	23	19	13	20
EPT	6	3	4	2	1	2
NST	2	2	3	4	1	2
SWD	1.96	2.29	1.69	1.50	1.39	2.34
MTS	4.84	4.77	4.70	4.42	4.00	4.70
MMIF	0.65	0.60	0.60	0.50	0.35	0.50
	D1B	D2B	D3B	D4B	D6B	D7B
Total N	675	546	1027	326	699	339
TAX	15	28	29	19	27	23
EPT	2	2	2	0	1	2
NST	2	6	7	3	8	5
SWD	1.11	2.40	2.19	2.22	2.24	2.48
MTS	4.80	4.79	4.76	4.53	5.04	4.87
MMIF	0.45	0.65	0.65	0.50	0.70	0.60
	D1C	D2C	D3C	D4C	D6C	D7C
Total N	314	527	516	567	267	415
TAX	17	18	22	22	20	21
EPT	3	2	4	2	4	3
NST	2	1	3	4	2	4
SWD	1.96	1.85	2.14	2.02	2.28	2.02
MTS	4.88	4.33	4.82	4.73	4.80	4.95
MMIF	0.55	0.50	0.65	0.60	0.55	0.60

Appendix 23A: PCA - Macroinvertebrates

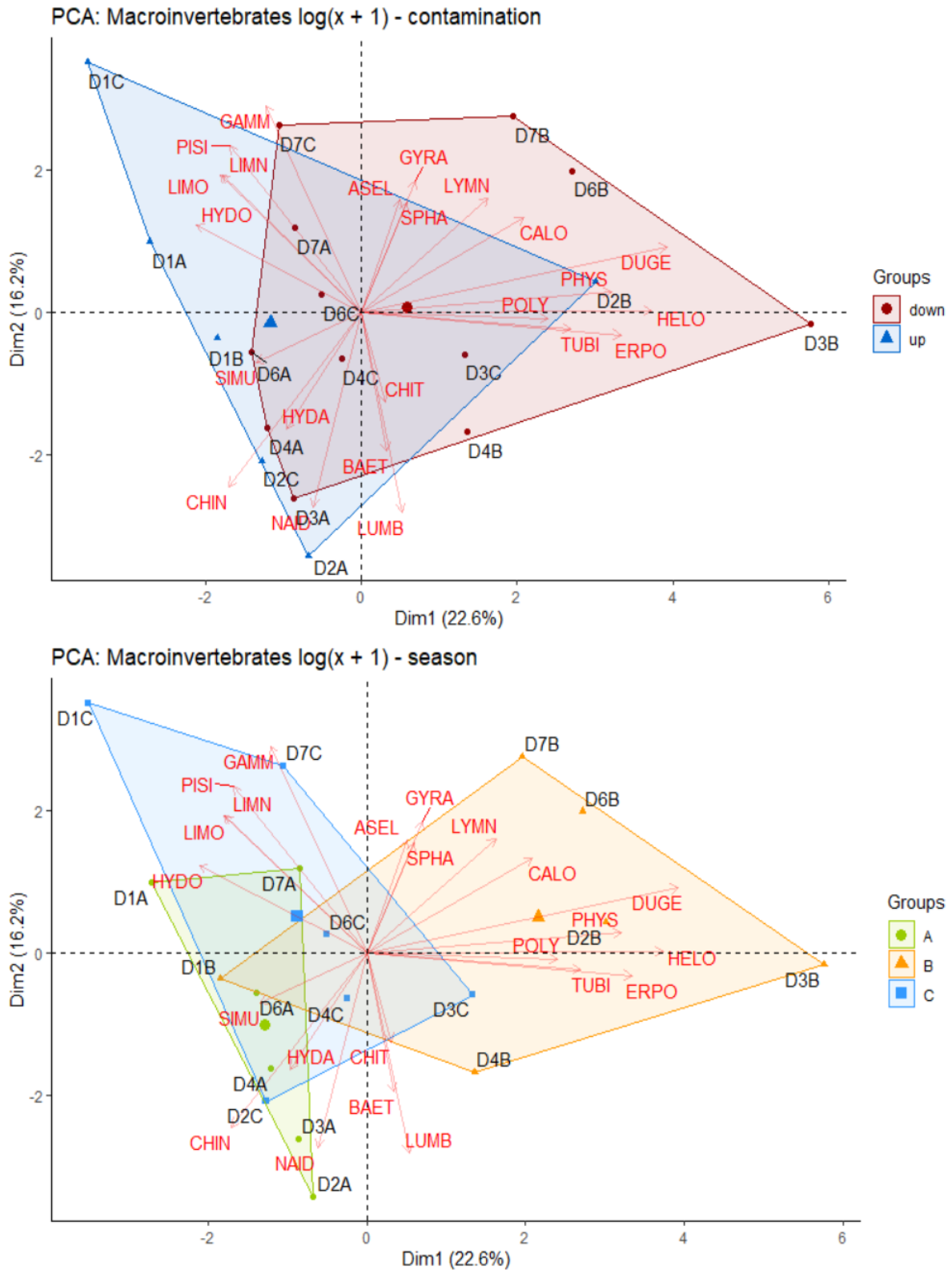


Figure 23A: Principal Component Analysis diagram for macroinvertebrate counts (proportions) with grouping based on ‘contamination’ (up vs downstream; **top**), and based on sampling campaign (‘season’; A: 17/04/2019; B: 21/08/2019; C: 24/01/2020; **bottom**), data log(x + 1) transformed. Top graph provided in text (Fig. 7) but shown enlarged here. Variables under investigation are indicated with red arrows. Additional information on the different PC axes can be found in Appendix 23B. Macroinvertebrate codes can be found in Appendix 19B.

Appendix 23B : PCA - Macroinvertebrates

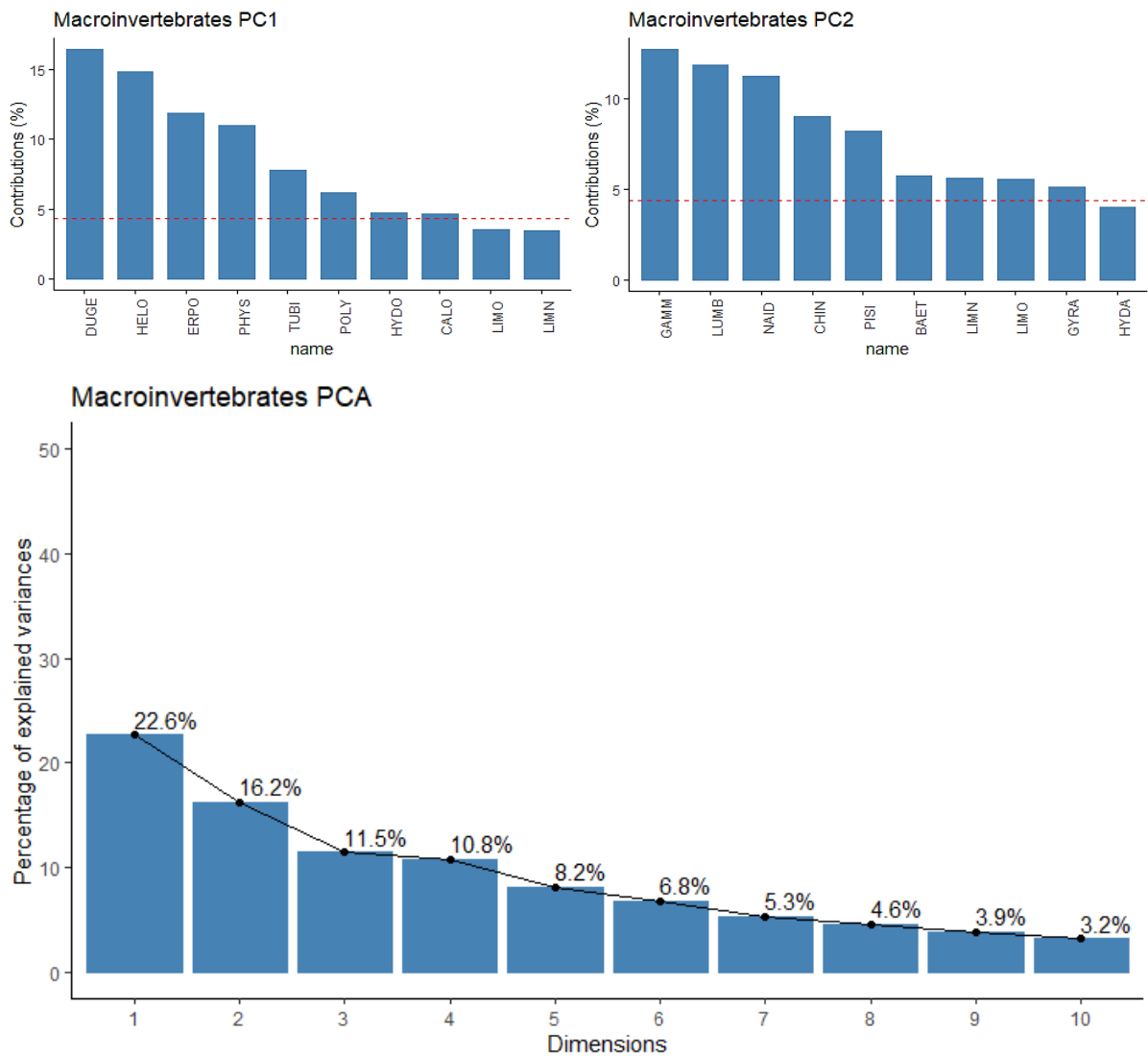


Figure 23B: Graphs supporting the PCA diagrams of Figure 7 and Appendix 23A. Graphs on top show the top 10 of variables contributing to either PC1 (Dim1; left) or PC2 (Dim2; right). The red dashed line serves as a reference which corresponds to the expected value if the contribution were uniform. The bottom graph shows the percentage of variance explained by the different PC dimensions.

Extracurricular thesis-related work

1 – Poster presentation: Fifth Annual Meeting on Plant Ecology and Evolution (AMPEE5) – Meise, Belgium 2019; p. 144

2 – Poster presentation: European Diatom Meeting – Cardiff, UK 2020; p. 145



Assessment of biological quality along a metal pollution gradient applying macroinvertebrates and diatoms

Stijn Van de Vondel^{1,2,3}, Lieven Bervoets³ & Bart Van de Vijver^{1,2}

¹Meise Botanic Garden, Research Department, Nieuwelaan 38, B-1860 Meise, Belgium

²University of Antwerp, Department of Biology, ECOBE, Universiteitsplein 1, B-2610 Wilrijk, Belgium

³University of Antwerp, Department of Biology, SPHERE, Groenenborgerlaan 177, B-2020 Antwerp, Belgium

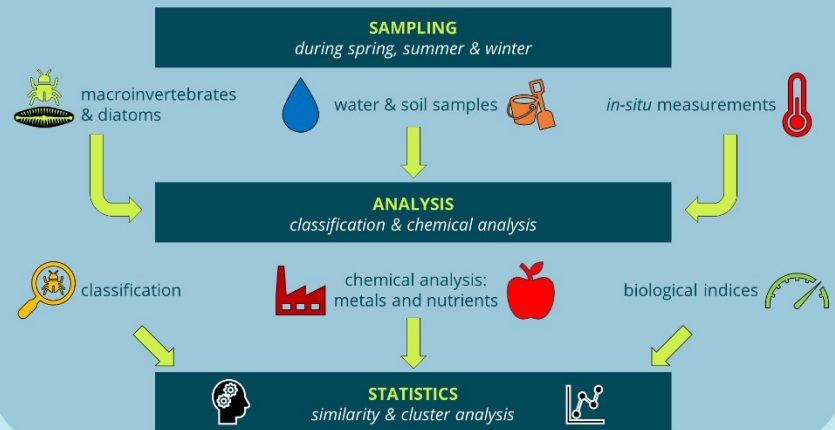
Introduction

The **EU Water Framework Directive** urges all EU member states to assess the water quality of their waterbodies using a range of aquatic organisms.

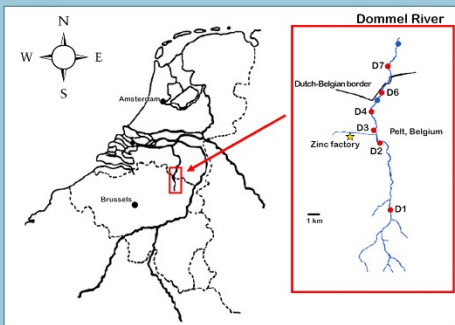
Here, **macroinvertebrates** and **diatoms** (micro-algae with cell walls made of silica) are used to determine **water quality** of the **Dommel river**, which shows a **metal pollution gradient** caused by historical contamination.

Diatoms sampled in **2007** will be reevaluated, to test the effect of recent changes in taxonomy on the water quality values.

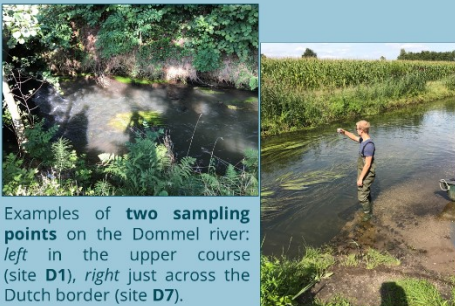
Methods



Study Area

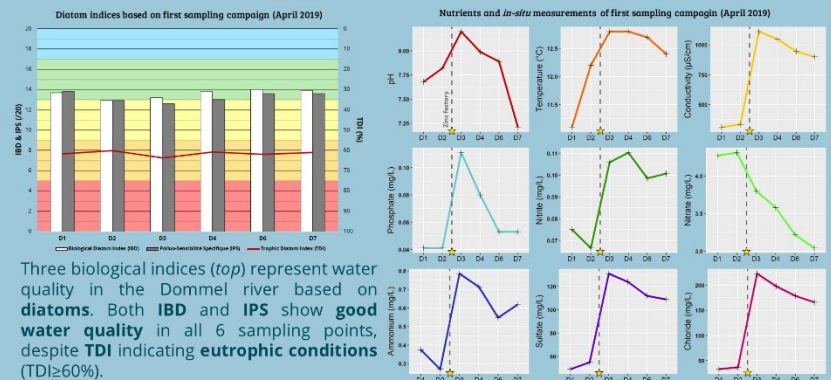


Map showing the location of the **Dommel river** with the chosen sampling points (after De Jonge et al. 2008).



Examples of **two sampling points** on the Dommel river: **left** in the upper course (site **D1**), **right** just across the Dutch border (site **D7**).

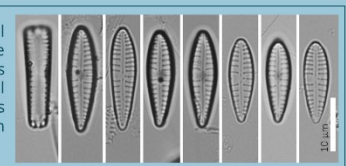
First Results



Three biological indices (*top*) represent water quality in the Dommel river based on **diatoms**. Both **IBD** and **IPS** show **good water quality** in all 6 sampling points, despite **TDI** indicating **eutrophic conditions** ($TDI \geq 60\%$).

On the *right*, several **in-situ measurements** are shown along with **nutrient concentrations** in the Dommel river. Additionally, the indicative location of the tributary running alongside the **zinc factory** is marked with a star. The measurements thereafter (D3 → D6) show **increased concentrations** for PO_4^{3-} , NO_2^- , NH_4^+ , SO_4^{2-} and Cl^- ; while NO_2^- concentration decreases.

An unknown diatom species was recorded in several samples from the upper Dommel course. As part of the genus *Gomphonema*, this species shows some similarities with other common taxa but differs in several morphological aspects. A detailed analysis to unravel its correct taxonomic position is being executed using both light and scanning electron microscopy techniques.





Assessment of biological quality along a metal pollution gradient applying macroinvertebrates and diatoms

Stijn Van de Vondel^{1,2,3}, Lieven Bervoets³ & Bart Van de Vijver^{1,2}

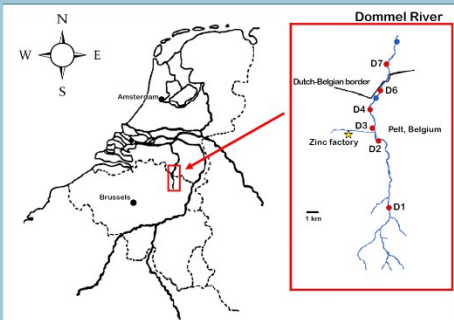
¹Meise Botanic Garden, Research Department, Nieuwelaan 38, B-1860 Meise, Belgium
²University of Antwerp, Department of Biology, ECOBE, Universiteitsplein 1, B-2610 Wilrijk, Belgium
³University of Antwerp, Department of Biology, SPHERE, Groenenborgerlaan 177, B-2020 Antwerp, Belgium

Introduction

The **EU Water Framework Directive** urges all EU member states to assess the water quality of their waterbodies using a range of aquatic organisms.

Here, **macroinvertebrates** and **diatoms** are used to determine **water quality** of the **Dommel river**, which shows a **metal pollution** gradient caused by historical contamination.

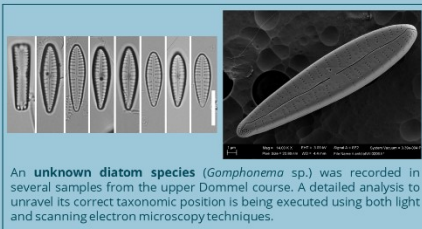
Diatom samples collected in **2007** by De Jonge et al. (2008) will be reassessed to test the effect of recent changes in taxonomy on the water quality values.



Map showing the location of the **Dommel river** with the chosen sampling points (after De Jonge et al., 2008).

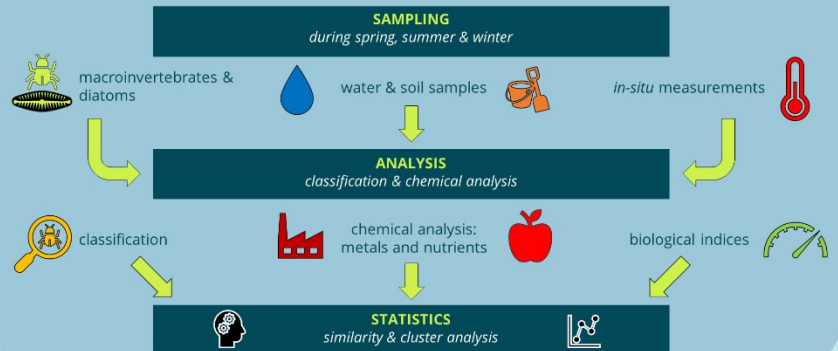
Discussion

- The **MMIF** clearly indicates a reduced ecological quality between upstream and downstream locations, while **diatom indices** remain relatively stable, which falls in line with conclusions by De Jonge et al. (2008).
- First observations suggest an **increase in nutrient and metal concentrations**, of which the latter is also supported by increased bioaccumulated metal concentrations in macroinvertebrates.

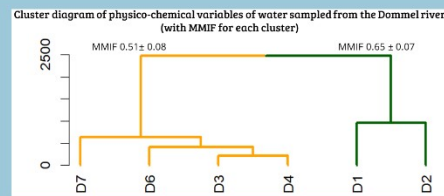


An **unknown diatom species** (*Gomphonema* sp.) was recorded in several samples from the upper Dommel course. A detailed analysis to unravel its correct taxonomic position is being executed using both light and scanning electron microscopy techniques.

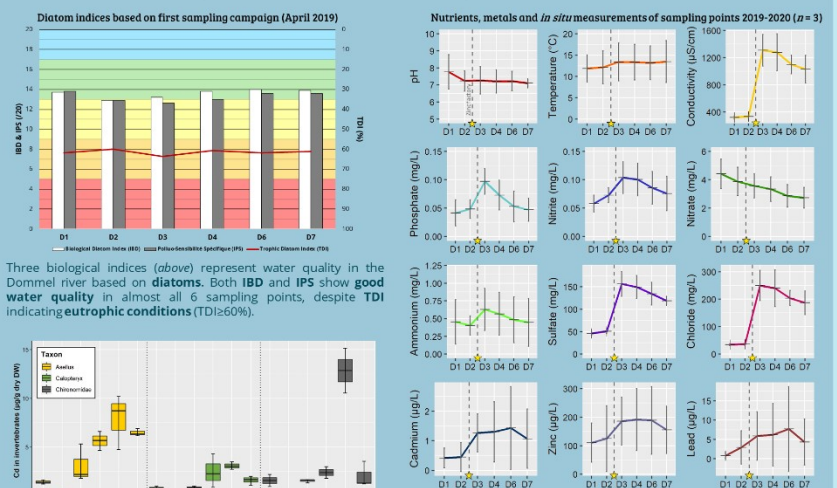
Methods



First Results



Hierarchical clustering based on squared Euclidean distances, with average **MMIF** (Multimetric Macroinvertebrate Index Flanders) shown for both clusters.



Three biological indices (above) represent water quality in the Dommel river based on **diatoms**. Both **IBD** and **IPS** show **good water quality** in almost all 6 sampling points, despite **TDI** indicating **eutrophic conditions** (TDI=60%).

Cadmium concentrations measured in 3 macroinvertebrate taxa sampled in August 2019, showing an **increase in Cd** from D2 to D3. Similar trends are found for several other metals (e.g. Zn and Pb; not shown here).

Several **in situ measurements** are shown along with **nutrient and metal concentrations** in water of the Dommel river from samples between April 2019 and January 2020 ($n = 3$). Additionally, the indicative location of the tributary running alongside the **zinc factory** is marked with a star. Most measurements show a positive, increasing trend from D2 to D3.

